



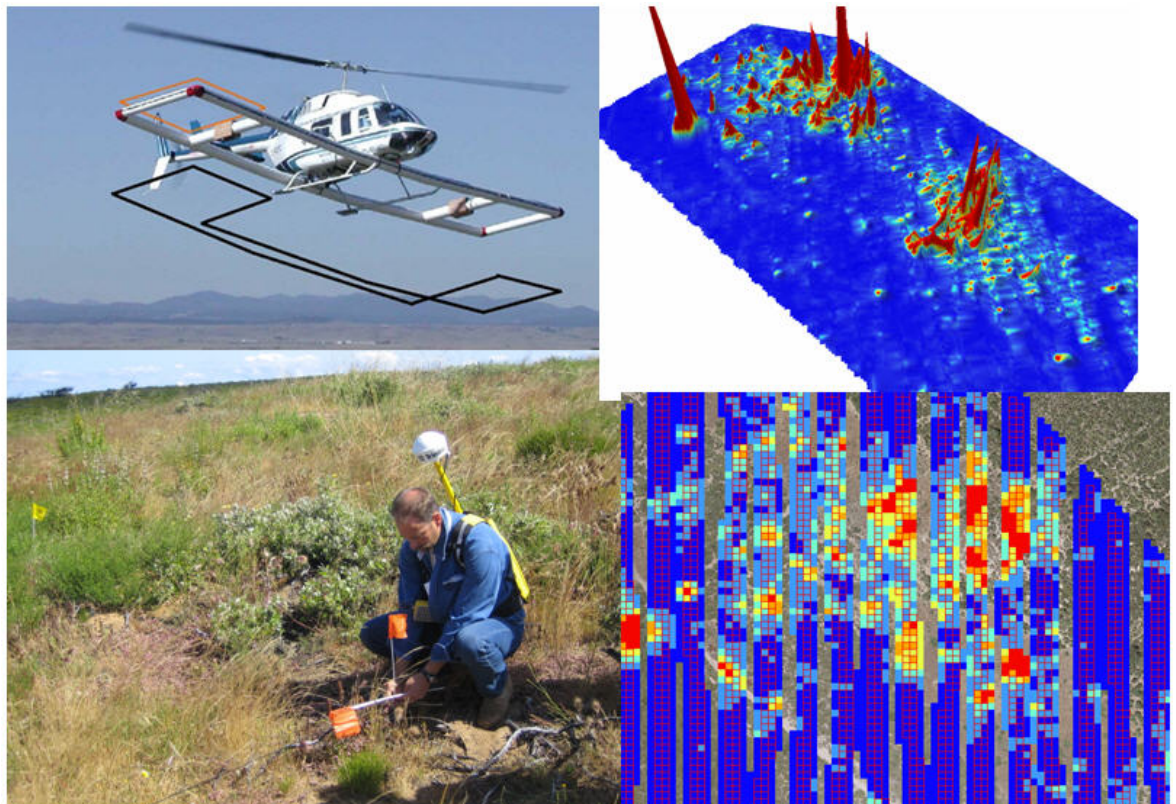
**US Army Corps  
of Engineers®**  
Engineer Research and  
Development Center

*Environmental Quality Technology Program*

## **Evaluation of Airborne Remote Sensing Techniques for Predicting the Distribution of Energetic Compounds on Impact Areas**

Mark R. Graves, Linda Peyman Dove, Thomas F. Jenkins,  
Susan Bigl, Marianne E. Walsh, Alan D. Hewitt, Dennis  
Lambert, Nancy Perron, Charles Ramsey, Jeff Gamey,  
Les Beard, William E. Doll, and Dale Magoun

September 2007



# **Evaluation of Airborne Remote Sensing Techniques for Predicting the Distribution of Energetic Compounds on Impact Areas**

Mark R. Graves and Linda Peyman Dove

*Environmental Laboratory  
U.S. Army Engineer Research and Development Center  
3909 Halls Ferry Road  
Vicksburg, MS 39180-6199*

Thomas F. Jenkins, Susan Bigl, Marianne E. Walsh, Alan D. Hewitt, Dennis Lambert,  
and Nancy Perron

*Cold Regions Research and Engineering Laboratory  
U.S. Army Engineer Research and Development Center  
Hanover, NH 03755*

Charles Ramsey

*EnviroStat, Inc.  
P.O. Box 636  
Fort Collins, CO 80522*

Jeff Gamey, Les Beard, and William E. Doll

*Battelle  
105 Mitchell Road, Suite 103  
Oak Ridge, TN 37830*

Dale Magoun

*University of Louisiana at Monroe, Dept. of Mathematics and Physics  
700 University Avenue  
Monroe, LA 71209*

Final report

Approved for public release; distribution is unlimited.

Prepared for Office of the Assistant Secretary of the Army  
(Acquisition, Logistics, and Technology)  
and U.S. Army Corps of Engineers  
Washington, DC 20314-1000

**Abstract:** The characterization of impact area munitions constituents has typically employed traditional soil sampling approaches. These sampling approaches do not accurately account for the distribution of such contaminants over the landscape due to the distributed nature of explosive compound sources throughout impact areas, the highly localized distribution of contaminants surrounding these sources, and inaccurate records of historical target locations.

Remote sensing and geographic information system (GIS) technologies were utilized to assist in the development of enhanced sampling strategies to better predict the landscape-scale distribution of energetic compounds. Remotely sensed magnetometer and electromagnetic (EM) data were used to detect and delineate areas of high densities of anomalies. The anomalies were considered to be related to targets and/or ranges likely to be highly contaminated with surface and subsurface ordnance and explosive items and artifacts. The Oak Ridge Airborne Geophysical System airborne magnetometer and time-domain EM systems were used.

The magnetometer data were analyzed using GIS technology to develop a soil sampling plan based on varying levels of metal content in the ground. Soil samples were then collected and analyzed for energetic compounds. Statistical techniques found that a possible relationship (correlation) between analytic signal and the energetics measured in the soil may exist.

**DISCLAIMER:** The contents of this report are not to be used for advertising, publication, or promotional purposes. Citation of trade names does not constitute an official endorsement or approval of the use of such commercial products. All product names and trademarks cited are the property of their respective owners. The findings of this report are not to be construed as an official Department of the Army position unless so designated by other authorized documents.

**DESTROY THIS REPORT WHEN NO LONGER NEEDED. DO NOT RETURN IT TO THE ORIGINATOR.**

# Contents

<b>Figures and Tables</b> .....	<b>v</b>
<b>Preface</b> .....	<b>viii</b>
<b>Unit Conversion Factors</b> .....	<b>ix</b>
<b>1 Introduction</b> .....	<b>1</b>
Background .....	1
Purpose.....	1
Project site description .....	3
<b>2 Airborne Geophysical Survey, Fort Ord, California</b> .....	<b>6</b>
Purpose.....	6
Airborne magnetometer and EM system description .....	8
<i>Airborne magnetometer system</i> .....	8
<i>Airborne EM system</i> .....	9
<i>Site-specific effects on boom-mounted helicopter systems</i> .....	11
Survey parameters and procedures.....	12
<i>Instrumentation</i> .....	13
<i>Survey areas</i> .....	13
<i>Magnetic data acquisition</i> .....	14
<i>EM data acquisition</i> .....	14
<i>Positioning</i> .....	15
Magnetic data processing.....	17
<i>Quality control</i> .....	17
<i>Time lag correction</i> .....	17
<i>Sensor dropouts</i> .....	18
<i>Aircraft compensation</i> .....	18
<i>Rotor noise</i> .....	18
<i>Heading corrections</i> .....	18
<i>Array balancing</i> .....	19
<i>Magnetic diurnal variations</i> .....	19
<i>Total magnetic field</i> .....	19
<i>Vertical magnetic gradient</i> .....	20
<i>Analytic signal</i> .....	21
<i>Altitude calculations</i> .....	22
<i>Altitude implications for magnetic fields</i> .....	23
<i>Anomaly density</i> .....	24
Electromagnetic data processing.....	25
<i>Quality control</i> .....	25
<i>Rotor and blade noise</i> .....	26
<i>EM response leveling</i> .....	26
Ordnance and resistivity calibration sites.....	26
<i>Magnetic data: Ordnance calibration site</i> .....	27

<i>EM data: Resistivity calibration site and ordnance calibration site</i> .....	36
Magnetic products and interpretation .....	39
<i>Total magnetic field</i> .....	39
<i>Vertical gradient</i> .....	40
<i>Analytic signal</i> .....	44
<i>Interpretation map</i> .....	45
<i>Anomaly density</i> .....	48
<i>MRS-16 site</i> .....	50
<i>Data and image archive</i> .....	51
EM products and interpretation .....	55
<i>Time-domain EM response</i> .....	55
<i>Interpretation of EM data</i> .....	57
<i>EM data and image archive</i> .....	59
Conclusions .....	62
<b>3 Soil Sampling and Analysis, Fort Ord, CA .....</b>	<b>65</b>
Soil sampling .....	65
Soil sample processing.....	65
Extract analysis .....	66
QA/QC .....	67
Results .....	72
<b>4 Statistical Analyses.....</b>	<b>76</b>
Scatterplots .....	79
Parametric analyses.....	79
Nonparametric analyses.....	82
Logistic analyses .....	83
<b>5 Conclusions.....</b>	<b>87</b>
<b>References.....</b>	<b>89</b>
<b>Appendix A: Airborne Geophysical Survey Daily Quality Control (QC) Results, Fort Ord, CA .....</b>	<b>91</b>
<b>Appendix B: Airborne Geophysical Survey Electromagnetic Data, Fort Ord, CA.....</b>	<b>100</b>
<b>Appendix C: Development of Soil Sampling Plan, Fort Ord, CA.....</b>	<b>116</b>
<b>Appendix D: SAS Program (All Observations Included) .....</b>	<b>134</b>
<b>Appendix E: SAS Program (Large Outlier Deleted).....</b>	<b>136</b>
<b>Appendix F: SAS Output (All Observations Included).....</b>	<b>138</b>
<b>Appendix G: SAS Output (Large Outlier Deleted) .....</b>	<b>164</b>
<b>Report Documentation Page</b>	

# Figures and Tables

## Figures

Figure 1. A portion of the Fort Ord impact area.....	2
Figure 2. Fort Ord survey areas.....	7
Figure 3. ORAGS-Arrowhead system in operation at Fort Ord.....	8
Figure 4. General system layout for ORAGS-Arrowhead.....	9
Figure 5. ORAGS-Arrowhead console as installed in the Bell 206 Long Ranger helicopter.....	10
Figure 6. ORAGS-TEM airborne EM induction system similar to that used at Fort Ord.....	10
Figure 7. ORAGS-TEM system in flight.....	11
Figure 8. Sample altitude profiles for heights above sea level and above ground level.....	16
Figure 9. Histogram and related statistics of altimeter data for all sensors after correction for orientation and topography.....	23
Figure 10. Illustration of falloff in magnetic anomaly amplitude with increased sensor height above a ferrous target.....	24
Figure 11. Altitude for nominal 2-m survey at the ordnance calibration site.....	29
Figure 12. Altitude for nominal 4-m survey at the ordnance calibration site.....	30
Figure 13. Altitude for nominal 5.5-m survey at the ordnance calibration site.....	31
Figure 14. Analytic signal for nominal 2-m survey at the ordnance calibration site.....	32
Figure 15. Analytic signal for nominal 4-m survey at the ordnance calibration site.....	33
Figure 16. Analytic signal for nominal 5.5-m survey at the ordnance calibration site.....	34
Figure 17. Sensor altitude plot over Ranges 43 and 48 with analytic signal anomaly peaks.....	35
Figure 18. EM response (mV) for time bin 1 at the resistivity calibration site.....	37
Figure 19. EM response (mV) for time bin 2 at the ordnance calibration site.....	38
Figure 20. Thumbnail of total magnetic field map of the survey area at Fort Ord.....	40
Figure 21. Thumbnail of sensor altitude above ground level map of the survey at Fort Ord.....	41
Figure 22. Thumbnail of vertical magnetic gradient map of the survey area at Fort Ord for altitudes <5 m.....	42
Figure 23. Thumbnail of vertical magnetic gradient map of the survey area at Fort Ord for altitudes <4 m.....	43
Figure 24. Thumbnail of analytic signal map of the survey area at Fort Ord for altitudes <5 m.....	44
Figure 25. Thumbnail of analytic signal map of the survey area at Fort Ord for altitudes <4 m.....	45
Figure 26. Thumbnail of interpretation map for the survey area at Fort Ord.....	46
Figure 27. Histogram of analytic signal map showing background noise peak at 0.2 nT/m.....	47

Figure 28. Thumbnail of anomaly density map of the survey area at Fort Ord.....	50
Figure 29. Histogram of altitude data at the MRS-16 site. ....	51
Figure 30. Thumbnail of analytic signal map of the MRS-16 area at Fort Ord. ....	52
Figure 31. Thumbnail of interpretation map of the MRS-16 area at Fort Ord.....	53
Figure 32. Typical EM response over a metallic conductor. ....	56
Figure 33. Insensitivity of Fort Ord soils to ORAGS-TEM. ....	56
Figure 34. EM response of EM Block A, 230 $\mu$ s after transmitter turnoff.....	57
Figure 35. Analytic signal of total magnetic field measured over EM Block A. ....	59
Figure 36. EM response of EM Block B, 230 $\mu$ s after transmitter turnoff. ....	60
Figure 37. Analytic signal of total magnetic field measured over EM Block B.....	61
Figure 38. Mean analytic signal at each sampling site at Fort Ord versus the total energetic content. ....	79
Figure 39. Mean analytic signal at each sampling site at Fort Ord versus the total energetic content without the high value outlier. ....	80
Figure 40. Plot of mean analytic signal versus probability of detection of energetics. ....	85
Figure A1. Magnetic QC lines from January 29/05. ....	92
Figure A2. Magnetic QC lines from January 30/05. ....	93
Figure A3. Magnetic QC lines from January 31/05. ....	94
Figure A4. Magnetic QC lines from February 01/05.....	95
Figure A5. Magnetic QC lines from February 02/05. ....	96
Figure A6. Magnetic QC lines from February 03/05. ....	97
Figure A7. Magnetic QC lines from February 04/05.....	98
Figure A8. Magnetic QC lines from February 08/05. ....	99
Figure B1. EM response (mV), time bin 1-93 microseconds after turnoff, EM Block A. ....	100
Figure B2. EM response (mV), time bin 2-230 microseconds after turnoff, EM Block A.....	101
Figure B3. EM response (mV), time bin 3-510 microseconds after turnoff, EM Block A. ....	102
Figure B4. EM response (mV), time bin 4 - 1065 microseconds after turnoff, EM Block A. ....	103
Figure B5. EM response (mV), time bin 5-1805 microseconds after turnoff, EM Block A. ....	104
Figure B6. EM response (mV), time bin 6-2270 microseconds after turnoff, EM Block A. ....	105
Figure B7. EM sensor altitude, EM Block A.....	106
Figure B8. Analytic signal computed from total magnetic field data, EM Block A. ....	107
Figure B9. EM response (mV), time bin 1-93 microseconds after turnoff, EM Block B.....	108
Figure B10. EM response (mV), time bin 2-230 microseconds after turnoff, EM Block B. ....	109
Figure B11. EM response (mV), time bin 3-510 microseconds after turnoff, EM Block B.....	110
Figure B12. EM response (mV), time bin 4-1065 microseconds after turnoff, EM Block B.....	111
Figure B13. EM response (mV), time bin 5-1805 microseconds after turnoff, EM Block B.....	112
Figure B14. EM response (mV), time bin 6-2270 microseconds after turnoff, EM Block B.....	113
Figure B15. EM sensor altitude, EM Block B.....	114

Figure B16. Analytic signal computed from total magnetic field, EM Block B.....	115
Figure C1. Raw magnetometer data. (Distance from side to side is approximately 55 m).....	117
Figure C2. 5-m resolution mesh of polygons generated using Hawth's Analysis Tools.....	119
Figure C3. Six classes generated using Jenck's Optimization techniques. ....	121
Figure C4. 5-m grids that fell totally within the flight lines.....	126
Figure C5. Mean analytic signal value in each 5-m potential sampling area broken into six classes.....	129
Figure C6. Soil sampling sites selected from airborne magnetometer data, Fort Ord, CA.....	133

## Tables

Table 1. Time bins for ORAGS TEM system.....	55
Table 2. Results from analysis of blank samples and blank spiked sample conducted with soil samples from Fort Ord, May 9-10, 2005. ....	68
Table 3. Results from analysis of replicate laboratory subsamples.....	68
Table 4. Results from analysis of replicate multi-increment samples from Fort Ord.....	70
Table 5. Analytical results for grid samples from Fort Ord, May 2005.....	72
Table 6. Listing of data used in statistical analyses.....	76
Table 7. Results of linear model (independent variable mean analytic signal).....	81
Table 8. Results of exponential model (independent variable mean analytic signal) .....	81
Table 9. Normality test results. ....	82
Table 10. Summary statistics by GRIDCODE.....	82
Table 11. Median test (number of points above median).....	82
Table 12. Logistic regression analysis parameter estimates.....	84
Table 13. Logistic regression. Observed versus Predicted.....	84

## Preface

This report was prepared as part of the Environmental Quality Technology Program, Site Characterization Issues and Analytical Tools and Procedures thrust area, Work Unit “Range and Landscape Level Characterization Methodology.” Research was conducted by the Environmental Laboratory (EL), U.S. Army Engineer Research and Development Center (ERDC), Vicksburg, MS, the Cold Regions Research and Engineering Laboratory, ERDC, Hanover, NH, EnviroStat, Inc., Fort Collins, CO, and Battelle, Oak Ridge, TN. Drs. Dale Magoun, Department of Mathematics and Physics, University of Louisiana, Monroe, LA, and Jay Geagan, Department of Experimental Statistics, Louisiana State University, Baton Rouge, LA, provided statistical analysis expertise for the project.

David Eisen, Fort Ord Base Realignment and Closure Office, assisted the remote sensing and soil sampling teams in gaining access to the impact areas, assisted with media events to educate the public prior to the remote sensing missions, and provided explosive ordnance disposal personnel to accompany the soil sampling team onto the impact area.

This project was performed under the general supervision of Dr. David Tazik, Chief, Ecosystems Evaluation and Engineering Division, EL. Reviews were provided by Dr. John Ballard, Jerrell R. Ballard, and Clifford Morgan, EL, and Dr. Dwain Butler, Alion Science and Technology Corporation. Dr. Beth Fleming was Director, EL.

COL Richard B. Jenkins was Commander and Executive Director of ERDC. Dr. James R. Houston was Director.

## Unit Conversion Factors

Multiply	By	To Obtain
acres	4,046.873	square meters
miles (U.S. statute)	1,609.347	meters

# 1 Introduction

## Background

The characterization of impact area munitions constituents has typically employed traditional soil sampling approaches, usually variation of stratified random techniques. These sampling approaches do not accurately account for the distribution of such contaminants over the landscape due to the distributed nature of explosive compound sources throughout impact areas, the highly localized distribution of contaminants surrounding these sources, and inaccurate records of historical target locations.

A great deal of research has been conducted by the U.S. Army Corps of Engineers related to sampling on impact areas around known targets or around low-order explosions that are visibly apparent on the surface (Jenkins et al. 1997, Jenkins et al. 2004a, 2004b, Hewitt et al. 2005). These studies have greatly increased the knowledge of how explosive residues may be distributed; however, they do not address large-scale characterization of those explosive contaminants over an entire landscape. In addition, on many impact areas, firing records are scarce and incomplete, and locations of previous target sites may be difficult to discern, particularly in highly vegetated areas.

To help predict the distribution of energetic compounds over large areas, and to locate former target sites that may represent sources of energetic compounds, there must be some related phenomenon that can be readily detected and measured that is associated with the distribution of these compounds.

Impact craters, a detectable surface expression of impact activity on firing ranges, have been found in previous studies to be of limited assistance in locating energetic compounds in soils (Jenkins et al. 2005). These features also may be short-lived, as they are subject to weathering and erosion. However, surface and near-surface metal in soil is a stable property of areas related to impacts that is relatively easy to map.

## Purpose

The purpose of this research was to utilize remote sensing and geographic information system (GIS) technologies to assist in the development of

enhanced sampling strategies to better predict the landscape-scale distribution of energetic compounds and, if possible, to develop a predictive model defining contaminant source terms. Remotely sensed magnetometer and electromagnetic (EM) data were used to thoroughly characterize metal content over a large impact area at Fort Ord, CA (Figure 1).



Figure 1. A portion of the Fort Ord impact area.

The project involved the application of the state-of-the-art Oak Ridge Airborne Geophysical System (ORAGS) airborne magnetometer and time-domain EM systems developed by Oak Ridge National Laboratory (ORNL) and deployed by Battelle of Oak Ridge, TN. The magnetometer data were analyzed using GIS technology to develop a soil sampling plan based on varying levels of metal content in the ground. Soil samples were then collected using this plan and analyzed for energetic compounds. Statistical techniques were then used to determine if a relationship existed between metal content and the distribution and amount of energetic compounds in the soil.

Products of this research include new techniques for characterizing impact areas, including new techniques for data fusion, integrated statistical analyses, and information extraction, and for developing sampling strategies that better define contaminant source terms.

## Project site description

Information in this section was taken from the Fort Ord Cleanup Web site maintained by MACTEC Engineering and Consulting, Inc.:

<http://www.fortordcleanup.com/foprimer/>

Fort Ord is near Monterey Bay in Monterey County, California, approximately 80 miles south of San Francisco. The base consists of approximately 28,000 acres near the cities of Seaside, Sand City, Monterey, Del Rey Oaks, and Marina. Laguna Seca Recreation Area and Toro Regional Park border Fort Ord to the south and southeast, respectively. Land use east of Fort Ord is primarily agricultural.

In 1917, the U.S. Army bought the present day East Garrison and nearby lands on the east side of Fort Ord to use as a maneuver and training ground for field artillery and cavalry troops stationed at the Presidio of Monterey. Before the Army's use of the property, the area was agricultural, as is much of the surrounding land today. No permanent improvements were made until the late 1930s, when administrative buildings, barracks, mess halls, tent pads, and a sewage treatment plant were constructed. From 1947 to 1975, Fort Ord was a basic training center. After 1975, the 7th Infantry Division occupied Fort Ord. Light infantry troops operated without heavy tanks, armor, and artillery. Fort Ord was selected in 1991 for decommissioning, but troop reassignment was not completed until 1994 when the post formally closed. Although Army personnel still operate parts of the base, no active Army division is stationed at Fort Ord.

The climate is characterized by warm, dry summers and cool, rainy winters. The Pacific Ocean is the principal influence on the climate at Fort Ord. Daily ambient air temperatures typically range from 5 to 20 °C, but temperatures in the low 40 °C range have occurred. Fog is common in the morning throughout the year. Winds are generally from the west. The average annual rainfall of 35 cm occurs almost entirely between November and April. Because the predominant soil is permeable sand, runoff is limited and streamflow only occurs intermittently within the very steep canyons in the eastern portion of Fort Ord.

Fort Ord is located on California's central coast, a biologically diverse and unique region. The range and combination of climactic, topographic, and soil conditions at Fort Ord support many biological communities. Various plant communities identified at the Fort Ord sites include coast live oak woodland, central maritime chaparral, central coastal scrub, vegetatively

stabilized dune, northern foredune grassland, landscaped, valley needle-grass grassland, seasonally wet grassland, vernal pool, upland ruderal, and wet ruderal. Central maritime chaparral is the most extensive natural community at Fort Ord, occupying approximately 5060 ha in the southcentral portion of the base. Oak woodlands are widespread at Fort Ord and occupy the next largest area, about 2020 ha. Grasslands, primarily in the southeastern and northern portions of the base, occupy approximately 1800 ha.

Elevations at Fort Ord range from approximately 275 m above mean sea level near Impossible Ridge, on the east side of the base, to sea level at the beach. The predominant topography of the area reflects morphology typical of the dune sand deposits that underlie the western and northern portions of the base. In these areas, the ground surface slopes gently west and northwest, draining toward Monterey Bay. The topography in the southeastern third of the base is notably different from the rest of the base. This area has relatively well-defined, eastward-flowing drainage channels within narrow, moderately to steeply sloping canyons. Runoff is into the Salinas Valley.

Fort Ord is within the Coast Ranges Geomorphic Province. The region consists of northwest-trending mountain ranges, broad basins, and elongated valleys generally paralleling the major geologic structures. In the Coast Ranges, older, consolidated rocks are characteristically exposed in the mountains but are buried beneath younger, unconsolidated alluvial fan and fluvial sediments in the valleys and lowlands.

The geology of Fort Ord generally reflects older, consolidated rock that is exposed at the surface near the southern base boundary and becomes buried under a northward-thickening sequence of poorly consolidated deposits to the north. Fort Ord and the adjacent areas are underlain, from depth to ground surface, by one or more of the following older, consolidated units:

- Mesozoic granite and metamorphic rocks
- Miocene marine sedimentary rocks of the Monterey Formation
- Upper Miocene to lower Pliocene marine sandstone of the Santa Margarita Formation (and possibly the Pancho Rico and/or Purisima Formations). Locally, these units are overlain and obscured by geologically younger sediments, including:
  - Plio-Pleistocene alluvial fan, lake, and fluvial deposits of the Paso Robles Formation

- Pleistocene eolian and fluvial sands of the Aromas Sand
- Pleistocene to Holocene valley fill deposits consisting of poorly consolidated gravel, sand, silt, and clay

A system of sand dunes lies between Highway 1 and the shoreline. The western edge of the dunes has an abrupt drop of 10 to 20 m, and the dunes reach an elevation of 43 m above mean sea level on the gentler, eastern slopes. The dunes provide a buffer zone that isolates the Beach Trainfire Ranges from the shoreline to the west. In some areas, spent ammunition has accumulated on the dune slopes as the result of years of range operation. Numerous former target ranges, ammunition storage facilities, and two inactive sewage treatment facilities lie east of the dunes.

Undeveloped land in the inland portions of Fort Ord includes infantry training areas and open areas used for livestock grazing and recreational activities such as hunting, fishing, and camping. A large portion of this undeveloped land is occupied by the Impact Area (formerly called the Multi-Range Area). This area was used for advanced military training operations.

An area known as the Impact Area is located in the southcentral portion of Fort Ord and is designated a Munitions Response (MR) site. Lands within the boundaries of the Impact Area are expected to have the highest density of Munitions and Explosives of Concern (MEC) with specific target areas having the highest densities. Types of MEC found at Fort Ord include artillery projectiles, rockets, hand grenades, land mines, pyrotechnics, bombs, demolition materials, and other items. Known MR sites are posted with warning signs and are off-limits to unauthorized people.

## **2 Airborne Geophysical Survey, Fort Ord, California**

### **Purpose**

The purpose of the airborne geophysical survey was to acquire, process, and analyze geophysical data for detecting and delineating areas of high densities of anomalies. The anomalies were considered to be related to targets and/or ranges likely to be highly contaminated with surface and subsurface ordnance and explosive items and artifacts. The survey was carried out jointly by Battelle and ORNL at Fort Ord within the area illustrated in Figure 2. The data acquired during this survey also assisted the Fort Ord Base Realignment and Closure (BRAC) Office and their contractors in a variety of characterization, screening-level, and removal activities associated with determination of the extent of potential unexploded ordnance (UXO) related contamination at the site.

The survey area was selected using LiDAR data and other imagery, aerial photography, and base map data. Within the defined survey area, the survey data collected consisted of a 1281-ha magnetic survey using the transect survey method on alternating lines (providing an effective coverage of 2562 ha when interpolating between transects). A 72-ha electromagnetic survey is located within the main Impact Area and was surveyed at full coverage (high-density). In addition, a supplemental 41-ha site, known as the MRS-16 area, was flown with the magnetic system at full coverage at the request of the Fort Ord BRAC Office. A well-established and well-documented geophysical prove-out site containing inert ordnance items was used as calibration for this survey.

The ORAGS magnetometer and EM systems have been previously deployed at Sierra Army Depot in California, the Badlands Bombing Range in South Dakota, Fort Detrick in Maryland, Nomans Land Island in Massachusetts, New Boston Air Force Station in New Hampshire, Camp Wellfleet in Massachusetts, and Shumaker Naval Ammunition Depot in Arkansas.

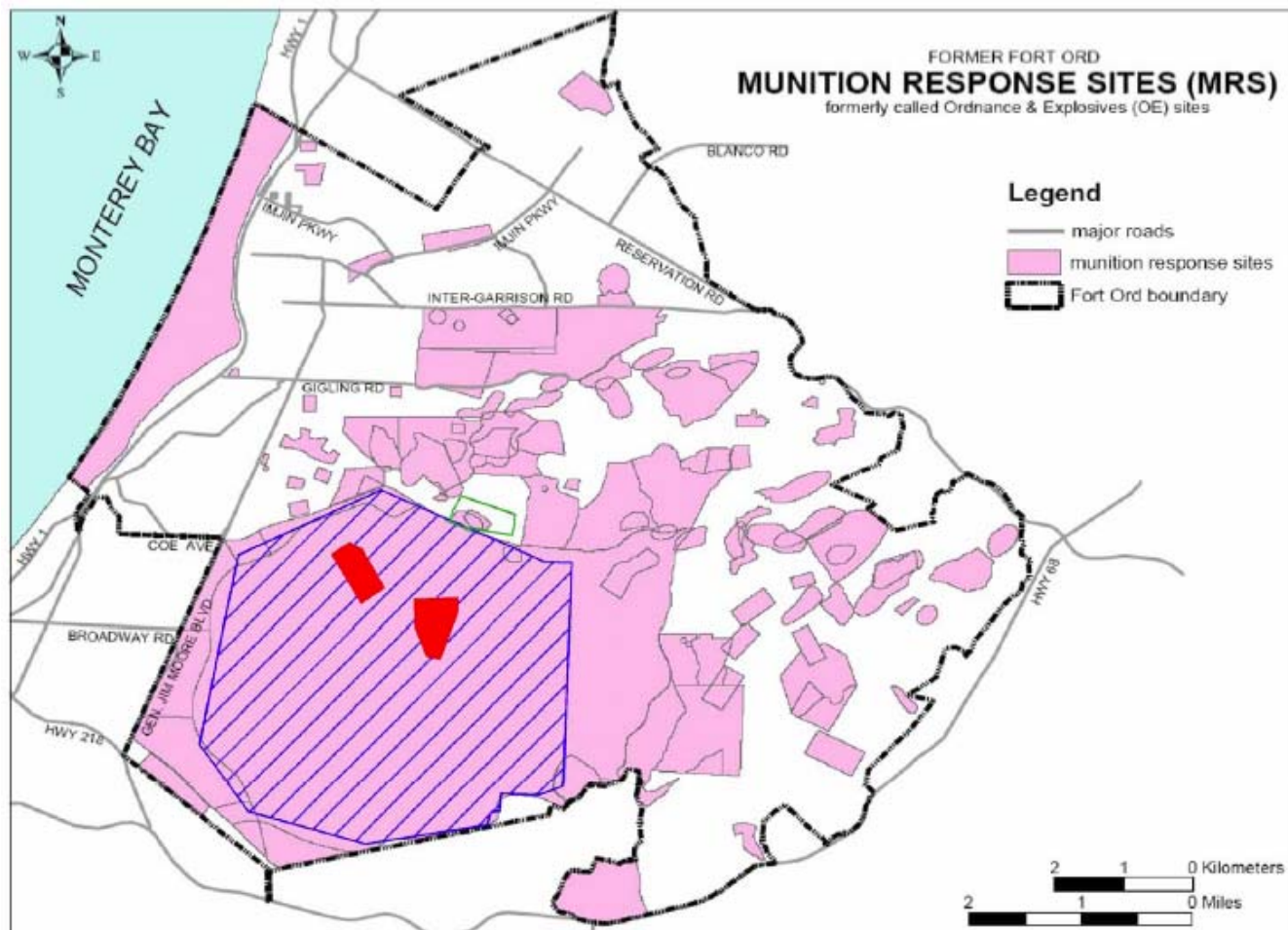


Figure 2. Fort Ord survey areas. Magnetometer survey is indicated by the blue hatched region, and the EM survey is indicated by the red blocks. The RS-16 survey area is outlined in green.

It is important to recognize that the airborne data are NOT suitable for declaring an area free of contamination because some ordnance types at Fort Ord fall below the detection threshold of the system, and only a percentage of other ordnance types will be detected. Furthermore, the transect method employed at Fort Ord reduces the 2562 ha of effective coverage to 50 percent actually surveyed in detail. Rough topography and tall vegetation increased flight height and reduced the coverage to 42 percent that has any potential for detecting large single pieces of ordnance. *Clusters of ordnance, however, represent a legitimate target for this technology and methodology* over the entire 2562 ha, allowing for interpolation between lines and across gaps caused by increased flight height. Thus, the goal of the project to identify locations of high anomaly densities that may be indicative of potential former target locations and/or ranges that are likely to be highly contaminated with UXO has been successfully met.

## Airborne magnetometer and EM system description

### Airborne magnetometer system

ORNL developed the airborne magnetometer system (Figure 3) that was used for data acquisition at Fort Ord. This system, known as the ORAGS-Arrowhead, is now operated by Battelle. It provides a substantial increase in detection capability compared to previous airborne systems (Aerodat HM-3 and ORNL Hammerhead) because of a new boom architecture designed to position more magnetic sensors at low-noise locations, a significantly higher sampling frequency, and a unique aircraft orientation system.

Four magnetometers at 1.7-m line spacing are located in the forward V-shaped boom (Figure 4), and two magnetometers are located in each of the lateral booms (eight total magnetometers). The Arrowhead system is mounted on a Bell 206 Long Ranger helicopter and flown as low to the earth's surface as safety permits (average 3.5 m at Fort Ord) in preprogrammed traverses over the survey areas. Survey speeds were approximately 20 m/s. Flight lines were spaced 25 m apart (providing nominal 50 percent coverage with a 12-m swath of sensors spaced 1.7 m apart) with data recorded at 120 Hz. Base station magnetic readings were recorded in order to monitor diurnal magnetic activity. This diurnal magnetic activity is removed from the data as part of the data processing. Airborne magnetic data are acquired during daylight hours only.



Figure 3. ORAGS-Arrowhead system in operation at Fort Ord.

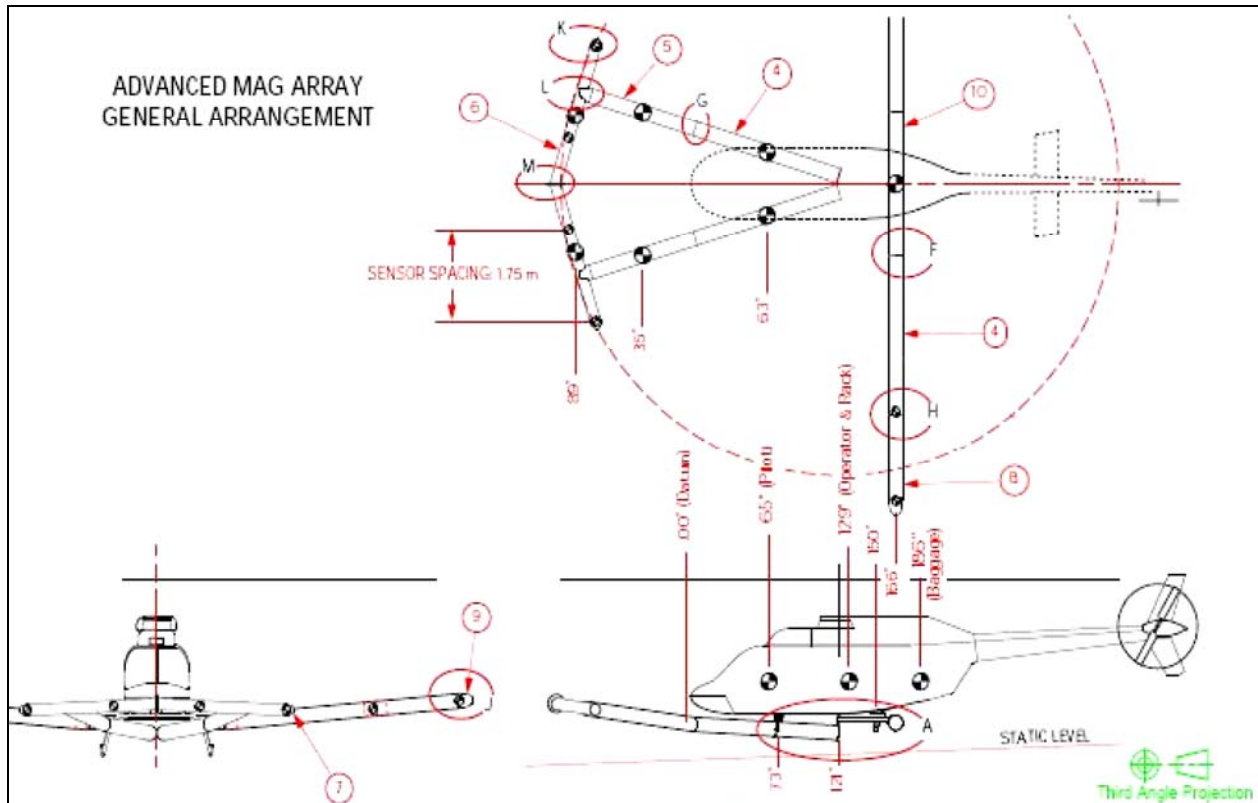


Figure 4. General system layout for ORAGS-Arrowhead.

The orientation system is based on four global positioning system (GPS) antennas. A fluxgate magnetometer is mounted in the forward assembly to compensate for the magnetic signature of the aircraft. A laser altimeter is mounted beneath the helicopter, at approximately the same altitude as the sensors to monitor sensor height above the ground. Data are recorded digitally on the ORAGS™ console (Figure 5) inside the helicopter in a binary format. The magnetometers are sampled at a 1200-Hz sample rate and desampled to 120 Hz to allow sufficient bandwidth to eliminate helicopter rotor noise.

### Airborne EM system

In addition to the ORAGS-Arrowhead system, ORNL also has recently completed performance evaluation of the airborne EM system that provided supporting data over a portion of the larger magnetic survey area at Fort Ord. The ORAGS-Time-domain Electromagnetic ORAGS (TEM) system is a boom-mounted EM induction system that mounts on rigid Kevlar and carbon fiber booms attached to the underside of a Bell 206 Long Ranger helicopter (Figure 6). As with the Arrowhead system, the rigid boom architecture enables the helicopter to fly closer to the ground,



Figure 5. ORAGS-Arrowhead console as installed in the Bell 206 Long Ranger helicopter.



Figure 6. ORAGS-TEM airborne EM induction system similar to that used at Fort Ord.

thus increasing system resolution, while also enabling precise control of receiver positions and more accurate determination of UXO locations.

For the Fort Ord survey, the transmitter coil was arranged in a rectangular two-lobed geometric configuration (Figure 7). A current is established in the loop, then rapidly switched off, inducing a secondary magnetic field in the earth, the decay of which is measured in the receiver coils. In this configuration, a transmitter cable is supported by a 12-m x 3-m rectangular, composite frame. The turnoff time for the lobed configuration is approximately 160  $\mu$ s. The receiver system consists of two large single turn loops having dimensions of about 2.7 m x 2.7 m (Figure 7).

### Site-specific effects on boom-mounted helicopter systems

Each survey site presents a unique set of conditions that can affect the performance and results of the boom-mounted helicopter systems. Variations in vegetation height forces changes in survey altitudes, and small individual ordnance items are less detectable as survey height increases. The presence of cultural features such as buildings, aboveground phone and power lines, and fences can also force higher survey altitudes, or totally exclude some areas from being surveyed. Weather conditions, in particular wind patterns, can cause attitudinal variations in helicopter systems, and these variations often will appear as low frequency variations in the EM or magnetic response with respect to targets of interest.



Figure 7. ORAGS-TEM system in flight. The red square shows the large receiver coil position, and the black line represents the rectangular two-lobed transmitter coil layout.

Topographic changes can produce similar low frequency effects as the helicopter's altitude above ground level changes. Variations in the magnetic susceptibility of underlying soil or rock can also produce anomalies. Usually these are low amplitude, long wavelength anomalies that are easily distinguishable from UXO anomalies, but at some sites localized magnetic soils or individual magnetic boulders can produce magnetic anomalies that are virtually indistinguishable from UXO anomalies, both in amplitude and wavelength. With respect to EM systems, long wavelength anomalies may be produced by variations in soil or rock conductivity, but these anomalies typically have very low amplitudes. Geological conditions can only rarely produce EM anomalies that mimic UXO anomalies in both amplitude and wavelength. With the exception of some metallic ore deposits and localized zones of high magnetic susceptibility, geological structures are usually less conductive than metals by several orders of magnitude (Telford et al. 1990). Larger UXO tends to produce narrow, high-amplitude anomalies that decay slowly in comparison to geological anomalies. Conductive, two-dimensional geological structures can produce high amplitudes and slow decay, but in map view, anomalies will appear elongate, unlike those produced by UXO. Compact geological features that may produce anomalies of the same wavelength as UXO also typically will produce much lower anomaly amplitudes because of their low conductivities relative to steel or aluminum. An exception occurs in areas where magnetic boulders or compact pockets of highly magnetically susceptible soils occur. The transient EM responses from these magnetic geological occurrences may be largely indistinguishable from that of smaller UXO anomalies (Billings et al. 2003).

## **Survey parameters and procedures**

The airborne survey was completed during the 20-day period (on-site) between January 29, 2005, and February 17, 2005. Surveying included total field magnetic and time-domain EM measurements. All surveys were flown at as low an altitude as possible, in keeping with topography, vegetation, and safety considerations. The magnetometer array was flown at 25-m line spacing. With a 12-m swath width, the survey of the Impact Area block provided an actual surface coverage of about 50 percent. The EM system, with two receiver coils separated laterally by 10 m center-to-center, was flown with an interleaved line spacing of 5 m to achieve essentially 100 percent surface coverage over two blocks within the area covered by the ORAGS-Arrowhead system.

Aircraft ground speed was maintained at approximately 10 to 15 m/s (20 to 35 mph). The survey aircraft was a Bell 206 Long Ranger helicopter. Operations were based at Monterey Peninsula Airport. The GPS base station was established at a known National Aeronautics and Space Administration monument at location North American Datum 1983 (NAD83) 120° 34' 29.85951" west, 40° 22' 35.23890" north, North American Vertical Datum (NAVD) 88 1263.725 m. The magnetic diurnal base station was established in a magnetically quiet region at the airport.

A comprehensive Operational Emergency Response Plan was developed and issued previously to address issues related to flight operations, safety, and emergency response. This plan was incorporated into an overall Mission Plan developed to manage field survey operations.

The survey crew included Les Beard, David Bell, William Doll, Jeff Gamey, and Jacob Sheehan from ORNL and Battelle, and Jeff Fullerton, Marcus Watson, and Derrick Wilkinson from National Helicopters Inc., Toronto, Canada.

### **Instrumentation**

Both the ORAGS-Arrowhead airborne magnetic system and the ORAGS-TEM airborne EM system were deployed at Fort Ord. A real-time differential GPS was used for navigation based on OmniStar satellite differential corrections. This provided the pilot with navigation information with a dynamic accuracy of 1 m. Differential corrections for data positioning were enabled by using a Novatel DL4 differential global positioning system (DGPS) base station for post-processing. A laser altimeter was used to monitor terrain clearance in-flight. The laser altimeter provided accuracy to 5 cm over the normal operational range. Ground-based magnetometer and GPS base stations were operated at the base of operations (Monterey Peninsula Airport) for positioning and magnetometer diurnal calibration purposes. A Gem Instruments GSM-19 magnetometer, recording background magnetic field at 3-s intervals, was used as the magnetic base station.

### **Survey areas**

The acquisition area for this project totaled 2603 ha, including the geophysical prove-out area. Survey boundary coordinates for the magnetic survey area were provided by BRAC personnel, as illustrated in Figure 2. Survey boundaries for the EM survey were provided by U.S. Army

Engineer Research and Development Center (ERDC) personnel. The main magnetic survey area of 2562 ha was flown in a “transect” mode (every other line, or 50 percent density), at the lowest achievable altitude (that is both safe and attainable) based on the targets of interest (size, depth) and terrain (safety). The 41-ha MRS-16 area was flown at full coverage at the request of the BRAC Office. In addition, the survey conducted over the geophysical prove-out area (located within the main magnetic survey area) included a variety of altitudes ranging from 2 m to 5.5 m in order to develop quantitative measures of sensor performance for the targets of interest (i.e., to address a *secondary* objective of assessing the potential of airborne surveys for individual ordnance item detection). The 72-ha EM survey area is located within the main area and was flown at full density.

### **Magnetic data acquisition**

The ORAGS-Arrowhead data were desampled in the signal processing stage to a 120-Hz recording rate. All other raw data were interpolated to a 120-Hz rate. This results in a down-line sample density of approximately 15 cm at typical survey speeds. Data were converted to an American Standard Code for Information Interchange (ASCII) format and imported into a Geosoft format database for processing. With the exception of the DGPS post-processing and the calculation of compensation coefficients, all data processing was conducted using the Geosoft software suite.

### **EM data acquisition**

EM data were acquired using the ORAGS-TEM system with the transmitter in dual lobed mode, as shown in Figure 7, and two single turn 2.7-m × 2.7-m receiver loops affixed to the underside of the boom assembly and coincident with the two transmitter loops. The choice of large single loop receivers over smaller receivers was based on the superior performance of the large loop receivers in field trials at Badland Bombing Range for 2- to 3-m survey heights (Beard et al. 2004). The centers of the receiver coils were 10 m apart. Lines were flown with nominal 5-m line spacing to achieve effective 100 percent coverage. High sample rates are required to measure the EM decay signal. One decay signal is stored for each transmitted pulse. The rate at which pulses are transmitted is known as the base frequency. The transient EM decays were acquired at a rate of 10,800 samples per second with a transmitter base frequency of 90 Hz. The decays were separated into six response decay bins. Bins 1-6 were arranged as follows: bin 1/sample 1, bin 2/samples 2-3, bin 3/samples 4-7, bin 4/samples 8-15, bin 5/samples 16-23, and bin 6/samples 24-25.

Sample N is the TEM response measured  $92.5 \times N$  microseconds after the end of the transmitter turnoff ramp. Decays were averaged over the bin samples and recorded in the database. The 90-Hz base frequency was chosen, based on data collected at Badlands Bombing Range, to deliver a strong response from ordnance (ORNL 2003). GPS and laser altimeter data were sampled at 30 Hz. All binned transient EM data were down-sampled to 30 Hz, and converted to ASCII format. The ASCII data were imported into a Geosoft database for processing. As with the magnetic data, the differential GPS were post-processed outside Geosoft, but otherwise, all other data were processed using Geosoft.

### **Positioning**

With both the magnetic and EM systems, the pilot was guided during flight by an onboard navigation system that used satellite-fed DGPS positions. This provided sufficient accuracy for data collection (approximately 1 m) but was inadequate for final data positioning. To increase the accuracy of the final data positioning, a base station GPS was established at a monument on Fort Ord (GSFC-7421) at location NAD83  $36^{\circ} 35' 21.71529''$  north  $121^{\circ} 46' 19.67986''$  west NAVD88 284.5 m. Raw data were collected in the aircraft and on the ground for differential corrections. These were applied in post-processing to provide 2-cm accuracy in the antenna positioning (based on the software's quality assurance parameters). The final latitude and longitude data were projected onto an orthogonal grid using the NAD83 Universal Transverse Mercator (UTM) Zone 10N, meters. After processing, data were re-projected onto NAD83 California State Plane Zone 4 in U.S. survey feet for a presentation consistent with the system used by the majority of surveyors at Fort Ord. All map products therefore are presented in units of U.S. survey feet.

The location of the true base station monument was confused by a nearly identical, undocumented monument in a more visible location. This discrepancy was detected during the first quality control (QC) check of the calibration grid and was rectified. The location of the undocumented monument was determined by a Fort Ord civil survey crew and the positioning data for that day were re-processed. Subsequent flights used the true base station monument.

The location of each magnetometer sensor was calculated using the GPS antenna location and the aircraft orientation, as measured by the Ashtech Attitude Determination Unit at a 2-Hz sample rate. This system is comprised of four GPS antennae spread across the boom array and linked to a

single processor that outputs pitch, roll, and azimuth. These data are combined with the physical geometry of the array to calculate the position and relative height of each magnetometer sensor.

Vertical positioning was monitored by laser altimeter with an accuracy of 2 cm. These data showed intermittent reflections from the top of the foliage canopy (Figure 8). They were processed to remove this effect to within 10 cm. Vertical positioning was also monitored by the GPS, which provides sensor height above the ellipsoid (HAE). A digital elevation map (DEM) was compiled using HAE and laser altimeter data, and was subsequently incorporated into the altitude calculations for each sensor. The DEM was compared to existing LiDAR (Light Detection and Ranging) data to confirm the relative accuracy of the processing. The DEM was based on the GPS altitude, which showed inherently less absolute accuracy than the LiDAR but represents a more complete data set with sufficient relative accuracy for measuring slope changes beneath the helicopter swath. Thus, the GPS-based DEM was sufficient for instrument altitude calculations (height above ground level), but should not be used for absolute topographic measurements (height above sea level).

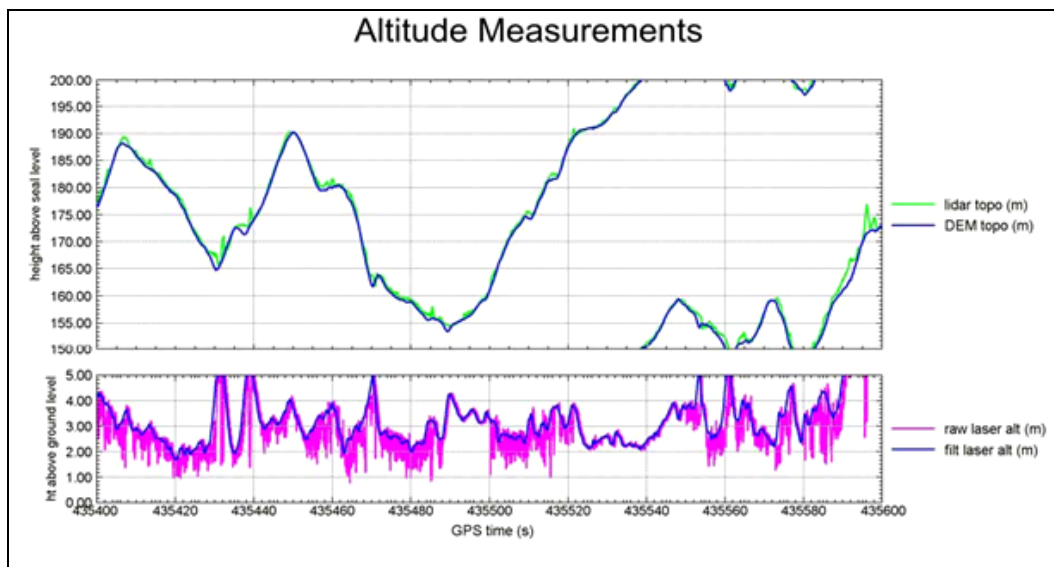


Figure 8. Sample altitude profiles for heights above sea level and above ground level (AGL). (top) LiDAR and GPS-based DEM topographic profiles. (bottom) Raw and processed laser altimeter data showing vegetation penetration.

These calculations reduce the absolute accuracy of the magnetometer sensor locations. The final accuracy of the sensor positions is estimated to be approximately 1 m horizontally based on the calibration grid results, and 15 cm vertically based on the range of the final altimeter data.

## **Magnetic data processing**

The magnetic data were processed in several stages. The stages included correction for time lags, removal of sensor dropouts, compensation for dynamic helicopter effects, removal of diurnal variation, correction for sensor heading error, array balancing, and removal of helicopter rotor noise. The calculation of the vertical magnetic gradient and the magnetic analytic signal (total gradient) was derived from the total field magnetic data. Anomaly density maps were also derived from the analytic signal peaks. For presentation purposes, the vertical gradient and analytic signal data were divided into high and low altitude maps to avoid misinterpretation of the data. The total field data show both high- and low-altitude data, and the anomaly density data are derived only from the low-altitude data.

### **Quality control**

The data were examined in the field to ensure sufficient data quality for final processing. Each of the processing steps listed above was evaluated and tested. The adequacy of the compensation data, heading corrections, time lags, orientation calibration, overall performance and noise levels, and data format compatibility were all confirmed during data processing. During survey operations, flight line locations were plotted to verify full coverage of the area. Missing lines or areas where data were not captured were rejected and reacquired. Data were also examined for high noise levels, data dropouts, unacceptable diurnal activity, or other unacceptable conditions. Lines deemed to be unacceptable were reflown during the acquisition stage. Occasional lines deviated from a straight flight path due to local topography. In instances where the pilot intentionally slid sideways down the hill in order to maintain uniform sensor clearance, the sensor altitude was given priority over uniform coverage unless adjacent swaths actually crossed. In total, four lines were rejected and reflown for coverage and quality issues that were not caught by the pilot and operator while in the field.

### **Time lag correction**

There is a lag between the time the sensor makes a measurement and when it is time-stamped and recorded. This applies to both the magnetometer and the GPS. Accurate positioning requires a correction for this lag. Time lags among the magnetometers, fluxgate, and GPS signals were measured by a proprietary ORAGS utility. This utility sends a single EM

pulse that is visible in the data streams of all three instruments. This lag was corrected in all data streams before processing.

### **Sensor dropouts**

Cesium vapor magnetometers have a preferred orientation to the Earth's magnetic field. As a result of the motion of the aircraft, the sensor dead zones will occasionally align with the Earth's field. In this event, the readings drop out, usually from a local average of over 53,000 nT to 0 nT. This usually occurs only during turns between lines, and rarely during on-line surveying (<1 sec of data loss per day). All dropouts were removed manually during processing.

### **Aircraft compensation**

The presence of the helicopter in close proximity to the sensors causes considerable deviation in the readings, which requires compensation. The orientation of the aircraft with respect to the sensors and the motion of the aircraft through the earth's magnetic field are contributing factors. A calibration flight is flown to record the information necessary to remove these effects. The maneuver consists of flying a box-shaped flight path at high altitude to gain information in each of the cardinal directions. During this procedure, the pitch, roll, and yaw of the aircraft are varied. This provides a complete picture of the effects of the aircraft at all headings in all orientations. The entire maneuver was conducted twice for comparison. The information was used to calculate coefficients for a 19-term polynomial for each sensor. The fluxgate data were used as the baseline reference channel for orientation. A polynomial is applied postflight to the raw data, and the results are referred to as the compensated data.

### **Rotor noise**

The aircraft rotor spins at a constant rate of about 400 rpm. This introduces noise to the magnetic readings at a frequency of approximately 6.6 Hz. Harmonics at multiples of this base are also observable, but have much smaller amplitudes. This frequency is usually higher than the spatial frequency created by near-surface metallic objects and is removed with a frequency filter.

### **Heading corrections**

Cesium vapor magnetometers are susceptible to heading errors. The result is that one sensor will give different readings when rotated about a

stationary point. This error is usually less than 0.2 nT. Heading corrections are applied to adjust readings for this effect.

### **Array balancing**

The sensors also show a lower degree of absolute accuracy than they do relative accuracy. Different sensors in identical situations will measure the same relative change, but they may differ as to whether the change was from 50,000 to 50,001 or from 50,100 to 50,101. After individual sensors are heading-corrected to a uniform background reading, the background readings of each sensor are corrected or balanced to one another across the entire array.

### **Magnetic diurnal variations**

The earth's magnetic field can vary by hundreds of nanoTesla (nT) over the course of a day. This means that measurements made in the air include a drifting background level. A base station sensor was established to monitor and record this variation every 3 sec. The time stamps on the airborne and ground units were synchronized to GPS time. The diurnal activity recorded at the base station was extremely quiet. In general, diurnal variations were less than 5 nT per hour. Processing included defaulting repeated values, linearly interpolating between the remaining points, and applying a 10-sec low-pass filter (equivalent to three points of raw data). The processed data were subtracted directly from the airborne data on a point-by-point basis.

### **Total magnetic field**

After the application of the previously cited geophysical corrections, the end result is the Total Magnetic Field Intensity, or Total Field. These data are interpolated onto a regular grid at 0.5-m intervals (pixel size) using a minimum curvature technique with an extrapolated footprint of 1.5 m (extension beyond the last data point). This forms the basis of the gridded data maps.

The total field data represent the Earth's magnetic field at approximately 3.5 m above the ground surface (average survey height). It responds to all magnetic sources to a depth equivalent to the area of the survey (i.e., several kilometers). Many of these sources are irrelevant to the scope of this project. It is therefore beneficial to remove effects that are caused by features at a much larger scale or greater depth than those of interest. In

particular, the north-south trend in all large area surveys can extend the dynamic range so that smaller anomalies do not span more than one color in the presentation palette. The regional magnetic field can be determined in several ways, and in general consists of anomalies that have much longer wavelengths than the features of interest. The regional response was removed using a one-dimensional minimum curvature method, B-Spline. The map that results from the subtraction of the regional magnetic field from the total magnetic field is called the residual magnetic map.

This residual technique was applied to the data at Fort Ord, but was only presented in the original field maps for QC purposes. The variations in altitude across the area called into question the appropriate cut-off for the residual calculation. Thresholds appropriate for lower altitude data will necessarily exclude the broader anomalies observed at higher altitudes, and broader thresholds begin to introduce low-frequency noise into the residual, deriving from magnetic variations in the soils or from roll of the helicopter. It was therefore determined to calculate and present the vertical gradient and analytic signal from the total field rather than the residual field.

### **Vertical magnetic gradient**

The vertical magnetic gradient is calculated from the total field data using a fast Fourier transform (FFT) function. This process reduces geologic influence and sharpens near-surface features. Typically, geologic blocks are reduced to contact points, and discrete targets are reduced to dipolar responses. Visually, this product is similar to the residual total field, but is less subjective in the selection of processing parameters.

These data were masked based on the gridded altimeter data so that null responses due to high altitude would not be confused with null responses due to lack of near-surface debris. Both high- and low-altitude data are presented in map form, with thumbnails of the low-altitude data provided in the text of this report. A cut-off of 5 m was chosen based on examination of the data, particularly in the ordnance detection and discrimination study (ODDS) test grid (see “Magnetic Data: Ordnance Calibration Site” section in this chapter) and the area of Range 43 and 48. The range area was known to be almost uniformly covered with debris and had a suitably wide range of survey heights from very low to very high. Assuming a uniform distribution, the loss of signal can be correlated to the altitude to determine a suitable cut-off threshold. Within this data set, some discrete

anomalies were still observable at 6 m altitude, but the number and amplitude of anomalies dropped significantly before this point.

The calibration grid was flown at three nominal altitudes (2, 4, and 5.5 m). Although this test grid was not representative of the high density clusters that were the objective of this survey, it was clear that even these collections of discrete objects were still detectable as a group at 5 m altitude. Supplementary maps with a 4-m altitude cut-off were also produced to represent the highest sensitivity sections of the data set.

### **Analytic signal**

The analytic signal is calculated from the gridded total field data as the square root of the sum of the squares of three orthogonal magnetic gradients (Hrvoic and Pozza 2006). It represents the maximum rate of change of the magnetic field in three-dimensional space – a measure of how much the readings would change by moving a small amount in the direction of maximum change.

There are several advantages to using the analytic signal. It is generally easier to interpret than total field or vertical gradient data for small object detection because it has a simple positive response above a zero background. The amplitude of the response depends on the strength of the magnetic anomaly. In comparison, total field and vertical gradient maps typically display a dipolar response to small, compact sources (having both a positive and negative deviation from the background). The actual source location is at a point between the two peaks that is dependent upon the magnetic latitude of the site and the properties of the source itself. Analytic signal is essentially symmetric about the target, is always a positive value, and is less dependent on magnetic latitude. More generally, the analytic signal highlights the corners of source objects, but for small targets at the latitude of this survey, these corners converge into a single peak almost directly over the target.

The dominant noise source in an analytic signal is line-to-line inconsistencies in the gridded data that impact the gradients. These may be caused by heading error, sensor balancing, altitude variation, or uncompensated aircraft effects. The minimum anomaly threshold was set above the analytic signal noise floor at 0.5 nT/m for single peaks. This represents the 2.5:1 signal:noise ratio based on a measured noise floor of 0.2 nT/m.

### **Altitude calculations**

As described above, the laser altimeter data detected reflections from both the ground and the upper canopy of the vegetation. These were processed to remove the effect of the foliage canopy as much as possible to an accuracy of approximately 10 cm. It should be noted, however, that this does not necessarily imply full penetration was achieved at all points. These data were then combined with the GPS HAE data to produce a DEM. The results compared well with the LiDAR data provided by Fort Ord. The GPS HAE measurement has sufficient accuracy to correct the sensor altitudes for local variations in topographic slope beneath the helicopter, but has inherently less absolute accuracy than the LiDAR. The DEM should therefore not be used for detailed topographic studies.

The laser DEM was then scanned into the database at each sensor location (rather than at the laser altimeter position). This provided sensor height above the ground, which included both orientation effects (pitch, roll, azimuth) and topography effects (slope of the ground under the helicopter). The resulting altitude map shows these effects as changes across the array. For example, a progressive altitude change from side-side across a swath indicates that the helicopter flew parallel to the slope. Where the helicopter flew directly up (or down) a slope, the effect shows higher (or lower) altitudes on the lateral sensors. This is the altitude parameter that was used to mask the grids into high and low certainty areas.

The median altitude for the main survey block was 3.5 m. The rough topography and erratic vegetation induced more variation in survey altitude than is ideal. To avoid misleading future analysts, the data were divided into low- and high-altitude (high and low sensitivity) maps. A histogram of the altitude data is presented in Figure 9. An analysis of the analytic signal data from the calibration grid (see “Magnetic Data: Ordnance Calibration Site” section in this chapter) indicated that small, discrete anomalies dropped below the noise threshold between 5 and 6 m altitude. As a result, an altitude threshold of 5 m was chosen as the cut-off. This placed 83 percent of the data in the high-confidence category. Supplementary maps with a 4-m cut-off (66 percent of the data) were produced to show only the highest sensitivity data.

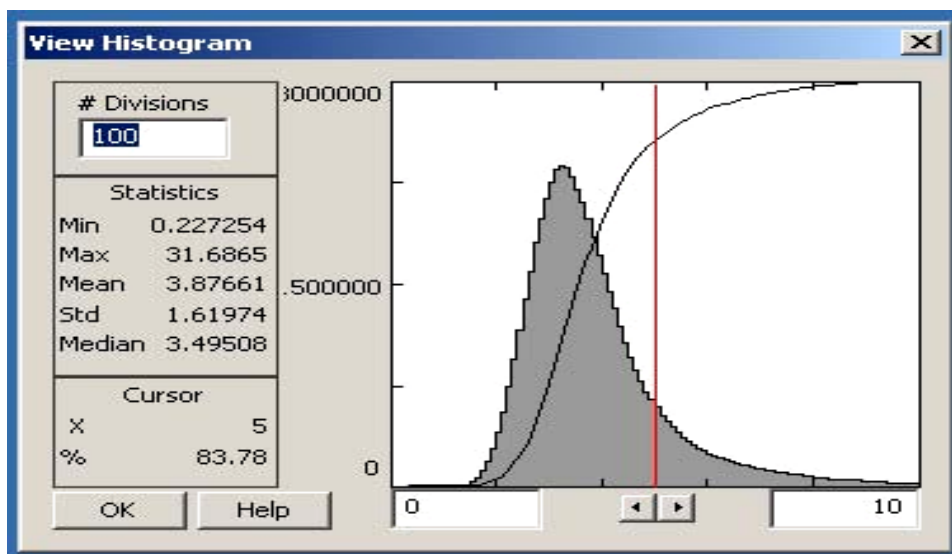


Figure 9. Histogram and related statistics of altimeter data for all sensors after correction for orientation and topography.

### Altitude implications for magnetic fields

The sensitivity of magnetic surveys is dependent upon the distance between the sensors and the object that is to be detected. As an example, Figure 10 shows the change in amplitude of a residual magnetic field anomaly produced by a ferrous object for varying sensor altitudes. The absolute amplitudes shown are scalable to the target in question but are roughly 50x higher than the typical ordnance at Fort Ord. In this model, all of the magnetization is induced by the earth's magnetic field. In most targets, particularly in scrap and metallic debris, additional signal amplitude will be contributed by permanent magnetization effects.

The anomalies are computed for local magnetic inclination and declination. The profiles are along a north-south line and the vertical distances between sensor and target are 2, 4, 8, and 16 m. Similar reductions in amplitude with increasing sensor height also occur in the analytic signal response. More complicated anomaly shapes, often cumulative in amplitude, are caused by target shape effects or overlapping anomalies from multiple natural or man-made sources. Such is the case with closely spaced sources such as those found in the clusters and range targets that are the objective of the Fort Ord survey.

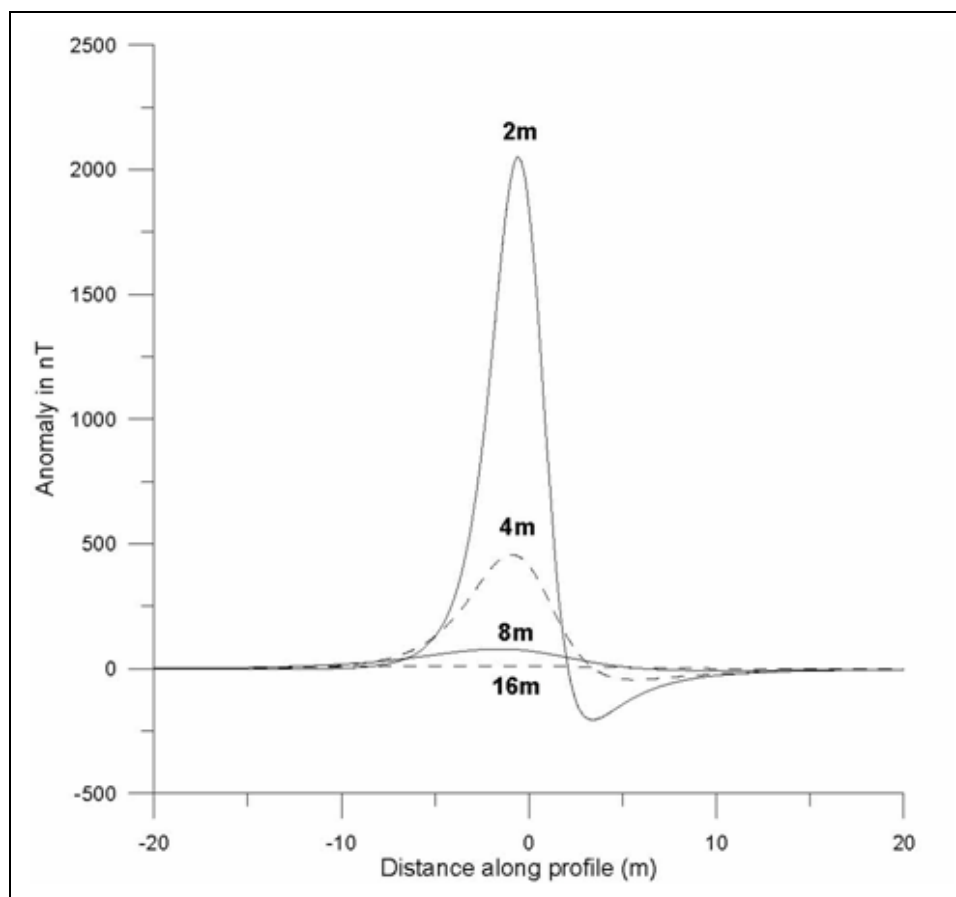


Figure 10. Illustration of falloff in magnetic anomaly amplitude with increased sensor height above a ferrous target.

### Anomaly density

Airborne magnetic anomalies were picked automatically from the gridded analytic signal data using a threshold of 0.5 nT/m. Peak selection was limited to grid points that *exceeded all of their neighbors*. This reduced the number of peaks selected over long, linear features such as pipelines and fences. This selection was further reduced by masking out all those where the sensor altitude was over 5 m. Since the goal of this project was to examine the potential relationship between metallic fragments and other debris, no other discrimination techniques were applied for this survey objective.

Anomaly density was calculated by counting the number of airborne anomalies in each 25-m × 25-m data window and dividing by the percentage of the window covered by magnetic data below 5 m altitude. On average, each survey swath is 12 m wide with 25-m line spacing. For every 25-m window, the average coverage should be about 50 percent. This is increased slightly by the small extrapolation at the edges of each swath,

but is reduced where the survey altitude is above 5 m. If the coverage decreased below 10 percent, no density was calculated. The number of anomalies per window was scaled to units of airborne anomalies per hectare.

The density of airborne anomalies was compared to corresponding ground anomaly densities acquired by Parsons Engineering. This was done by simply dividing the airborne- and ground-based anomaly density grids. The area of comparison was quite small and the ratio of ground-to-airborne densities was irregular and inconclusive, ranging from 2:1 to 9:1. An average of 5:1 would represent a reasonable scaling factor between the two survey modes, but is only accurate to a factor of two. It should be noted that the ground survey will detect much smaller targets regardless of the anomaly density, so that any comparison between the two can never be more than qualitative.

For altitudes at and below the 5-m threshold, the ODDS test grid is sufficiently sensitive to detect the ordnance debris clusters that are the targets of this survey. This too was demonstrated at the ODDS test grid because even with the low density of targets there, they combined for recognizable clusters. Areas with low density counts (below that in the test grid), however, are not necessarily clear of ordnance. The density measurements presented here are only approximations based on magnetic anomalies.

## **Electromagnetic data processing**

The quality assurance/quality control (QA/QC) and time lag stages of EM data processing are similar to those for the magnetic data. However, sensor dropouts are not an issue with active source EM data, nor are compensation, heading, or diurnal corrections necessary. Single loop receivers on the port and starboard side of the helicopter were of identical dimension and mounting, and so the sensors were in this sense balanced.

### **Quality control**

The data were examined in the field to ensure sufficient data quality for final processing. Each of the processing steps listed above was evaluated and tested. The adequacy of time lags, noise levels, and data format compatibility were all confirmed during data processing. During survey operations, flight line locations were plotted to verify full coverage of the area. Missing lines or areas where data were not captured were rejected and reacquired. Data were also examined for high noise levels, or other

unacceptable conditions. Lines deemed to be unacceptable were reflight during the acquisition stage.

### **Rotor and blade noise**

The aircraft rotor spins at a constant rate of approximately 400 rpm and the blades have twice this frequency. This introduces noise to the EM readings at frequencies of approximately 6.6 and 13.2 Hz. Harmonics at multiples of this base are also observable, but are much smaller. These frequencies are usually higher than the spatial frequency created by near-surface metallic objects and is removed with a frequency filter.

### **EM response leveling**

EM leveling involves application of methodologies to correct for drift, or offsets between adjacent flight lines in order to generate a corrected map product that accurately represents resistivity (ohm-m or mS/m) or response to buried metals (mV). The EM (mV) response of the receiver coils can be affected by a number of factors such that the base level of the measurement is nonzero even in an entirely nonconductive environment. To correct for this shift and drift, high-altitude excursions 50 to 100 m AGL were flown after every few survey lines. From the high-altitude background excursions, background curves were constructed for each flight and were removed from the binned EM responses. This method is required for conductivity estimation. However, the maps produced using this method retained small offsets between lines, causing them to have a striped or corrugated appearance, so this method was abandoned and an alternative leveling approach was used in which the background EM field was estimated using multiple B-spline iterations on a given flight, then the background field response was subtracted. This produced better quality maps from a visual perspective for anomaly detection than did the use of high-altitude excursions.

### **Ordnance and resistivity calibration sites**

Two calibration sites were used to support the airborne survey. The primary site was used to assess sensitivity of the magnetic system to ordnance. In addition, a second site was established for ground-truthing the EM system for resistivity calculations. Both sites are described in this section.

**Magnetic data: Ordnance calibration site**

The ordnance calibration grid data are analyzed in two sections. The first is the daily QC flights over a line of three pipes simulating 2.75-in. rockets established by Battelle to verify positioning and system performance. This line was flown in two directions (northbound, southbound) each day. Results are presented in Appendix A.

This procedure successfully identified a problem with the base station GPS location coordinates that was immediately resolved as described in the “Survey Parameters and Procedures, Positioning” section in this chapter. In Figure A1, note that only two targets are visible. This is because the set of double pipes was oriented in such a way that the permanent magnetization of one almost completely cancelled that of the other. Analysis of the data shows that positioning accuracy and repeatability are within 1 m.

The second part of the ordnance calibration grid was the ODDS test grid. Magnetic and EM data were acquired over the geophysical prove-out area to develop and determine “signatures” of ordnance and ordnance-related items, clusters, and groupings that form the objectives of the airborne survey. In addition, these data were used during the interpretation of the airborne data to aid in QC and classification of anomalies of interest for further investigation.

The location and contents of the geophysical prove-out area were provided to ORNL and Battelle staff by Parsons Engineering and the U.S. Army Corps of Engineers. This site is broken into four blocks. Target information was provided for only two of these blocks. The content of the other two blocks remained unknown to the team, but it was understood that the density of targets was considerably higher in these blocks. To our knowledge, a “cluster” of UXO has never been adequately defined. For this survey, a cluster is defined as a collection of ordnance or debris with sufficient spatial density such that their combined magnetic moments meet or exceed the moments of individual targets in the ODDS test grid. Because these emplaced items were meant to be detectable as discrete items with a ground-based system, and because the density of debris on known ranges greatly exceeds this level, this should be viewed as a conservative definition.

This site was flown at three different heights with the magnetometer system in order to estimate the detection capabilities of the system over the typical range of flight altitudes. Altitude and analytic signal maps for

the magnetic data are shown in Figures 11-16. The median height achieved for these three passes was 2.0, 3.9, and 5.5 m. It should be noted that the sensor altitude on each swath is higher on the east side of each swath due to the local topography. Targets larger than 90 mm in diameter are plotted as circles on each map. Targets smaller than 90 mm that registered as a distinct peak in the 2-m analytic signal map are plotted as plus signs. The 2.75-in. pipes are shown as crossed circles.

The analytic signal map at the 2-m flight height indicates that objects larger than 90 mm in diameter can be detected with a high degree of certainty where very low altitudes can be achieved. Several objects smaller than this were also detected, but with low signal-to-noise ratio. Numerous additional objects, and possibly clusters of objects or fragments, were detected in the two “Unknown Blocks.” This altitude was only rarely achieved during the actual survey (1 percent).

At the 4-m altitude most of the discrete targets have dropped below the detection threshold. Only the pipes and the largest of the single targets are clearly visible. The presumed clusters in the “Unknown Blocks” are still clearly above the detection threshold. Data at this altitude and lower represent 61 percent of the total survey block.

The 5.5-m altitude data are above the cut-off threshold used for the main survey block, but the pipes and the largest of the clusters are still visible. Although they were not the focus of this project, it should be mentioned that discrete objects at this altitude cannot be detected unless they are as large as the pipes. Data at this altitude and below represent 88 percent of the total survey block. This evidence supports the decision to use a 5-m altitude cut-off threshold for detection of clusters of ordnance and debris. The MRS-16 site, however, was largely flown at altitudes greater than this. It is unlikely that clusters of this size would be detectable at the 6.4-m median altitude flown over that block.

Further support for the cut-off thresholds was derived from actual survey data over Ranges 43 and 48. Figure 17 shows the sensor altitudes with anomaly peaks shown as black dots. (Note that the color scale in this map has been altered from the main map thumbnailed in Figure 21 to enhance the altitude range of interest.) Target debris was assumed to be relatively uniformly distributed across the area. The irregular black polygon indicates an area where the anomalies show very little correlation with altitude

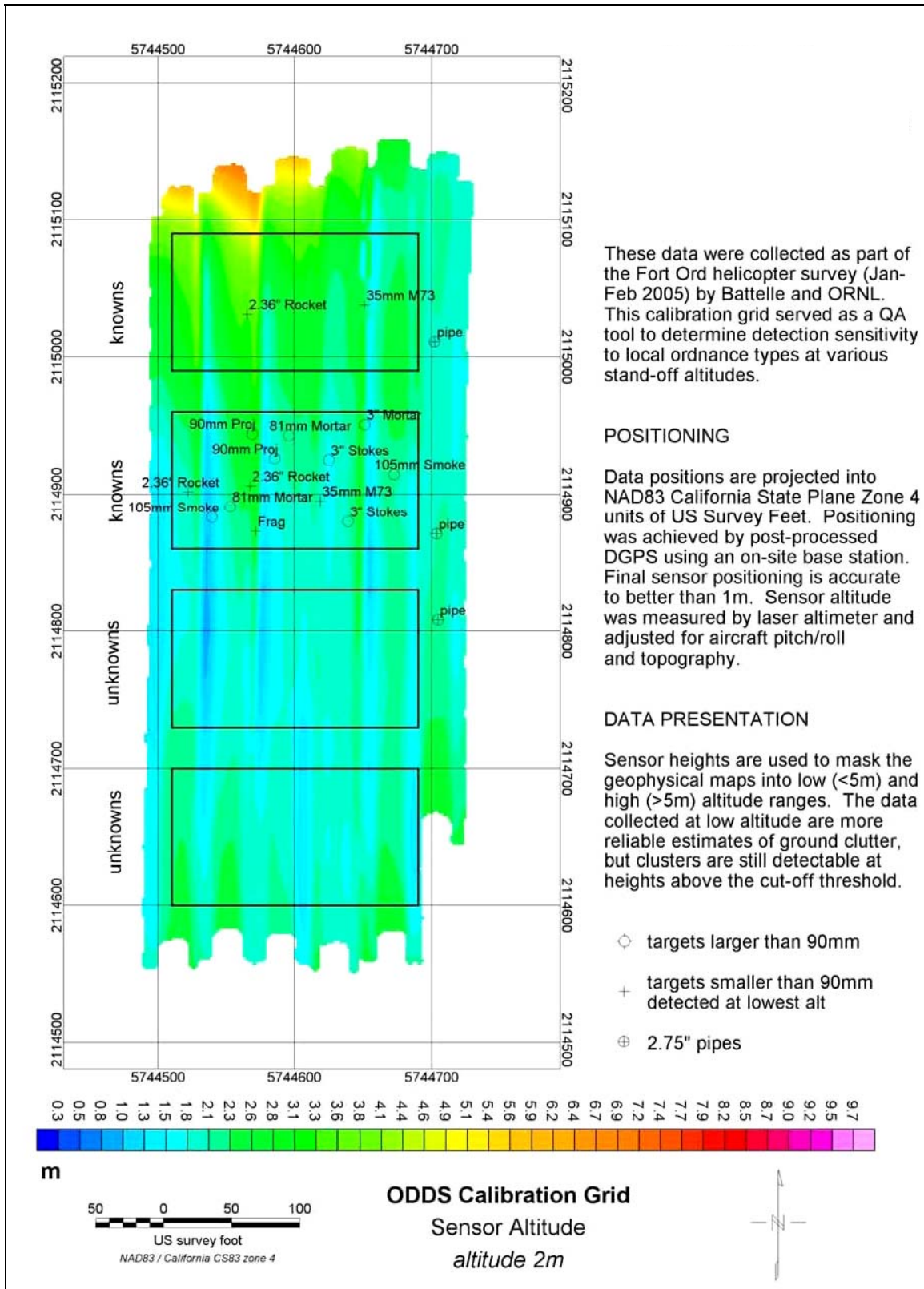


Figure 11. Altitude for nominal 2-m survey at the ordnance calibration site.

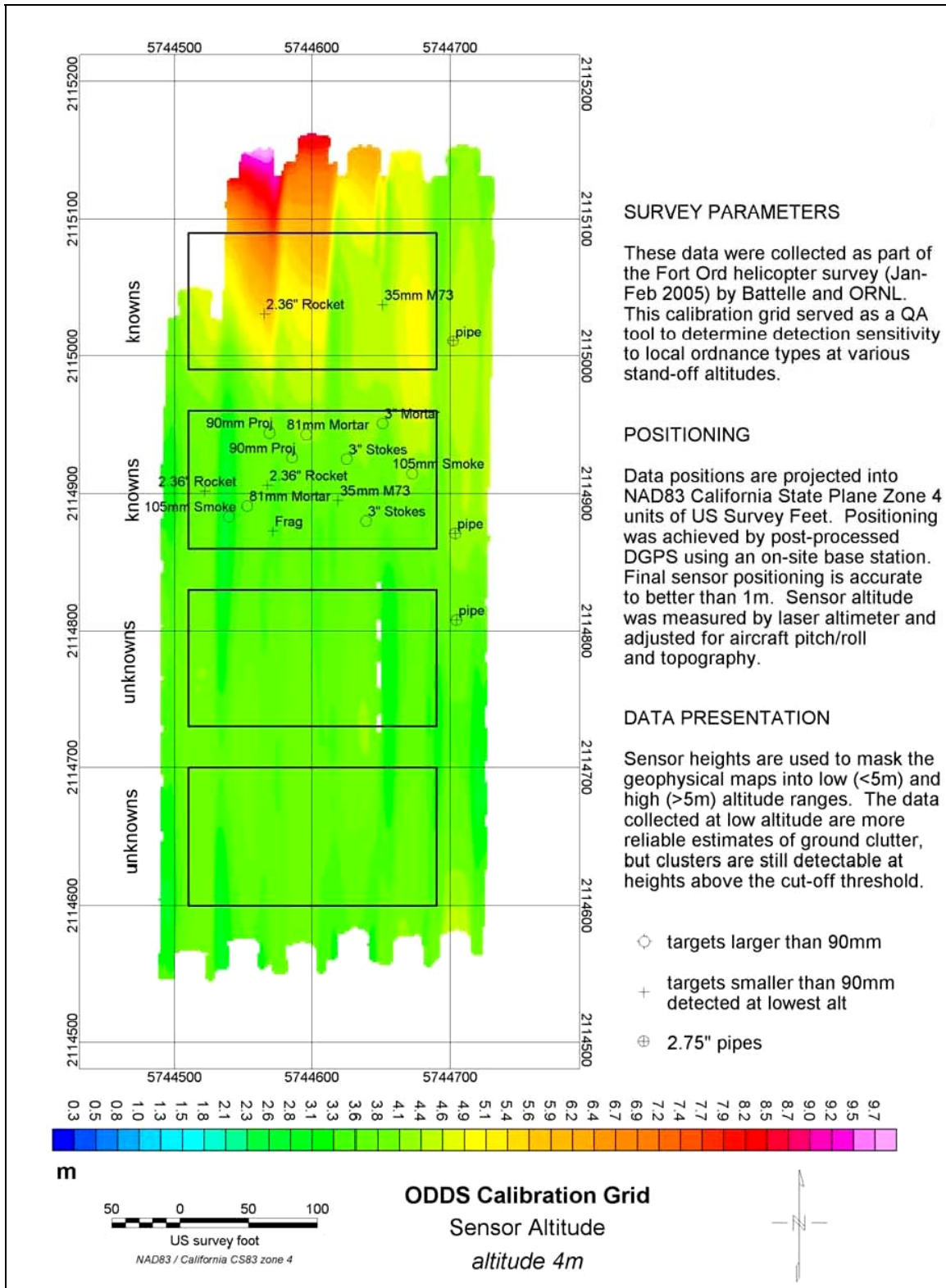


Figure 12. Altitude for nominal 4-m survey at the ordnance calibration site.

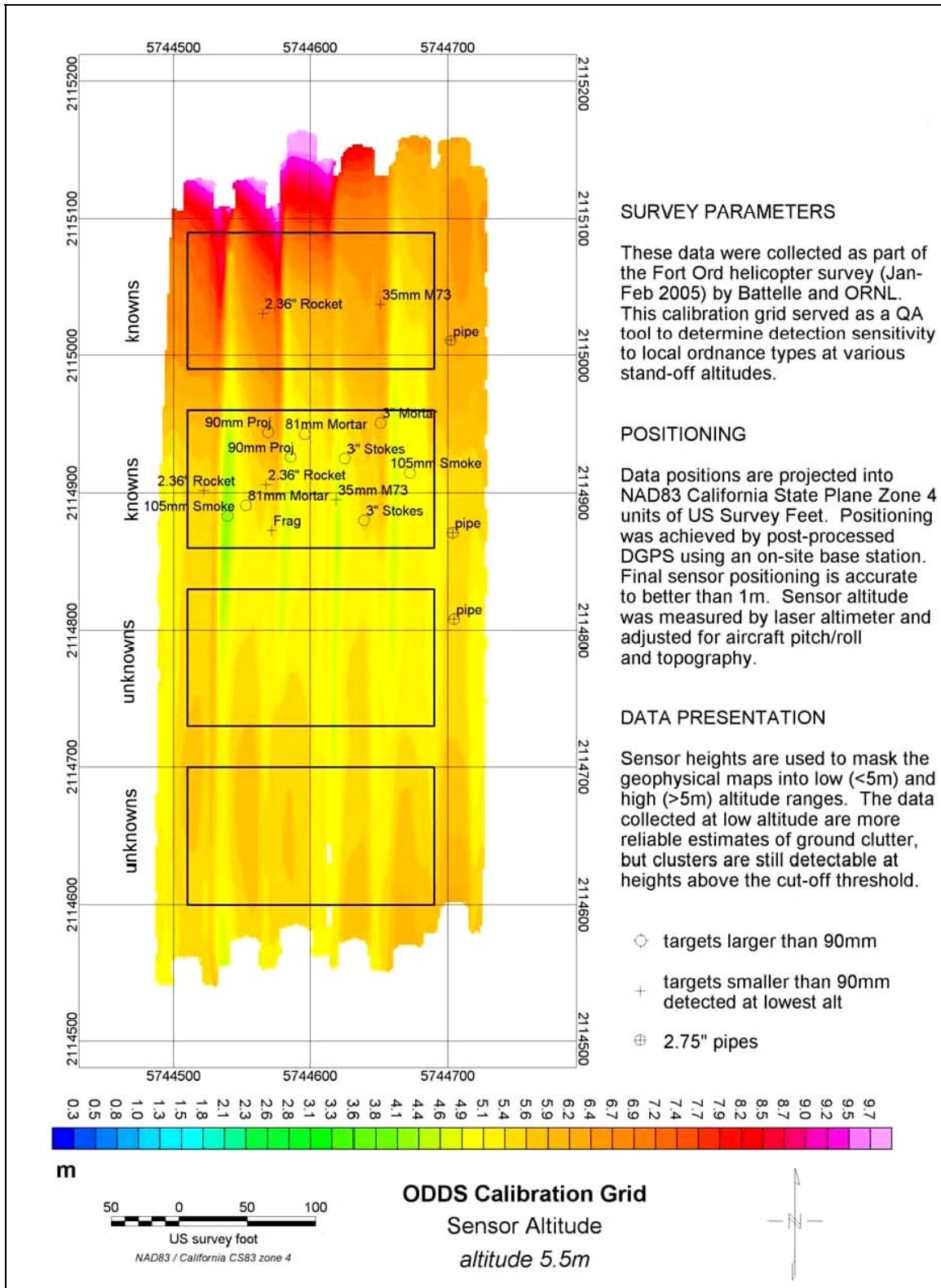


Figure 13. Altitude for nominal 5.5-m survey at the ordnance calibration site.

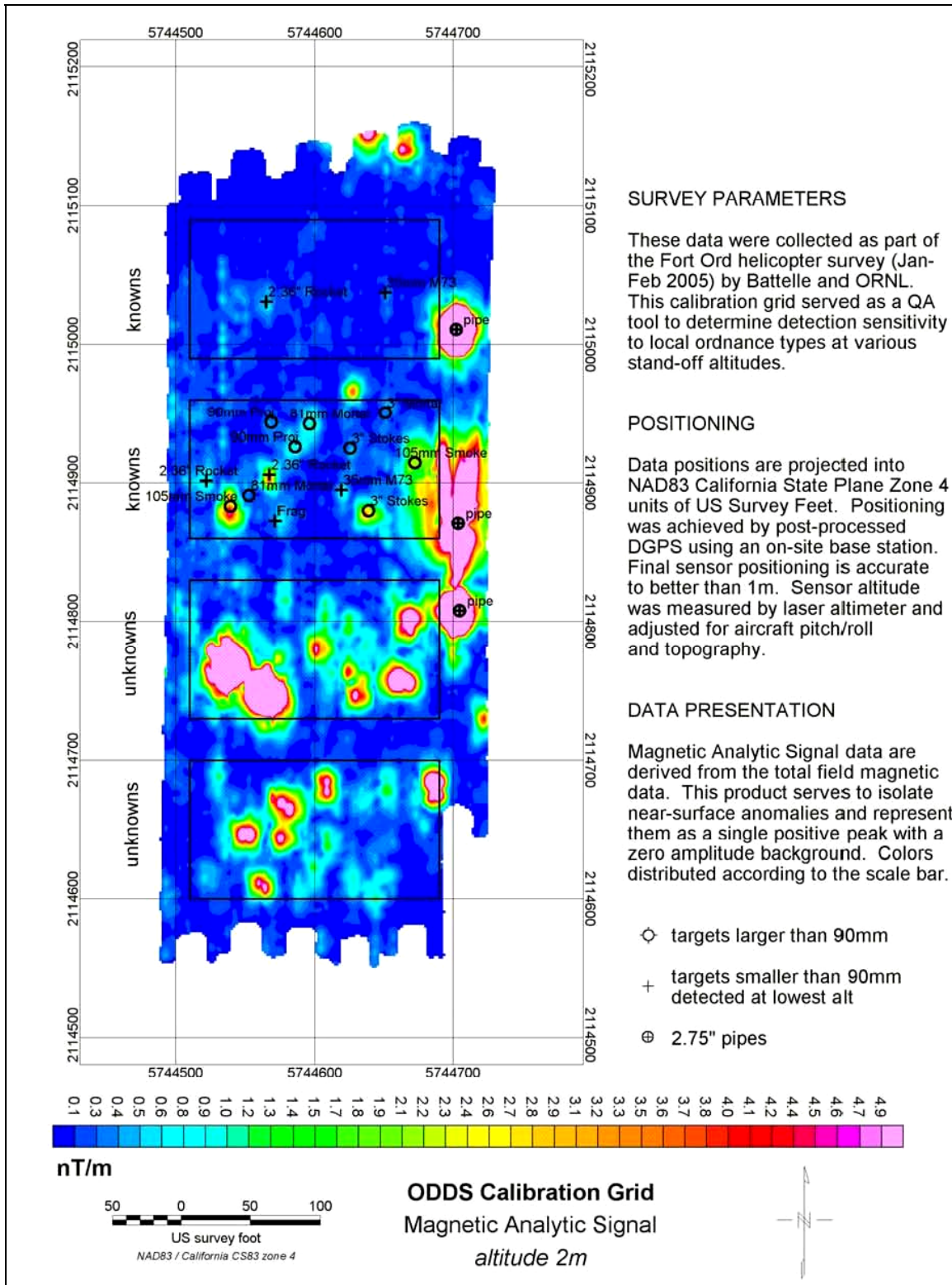


Figure 14. Analytic signal for nominal 2-m survey at the ordnance calibration site.

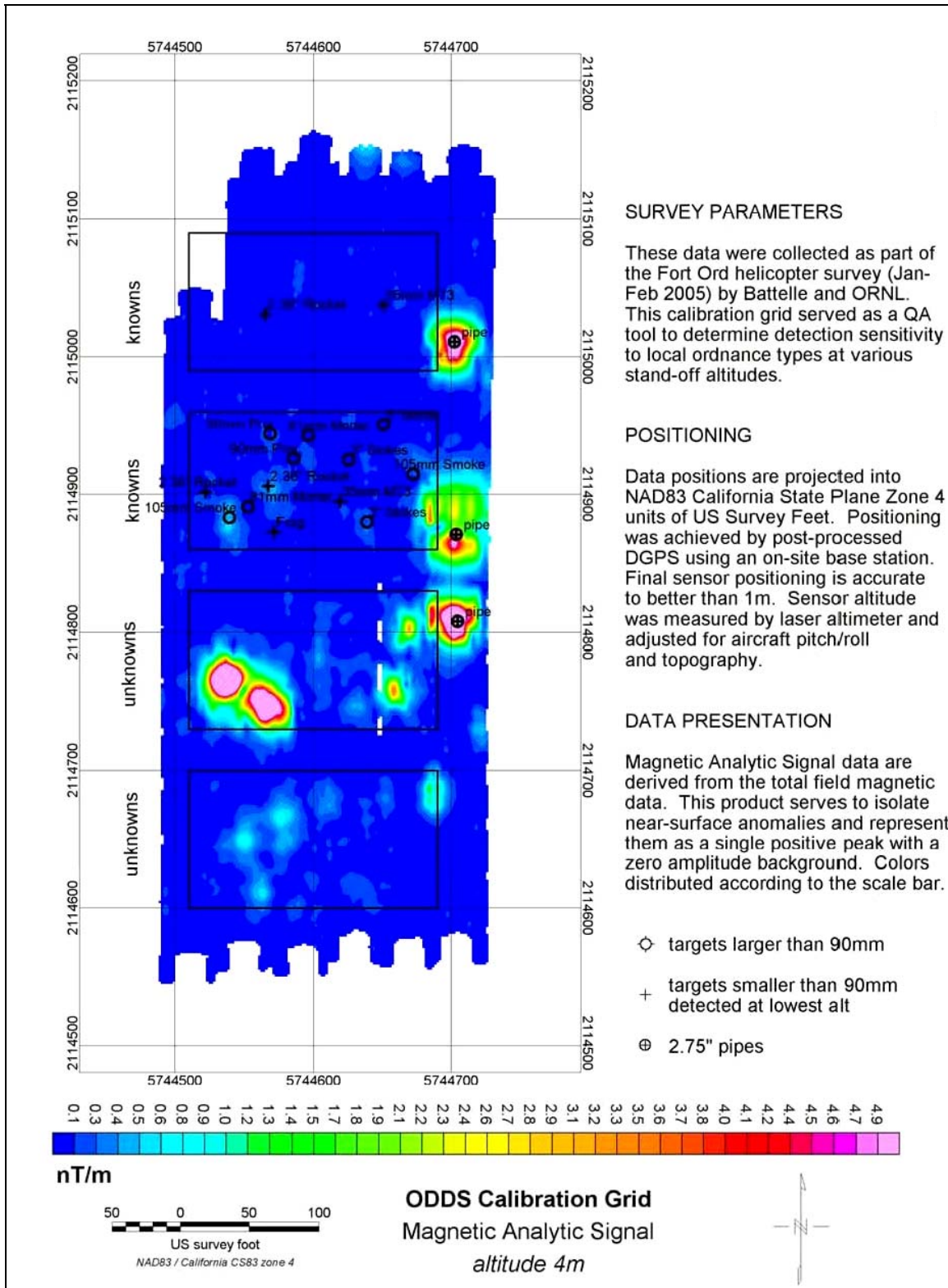


Figure 15. Analytic signal for nominal 4-m survey at the ordnance calibration site.

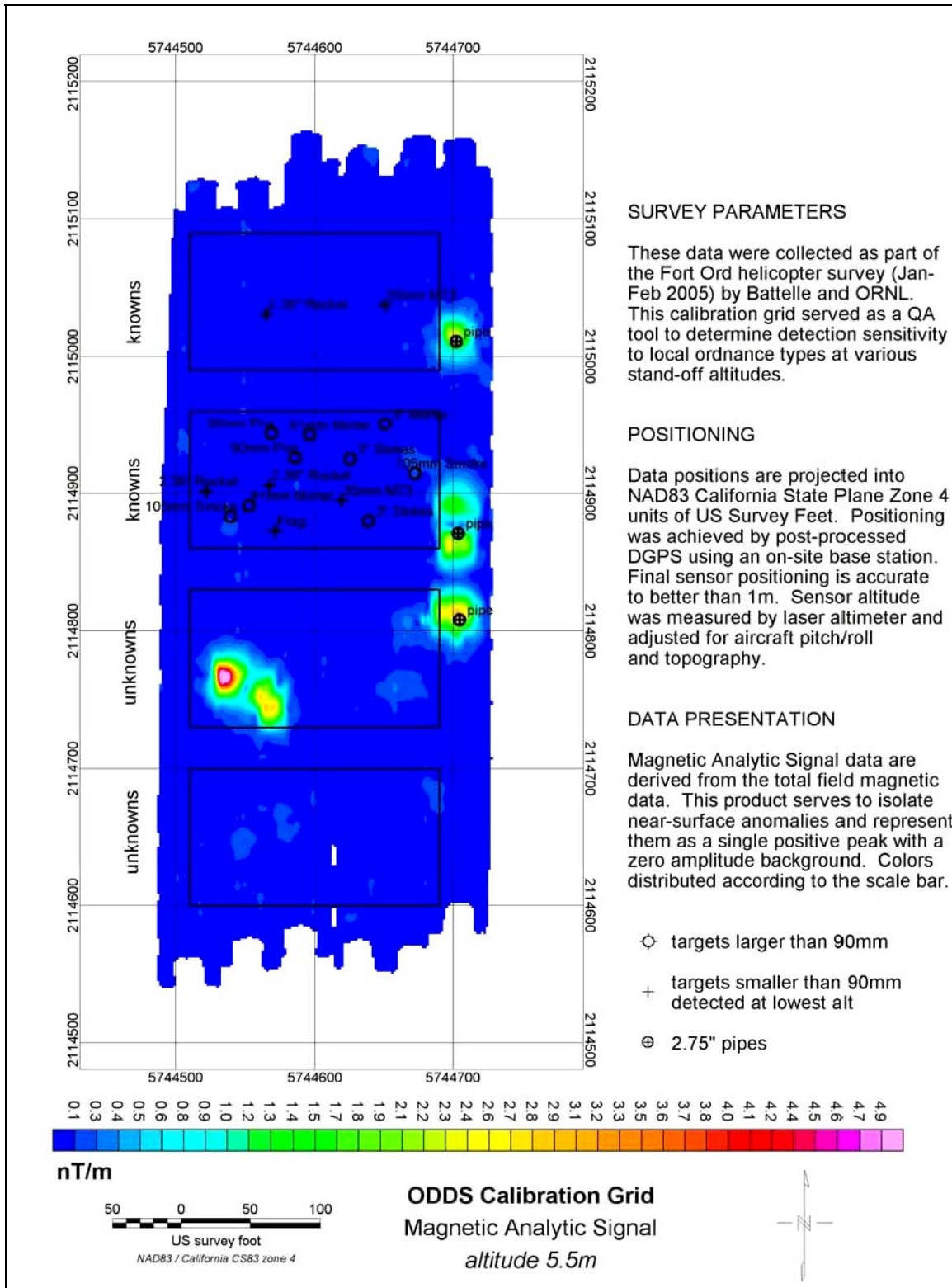


Figure 16. Analytic signal for nominal 5.5-m survey at the ordnance calibration site.

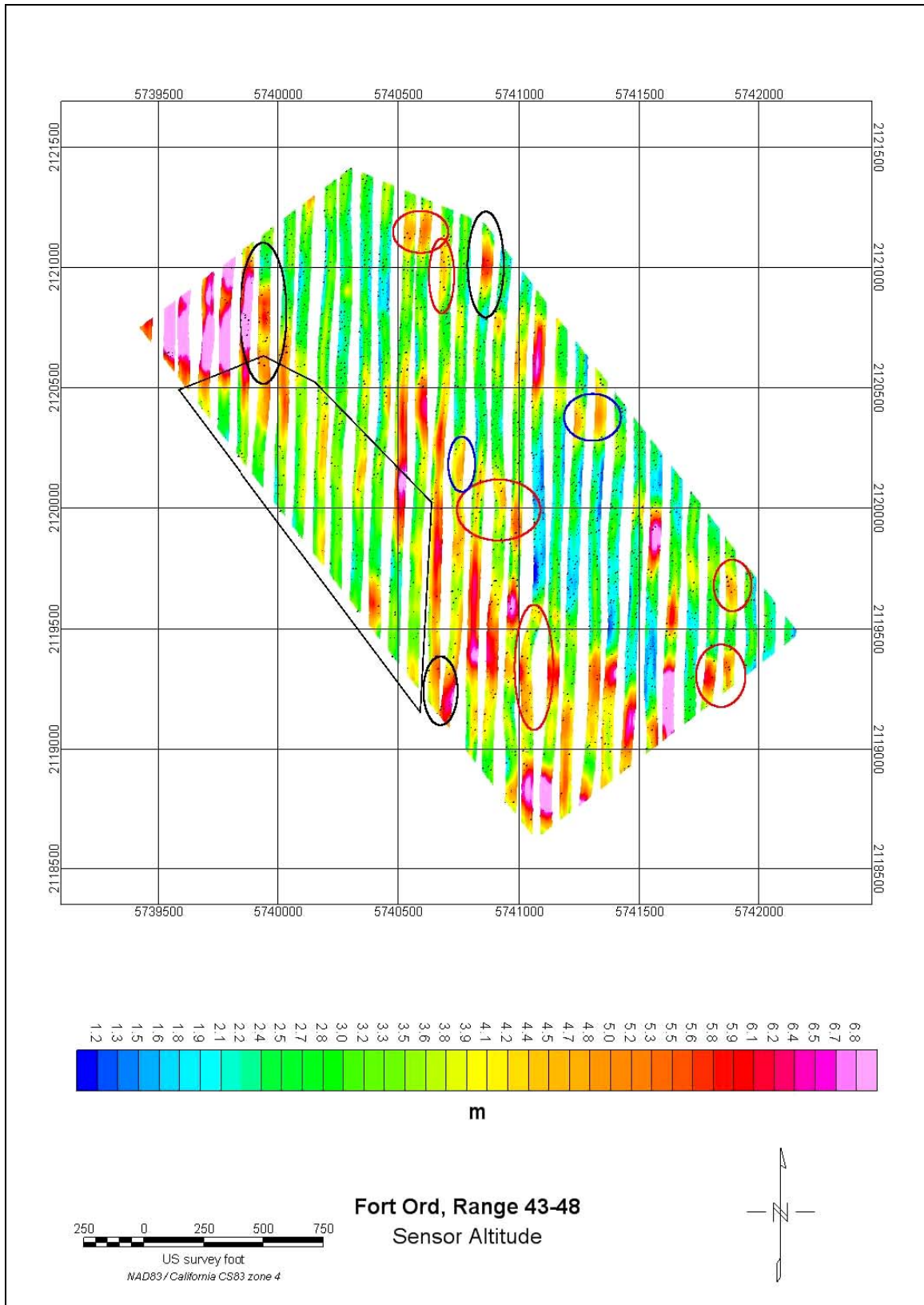


Figure 17. Sensor altitude plot over Ranges 43 and 48 with analytic signal anomaly peaks.

even though much of the survey was flown below 4 m. This would imply that the debris is not as uniformly distributed as originally thought. The general distribution of anomalies, however, clearly indicates that higher altitudes detected far fewer anomalies, as would be expected.

The black ovals plotted on the map indicate areas where discrete anomalies were detected at altitudes higher than 6 m. This is an unusual situation and is probably the result of very large targets. The remaining ovals highlight areas between 4 and 5 m altitude. The red ovals show areas where anomalies were detected, while the blue ovals are areas where no anomalies were detected but were expected. These gaps in the detection at the 5-m altitude are too small and too few to alter the overall interpretation of the data, but presentations of the data with a 4-m cut-off are also provided to display the data with a higher level of sensitivity and overall confidence.

#### **EM data: Resistivity calibration site and ordnance calibration site**

The EM system used a calibration test site outside the impact zone as a resistivity calibration grid. A subarea of the resistivity calibration grid was surveyed with ground magnetometry and with an EM-31 ground conductivity meter. The ground surveys indicated the area was relatively clear of metallic debris, and the EM-31 showed only modest variations in resistivity between 70 and 130 ohm-m. As shown in Figure 18, the leveled, gridded helicopter EM response was also smooth and of low variation over the area, as confirmed by the ground assessment. However, researchers were unable to use the resistivity calibration grid data to estimate ground resistivity. The at-altitude EM response of the system is as large as or larger than the response at a 2-m altitude over ground that, from inspection, is presumably free of metallic debris. The ground at this location is essentially unresponsive to the TEM system. This also proved to be the case inside the impact zone.

The primary focus of the EM portion of the Fort Ord survey was to attempt to use the EM system to obtain estimates of soil resistivity that might be associated with contaminants. A *secondary* focus for the EM data, requested by Fort Ord, was for UXO detection. The primary focus was untested and presented a challenge, as the system was designed for UXO detection. The ordnance calibration site was flown on only one occasion because of the limited time allotted by the client for deploying this system over two specified areas. Shown in Figure 19 is the bin 2 EM response over the site. The response of the system was low throughout the site, and the anomalies shown in the figure do not correlate well with magnetic

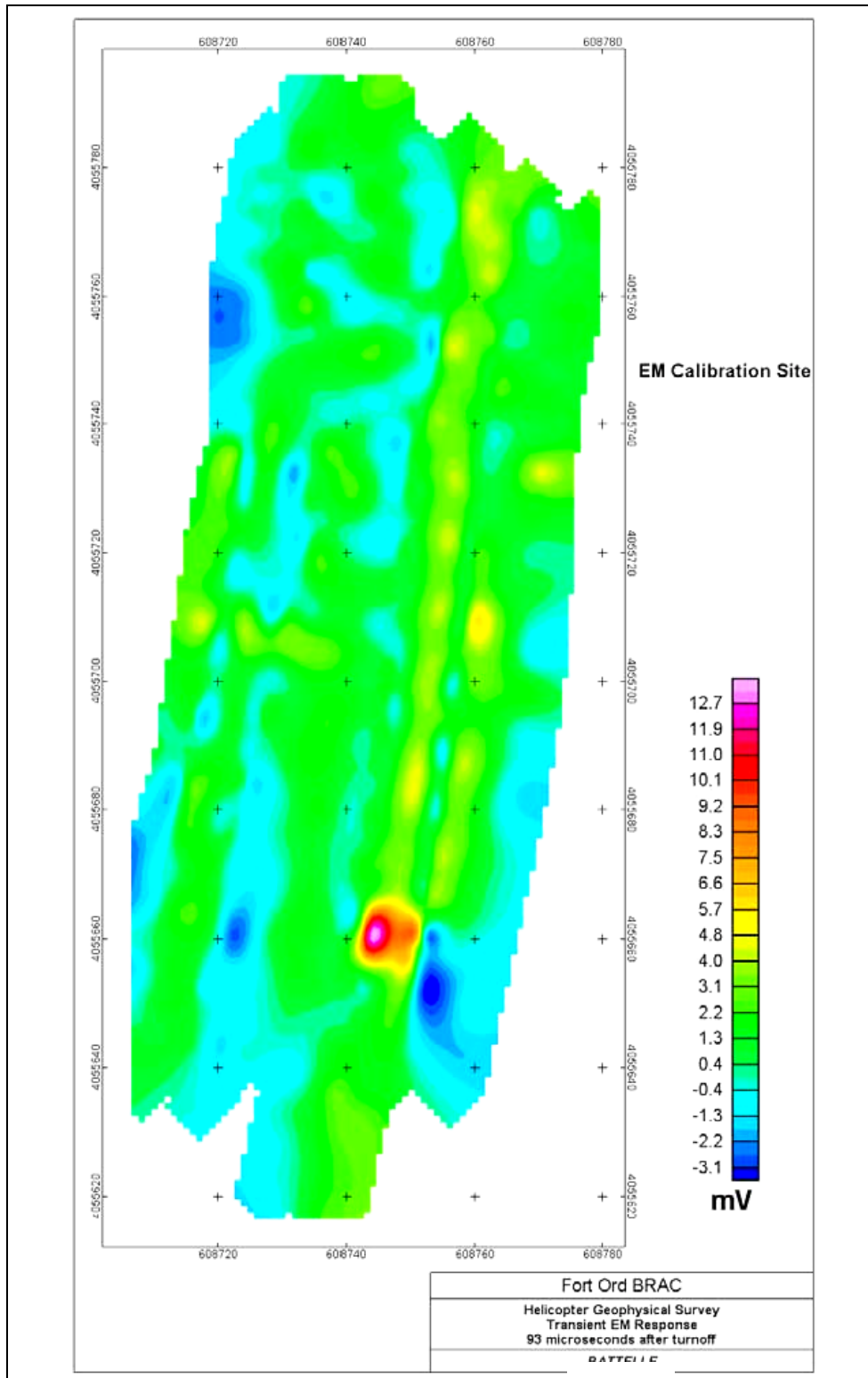


Figure 18. EM response (mV) for time bin 1 at the resistivity calibration site.

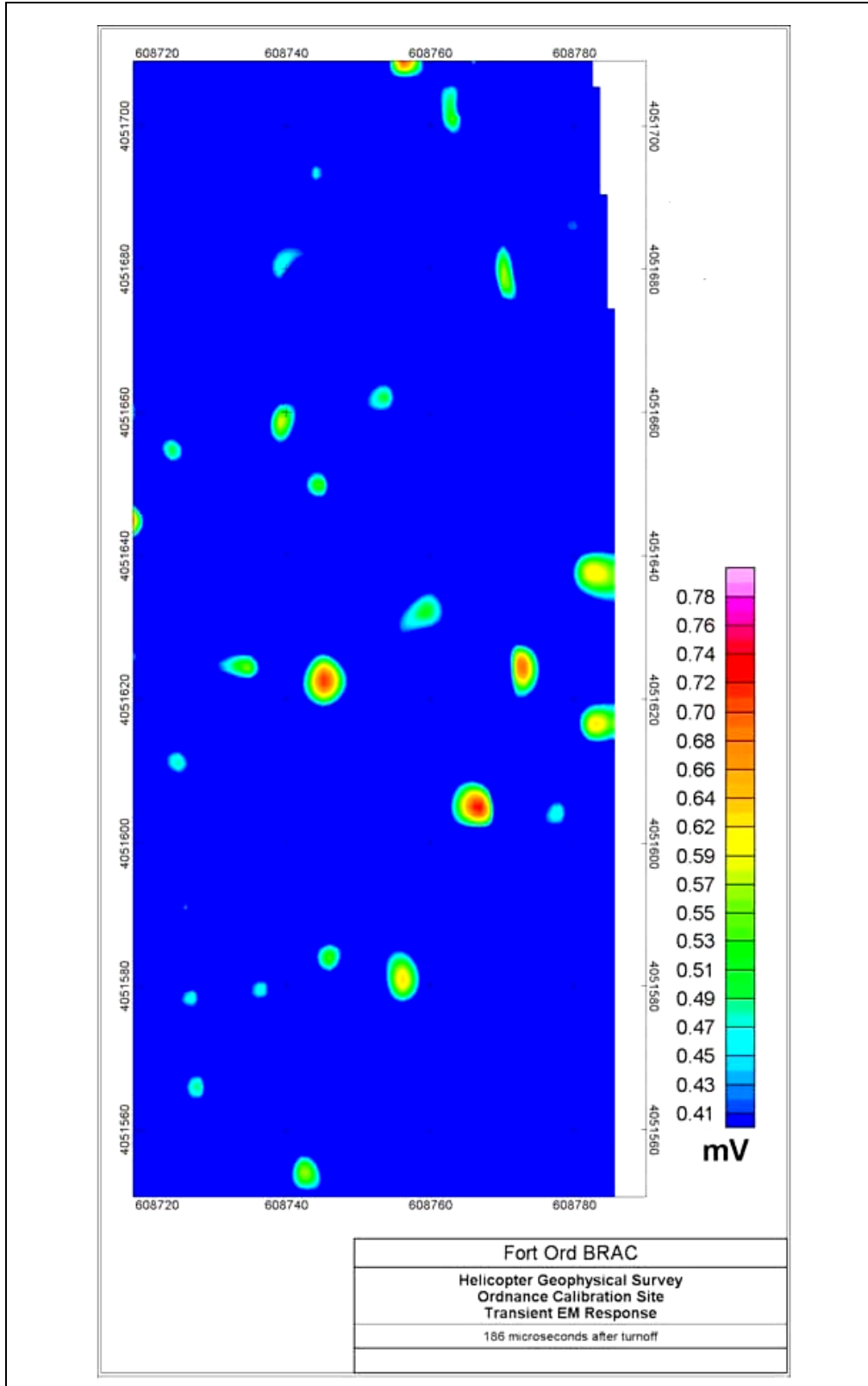


Figure 19. EM response (mV) for time bin 2 at the ordnance calibration site.

anomalies over the same area. Although small anomalies from the marker pipes used to QC the magnetic survey appear in the data, most of the anomalies appear to be related to an unusual variable frequency oscillation, the source of which has not been ascertained. This noise is further discussed in the “Interpretation of Electromagnetic Data” section.

## **Magnetic products and interpretation**

The maps referenced in this section are provided as thumbnail figures in the text of the report and in a variety of digital formats as detailed in the “Data and Image Archive” section in this chapter. The magnetic interpretation is divided into the main survey area and the MRS-16 site flown at the request of the BRAC Office. Due to the relatively high flight height over the MRS-16 site, most of the interpretation focuses on the main survey area.

### **Total magnetic field**

The dominant feature of the total field map (Figure 20) is the regional north-south trend. This can generally be ignored as irrelevant to the survey objectives, but it makes interpretation difficult. In most cases, the regional field dominates so that discrete anomalies of interest are compressed into a narrow band of the color spectrum, and become difficult to discern. In order to produce a residual magnetic map to show localized geology and ordnance, large-scale features must be removed. Residual calculations using a plane and the International Geomagnetic Reference Field only removed a portion of the regional effect and were discarded. The remaining deep-seated geology still dominated. Residual calculations using standard B-spline techniques (such as those used on the field QC maps) produced a visually appealing map, but distorted many of the near-surface anomalies. This was especially true of those on the flanks of deeper geologic features. In comparison, some mid-depth features exceeded the residual cut-off threshold and produced false anomalies. These could be discounted by comparing the residual and total field, but would be very time-consuming on a survey-wide basis. The variation in survey altitude (Figure 21) also made it difficult to set a single residual cut-off threshold, because changes in altitude shift the spatial spectrum of the anomalies. It was decided, therefore, to concentrate interpretation on the vertical gradient and analytic signal maps and discard the residual maps created for QC in the field.

The figures printed in this section are thumbnails only. The resolution here is insufficient for detailed interpretation.

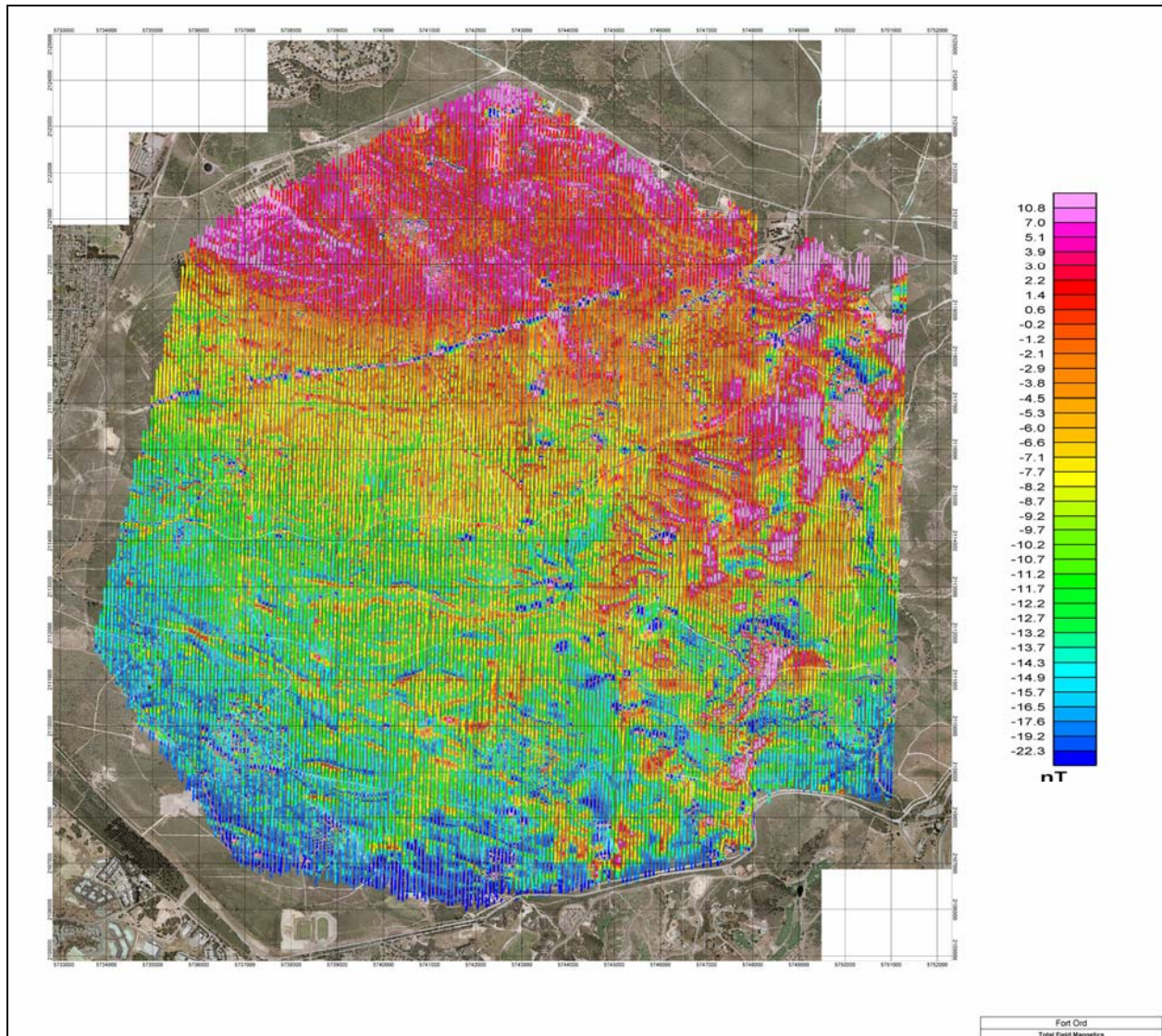


Figure 20. Thumbnail of total magnetic field map of the survey area at Fort Ord.

### Vertical gradient

The vertical gradient map (Figures 22 and 23) was calculated from the gridded total field data using an FFT vertical derivative function. This is an intermediate product, which is visually similar to the residual total field, between the total field and the analytic signal. Near-surface anomalies appear as dipolar responses with a smaller spatial extent than the total field anomalies. The amplitude of the response is dependent upon the sensor height, magnetic susceptibility, size, and mass distribution of the source. The sensor height is particularly important because it is the only one that is independent of the target. Although not the focus of this study, if these data are analyzed in the future with an emphasis on UXO detection, the data

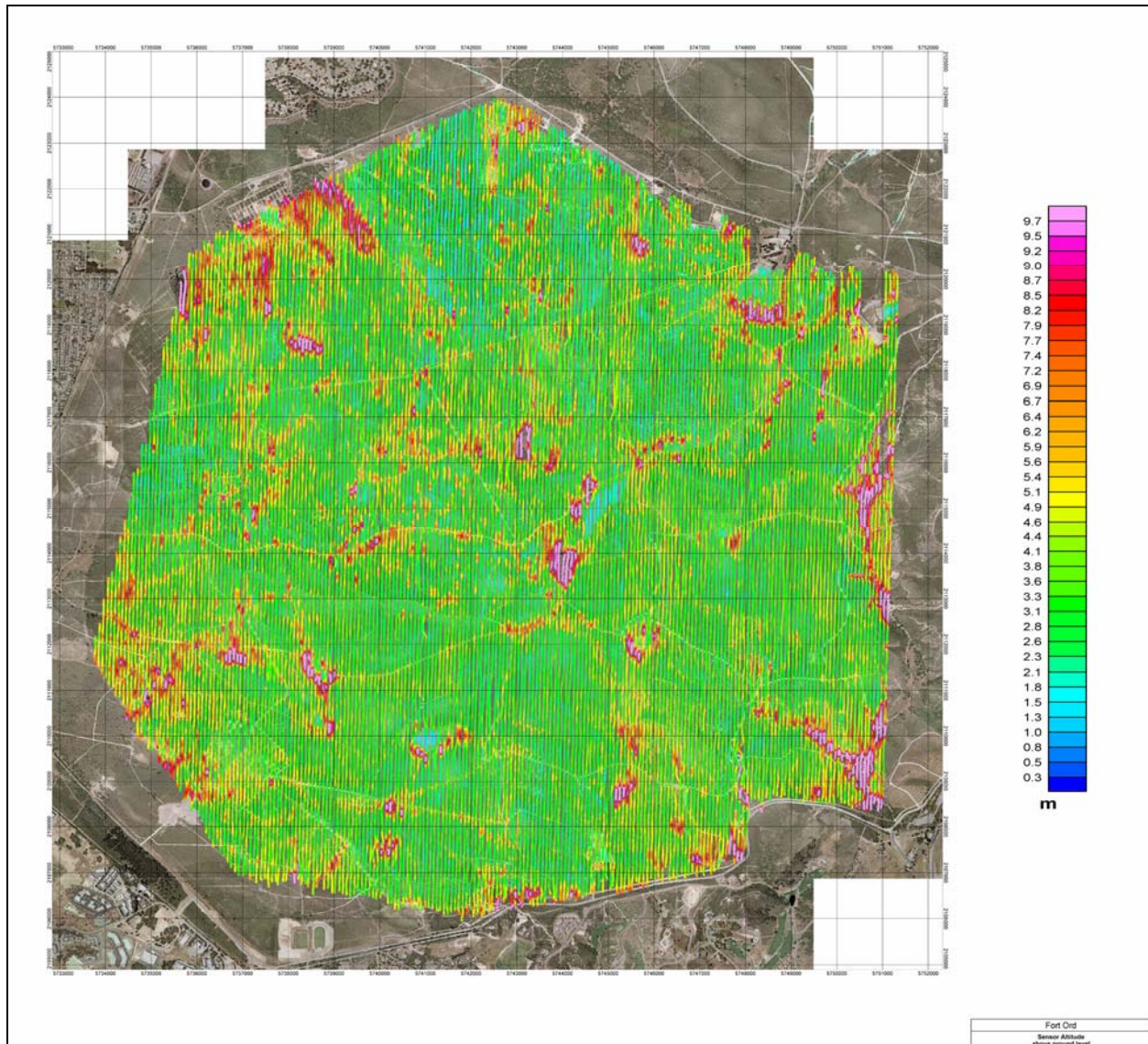


Figure 21. Thumbnail of sensor altitude above ground level map of the survey at Fort Ord.

must be analyzed with due consideration given to the actual sensor altitude achieved at each anomaly. To restrict the presented data to an acceptable range of sensor heights, results were masked for those portions of the survey area where the flight height was greater than 5 m (Figure 22). The masked areas comprise approximately 17 percent of the total map area, and represent places where vegetation or topography prevented successful acquisition of data suitable for detection of individual UXO items or clusters at this site. Supplemental maps with a 4-m altitude cut-off (Figure 23) allow the user to see the effect of altitude with respect to reduced area coverage and increased target sensitivity. In general, the 5-m data were used for interpretation, with a greater level of confidence implied for the 4-m data.

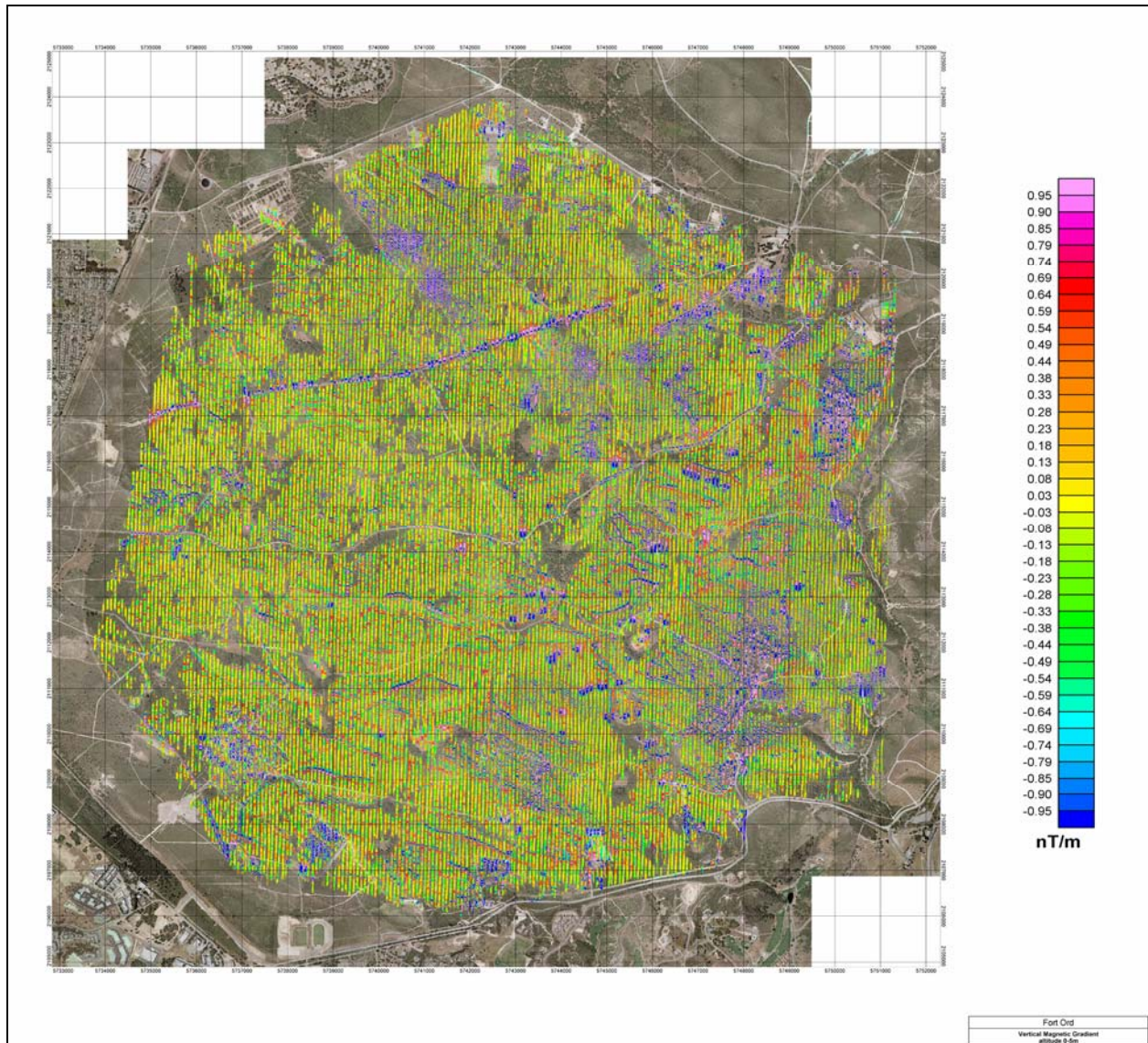


Figure 22. Thumbnail of vertical magnetic gradient map of the survey area at Fort Ord for altitudes <5 m.

The dominant feature of the vertical gradient map is the linear pipeline running east-northeast from the west side of the survey block. Areas of high contamination are highlighted as red/blue pockets against the yellow “zero-mean” response. Areas of moderate debris are less obvious orange/green responses. Some low-amplitude, linear features undulate across the area in a general east-west direction. These are interpreted as geologic or topographic sources.

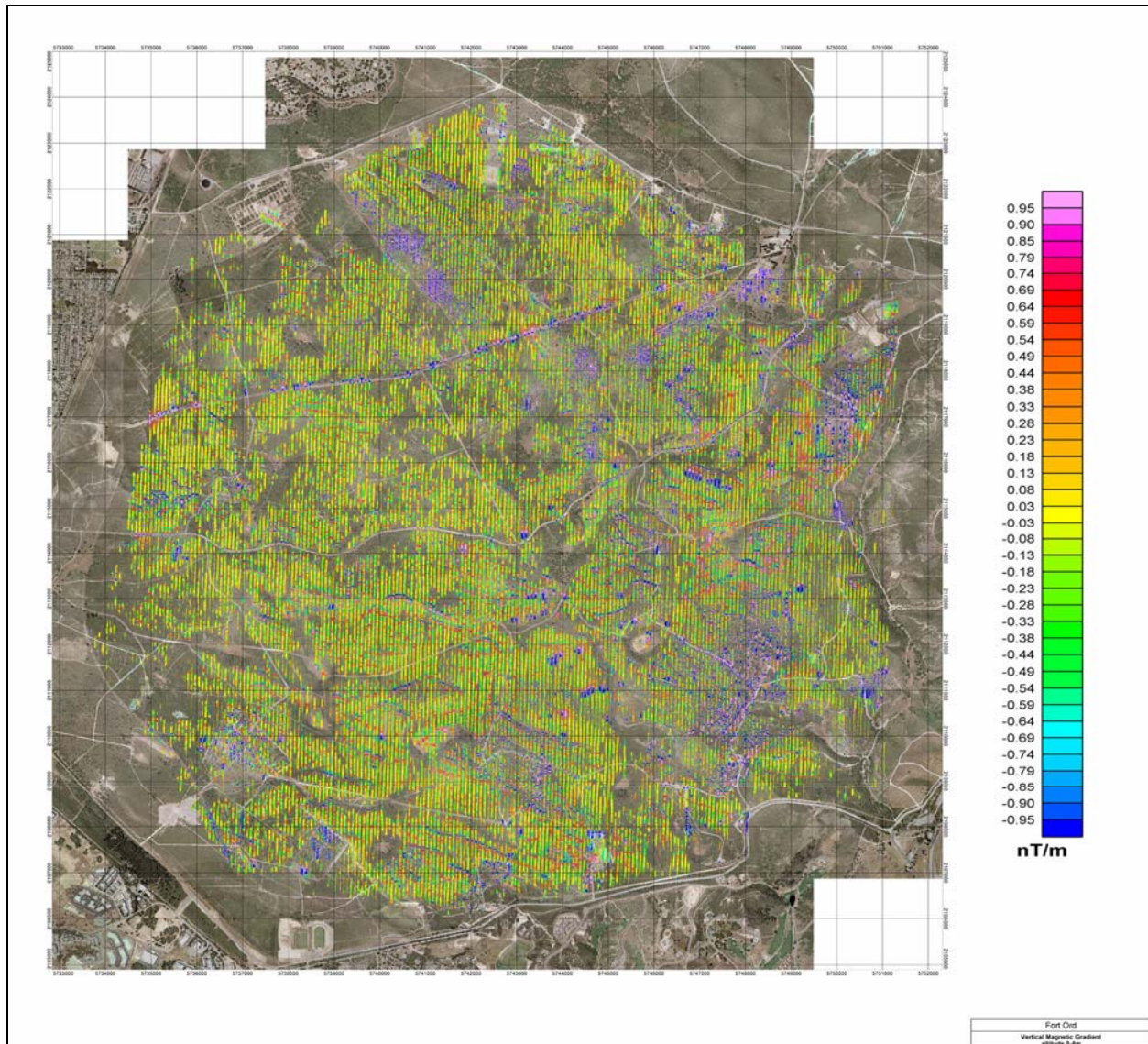


Figure 23. Thumbnail of vertical magnetic gradient map of the survey area at Fort Ord for altitudes <4 m.

It should be noted that there is a strong correlation between geology, topography, cultural and historic land use, and survey altitude. For example, geology often controls topography; cultural features such as roads, trails, power lines, and impact ranges are often dictated by topography; and survey height is strongly controlled by the necessity to avoid both topography and cultural obstacles. This makes detailed interpretation regarding the source of each geophysical anomaly difficult. This level of analysis is not, however, an objective of this project. If such an analysis is conducted, the altimeter data must be considered as a primary factor.

## Analytic signal

An analytic signal map is presented in Figures 24 and 25. As described in the “Analytic Signal” section of this report, the analytic signal can be understood as the total gradient. It is similar to the vertical gradient, but it factors in the horizontal gradients as well. The result is a “zero-minimum” product with all peaks being positive, and the amplitude proportional to the size and magnetic susceptibility. In most magnetometer UXO surveys, this map serves as the basis for UXO detection. For this project, anomaly peaks and most of the interpretation were based on this product.

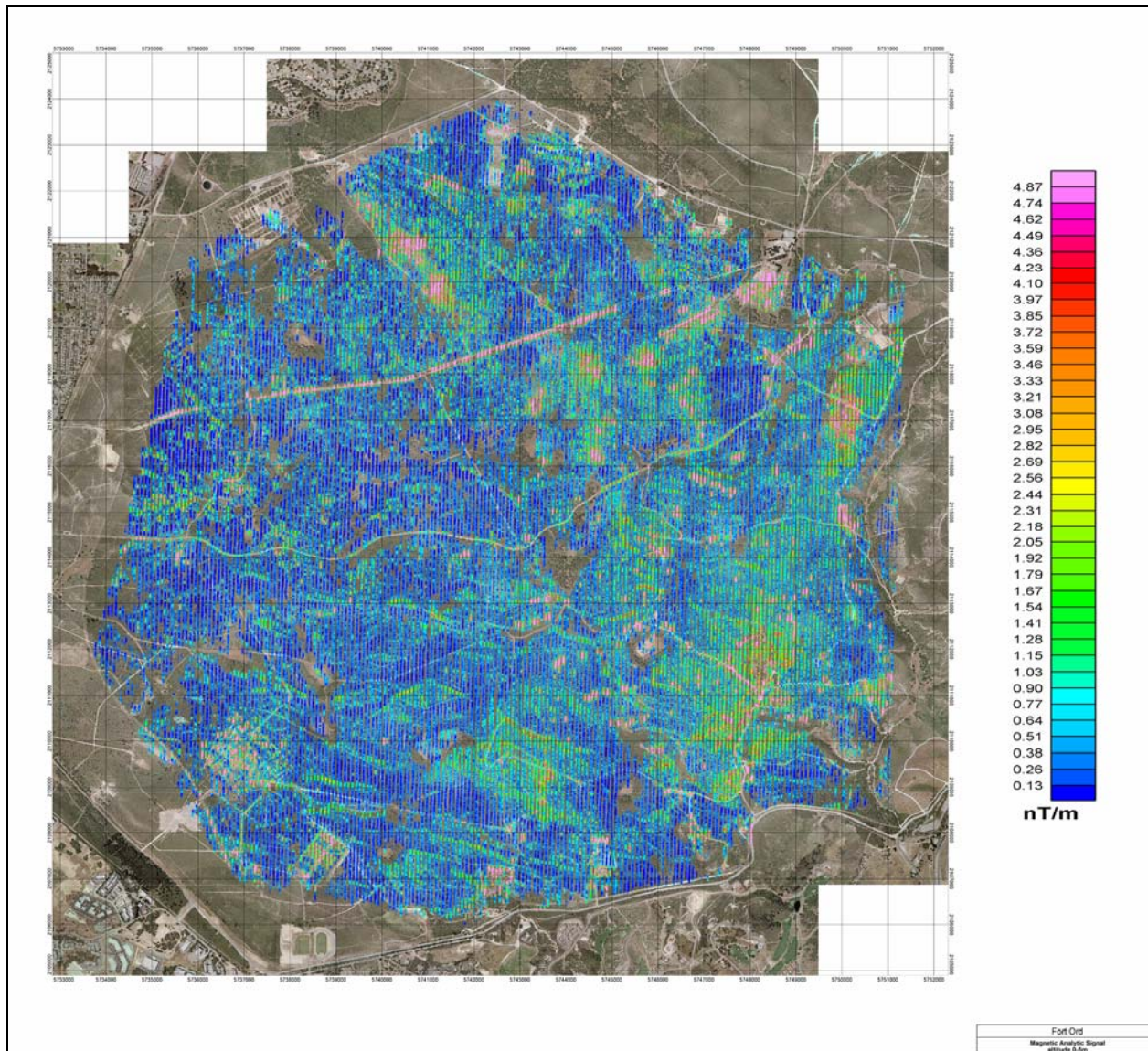


Figure 24. Thumbnail of analytic signal map of the survey area at Fort Ord for altitudes <5 m.

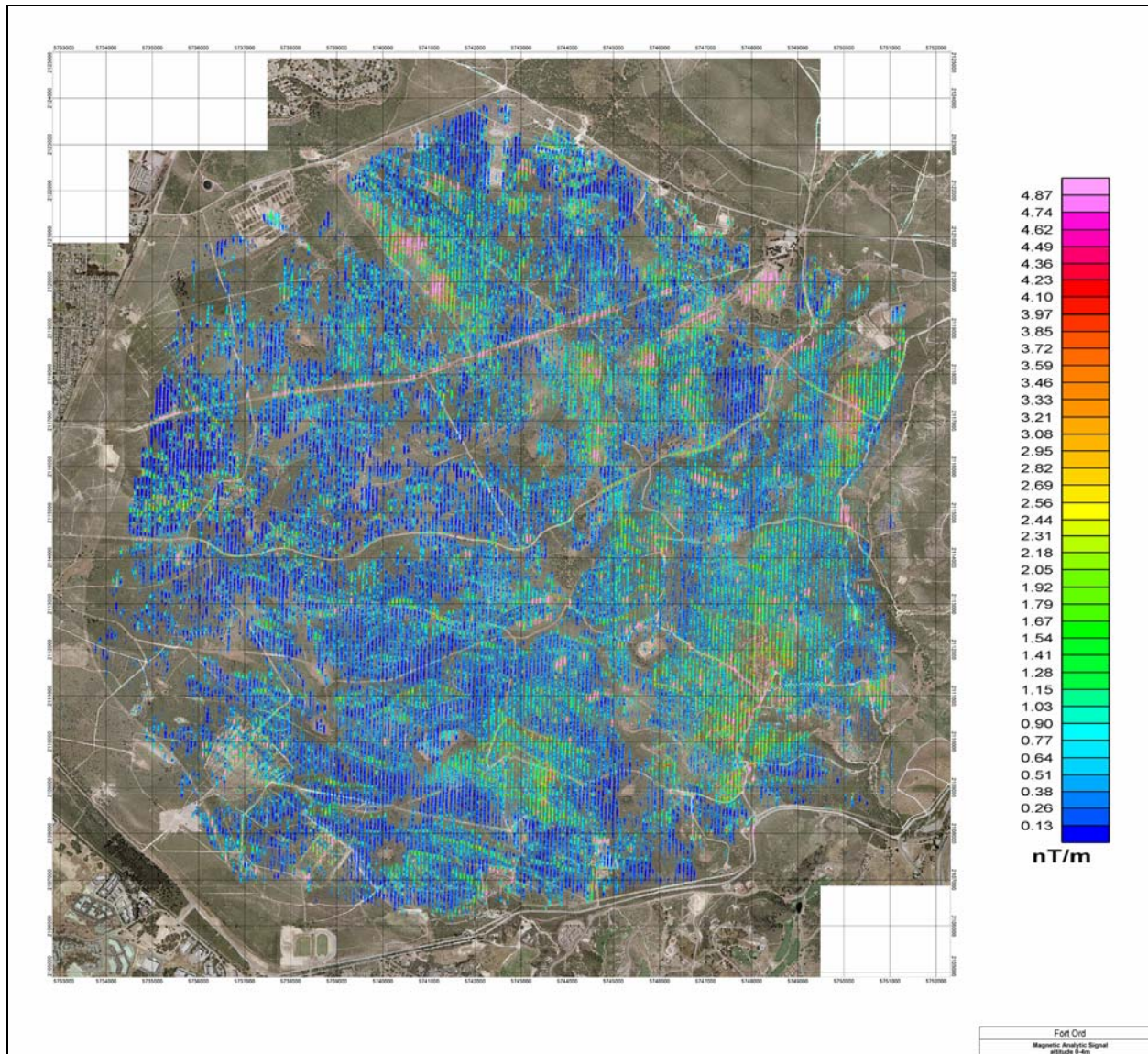


Figure 25. Thumbnail of analytic signal map of the survey area at Fort Ord for altitudes <4 m.

### Interpretation map

From the analytic signal map, various linear features associated with roads, tracks, pipelines or other cultural features were plotted by hand. These features appear on the interpretation map (Figure 26) as black line segments. The most obvious of these is the interpreted pipeline across the northern portion of the survey block. This response is discontinuous, presumably because sections have been removed from the ground. A smaller discontinuous line runs through the center of the block. A third line along the southwest boundary of the block is interpreted as associated with a boundary fence.

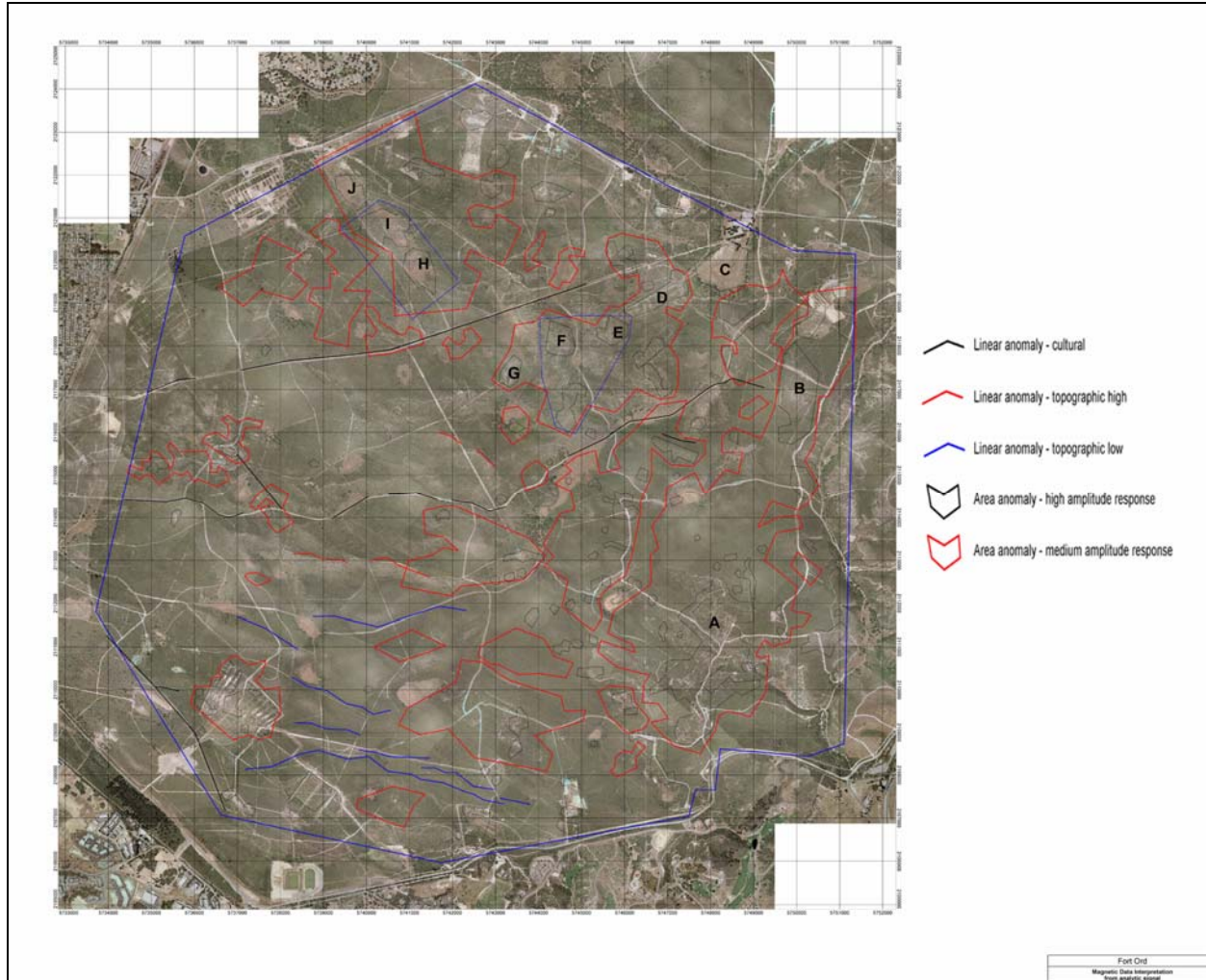


Figure 26. Thumbnail of interpretation map for the survey area at Fort Ord. (Blocks A-J are explained in the text.)

Other linear features were mapped with red and blue lines. The red lines correspond to analytic signal anomalies that trace topographic ridge lines. These may be geologic in origin. The blue lines correspond to analytic signal anomalies that trace topographic troughs. These may be associated with collections of debris that have settled in local depressions.

In addition to linear trends, anomaly peaks in the analytic signal were analyzed and collected into various groups. A histogram of the analytic signal map (Figure 27) shows that the background noise level is 0.2 nT/m. From this basis, amplitude thresholds were established at 10:1 (2 nT/m) and 2.5:1 (0.5 nT/m) signal-noise ratios for strong and weak anomalies, respectively. Anomalies were thus divided into low- (0.2 to 0.5 nT/m), medium- (0.5 to 2.0 nT/m), and high- (>2 nT/m) amplitude responses.

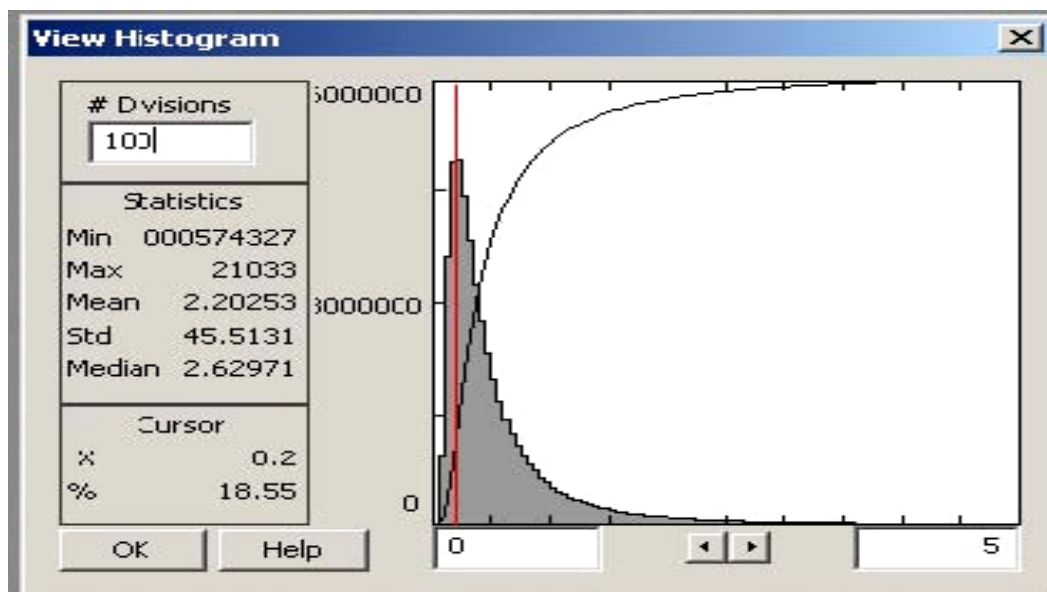


Figure 27. Histogram of analytic signal map showing background noise peak at 0.2 nT/m.

The low-amplitude anomalies are not included in this analysis. The remaining anomalies are divided 80/20 percent between medium- and high-amplitude responses. These were manually grouped into contiguous blocks and plotted on the interpretation map. Very-high-amplitude anomalies ( $>20$  nT/m or 100:1 signal-noise) represent 3 percent of the total anomaly count.

Large contiguous blocks (two or more lines) of high-amplitude response ( $>2$  nT/m) were outlined with handdrawn polygons in grey. The boundaries of these polygons should not be taken as physical target boundaries. They are merely an attempt to outline the highest amplitude responses. In many cases, dozens or hundreds of individual items may be combining to create a single anomaly that effectively saturates the system's ability to resolve them. Also, many responses are caused by sources that have forced the survey altitude above the 5-m altitude threshold. In this situation, the boundaries of the response are impossible to define because the relevant data have been masked out.

Other polygons were drawn in red around blocks of medium-amplitude response ( $>0.5$  nT/m), which may be associated with lesser densities of debris. That is not to say that ordnance does not exist outside the polygons shown, but the responses outside the blocks appear to be more consistent with geologic sources than the ordnance types expected at this site and at the actual survey altitude. Several of these moderate-amplitude responses exist within the survey area, but these are interpreted to be more likely geologic in nature. This would be the result of magnetically susceptible

rocks eroding in from other locations, although random rock samples were tested with a susceptibility meter and were not found to be particularly magnetic. The true source of these moderate-amplitude but lower priority anomalies cannot be ascertained without ground followup.

The largest contiguous block of high-amplitude data in this map is in the southeast corner of the survey area (A). It is part of a larger medium-amplitude block that extends to the north northeast and encompasses the second largest single high-amplitude block (B). Blocks C-G represent a line of high-amplitude blocks that are smaller in extent, but equally strong in amplitude. Blocks D-G are located on topographic highs, but block C almost completely fills a local valley. Blocks H-J represent equally strong responses and are known ranges under remediation. Numerous other high-amplitude blocks have been identified and require additional ground followup, but letters have not been assigned to these areas. In general, these other blocks have amplitudes comparable to the lettered blocks, but are smaller in their extent.

Most of the high-amplitude blocks are contained within a larger medium-amplitude block. This would indicate that there is a considerable amount of scattered debris around a central cluster. Not all high-amplitude blocks have an associated halo of debris, however. In these cases, the response may be caused by a single large object rather than a cluster of smaller ones. The lack of a response from a debris halo is not an indication of a lack of small ordnance. Much of the ordnance expected at this site is below the detection threshold of an airborne magnetometer system, and the existence of a large, discrete object is an indication of human activity that should be followed up.

### **Anomaly density**

A total of 140,166 discrete anomaly peaks were detected in the analytic signal grid with a minimum amplitude threshold of 0.5 nT/m, which is 2.5 times the background noise level of 0.2 nT/m. The average amplitude of these peaks was 6.5 nT/m and the maximum was 21,000 nT/m. Of these, 12,702 were eliminated because the associated sensor altitude was greater than 5 m, leaving a total of 127,464 airborne anomaly peaks. As described earlier, 80 percent of the anomalies were between 0.5 and 2.0 nT/m, and 3 percent of the anomalies were above 20 nT/m.

Airborne anomaly densities, in units of counts per hectare, were calculated from these peaks and the low-altitude, analytic signal coverage. These were compared to the ground magnetic anomaly density figures provided by Parsons Engineering through the Corps of Engineers. The differences in sensitivity between the two survey modes make quantitative comparisons difficult. The ratio of the ground-to-airborne densities was calculated by simply dividing the airborne- and ground-based density maps. The ratios ranged from 2:1 to 9:1, with no single dominant ratio. A 5:1 ratio represents an average scaling factor between ground and airborne densities, but the numeric accuracy of such scaling is accurate only within a factor of +/-2 at best. It should be noted that low, or even zero, density responses in the airborne data are insufficient justification to declare an area clear of ordnance.

The resulting map (Figure 28) shows a strong correlation with the polygons of the moderate analytic signal response (red polygons). Most of the linear cultural features are suppressed but not eliminated because they form longer anomalies rather than discrete peaks. The linear features associated with local topographic features are not particularly suppressed. This is because they are strings of discrete anomalies rather than a long continuous anomaly. The high-amplitude analytic signal responses (grey polygons) do not show as high a correlation with the density as expected. In this product, a single large amplitude response counts with the same weight as a single low-amplitude response. The analytic signal may reflect the bulk or volume or mass of metallic debris, whereas the density measurement attempts to represent a count of debris pieces.

The dominant feature of this map is the very high density found in the vicinity of Range 43 and 48 (Blocks H-J). Blocks C-G have comparable anomaly densities. By comparison, Blocks A and B, which dominated the analytic signal amplitude response, show noticeably lower densities. The broad medium-amplitude response block surrounding Blocks A and B shows ordnance densities comparable to those in the ODDS calibration grid.

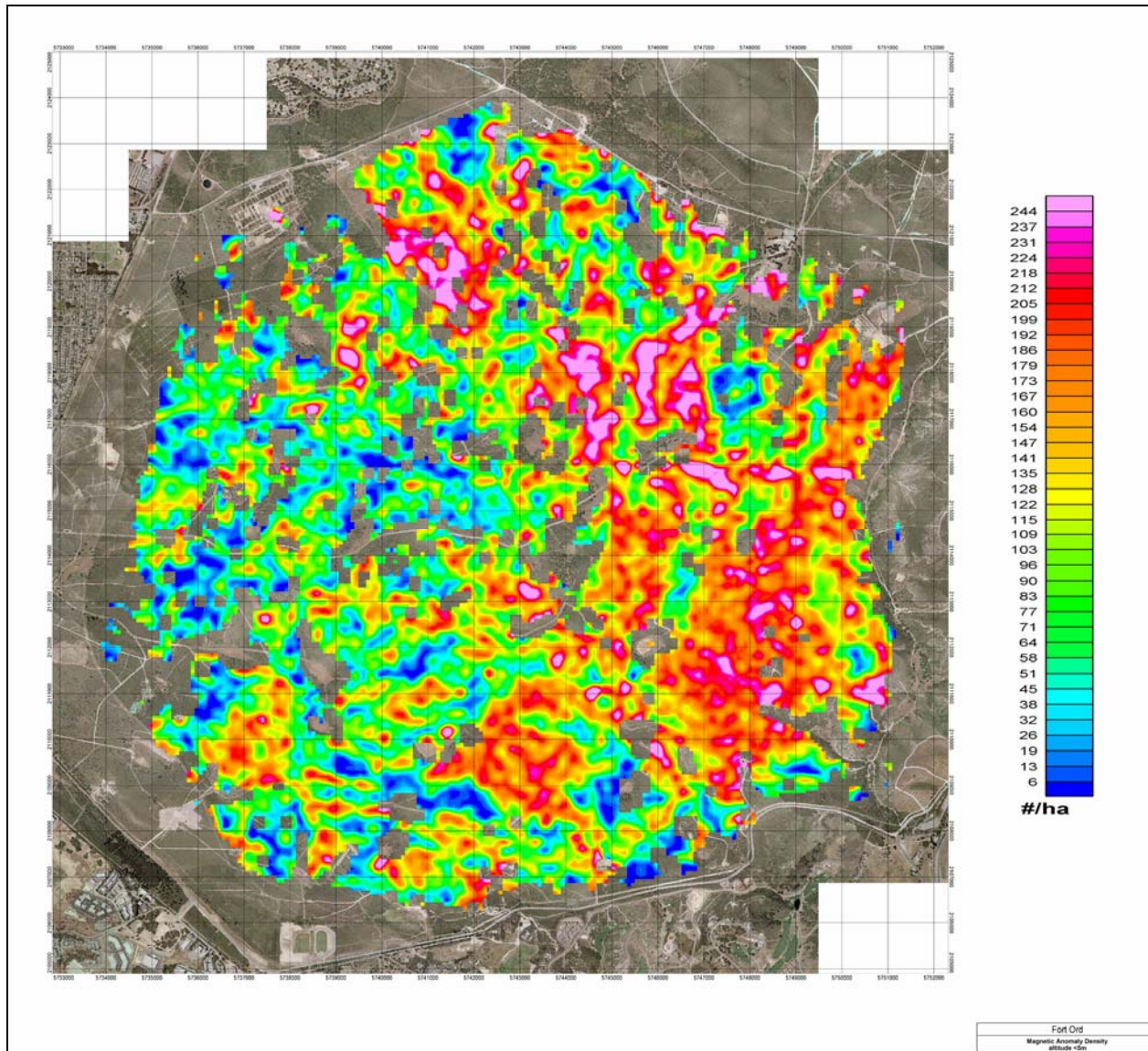


Figure 28. Thumbnail of anomaly density map of the survey area at Fort Ord.

### MRS-16 site

At the request of the Fort Ord BRAC Office, an additional block known as the MRS-16 site was flown to the north of the main survey area. This area had heavy tree cover and was under consideration for clearance burning. The area was flown with full coverage using 12-m line spacing. The vegetative cover prevented low-level surveying in all but one small section of the area. Although the range of altitudes was comparable to the main survey block, the median height was approximately double at 6.4 m. Figure 29 shows the histogram and general statistics for the MRS-16 site. The vertical red line shows the cut-off altitude used on the main block.

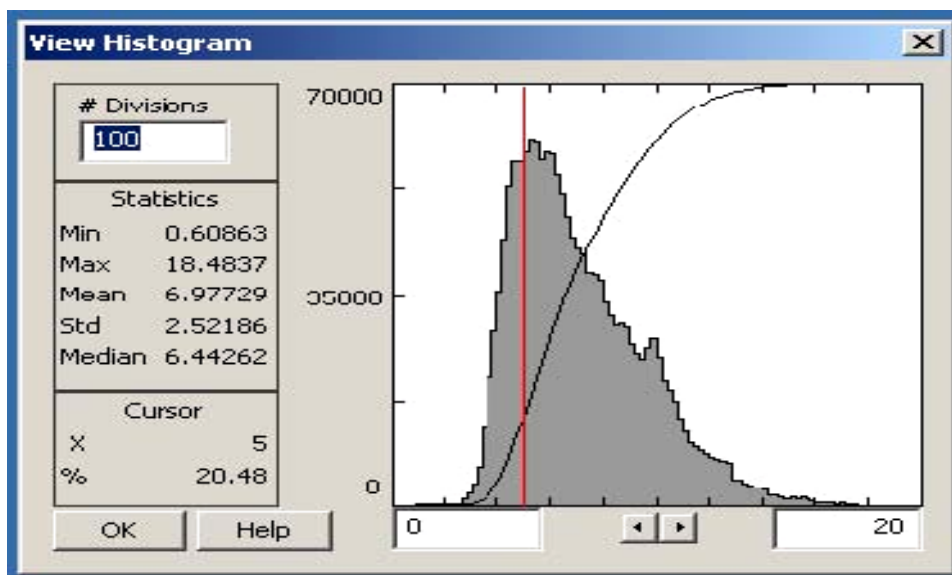


Figure 29. Histogram of altitude data at the MRS-16 site. The median altitude is 6.4 m. The 5-m cut-off threshold used in the main survey area would eliminate 79.5 percent of the data from consideration.

In general, the survey height was too great to discriminate individual objects. Clusters of objects may also be masked at this altitude. Infrastructure such as fences and roads is the most likely source of the observable anomalies; however, there were about a dozen small, discrete anomalies that should be assessed. These are marked on the analytic signal map (Figure 30) and the interpretation map (Figure 31). The approach to interpretation was similar to that used for the main survey area. Linear and cultural features were traced by hand, as were areas of high and moderate anomaly intensity. In addition, several discrete anomalies that occurred outside the moderate intensity polygons are recommended for assessment by the BRAC Office.

### Data and image archive

ORNL provided ERDC, Vicksburg, original Geosoft format files as the principal digital format. This includes database files with georeferenced point data (GDB), and interpolated grid files (GRD). A free data viewer is included with the digital data or is available online at [www.geosoft.com](http://www.geosoft.com) (Oasis Montaj Viewer 6.1). Supplemental copies of map data are provided as image files in compressed tagged information file (TIF) format in addition to the smaller reproductions included in this report. These maps were provided with a digital resolution of 150 and 300 dpi. GeoTiff format files of the geophysical data alone are provided for quick inclusion into other GIS platforms, but the resolution is not as high as the original Geosoft GRD files.

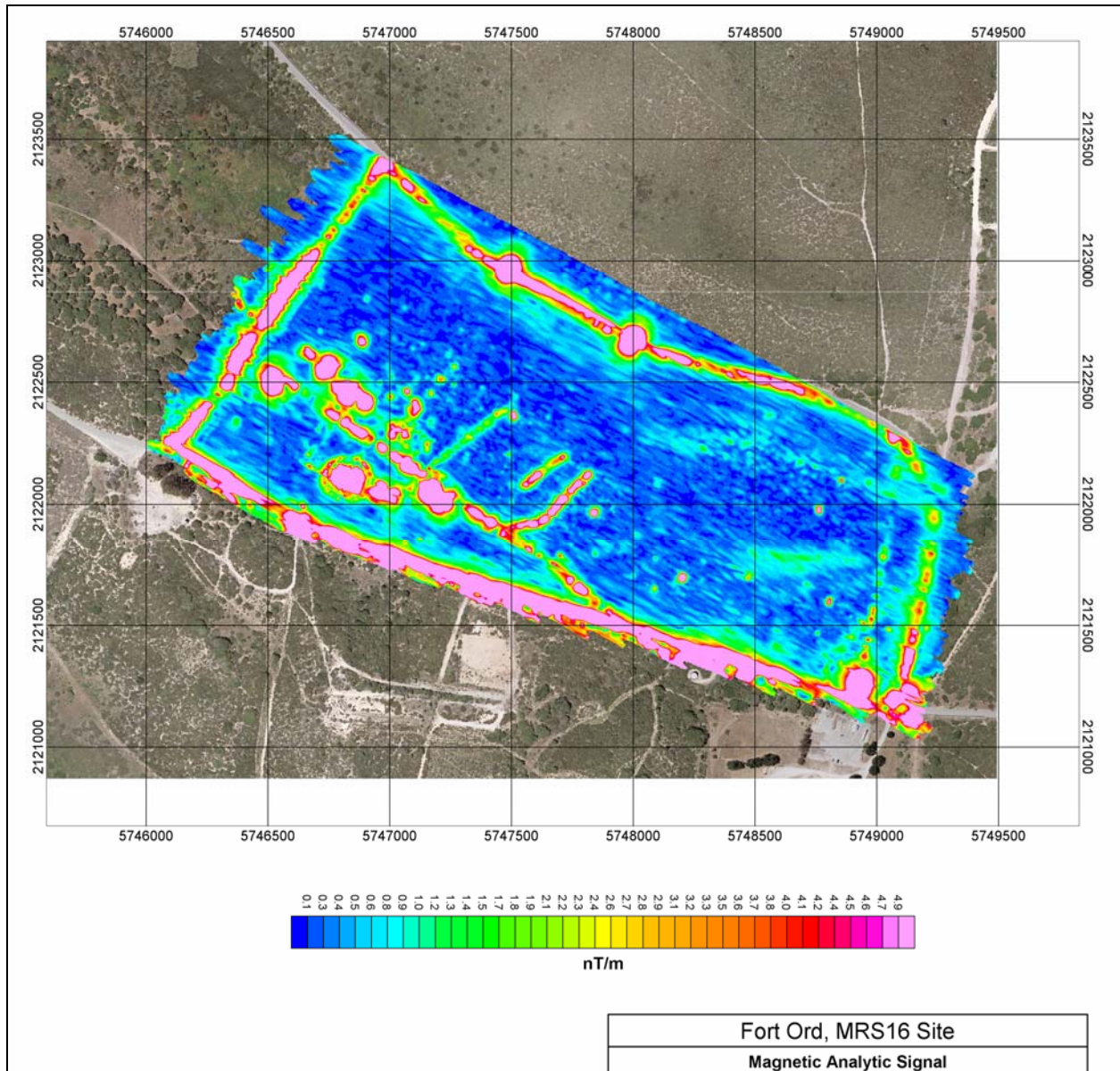


Figure 30. Thumbnail of analytic signal map of the MRS-16 area at Fort Ord.

The Geosoft databases (GDB) are the primary data source. They represent the highest data resolution, but have no visual component. Files are named “ord\_final\_A”, where A designates the survey area covered. Areas include the calibration grid (calgrid), area MRS16, and the main survey block broken roughly into four quadrants (q1, q2, q3, q4). Lines in the database represent the trace of a single sensor as it travels down the line. Lines are numbered “Q####.S”, where Q is the quadrant number, #### is the survey line number, and S is the sensor number (0-7 from left to right across the array). Data columns or channels in the database are:

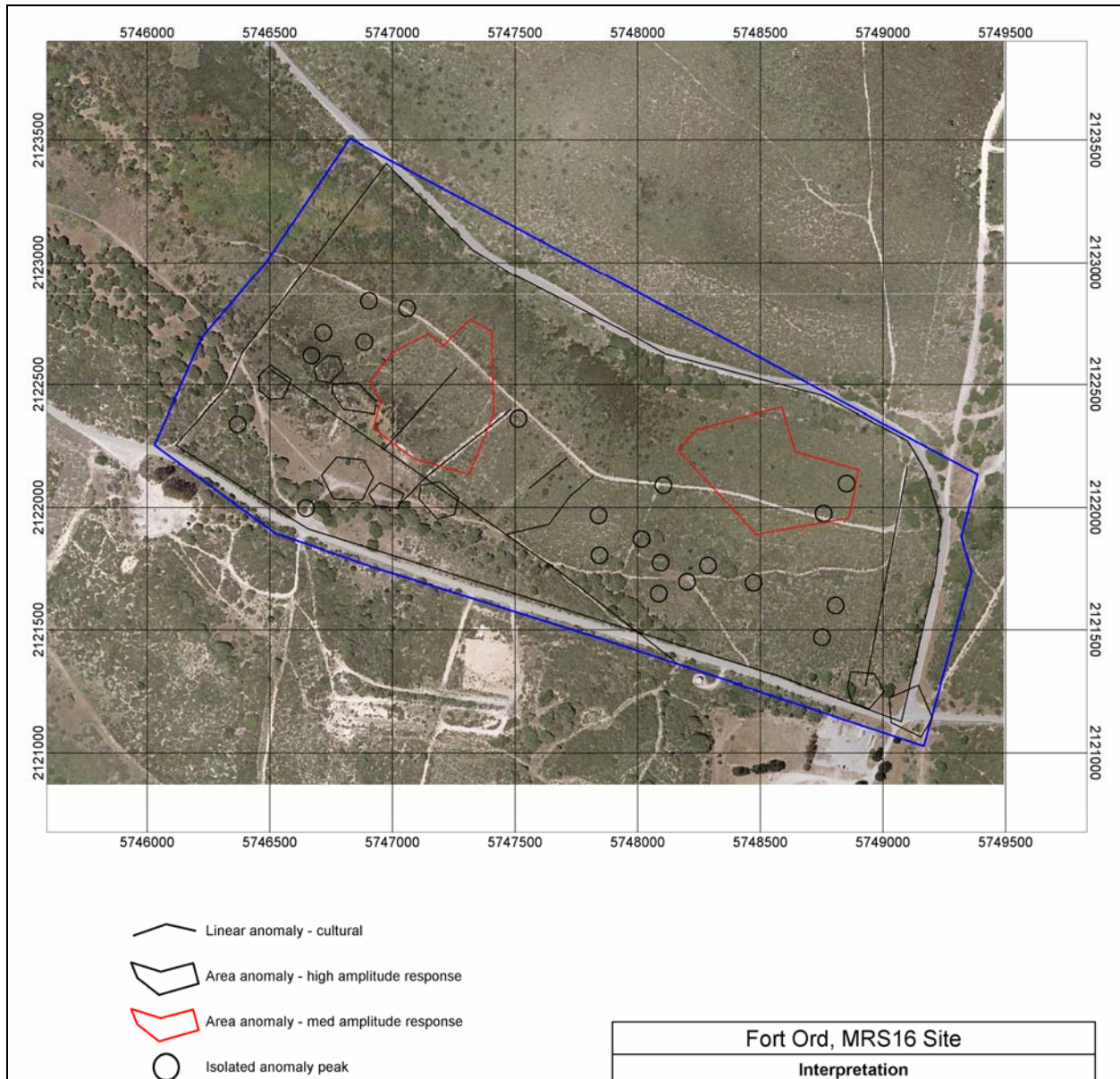


Figure 31. Thumbnail of interpretation map of the MRS-16 area at Fort Ord.

- X\_UTM – Easting coordinate in NAD83 UTM Zone 10N meters.
- Y\_UTM – Northing coordinate in NAD83 UTM Zone 10N meters.
- Z\_agl – Sensor altitude above ground level in meters.
- Mag\_tf – Total field magnetic values in nanoTesla.
- Mag\_resid – Residual total field magnetic values in nanoTesla.

The Geosoft grids (GRD) are the database values interpolated onto a regular grid for contouring and visualization. Additional products such as vertical gradient and analytic signal are calculated exclusively in gridded format. Gridded data use the naming convention “A\_PROD\_SPC”, where A is the survey area (calgrid, MRS16, ord). The calibration grid data are

divided into three heights of 5, 10, and 15 ft AGL. PROD is the data product as described in the bullets below. The SPC extension is included to remind users that the coordinates for the gridded data use the California State Plane Coordinates, NAD83 Zone4, U.S. survey feet.

- TF – Total field magnetic values in nanoTesla
- VGhi – Vertical gradient values above 5-m sensor height in nanoTesla/meter.
- VGlo4 – Vertical gradient values below 4-m sensor height in nanoTesla/meter.
- VGlo5 – Vertical gradient values below 5-m sensor height in nanoTesla/meter.
- AS – Analytic signal values for all heights in nanoTesla/meter.
- AShi – Analytic signal values above 5-m sensor height in nanoTesla/meter.
- ASlo4 – Analytic signal values below 4-m sensor height in nanoTesla/meter.
- ASlo5 – Analytic signal values below 5-m sensor height in nanoTesla/meter.
- ALT2 – Sensor altitudes AGL in meters.
- DENS – Magnetic anomaly density in peaks/hectare.

Geosoft maps (MAP) present the gridded data at 1:10,000 scale (1:5,000 scale for MRS-16) with orthophoto background, coordinate grids, title blocks, and legends. These are the files that are used for the final data presentation. The naming convention is identical to that of the GRD files, except that the SPC designation has been dropped and interpretation maps (interp) have been added to the product list. TIF files of these maps have been prepared at 150 and 300 dpi. The naming convention is the same as the MAP files with the addition of the image resolution information (\_MAP150 or \_MAP300).

GeoTIF files have been prepared from GRD files at 150-dpi resolution. These are similar to the TIF files described above, except that they include the data only (no orthophoto background, title blocks, etc.) and include supplementary files (IPJ) for georeferencing the images. The naming convention is the same as the GRD files with the addition of the image resolution information (\_DATA150). The prefix DATA has been used to differentiate these files from the TIF of the MAP files, which include background information.

## EM products and interpretation

### Time-domain EM response

ORAGS-TEM data were collected in only two large areas at Fort Ord. The locations of EM Blocks A and B are shown by the red polygons in Figure 2. EM Block A is roughly rectangular and comprises 35 ha. EM Block B is somewhat triangular in shape and comprises 37 ha. EM data were also collected at the geophysical prove-out grid and at a site designated as the resistivity calibration area. Maps were made of EM response in millivolts for data averaged over specific time windows. Table 1 shows details of the six time bins with units in microseconds after the end of the transmitter pulse. Figure 32 shows the typical decay of the EM response over a good conductor. Over most metallic conductors found in EM Blocks A and B, the EM response decays to background levels usually by the fourth time bin, i.e., by about 1.4 milliseconds after transmitter turnoff. However, a few conductors in both areas showed above-background responses through all six time bins.

Table 1. Time bins for ORAGS TEM system.

Time Bin	Decay Samples Averaged	Start Time, $\mu\text{s}$	End Time, $\mu\text{s}$	Mean Bin Time, $\mu\text{s}$
1	1	92.5	92.5	92.5
2	2,3	185	277.5	231
3	4,5,6,7	370	647.5	509
4	8,9,10,11,12,13,14,15	740	1387.5	1064
5	16,17,18,19,20,21,22,23	1480	2127.5	1804
6	24,25	2220	2312.5	2266

Experience with the ORAGS-TEM system in tests at the Badlands Bombing Range led researchers to believe that they might see EM response change with (assumed) changes in soil conductivity (ORNL 2003). At the Badlands Bombing Range, the earliest time gates showed long period variations superimposed on the short period anomalies from UXO. The source of this long period variation was never firmly established. At Fort Ord neither of the EM survey blocks shows unambiguous responses from soil cover. All anomalies appear to be produced by large metallic debris, or collections thereof. Most of the time the high-altitude EM background was virtually indistinguishable from the EM response near the ground surface in areas clear of large conductors. Figure 33 shows

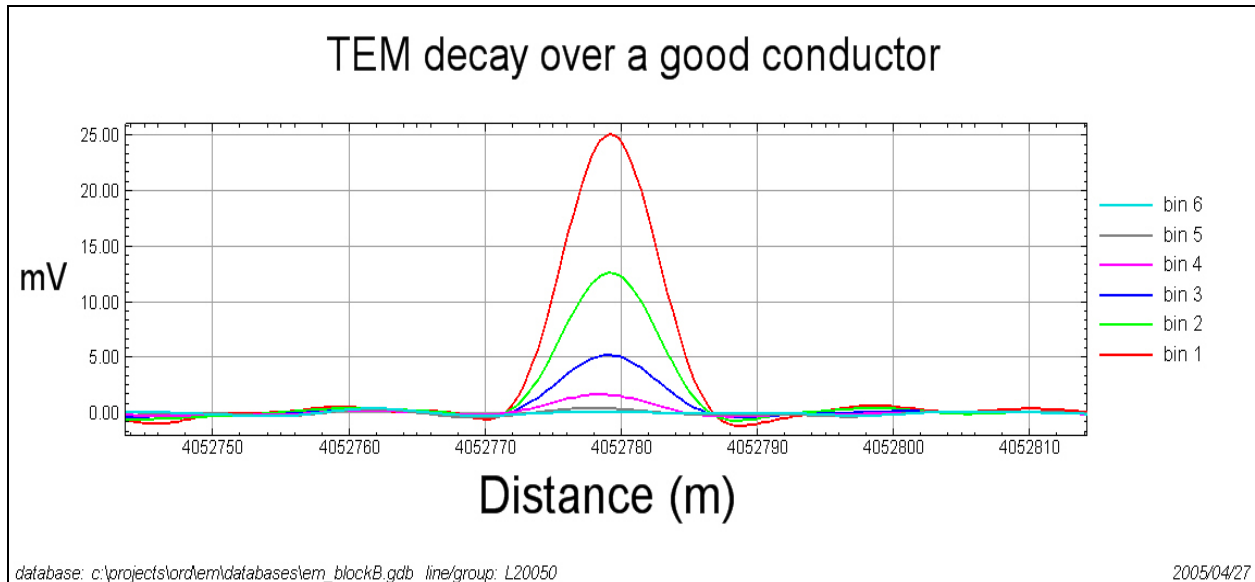


Figure 32. Typical EM response over a metallic conductor. Time bins correspond to those listed in Table 1.

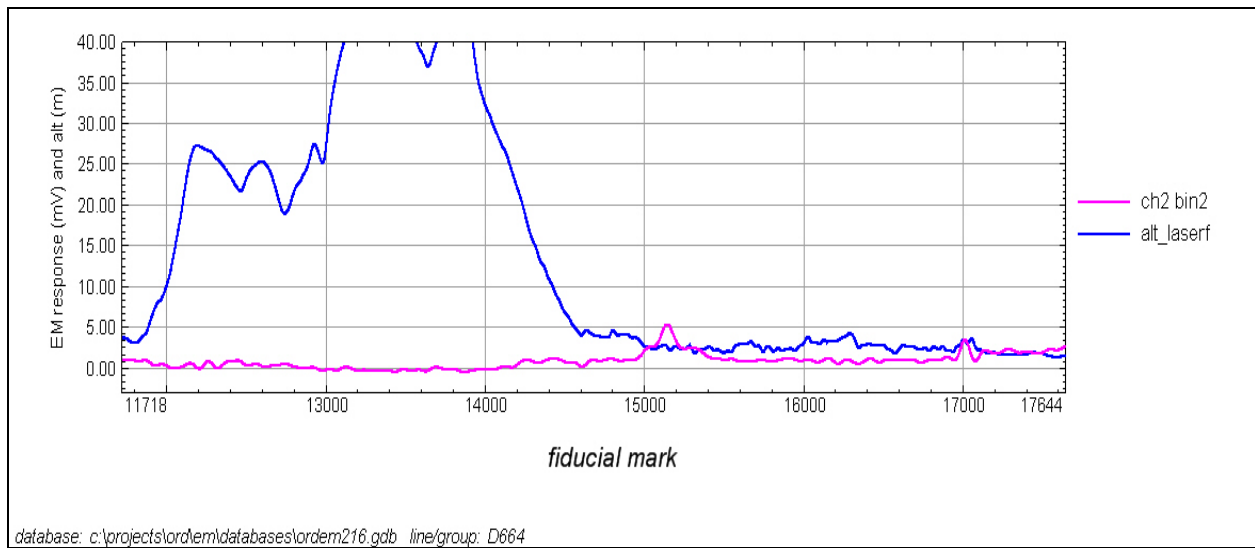


Figure 33. Insensitivity of Fort Ord soils to ORAGS-TEM. The EM response near the ground (fids 15000-17000) is virtually the same as the at-altitude response (fids 13000-14000).

data from time bin 2 (185  $\mu$ s after transmitter turnoff) collected along a survey line at an altitude of about 2 m AGL and also along a high-altitude background excursion at over 80 m AGL. The mean millivolt response at 2 m is virtually indistinguishable from the high-altitude millivolt response. Based on this and other results, it was concluded that it would not be possible to use the Fort Ord TEM data for ground conductivity mapping.

### Interpretation of EM data

For small targets and small transmitter and receiver coils, the EM response falls off with coil-to-target separation  $R$  at about  $1/R^6$ . The ORAGS-TEM system has a transmitter that is large with respect to the UXO target, and researchers found that fields from most UXO sources decay as  $1/R^5$  to  $1/R^4$ , a rate that is nonetheless more extreme than the  $1/R^3$  falloff in the case of magnetic fields. The ORAGS-TEM system therefore shows even more height dependence than do the magnetic systems. This is particularly apparent in EM Block A, where taller vegetation forced higher survey altitudes (3 to 5 m AGL) in the southwest half of the area. On this side of the survey block there are virtually no anomalies, as can be seen in Figure 34, which shows the EM response of time bin 2. On the northeast half, where survey heights were generally at or below 2 m AGL, EM anomalies are prevalent. Most sources appear to be from clusters of UXO rather than individual items.

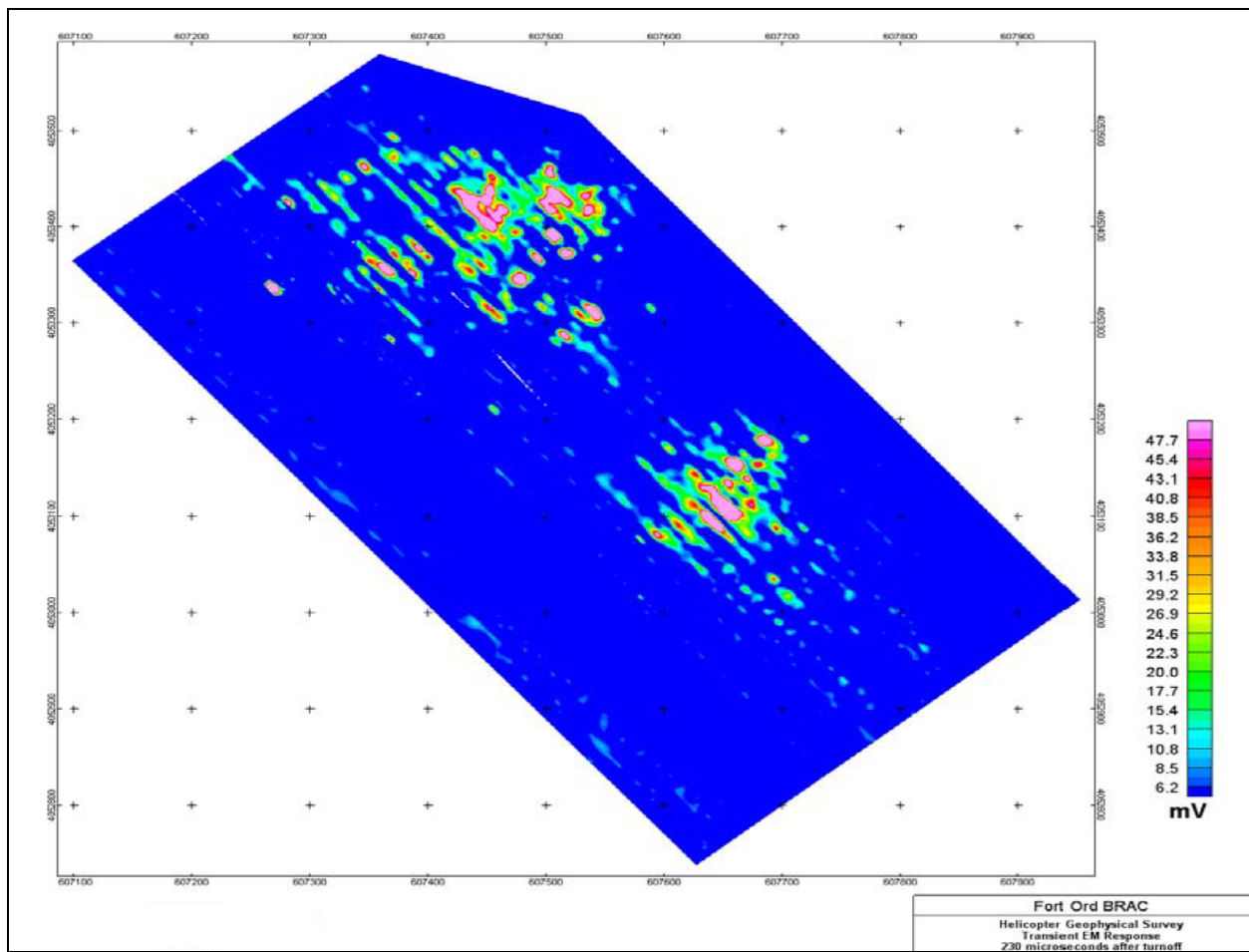


Figure 34. EM response of EM Block A, 230  $\mu$ s after transmitter turnoff (time bin 2).

Comparing the EM map with the analytic signal map derived from magnetic field data over EM Block A, it can be seen that the analytic signal appears more sensitive to smaller items than does the EM system. The analytic signal shown in Figure 35 shows small anomalies even over the southwest half of the area where survey heights were in the vicinity of 5 m. The EM map also appears more striped than the analytic signal map. The magnetic sensors were 1.7 m apart, and the change in signal between adjacent sensors from height differences is small. In contrast, the centers of the port and starboard EM receivers were 10 m apart, and small changes in helicopter roll can produce substantial EM response differences. For example, a 2-deg roll can produce a 24-cm height difference in the receivers. This can in turn produce up to a 100 percent difference in the EM responses of the port and starboard sensors. These line-to-line response differences cause the EM anomalies to appear discontinuous and give the two-receiver data a corrugated or striped appearance.

The situation in EM Block B is similar to that of EM Block A. Again, the EM data mainly show what appear to be concentrations of UXO or scrap, and do not show small individual items. A comparison of the EM bin 2 response in Figure 36 with the analytic signal in Figure 37 shows that virtually every clearly visible EM anomaly corresponds to a large analytic signal anomaly. Ordnance *concentrations* can be well-located using the Fort Ord EM data. It is the small individual ordnance items that are difficult for EM to define in the Fort Ord data sets. Survey altitudes in EM Block B ranged from 1 m to over 7 m, and averaged 2.6 m AGL.

In tests at the Badlands Bombing Range, individual M-38 practice bombs were clearly visible in low-altitude data (Beard et al. 2004), and items as small as 81-mm mortars could be detected, although less consistently. However, at Fort Ord, taller vegetation and rougher topography forced the pilot to consistently fly above 2.5 m AGL, and at these heights items smaller than individual bombs cannot be seen. However, clusters of clutter – the focus of this project – can still be readily discerned.

Another problem with the Fort Ord EM data was a variable period oscillation that appeared in the data, the source of which has not yet been ascertained. The most likely sources are either an overdriven transmitter, or boom vibration. In some cases the oscillation is substantial – over 10 mV – and could hide small anomalies produced by individual ordnance items.

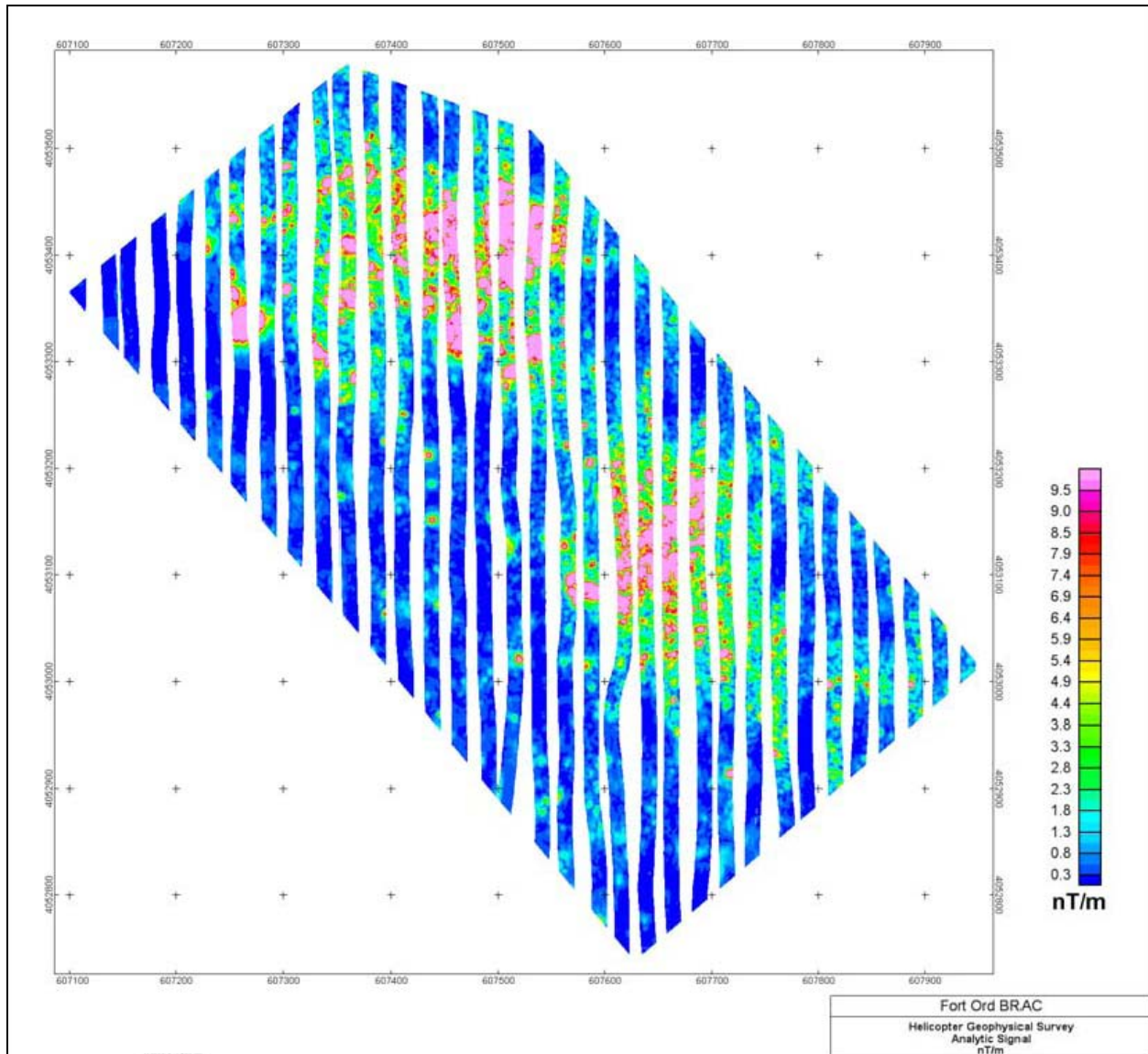


Figure 35. Analytic signal of total magnetic field measured over EM Block A.

All EM maps for EM Blocks A and B, including EM sensor altitude and a comparison with analytic signal, are shown in Appendix B.

### EM data and image archive

Geosoft format files were provided from ORNL to ERDC, Vicksburg, as the principal digital format. This includes database files with georeferenced point data (GDB), and interpolated grid files (GRD). Copies of map data were provided as image files in JPG format in addition to the smaller reproductions included in this report. These maps have a digital resolution of 100 dpi. Eight JPG files have been made for both of the EM survey

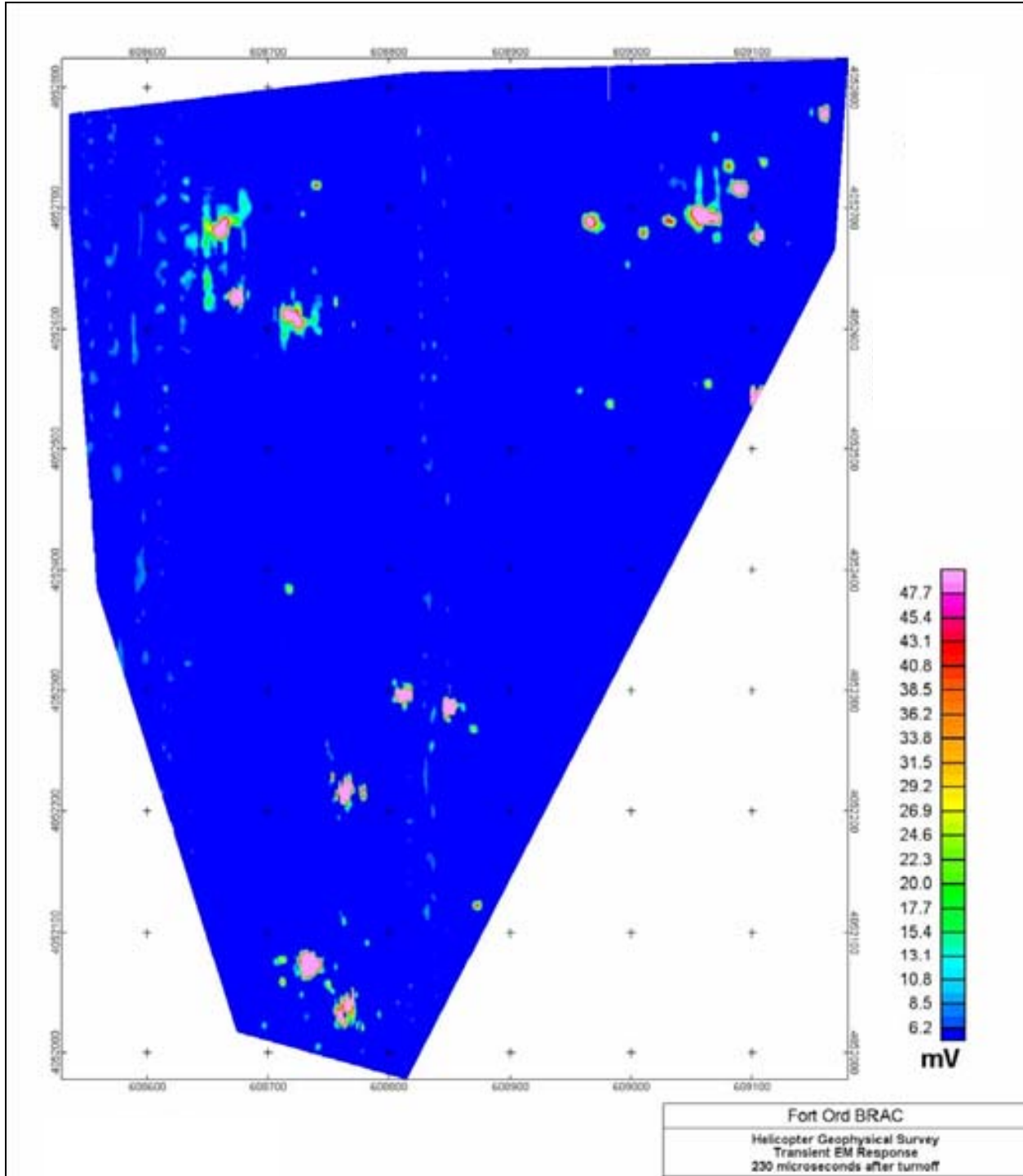


Figure 36. EM response of EM Block B, 230  $\mu$ s after transmitter turnoff (time bin 2).

areas: six EM response bins, altitude, and analytic signal. The EM response files are named to describe time bin and the survey block, e.g., em1A.jpg.

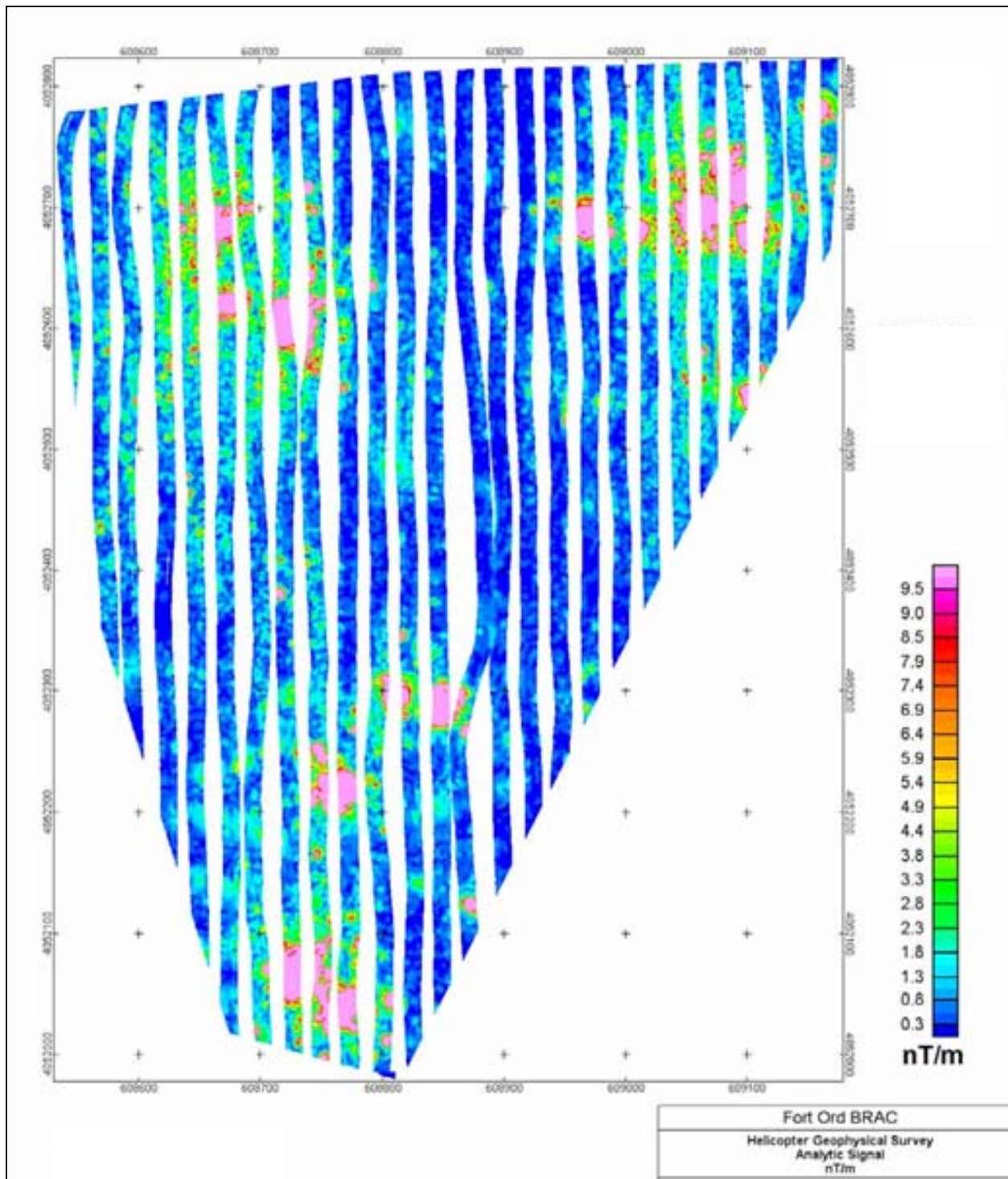


Figure 37. Analytic signal of total magnetic field measured over EM Block B.

The Geosoft databases (filename.gdb) containing the electromagnetic data are named after the 100-acre areas where EM data were collected. They are “EM\_blkA.gdb” and “EM\_blkB.gdb”. Lines in the database represent the trace of a single sensor as it travels down the line. Data columns or channels in the database are shown below:

- Xm – Easting coordinate in NAD83 UTM Zone 10N meters.
- Ym – Northing coordinate in NAD83 UTM Zone 10N meters.
- date – year/month/day.
- hae – Sensor height above ellipsoid.
- alt – Sensor altitude above ground level in meters.
- gps\_synch – GPS synchronized time in seconds.
- line – Flight line number.
- line2 – Flight line number with receiver indicator (0, port; 1, starboard).
- em1ffB – Levelled, filtered EM channel 1—93  $\mu$ s after transmitter turnoff.
- em2ffB – Levelled, filtered EM channel 2—230  $\mu$ s after transmitter turnoff.
- em3ffB – Levelled, filtered EM channel 3—510  $\mu$ s after transmitter turnoff.
- em4ffB – Levelled, filtered EM channel 4—1065  $\mu$ s after transmitter turnoff.
- em5ffB – Levelled, filtered EM channel 5—1085  $\mu$ s after transmitter turnoff.
- em6ffB – Levelled, filtered EM channel 6—2270  $\mu$ s after transmitter turnoff.

Geosoft grid files (filename.grd) are the database values interpolated onto a regular grid for contouring and visualization. The grids are NAD83 Zone 10N, meters. Grids were made for the two survey areas: Block A and Block B. The eight grids for each block consist of one altitude grid, an analytic signal magnetic grid, and grids for each of the six time bins. For example, “em1ffB\_A.grd” represents the grid for time bin 1 in Block A.

Geosoft maps (filename.map) present the gridded data at 1:2500 scale with coordinate grids, title blocks, and legends. These are the files that are used for the final data presentation. The maps for the six EM time bins are named according to time bin and block. For example, the EM response of time bin 3 in block B is em3\_B.map.

## Conclusions

The survey at Fort Ord consisted of a 1281-ha magnetic survey using the transect survey method on alternating lines (providing an effective coverage of 2562 ha when interpolating between transects). Rough topography and tall vegetation increased flight height and reduced the survey data coverage from 50 to 42 percent of the effective total. Clusters of ordnance,

however, represent a legitimate target for this technology over the entire 2562 ha, allowing for interpolation between lines and across gaps caused by increased flight height.

A 72-ha electromagnetic survey was also conducted within the main area and was flown at full density (10-m line spacing). In addition, a supplemental 41-ha magnetic survey was flown at the MRS-16 area at full coverage (100 percent at 1.7-m line spacing) at the request of the Fort Ord BRAC Office. A well-established and documented geophysical prove-out site containing inert ordnance items was used as calibration targets for this survey.

Map products that were developed for the main magnetic survey area included total magnetic field, vertical magnetic gradient, analytic signal, anomaly density, and interpretation maps. These are suitable for ground followup and other analyses intended to understand the relationship between potential energetic compounds and the presence of clusters of ordnance debris. The airborne data are NOT suitable for declaring an area free of contamination, as individual, isolated ordnance types can fall below the detection threshold of the system and not be detected. This is particularly true for the transect method that was employed in the main survey area at Fort Ord, in which only about half of the area of interest was surveyed. Further, areas of rough topography or tall vegetation forced increased flight height in those areas (as in the MRS-16 area), and rendered a portion of the data unsuitable for detection of the targets of interest. These factors are consistent with the goal of the project, which was to delineate areas of magnetic anomalies, many of which may be indicative of targets where an abundance of explosive compound contaminants may be found.

In general, the survey height in the MRS-16 area was too great to discriminate individual objects. Clusters of objects may also be masked at this altitude. Infrastructure such as fences and roads is the most likely source of the observable anomalies; however, there are about a dozen small, discrete anomalies that should be assessed. Several discrete anomalies outside the moderate intensity polygons are recommended for assessment by the BRAC Office.

The ORAGS-TEM system shows even more height dependence than the magnetic system. This is particularly apparent in EM Block A, where taller vegetation forced higher survey altitudes (3 to 5 m AGL) in the southwest

half of the area. On this side of the survey block there were virtually no anomalies. On the northeast side, where survey heights were generally at or below 2 m AGL, EM anomalies were prevalent. Sources appeared to be both clusters of UXO and individual items.

Data, survey results, and all associated information obtained during the course of the project were made available to the ERDC, Vicksburg, and the Fort Ord BRAC Office for use by various project team members, including explosive ordnance disposal technicians and contractors.

Also, during the course of this project, several ORNL project staff moved from ORNL to Battelle, where they continued to work on this project. At the time of the writing of this report, all project staff had successfully moved from ORNL to Battelle, thereby completing the commercialization of the technology from a government laboratory (ORNL) to a private sector firm (Battelle).

### **3 Soil Sampling and Analysis, Fort Ord, CA**

Chapter 3 described the analysis of the airborne magnetometer data collected at Fort Ord for delineating locations of UXO contamination as evidenced by concentrations of surface and buried intact ordnance and ordnance fragments. This chapter describes the soil sampling procedure and analysis at these locations.

#### **Soil sampling**

The locations developed from the airborne magnetometer data were located using a Trimble ProXR GPS with a TSC1 data collector (with about 1 m accuracy), a 5-m by 5-m grid was established on a north-south axis with the indicated position as the center point. Soil samples were collected in each grid by combining 25 increments from the surface to a 2.5-cm depth. Because the soil texture differed substantially from grid to grid, some samples were collected using a metal scoop, manufactured by AMS, and others were collected using a soil corer developed by Walsh (Walsh et al. 2004). The individual increments within the grid were collected using a systematic sampling pattern with a random starting point (Hewitt et al. 2005). This sampling design is referred to as a systematic-random design. Three replicate grid samples were collected in 19 randomly selected grids divided evenly among the six classes established from the magnetometer data (see Chapter 3). In grids 44 and 63, replicate samples were collected using both scoops and corers.

#### **Soil sample processing**

All soil samples were returned to the ERDC Cold Regions Research and Engineering Laboratory by overnight carrier. Samples were air-dried in the laboratory and passed through a 10-mesh (2-mm) sieve to remove oversized material. The < 2-mm fraction was ground on a Lab TechEssa LM2 (LabTech Essa Pty. Ltd., Bassendean, WA, Australia) puck-mill grinder for 90 seconds, which reduced the particle size of the material to a flour (< 70  $\mu\text{m}$ ). After grinding, samples were mixed thoroughly and spread to form a 1-cm-thick layer; subsamples were obtained by collecting 30 increments randomly through the entire thickness of the layer of ground material to obtain a subsample mass of about 10 g. Triplicate laboratory subsamples were obtained from the ground soil samples from grids 44, 63, and 74.

The 10-g portions of soil were extracted on a shaker table for 18 hr using 20 mL of acetonitrile. The extracts were filtered by passing each through a Millex-FH PTFE 0.45 syringe filter (Millipore Corp.). For gas chromatograph – electron capture detector (GC-ECD) analysis, this extract was injected without further dilution. For reverse phase – high performance liquid chromatographic – ultraviolet (RP-HPLC-UV) analysis, this extract was diluted 1 to 3 with deionized water to match the solvent strength of the HPLC eluent.

## Extract analysis

All sample extracts except those from grids 63, 65, and 68 were analyzed by GC-ECD according to Environmental Protection Agency (EPA) SW846 Method 8095 (U.S. EPA 1999). Extracts from grids 63, 65, 68, and others in which the GC-ECD analysis indicated that extract concentrations were greater than 0.5 mg/L, or there appeared to be interferences in the GC-ECD analyses, were analyzed by RP-HPLC-UV according to EPA SW846 Method 8330 (U.S. EPA 1994).

The GC-ECD analyses were conducted on an HP 6890 gas chromatograph equipped with a micro ECD detector. Direct injection of 1  $\mu$ L of soil extract was made into a purged packed inlet port (250 °C) equipped with a deactivated Restek Uniliner. Primary separation was conducted on a 6-m  $\times$  0.53-mm ID fused-silica column, with a 0.5- $\mu$ m film thickness of 5 percent diphenyl–95 percent dimethyl polysilicate (Rtx<sup>®</sup>-5, Restek, Bellefonte, PA). The GC oven was temperature-programmed as follows: 100 °C for 2 min, 10 °C/min ramp to 280 °C. The carrier gas was hydrogen at 10 mL/min (linear velocity approximately 90 cm/sec). The ECD detector temperature was 310 °C and the makeup gas was nitrogen flowing at 45 mL/min. All GC-ECD samples were reanalyzed on a confirmation column, 6 m  $\times$  0.53 mm ID having a 1.5- $\mu$ m film thickness of a proprietary polymer (Rtx-TNT-2 from Restek). The GC oven was temperature-programmed as follows: 130 °C for 1 min, 10 °C /min ramp to 280 °C. The carrier gas was helium at 20 mL/min (linear velocity approximately 180 cm/sec) and the nitrogen makeup gas was flowing at 60 mL/min. Inlet and detector temperatures were the same as above. Multianalyte standards were purchased from Restek, and the instrument was calibrated over five concentrations. Because of interferences, the detection limits for GC-ECD analysis was raised to 0.02 mg/kg.

HPLC analysis was conducted on a modular RP-HPLC system from Thermo Finnigan composed of a SpectraSYSTEM Model P1000 isocratic pump, a SpectraSYSTEM UV2000 dual wavelength UV/VS absorbance detector set at 210 and 254 nm (cell path 1 cm), and a SpectraSYSTEM AS300 auto sampler. Samples were introduced by overfilling a 100- $\mu$ L sampling loop. Separations were made on a 15-cm  $\times$  3.9-mm (4- $\mu$ m) NovaPak C-8 column (Waters Chromatography Division, Milford, MA) maintained at 28 °C and eluted with 15:85 isopropanol/water (v/v) at 1.4 mL/min. Concentrations were estimated from peak heights compared to commercial multianalyte standards (Restek). Detection limits for RP-HPLC analyses were also 0.02 mg/kg for all target analytes. The target analytes for both GC-ECD and RP-HPLC analyses were the 14 energetic compounds of SW846 Method 8330 (U.S. EPA 1994) with the addition of nitroglycerin.

## QA/QC

The total uncertainty in the characterization results was investigated by collecting triplicate 25-increment samples in grids 7, 8, 12, 13, 23, 31, 34, 43, 44, 53, 63, 65, 69, 72, 74, 84, 85, 98, and 99. Most of the total uncertainty is expected to be due to sampling error. To evaluate the uncertainty due to laboratory processing and analysis, triplicate laboratory subsamples from grids 44, 63, and 74 were analyzed. An attempt was made to compare results for samples collected with scoops and corers as well by collecting replicate samples using both approaches in grids 8, 12, and 44. However, these samples were largely blank with respect to the detection of energetic compounds.

Six blank soils were processed along with the soil samples from Fort Ord. Three control spike samples were processed as well. Analyte concentrations for all six blanks were less than 0.01 mg/L (Table 2). Only one of the spike samples was analyzed along with the sample extracts and the results indicated that analyte recoveries ranged from 89.6 to 119 percent with a mean recovery of 99.6 percent.

Results from the analysis of laboratory triplicate subsamples for samples from grids 44, 63, and 74 are presented in Table 3. The results for subsamples from Grid 44 were generally less than the detection limit of 0.02 mg/kg. For grids 63 and 74, however, TNT, 4-Am-DNT, and 2-Am-DNT were detected in all replicates above the 0.02-mg/kg limit.

**Table 2. Results from analysis of blank samples and blank spiked sample conducted with soil samples from Fort Ord, May 9-10, 2005.**

Sample	Extract Concentration, mg/L									
	NG	2,6-DNT	2,4-DNT	1,3,5-TNB	TNT	RDX	4 Am-DNT	2 Am-DNT	Tetryl	HMX
ORD-BIk4	<0.01	<0.01	<0.01	<0.01	<0.01	<0.01	<0.01	<0.01	<0.01	<0.01
ORD-BIk5	<0.01	<0.01	<0.01	<0.01	<0.01	<0.01	<0.01	<0.01	<0.01	<0.01
ORD-BIk6	<0.01	<0.01	<0.01	<0.01	<0.01	<0.01	<0.01	<0.01	<0.01	<0.01
ORD-BIk1	<0.01	<0.01	<0.01	<0.01	<0.01	<0.01	<0.01	<0.01	<0.01	<0.01
ORD-BIk2	<0.01	<0.01	<0.01	<0.01	<0.01	<0.01	<0.01	<0.01	<0.01	<0.01
ORD-BIk3	<0.01	<0.01	<0.01	<0.01	<0.01	<0.01	<0.01	<0.01	<0.01	<0.01
ORD-LCS1 (Conc.=0.050 mg/L)*		0.0466	0.0476	0.0471	0.0490	0.0448	0.0598	0.0486	0.0490	0.0533
% recovery		93.2	95.2	94.2	98.0	89.6	119.6	97.2	98.0	106.6

\* LCS = laboratory control sample.

**Table 3. Results from analysis of replicate laboratory subsamples.**

Grid #	Replicate Type	Concentration, mg/kg								
		TNT	RDX	Tetryl	1,3,5-TNB	4-Am-DNT	2-Am-DNT	NG	2,4-DNT	HMX
ORD-044 Ax	Lab Rep	<d	<d	<d	<d	<d	<d	<d	<d	<d
ORD-044 Ay	Lab Rep	<d	<d	<d	<d	<d	<d	<d	<d	<d
ORD-044 Az	Lab Rep	<d	<d	<d	<d	<d	<d	<d	<d	<d
ORD-044 Bx	Lab Rep	<d	<d	0.151	<d	<d	<d	<d	<d	<d
ORD-044 By	Lab Rep	<d	<d	<d	<d	<d	<d	<d	<d	<d
ORD-044 Bz	Lab Rep	<d	<d	<d	<d	<d	<d	<d	<d	<d
ORD-044 Cx	Lab Rep	<d	<d	<d	<d	<d	<d	<d	<d	<d
ORD-044 Cy	Lab Rep	<d	<d	<d	<d	<d	<d	<d	<d	<d
ORD-044 Cz	Lab Rep	<d	<d	<d	<d	<d	<d	<d	<d	<d
ORD-063 A1x	Lab Rep	1.136	<d	0.015	<d	0.082	0.078	<d	<d	<d
ORD-063 A1y	Lab Rep	1.162	<d	<d	<d	0.086	0.070	<d	<d	<d
ORD-063 A1z	Lab Rep	1.148	<d	<d	<d	0.090	0.078	<d	<d	<d
	Mean	1.149				0.086	0.075			
Stats-063A1	SD	0.013				0.004	0.005			
	%RSD	1.133				4.651	6.131			
ORD-063 A2x	Field & Lab Reps	0.042	<d	<d	<d	0.060	0.060	<d	<d	<d
ORD-063 A2y	Field & Lab Reps	0.038	<d	<d	<d	0.048	0.052	<d	<d	0.020
ORD-063 A2z	Field & Lab Reps	0.032	<d	<d	<d	0.042	0.064	<d	<d	0.030
	Mean	0.037				0.050	0.059			
Stats-063A2	SD	0.005				0.009	0.006			
	%RSD	13.482				18.330	10.415			
ORD-063 A3x	Field & Lab Reps	2.420	<d	<d	<d	0.138	0.136	<d	<d	<d
ORD-063 A3y	Field & Lab Reps	2.640	<d	<d	<d	0.148	0.132	<d	<d	<d

Grid #	Replicate Type	Concentration, mg/kg								
		TNT	RDX	Tetryl	1,3,5-TNB	4-Am-DNT	2-Am-DNT	NG	2,4-DNT	HMX
ORD-063 A3z	Field & Lab Reps	2.420	<d	<d	<d	0.154	0.132	<d	<d	<d
	Mean	2.493				0.147	0.133			
Stats-063A3	SD	0.127				0.008	0.002			
	%RSD	5.094				5.511	1.732			
ORD-074 Ax	Field & Lab Reps	0.084	<d	<d	<d	0.043	0.027	<d	<d	<d
ORD-074 Ay	Field & Lab Reps	0.072	<d	<d	<d	0.031	0.030	<d	<d	<d
ORD-074 Az	Field & Lab Reps	0.078	<d	<d	<d	0.040	0.027	<d	<d	<d
	Mean	0.078				0.038	0.028			
Stats-074A	SD	0.006				0.006	0.002			
	%RSD	7.539				16.718	6.669			
ORD-074 Bx	Field & Lab Reps	0.028	<d	<d	<d	0.018	0.017	<d	<d	<d
ORD-074 By	Field & Lab Reps	0.034	<d	<d	<d	0.022	0.017	<d	<d	<d
ORD-074 Bz	Field & Lab Reps	0.040	<d	<d	<d	0.032	0.018	<d	<d	<d
	Mean	0.034				0.024	0.017			
Stats-074B	SD	0.006				0.007	0.001			
	%RSD	17.463				29.733	2.882			
ORD-074 Cx	Field & Lab Reps	0.038	<d	<d	<d	0.027	0.021	<d	<d	<d
ORD-074 Cy	Field & Lab Reps	0.040	<d	<d	<d	0.029	0.022	<d	<d	<d
ORD-074 Cz	Field & Lab Reps	0.040	<d	<d	<d	0.031	0.021	<d	<d	<d
	Mean	0.039				0.029	0.021			
Stats-074C	SD	0.001				0.002	0.001			
	%RSD	3.107				7.975	3.023			
Mean %RSD		8.0				13.8	5.1			

The mean relative standard deviations were 8.0 percent for TNT, 13.8 percent for 4-Am-DNT, and 5.1 percent for 2-Am-DNT, indicating the sample processing and subsampling procedures were adequate, even for concentrations that were just above analytical detection limits.

The results from the analysis of field triplicate multi-increment samples from the selective grids are shown in Table 4. In most cases the concentrations of energetic compounds were below a detection limit of 0.02 mg/kg in all three replicates of the field samples. However, in seven of the grids, TNT concentrations were above the detection limit in all three replicates. The %RSD values for these grids varied from 21.9 to 125 percent with a mean value of 57.3 percent. Only the samples from grid 63 had TNT concentrations greater than 1 mg/kg.

Table 4. Results from analysis of replicate multi-increment samples from Fort Ord.

Grid #	Concentration, mg/kg									
	Replicate Type	TNT	RDX	Tetryl	1,3,5-TNB	4-Am-DNT	2-Am-DNT	NG	2,4-DNT	HMX
ORD-023A	Field Reps	0.044	<d	0.098	<d	<d	<d	<d	<d	<d
ORD-023B	Field Reps	0.024	<d	0.124	<d	<d	0.026	<d	<d	<d
ORD-023C	Field Reps	0.022	<d	0.184	<d	<d	0.038	<d	<d	<d
	Mean	0.030		0.135						
Field	SD	0.012		0.044						
	%RSD	40.552		32.591						
ORD-031A	Field Reps	0.107	<d	<d	<d	0.041	<d	1.366	<d	<d
ORD-031B	Field Reps	0.080	<d	<d	<d	0.022	<d	0.436	<d	<d
ORD-031C	Field Reps	0.125	<d	<d	<d	0.057	<d	<d	<d	<d
	Mean	0.104				0.040				
Field	SD	0.023				0.017				
	%RSD	21.861				42.864				
ORD-034A	Field Reps	<d	<d	<d	<d	<d	<d	<d	<d	<d
ORD-034B	Field Reps	<d	<d	<d	<d	<d	<d	<d	<d	<d
ORD-034C	Field Reps	<d	<d	<d	<d	<d	<d	<d	<d	<d
ORD-043A	Field Reps	<d	<d	<d	<d	<d	<d	<d	<d	<d
ORD-043B	Field Reps	<d	<d	<d	<d	<d	<d	<d	<d	<d
ORD-043C	Field Reps	<d	<d	<d	<d	<d	<d	<d	<d	<d
ORD-043D	Field Reps	<d	<d	<d	<d	<d	<d	<d	<d	<d
ORD-044A	Field Reps	<d	<d	<d	<d	<d	<d	<d	<d	<d
ORD-044B	Field Reps	<d	<d	0.05	<d	<d	<d	<d	<d	<d
ORD-044C	Field Reps	<d	<d	<d	<d	<d	<d	<d	<d	<d
ORD-053A	Field Reps	<d	<d	0.224	<d	<d	<d	0.043	<d	<d
ORD-053B	Field Reps	<d	<d	0.238	<d	<d	<d	<d	<d	<d
ORD-053C	Field Reps	<d	<d	1.870	<d	<d	<d	0.029	<d	<d
	Mean			0.777						
Field	SD			0.946						
	%RSD			121.737						
ORD-063A		1.149				0.086	0.08			
ORD-063B		0.037				0.050	0.059			
ORD-063C		2.493				0.147	0.133			
	Mean	1.226				0.094	0.091			
Field	SD	1.230				0.049	0.038			
	%RSD	100.277				51.851	42.0			
ORD-065A	Field Reps	<d	<d	0.088	<d	<d	<d	<d	<d	<d
ORD-065B	Field Reps	<d	<d	0.114	<d	<d	<d	<d	<d	<d
ORD-065C	Field Reps	0.029	<d	0.026	<d	<d	<d	<d	<d	<d
	Mean			0.076						

Grid #	Concentration, mg/kg									
	Replicate Type	TNT	RDX	Tetryl	1,3,5-TNB	4-Am-DNT	2-Am-DNT	NG	2,4-DNT	HMX
Field	SD			0.045						
	%RSD			59.034						
ORD-069A	Field Reps	<d	<d	0.080	<d	<d	<d	<d	<d	<d
ORD-069B	Field Reps	<d	<d	0.083	<d	<d	<d	<d	<d	<d
ORD-069C	Field Reps	<d	<d	<d	<d	<d	<d	<d	<d	<d
ORD-072A	Field Reps	0.058	<d	<d	<d	<d	<d	<d	<d	<d
ORD-072B	Field Reps	0.032	<d	<d	<d	<d	<d	1.386	<d	<d
ORD-072C	Field Reps	0.035	<d	<d	<d	0.038	<d	<d	<d	<d
	Mean	0.041								
Field	SD	0.014								
	%RSD	34.301								
ORD-074A	Field Reps	0.078				0.038	0.028			
ORD-074B	Field Reps	0.034				0.024	0.017			
ORD-074C	Field Reps	0.039				0.029	0.021			
	Mean	0.050				0.030	0.022			
Field	SD	0.024				0.007	0.005			
	%RSD	48.020				23.351	23.705			
ORD-084A	Field Reps	<d	<d	<d	<d	<d	<d	<d	<d	<d
ORD-084B	Field Reps	<d	<d	<d	<d	<d	<d	<d	<d	<d
ORD-084C	Field Reps	<d	<d	<d	<d	<d	<d	<d	<d	<d
ORD-085A	Field Reps	<d	<d	<d	<d	<d	0.020	<d	<d	<d
ORD-085B	Field Reps	<d	<d	<d	<d	<d	0.021	<d	<d	<d
ORD-085C	Field Reps	<d	<d	<d	<d	<d	0.019	<d	<d	<d
	Mean						0.020			
Field	SD						0.001			
	%RSD						5.601			
ORD-098A	Field Reps	<d	<d	<d	<d	<d	<d	<d	<d	<d
ORD-098B	Field Reps	<d	<d	<d	<d	<d	<d	<d	<d	<d
ORD-098C	Field Reps	0.016	<d	<d	<d	<d	<d	<d	<d	<d
ORD-099A	Field Reps	<d	<d	<d	<d	<d	<d	<d	<d	<d
ORD-099B	Field Reps	<d	<d	<d	<d	<d	<d	<d	<d	<d
ORD-099C	Field Reps	<d	<d	<d	<d	<d	<d	<d	<d	<d
<b>Summary of RSD Values for Field Replicates</b>										
		TNT	RDX	Tetryl	1,3,5-TNB	4-Am-DNT	2-Am-DNT	NG	2,4-DNT	HMX
	Max	125.0%	84.1%	122%		51.9%	42%			
	Min	21.9%	84.1%	32.6%		23.4%	5.6%			
	Mean	57.3%	84.1%	71.1%		39.4%	19.9%			





Grid #	Concentration, mg/kg									Total Energetic Conc. mg/kg
	TNT	RDX	Tetryl	1,3,5-TNB	4-Am-DNT	2-Am-DNT	NG	2,4-DNT	HMX	
ORD-072	0.04	<d	<d	<d	0.02	<d	0.46	<d	<d	0.52
ORD-073	0.06	<d	<d	<d	0.04	0.02	<d	<d	<d	0.12
ORD-074	0.05	<d	<d	<d	0.03	0.02	<d	<d	<d	0.10
ORD-075	<d	<d	<d	<d	<d	<d	<d	<d	<d	<0.02
ORD-076	0.04	<d	<d	<d	0.03	<d	<d	<d	<d	0.08
ORD-077	145.40	<d	<d	0.14	1.21	0.94	<d	0.07	<d	147.76
ORD-078	0.95	<d	0.02	<d	0.02	0.02	<d	<d	<d	1.02
ORD-079	0.02	<d	<d	<d	<d	<d	<d	<d	<d	<0.02
ORD-080	<d	<d	<d	<d	<d	0.02	<d	<d	<d	0.02
ORD-081	0.06	<d	<d	<d	0.13	0.15	<d	<d	<d	0.34
ORD-082	<d	<d	<d	<d	<d	<d	<d	<d	<d	<0.02
ORD-084	<d	<d	<d	<d	<d	<d	<d	<d	<d	<0.02
ORD-085	<d	<d	<d	<d	<d	0.02	<d	<d	<d	0.02
ORD-086	<d	<d	<d	<d	<d	<d	<d	<d	<d	<0.02
ORD-088	<d	<d	<d	<d	<d	<d	<d	<d	<d	<0.02
ORD-089	<d	<d	<d	<d	<d	<d	<d	<d	<d	<0.02
ORD-091	0.06	<d	<d	<d	<d	<d	<d	<d	<d	0.06
ORD-092	0.05	<d	<d	<d	0.03	0.02	<d	<d	<d	0.11
ORD-093	7.26	<d	<d	<d	0.21	0.23	<d	<d	<d	7.70
ORD-094	<d	<d	<d	<d	<d	<d	<d	<d	<d	<0.02
ORD-095	0.03	<d	<d	<d	<d	<d	<d	<d	<d	0.03
ORD-096	<d	<d	<d	<d	<d	<d	<d	<d	<d	<0.02
ORD-098	<d	<d	<d	<d	<d	<d	<d	<d	<d	<0.02
ORD-099	<d	<d	<d	<d	<d	<d	<d	<d	<d	<0.02
ORD-100	<d	<d	<d	<d	<d	<d	<d	<d	<d	<0.02
ORD-101	<d	<d	<d	<d	<d	<d	<d	<d	<d	<0.02
ORD-102	<d	<d	<d	<d	<d	<d	<d	<d	<d	<0.02
ORD-103	<d	<d	<d	<d	<d	<d	<d	<d	<d	<0.02
Maximum Concentration, mg/kg	145.40	0.08	1.99	0.14	1.21	0.94	0.06	0.07	0.02	147.76
Reporting Limits, mg/kg	d=0.02	d=0.02	d=0.02	d=0.02	d=0.02	d=0.02	d=0.02	d=0.02	d=0.02	

The energetic compound most often found in these samples was TNT, which was detected in 43 of the 92 grids sampled with concentrations ranging from below the detection limit of 0.02 to as high as 145 mg/kg for grid 077. However, only four grids (022, 063, 077, 093) had TNT concentrations above 1 mg/kg. The next most frequently detected energetic compound was tetryl, which was detected in 26 of the 93 grids. The maximum concentration detected for tetryl was 1.99 mg/kg for grid 055, but only grids 054 and 055 had tetryl concentrations above 1 mg/kg. Tetryl is no longer used as a high explosive, but prior to 1977, it was used in concert with TNT in an explosive called tetratol. The next most often detected were

4-Am-DNT and 2-Am-DNT, which were found in 22 and 18 grids, respectively, with maximum concentrations of 1.21 and 0.94 mg/kg. Also detected was 1,3,5-TNB, but only in two grids with a maximum concentration of 0.14 mg/kg. The compounds 4-Am-DNT, 2-Am-DNT, and 1,3,5-TNB are environmental transformation products of TNT. Also detected in one grid was 2,4-DNT with a concentration of 0.07 mg/kg. It is a manufacturing impurity in the production of TNT. Nitroglycerin was detected in four grids, but the maximum concentration detected was only 0.06 mg/kg. RDX and HMX were detected in two grids and one grid, respectively, with maximum concentrations of 0.08 and 0.02 mg/kg. Overall, the concentrations of these energetic compounds were quite low compared with concentrations found at other artillery range impact areas (Jenkins et al. in press). The Fort Ord range has been closed for over 10 years, and most of the surface debris has been removed. Thus, only in a few instances were researchers able to find locations of targets, and, in most cases, researchers were not able to visually locate areas and collect samples in areas where the highest concentrations were expected to be present.

## 4 Statistical Analyses

The data collected from the soil sampling and airborne magnetometer were statistically analyzed using scatterplots and parametric, nonparametric, and logistic analyses to determine if any relationship existed between the mean analytic signal measured by the airborne magnetometer and the total energetic content of the soil. The results are presented in this chapter. The raw data used in the analyses, as well as SAS programs and associated log files, are listed in Appendices C–F.

Table 6 summarizes the data used in the statistical analyses. The dependent variable in the statistical analyses was the total energetic content of the soil (ENERGETICS). This variable is the sum of the individual energetic components detected [ENERGETICS = (TNT + RDX + TETRYL + TNB\_135 + DNT\_4\_AM + DNT\_2\_AM + DNT\_2\_4 + NG + HMX)]. One independent variable of the statistical analyses was the mean analytic signal from the airborne magnetometer within the 5 m × 5 m sampling sites (MEAN). The other independent variable was GRIDCODE, which represents the six ranges of analytic signal used to develop the soil sampling plan (see Chapter 3).

Table 6. Listing of data used in statistical analyses.

Obs #	GRIDCODE	MEAN ANALYTIC SIGNAL, nT/m	IDENTIFIER FOR SAMPLING SITES	ENERGETICS mg/kg	DETECTABLE
1	1	0.5975	1	0	NO
2	1	0.3735	2	0	NO
3	1	0.9051	3	0	NO
4	2	3.64	4	0	NO
5	3	6.3144	5	0	NO
6	1	0.4086	6	0.032	YES
7	4	17.329	7	0.024	YES
8	5	23.383	8	0.015	NO
9	5	28.2375	9	0	NO
10	3	5.5343	10	0.402	YES
11	5	25.8849	11	0.155	YES
12	2	2.016	12	0.13	YES
13	6	68.7318	13	0.208	YES
14	3	5.5446	14	0.02	NO
15	2	3.5198	15	0.02	YES
16	5	29.8993	16	0.23	YES

Obs #	GRIDCODE	MEAN ANALYTIC SIGNAL, nT/m	IDENTIFIER FOR SAMPLING SITES	ENERGETICS mg/kg	DETECTABLE
17	2	3.0913	17	0.02	NO
18	4	11.2894	18	0.066	YES
19	5	19.5779	19	0.165	YES
20	5	27.6896	20	0.158	YES
21	3	5.3924	21	0.028	YES
22	2	3.8342	22	2.752	YES
23	5	22.3613	23	0.191	YES
24	4	14.1836	24	0.038	YES
25	6	76.2974	25	0.079	YES
26	6	34.4811	26	0.032	YES
27	5	20.1159	27	0.02	NO
28	4	12.2318	28	0.197	YES
29	4	17.1124	29	0	NO
30	3	6.7223	30	0.04	YES
31	3	7.1761	31	0.74	YES
32	2	1.9434	32	0	NO
33	4	12.5499	33	0	NO
34	1	0.3073	34	0	NO
35	5	21.2925	35	0.135	YES
36	6	35.1617	36	0	NO
37	5	26.3907	39	0.214	YES
38	3	9.309	40	0.336	YES
39	4	15.8233	41	0	NO
40	6	36.2997	42	0	NO
41	3	5.378	43	0	NO
42	6	48.5423	44	0.02	YES
43	3	7.7568	45	0.152	YES
44	2	1.8374	46	0.384	YES
45	6	37.8995	50	0.248	YES
46	5	23.8641	51	0.259	YES
47	4	13.5964	52	0.224	YES
48	2	2.7404	53	0.807	YES
49	2	2.475	54	1.97	YES
50	5	27.2801	55	2.122	YES
51	2	2.8409	56	0.252	YES
52	4	15.8211	58	0.276	YES
53	3	5.4322	61	0.246	YES
54	3	6.0226	62	0.082	YES
55	6	47.955	63	1.41	YES
56	6	34.6362	64	0.816	YES

Obs #	GRIDCODE	MEAN ANALYTIC SIGNAL, nT/m	IDENTIFIER FOR SAMPLING SITES	ENERGETICS mg/kg	DETECTABLE
57	5	22.1332	65	0.076	YES
58	4	12.9211	66	0.033	YES
59	3	8.9993	67	0.064	YES
60	6	42.8153	68	0.07	YES
61	3	6.9134	69	0.06	YES
62	6	37.4711	70	0.085	YES
63	2	1.9725	71	0	NO
64	4	13.2006	72	0.52	YES
65	4	18.6911	73	0.118	YES
66	6	47.7244	74	0.103	YES
67	1	0.2298	75	0	NO
68	3	8.6438	76	0.075	YES
69	5	23.5714	77	147.756	YES
70	3	6.0146	78	1.018	YES
71	5	27.3248	79	0.018	NO
72	4	17.4712	80	0.019	NO
73	4	16.6639	81	0.342	YES
74	2	4.0242	82	0	NO
75	4	12.2959	84	0	NO
76	2	1.9734	85	0.02	NO
77	1	0.3653	86	0	NO
78	1	0.6905	88	0	NO
79	1	0.106	89	0	NO
80	6	31.1573	91	0.061	YES
81	6	32.3068	92	0.109	YES
82	6	77.5767	93	7.702	YES
83	2	0.2474	94	0	NO
84	2	4.4785	95	0.029	YES
85	1	1.2364	96	0	NO
86	1	1.6145	98	0	NO
87	1	1.4408	99	0	NO
88	1	1.5788	100	0	NO
89	1	1.0437	101	0	NO
90	1	1.3164	102	0	NO
91	1	1.3045	103	0	NO

## Scatterplots

Figure 38 provides a graphic depiction of the mean analytic signal (nT/m) at each sampling site versus the total energetic content (mg/kg). This figure illustrates that most of the samples had low values of total energetic content, with the exception of one very high value (see observation #69 in Table 6). No real trend is apparent in this plot and the very low detection of energetics relative to the one very high outlier is quite marked.

Figure 39 provides a plot of the mean analytic signal versus the total energetic concentration without the high outlier. Only a subtle trend is readily apparent in this figure.

## Parametric analyses

The parametric analyses included simple linear regression on the independent variable MEAN (representing the mean analytic signal measured by the airborne magnetometer within each 5 m × 5 m sampling area), exponential model using the logarithm of ENERGETICS on the independent variable MEAN, and analysis of variance (ANOVA) on the independent variable GRIDCODE.

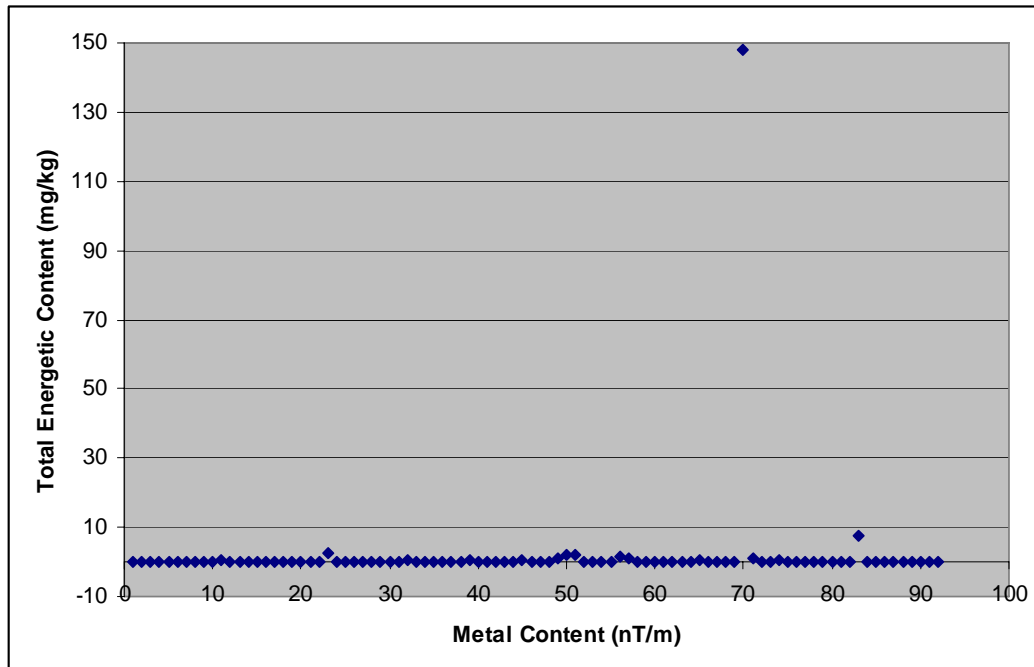


Figure 38. Mean analytic signal (nT/m) at each sampling site at Fort Ord versus the total energetic content (mg/kg).

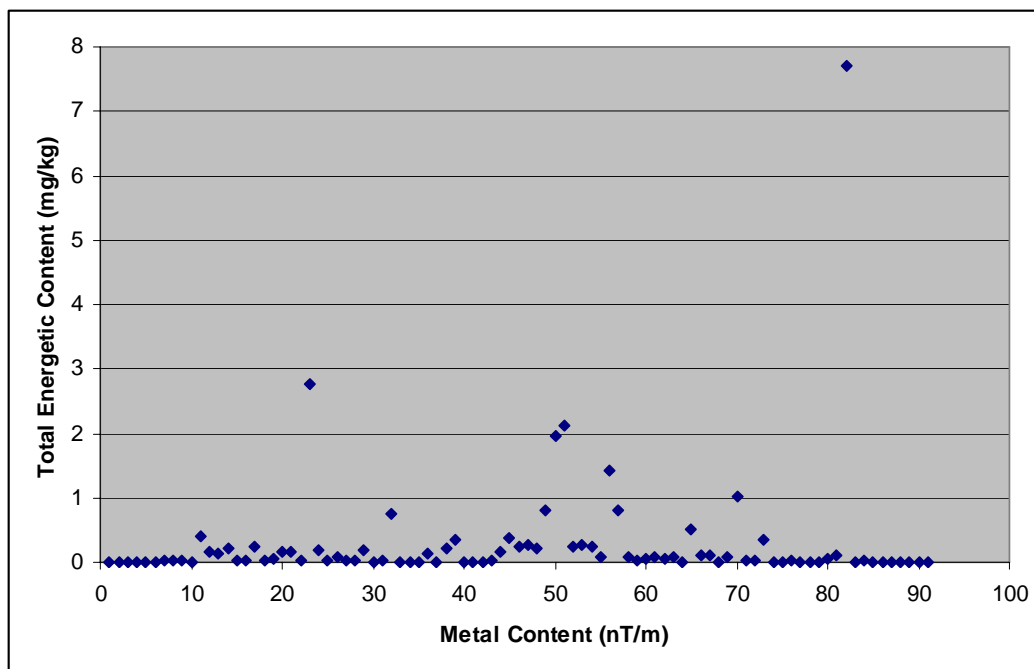


Figure 39. Mean analytic signal (nT/m) at each sampling site at Fort Ord versus the total energetic content (mg/kg) without the high value outlier.

Analyses of the original dataset were dominated by a single observation (see Table 6, observation #69 with a total energetics content value of 147.756). Even though the observation may be a true value, it was omitted from most of the analyses since it is an outlier (two times one order of magnitude larger than the second largest value). It is noted below if the outlier was included in the analyses. (All analyses were run both with and without observation #69 present, and are included in output files in the appendices).

A simple linear regression model and an exponential model (using the dataset that excludes observation #69) were analyzed with the independent variable MEAN. The quantitative variable MEAN showed a significant relationship with energetics in both the linear form ( $P = 0.0005$ ) and exponential model (using  $\log(\text{energetics})$ ) ( $P = 0.0028$ ). Neither model met the assumption of normality, but the exponential model was closer to meeting the assumptions than the linear model. Although the fitting of the model provides a least squares fit regardless of the assumption of normality, the assumption of normality is needed for testing hypotheses and fitting confidence intervals. A strong skew of the residuals in both cases indicates that the tests of hypotheses and confidence intervals are suspect for these models. Though, however weak, the strength of the relationships would suggest a real correlation likely exists between the presence of energetic compounds and the mean analytic signal.

Due to the simplicity of the linear model, and the strength of the test, the linear model was viewed as the best choice among the parametric analytical techniques (Table 7). This test indicates that the best predictive model for energetics was the linear model “energetics = -0.02599 + 0.01976\*MEAN”. This model explained 12.9 percent of the total variance (R-Square). The intercept for this model is negative, but not significantly different from zero, suggesting that energetics may reach zero when the mean is zero.

Table 7. Results of linear model (independent variable mean analytic signal)

Variable	DF	Parameter Estimate	Standard Error	t Value	Pr >   t	95% Confidence Limits
Intercept	1	-0.00994	0.12302	-0.08	0.9358	-0.25441 to 0.23453
Mean	1	0.01923	0.00533	3.61	0.0005	0.00864 to 0.02982

The only model found to have predictive value (using the dataset that includes observation #69) was the exponential model ( $P = 0.0447$ ). This model is originally  $Y_i = b_0 e^{b_1 X_i} e_i$  which after the logarithmic transformation becomes a simple linear regression ( $\ln(Y_i) = \ln(b_0) + b_1 X_i + \ln(e_i)$ ). Table 8 gives the value of the intercept ( $\ln(b_0)$ ) and slope ( $b_1$ ). Note, the dependent variable was transformed using  $\log(\text{MEAN}+1)$  in order to shift the dependent variable axis away from zero. The analysis using observation #69 was dominated by that observation and significant only when a logarithm was used, which tends to deemphasize extreme values. Although the analysis indicates a significant slope ( $t = 2.04$ ,  $p\text{-value} = 0.0447$ ), the model only explained 4.5 percent of the total variance (R-Square).

Table 8. Results of exponential model (independent variable mean analytic signal)

Variable	DF	Parameter Estimate	Standard Error	t Value	Pr >   t	95% Confidence Limits
Intercept	1	0.10398	0.08533	1.22	0.2262	-0.06556 to 0.27353
Mean	1	0.00782	0.00369	2.04	0.0447	0.0001821 to 0.01486

ANOVA (using the dataset that excludes observation #69) on the independent variable GRIDCODE showed no significance when fitted to either ENERGETICS ( $P = 0.3094$ ) or  $\log(\text{energetics})$  ( $P = 0.1523$ ). This variable could be useful if some complicated curvature existed across the values of the variable MEAN. If not, it uses 5 degrees of freedom to accomplish what might be accomplished by a linear fit, or simple curved fit, to the variable using only 1 degree of freedom.

## Nonparametric analyses

Since the data failed the assumptions of homogeneity of variance and normality (Table 9), nonparametric procedures were employed to determine if the level of ENERGETICS in the six different levels of GRIDCODE were statistically different. Certain nonparametric procedures, such as the median test, are free of the assumptions required of parametric procedures.

Table 9. Homogeneity of variance test results.

Test	Test Statistic Value	Degrees of Freedom	Number of Observations	Probability
Levene	3.8677	5	84	0.0033
Bartlett	42.0850	5	.	<.0001

The summary statistics by GRIDCODE are given in Table 10. From this table it is readily seen that the larger values of energetics are found in the higher grid cells.

Table 10. Summary statistics by GRIDCODE.

GRIDCODE	N	Mean	Median	Std Deviation
1	16	0.0020	0	0.0081
2	15	0.4256	0.0204	0.8289
3	15	0.2176	0.0754	0.2995
4	15	0.1238	0.0384	0.1568
5	14	0.2685	0.1566	0.5404
6	15	0.7296	0.0852	1.9665

The data were analyzed using the nonparametric median test. The results of this procedure are given in Table 11. The Chi-Square test statistic for these median values is 24.5855 with associated degrees of freedom of 5. The resulting p-value for this test was 0.0002.

Table 11. Median test (number of points above median).

Level	Count	Score Sum	Score Mean	Q <sup>1</sup>
1	16	0	0.000000	*
2	15	6	0.400000	3.065
3	15	10	0.666667	5.109
4	15	7	0.466667	3.576
5	15	11	0.733333	5.620
6	15	11	0.733333	5.620

<sup>1</sup> Q = (Score Sum for Level j - Score Sum for Level 1)/SE

As with parametric procedures, ancillary techniques do exist for post-analysis of the median test. The procedure is very similar to John Tukey’s Q-test in that it uses the number of points above the grand median as a measure of departure between the central values of the distributions. The standard error for the post-median test depends on whether or not the sample size is even or odd and is given by the formulas:

$$\sqrt{\frac{n(N+1)}{4N}} \text{ if } N \text{ is odd}$$

$$\sqrt{\frac{n(N+1)}{4(N-1)}} \text{ if } N \text{ is even}$$

Additionally, since the median test is not affected by outliers, then the extreme value, as mentioned above, does not have to be excluded from the analysis. Since N is odd (91), the standard error for this data is 1.95733. Using John Tukey’s Q-table and the harmonic mean of n (15.15789), the critical value of the studentized range is computed at the appropriate alpha level, with g groups and infinite degrees of freedom. For these data, the critical value of Q is 4.03. Thus, the conclusions from this procedure indicate that Grid Code 1 is not different from Grid Codes 2 and 4; however, it is different from Grid Codes 3, 5, and 6. Additionally, Grid Codes 2 and 4 are not different from 3, 5, and 6. Using the line notation, this is best summarized as:

	GRIDCODE					
	1	2	4	3	5	6
Score Sum	0	6	7	10	11	11

---

As can be observed from the line notation, there are two homogeneous groups with Grid Codes 2 and 4 being inclusive in each of these two groups. Thus, it can be concluded that the larger grid codes are associated with larger energetic values.

**Logistic analyses**

An ancillary procedure to both the parametric and nonparametric methods above is a technique that models categorical responses to quantitative data. Typically for a binary response variable Y and an

explanatory variable X, the procedure models the probability of Y for a given X as:

$$\pi(x) = \frac{\exp(\alpha + \beta x)}{1 + \exp(\alpha + \beta x)}$$

Equivalently, the log odds, called the logit, has the linear relationship of:

$$\text{logit}(\pi(x)) = \log\left(\frac{\pi(x)}{1 - \pi(x)}\right) = \alpha + \beta x$$

This equates the logit link function to the linear predictor.

Using this technique of the presence/absence of material in the grid cells produces a model given in Table 12.

Table 12. Logistic regression analysis parameter estimates.

Term	Estimate	Std Error	ChiSquare	Prob>ChiSq	Odds Ratio
Intercept	0.47534802	0.3257362	2.13	0.1445	.
Mean	-0.069085	0.0214574	10.37	0.0013	0.00473836

For log odds of NO/YES

The linear model of  $Y = 0.47534802 - 0.069085 * \text{Mean}$  gives a value of the logit that can be converted back to a probability using the inverse relationship of:

$$p = \frac{\exp(y)}{1 + \exp(y)}$$

For our data, since we were modeling NO/YES, the results would be classified as NO if p is smaller than 0.5 and as yes if it is greater (see Table 6, variable DETECTABLE). Table 13 shows the results of this model.

Table 13. Logistic regression, observed versus predicted.

Observed	Predicted	
	No	Yes
No	25 69.4%	11 30.6%
Yes	16 29.6%	38 70.4%

Thus, the results of this model correctly predicted 69.4 percent and 70.4 percent of the grid cells with no contaminants and with contaminants; it misclassified 30.6 percent of the grids with no contaminants and 29.6 percent of the grids with contaminants. Although these misclassification percentages appear to be large, these results do support both the non-parametric median test and the parametric Welch's approximate F-test in that it does appear that magnetometer data can be used as a predictor of grid cell contaminants.

The results for this model were highly significant. Based on the Likelihood Ratio test, the probability was  $<0.0001$ . Another test, the Wald test (not quite as good but providing confidence intervals) puts the level of significance at  $P = 0.0013$ . There is no assumption of normality, so that is not an issue with this analysis. The model is  $\log(\text{odds}) = -0.4754 + 0.0691\text{Mean}$ . A plot of the resulting probabilities is presented in Figure 40.

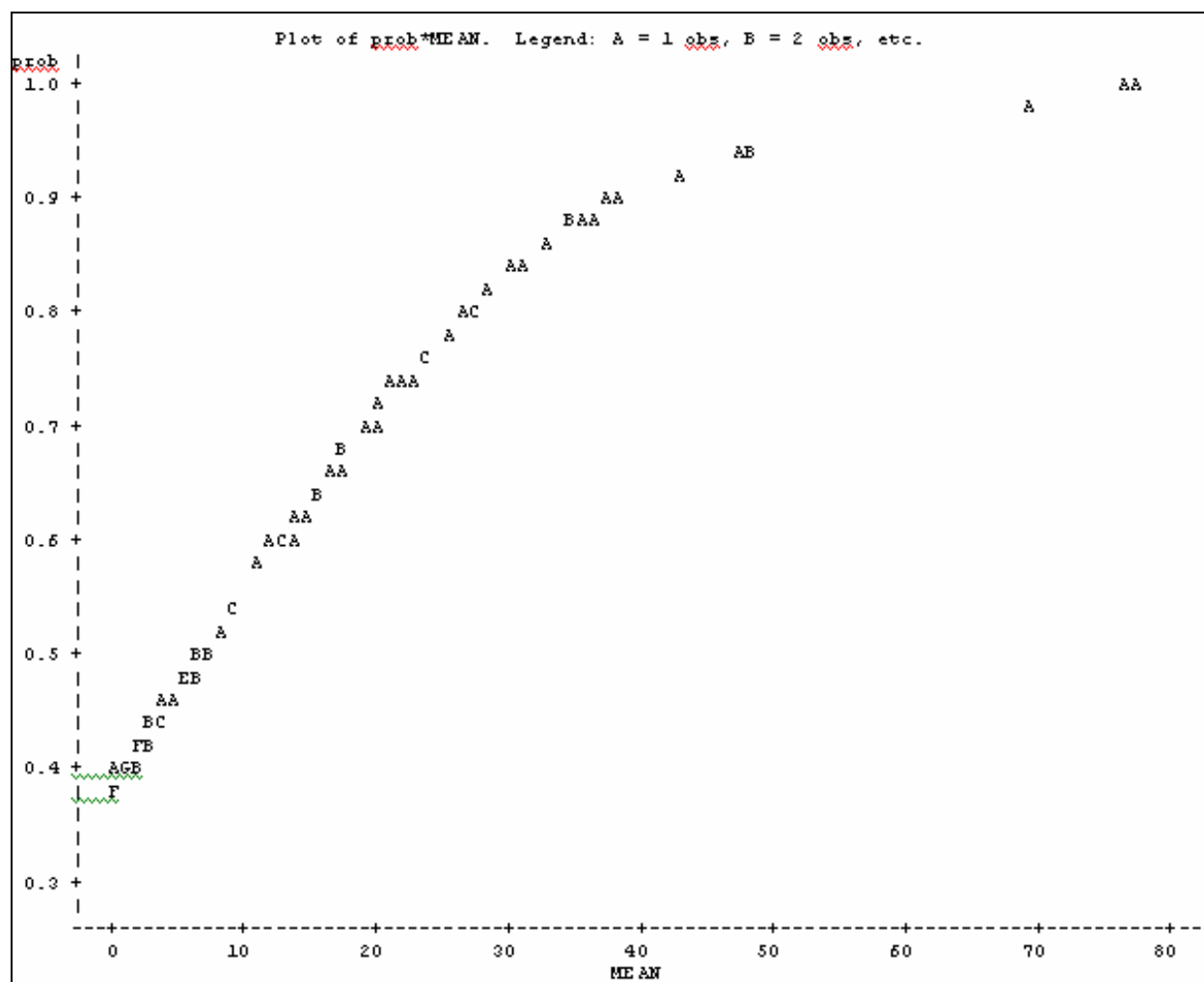


Figure 40. Plot of mean analytic signal versus probability of detection of energetics.

The results indicate that the probability of detecting energetics is about 0.38508 (between 0.24911 and 0.54173) at the lowest value of the mean (0.1060). This is not unreasonable as the study did not have a control area. A 50 percent chance of detecting energetics occurred at a mean level of about 6.9134 (between 0.38233 and 0.61874). By the time the mean was 27.2801, there was an over 80 percent chance of detecting energetics (0.80366, between 0.63959 and 0.90422).

## 5 Conclusions

Helicopter-based magnetometry and EM remote sensing techniques, developed primarily for the detection of UXO, may prove useful for other impact area applications such as assisting in estimating cleanup costs over large areas and the development of sampling strategies on closed impact areas. Often, due to poor firing records, it is difficult to locate concentrated spots of potential energetic sources (as well as heavy metals and other contaminants) due to vegetation, difficult terrain, etc. These remote sensing techniques make it possible to characterize large areas relatively quickly. While these techniques are expensive, the cost of such operations may be offset by their utility for applications beyond UXO detection.

Unfortunately, due to wartime circumstances and associated heightened training requirements, it was impossible to gain access to the active impact areas originally planned for this work. Fort Ord has been closed for over 10 years and did not represent an ideal study site. The soil samples gathered were found to have very low levels of energetics, perhaps due to a number of factors such as the length of time the impact area has been closed, photodegradation of the energetics, and possible vertical migration into the primarily sandy soil. The study area at Fort Ord also had been surface-cleared, meaning all UXO clearly visible on the surface had been removed. The items that were removed represented a great deal of metal as well as potential sources for energetics. Their removal almost certainly affected the analyses to some degree.

This study provides evidence that indicates that a possible relationship (correlation) between analytic signal and the energetics measured may exist. From a parametric point of view, the failure to meet the necessary assumptions of homogeneity of variances and normality tends to dampen the results and, hence, the conclusions about the predictive nature of using the underlying model. The failure of the experimental data to meet these assumptions affects both the conclusions about linear predictor relations and the conclusion that may be made from analysis of variance procedures. From the later point of view, the analysis of variance, Welch's approximate F-test did indicate that differences among the mean energetic levels for the six different grid codes did exist and that the larger mean analytic signal values were observed at the highest levels of GRIDCODE. The nonparametric median test supported the conclusion of Welch's approximate F-test, and the subsequent postexamination of the data did

conclude that higher levels of analytic signal are associated with greater levels of energetics.

A logistic analysis, which like nonparametric tests does not require the assumption of normality, also supported the evidence that a relationship between analytic signals and the detection of contaminants did exist. The logit model indicates that the probability of finding detectable chemical traces increases sharply as analytic signal (variable MEAN) increases. The probabilities range from about 38 percent at the lowest values of analytic signal to over 90 percent by the time the analytic signal is in the 40s.

## References

- Beard, L. P., W. E. Doll, J. S. Holladay, T. J. Gamey, J. L. C. Lee, and D. T. Bell. 2004. Field tests of an experimental helicopter time-domain electromagnetic system for unexploded ordnance detection. *Geophysics* 69:664-673.
- Beyer, H. L. 2004. Hawth's analysis tools for ArcGIS. <http://www.spataleecology.com/htools>.
- Billings, S. D., L. R. Pasion, D. W. Oldenburg, and J. Foley. 2003. *The influence of magnetic viscosity on electromagnetic sensors: EUDEM-SCOT2 2003*. International Conference on Requirements and Technologies for the Detection, Removal and Neutralization of Landmines and UXO, Brussels, September 15-18, 2003.
- Environmental Systems Research Institute, Inc. 2005. *Arc/Info GIS computer software*. Redlands, CA: Environmental Systems Research Institute.
- Hewitt, A. D., T. F. Jenkins, C. A. Ramsey, K. L. Bjella, T. A. Ranney, and N. M. Perron. 2005. *Estimating energetic residue loading on military artillery ranges: Large decision units*. ERDC/CRREL TR-05-7. Hanover, NH: U.S. Army Engineer Research and Development Center.
- Hrvoic, D., and M. R. Pozza. 2006. Mapping marine ferrous targets using real-time 3D analytic signal data. *The leading edge* 25(1):54-56.
- Jenkins, T. F., A. D. Hewitt, C. L. Grant, S. Thiboutot, G. Ampleman, M. E. Walsh, T. A. Ranney, C. A. Ramsey, A. Palazzo, and J. C. Pennington. in press. Identity and distribution of residues of energetic compounds at Army live-fire training ranges. *Chemosphere*.
- Jenkins, T. F., A. D. Hewitt, T. A. Ranney, C. A. Ramsey, D. J. Lambert, K. L. Bjella, and N. M. Perron. 2004a. *Sampling strategies near a low-order detonation and a target at an artillery impact area*. ERDC/CRREL TR-04-14. Hanover, NH: U.S. Army Engineer Research and Development Center.
- Jenkins, T. F., C. L. Grant, G. S. Brar, P. G. Thorne, P. W. Schumacher, and T. A. Ranney. 1997. Assessment of sampling error associated with the collection and analysis of soil samples at explosives contaminated sites. *Field Analytical Chemistry and Technology* 1:151-163.
- Jenkins, T. F., S. Thiboutot, G. Ampleman, A. D. Hewitt, M. E. Walsh, T. A. Ranney, C. A. Ramsey, C. L. Grant, C. M. Collins, S. Brochu, S. R. Bigl, and J. C. Pennington. 2005. *Identity and distribution of residues of energetic compounds at military live-fire training ranges*. ERDC TR-05-10. Hanover, NH: U.S. Army Engineer Research and Development Center.
- Jenkins, T. F., T. A. Ranney, A. D. Hewitt, M. E. Walsh, and K. L. Bjella. 2004b. *Representative sampling for energetic compounds at an antitank firing range*. ERDC/CRREL TR-04-7. Hanover, NH: U.S. Army Engineer Research and Development Center.

- MACTEC Engineering and Consulting, Inc. 2005. Fort Ord cleanup.  
<http://www.fortordcleanup.com/foprimer/>.
- Oak Ridge National Laboratory (ORNL). 2003. *Demonstration of airborne electromagnetic systems for detection and characterization of unexploded ordnance at the Badlands Bombing Range, South Dakota*. ESTCP Project 200101 Final Report. Oak Ridge, TN: Oak Ridge National Laboratory.
- Telford, W. M., L. P. Geldart, and R. E. Sheriff. 1990. Electrical properties of rocks and minerals. In *Applied geophysics*, 2nd ed., Chapter 5. New York: Cambridge University Press.
- U.S. Environmental Protection Agency. 1994. *Nitroaromatics and nitramines by HPLC*. Second Update SW846 Method 8330.
- \_\_\_\_\_. 1999. *Nitroaromatics and nitramines by GC-ECD*. Fourth Update SW846 Method 8095.
- Walsh, M. R. 2004. *Field sampling tools for explosives residues developed at CRREL*. ERDC/CRREL TN 04-1. Hanover, NH: U.S. Army Engineer Research and Development Center.
- Walsh, M. E., C. M. Collins, A. D. Hewitt, M. R. Walsh, T. F. Jenkins, J. Stark, A. Gelvin, T. S. Douglas, N. Perron, D. Lambert, R. Bailey, and K. Myers. 2004. *Range characterization studies at Donnelly Training Area, Alaska: 2001 and 2002*. ERDC/CRREL TR-04-3. Hanover, NH: U.S. Army Engineer Research and Development Center.

## **Appendix A: Airborne Geophysical Survey Daily Quality Control (QC) Results, Fort Ord, CA**

A single swath was flown over a line of pipes laid out on the surface of the ground at the start of each day. The results were analyzed for positional accuracy and sensor functionality. The following plots show the analytic signal in nanoTesla per meter (nT/m) for the northbound and southbound lines separately. Altitudes varied slightly from line to line, but averaged 2 m. Dates are shown on the map in a m-dd format. The target pipes were moved after positioning problems were detected and resolved on January 29/05 (Figure A1). This accounts for the difference in response on that day.

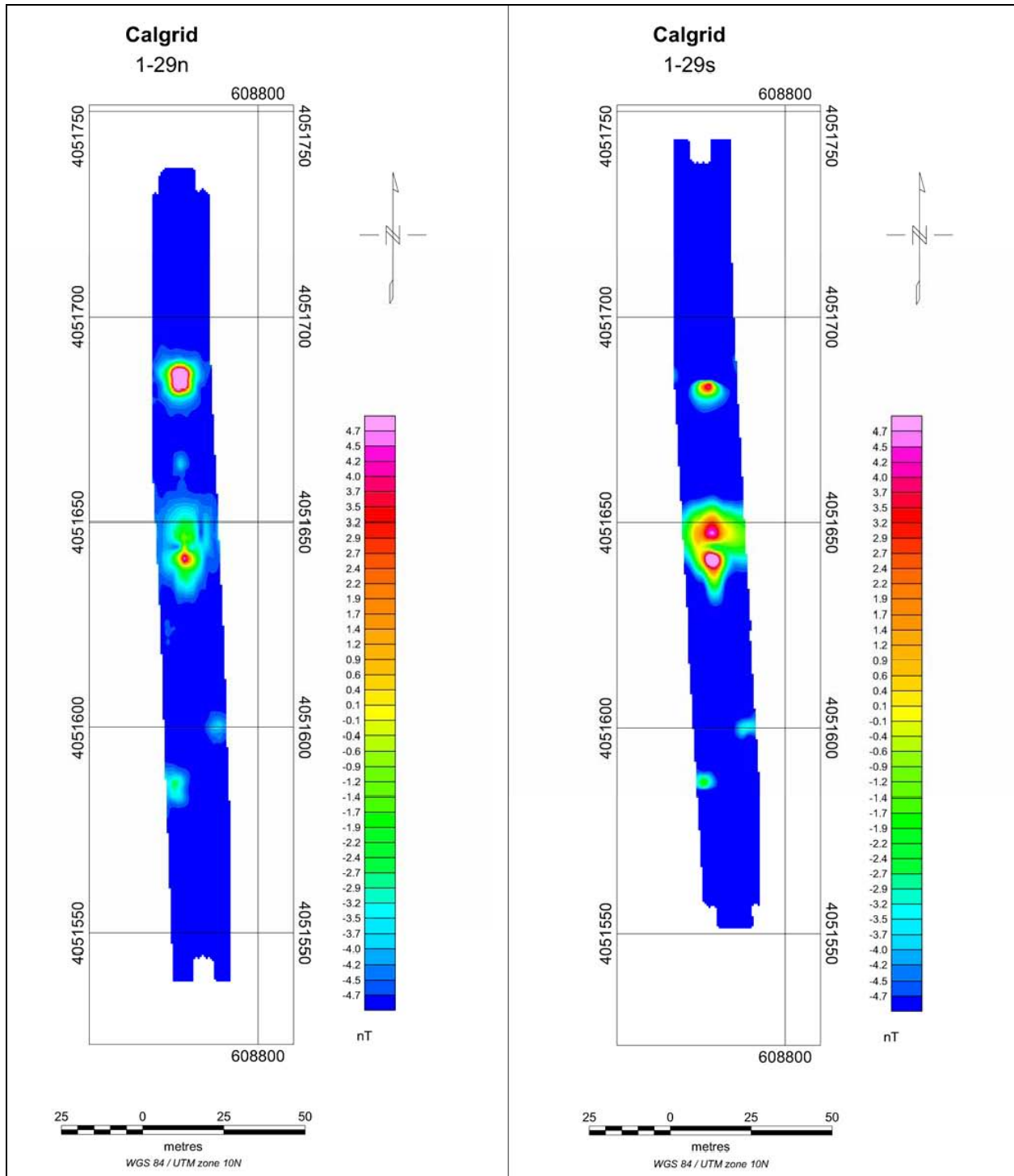


Figure A1. Magnetic QC lines from January 29/05.

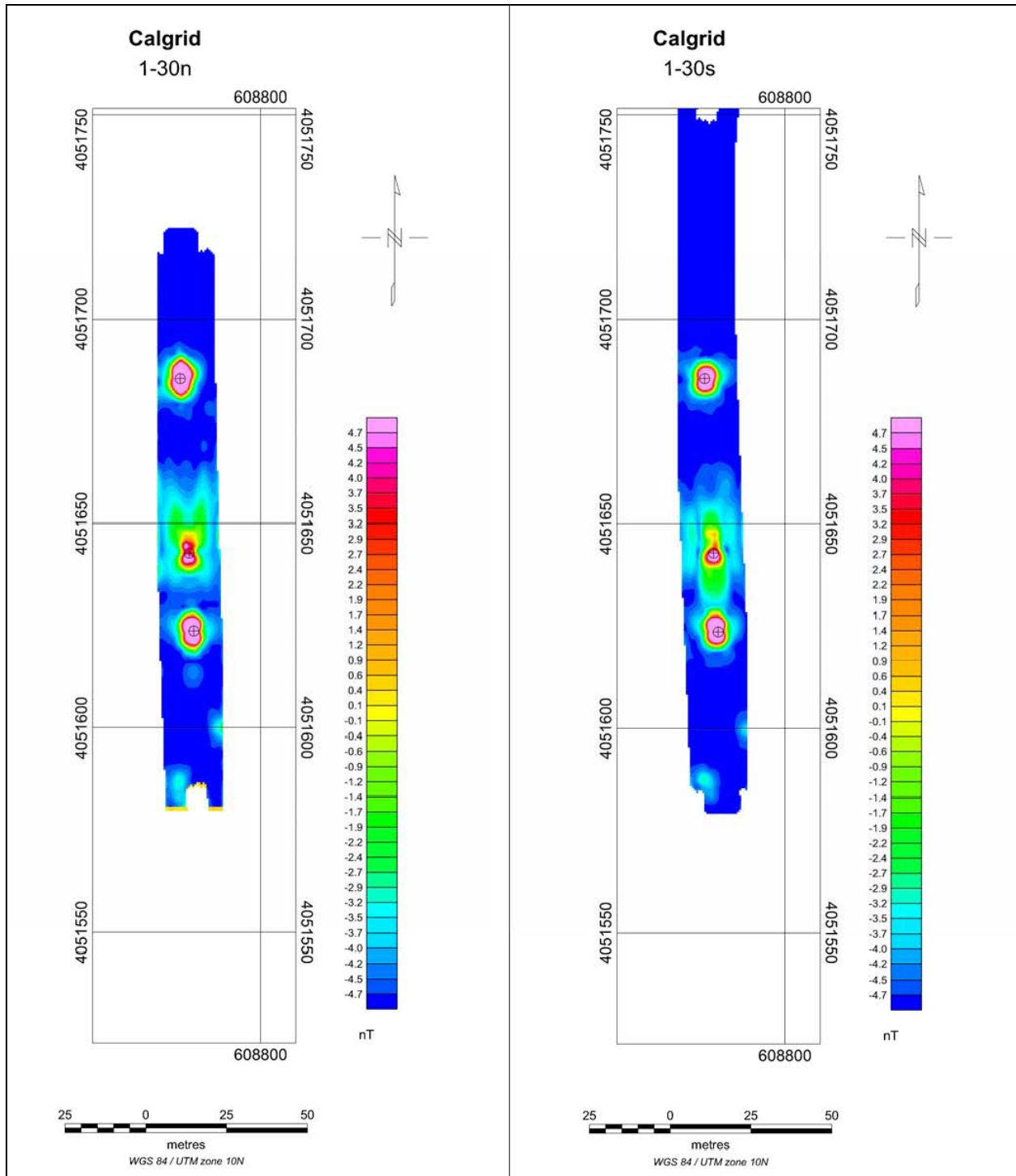


Figure A2. Magnetic QC lines from January 30/05.

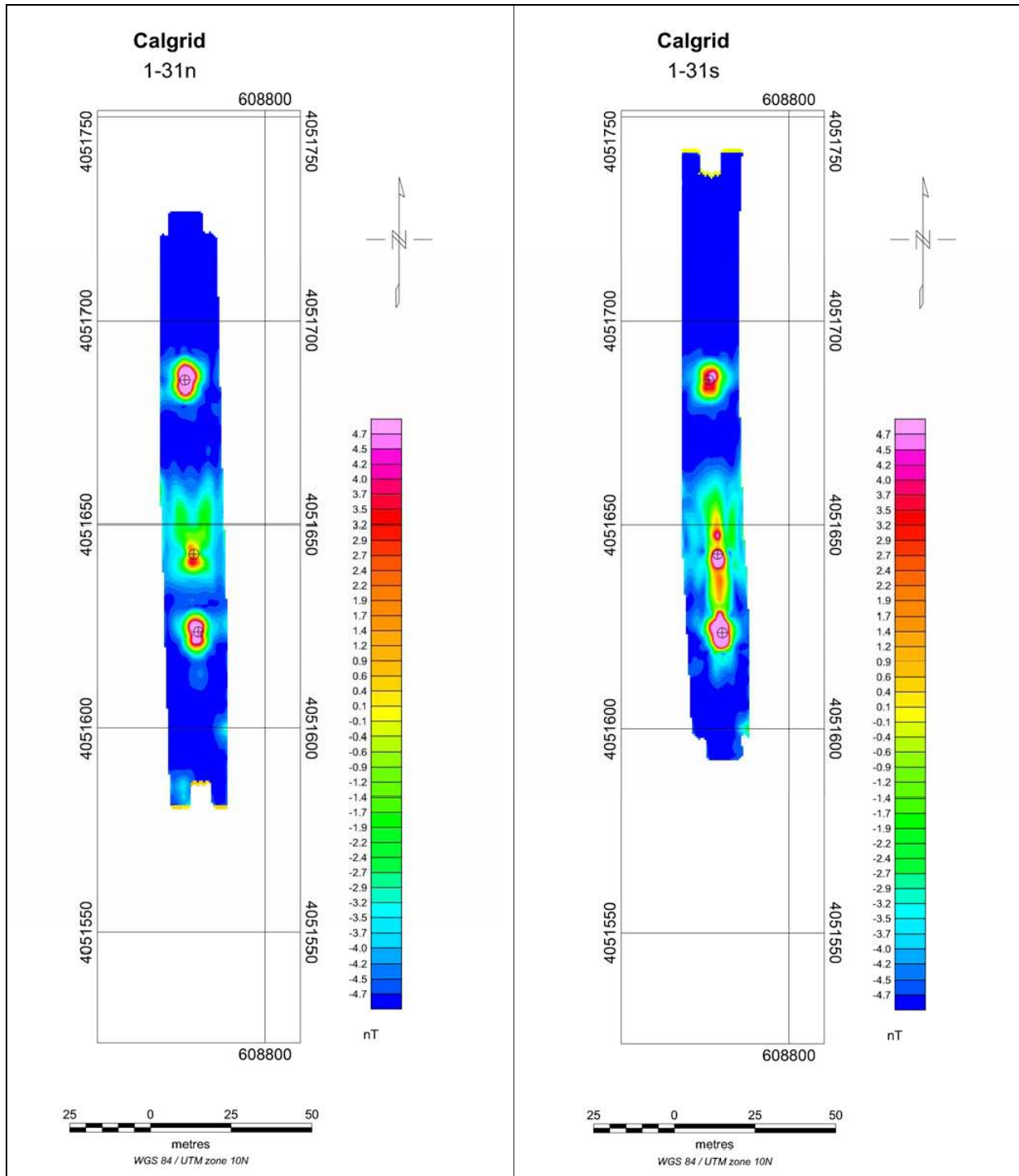


Figure A3. Magnetic QC lines from January 31/05.

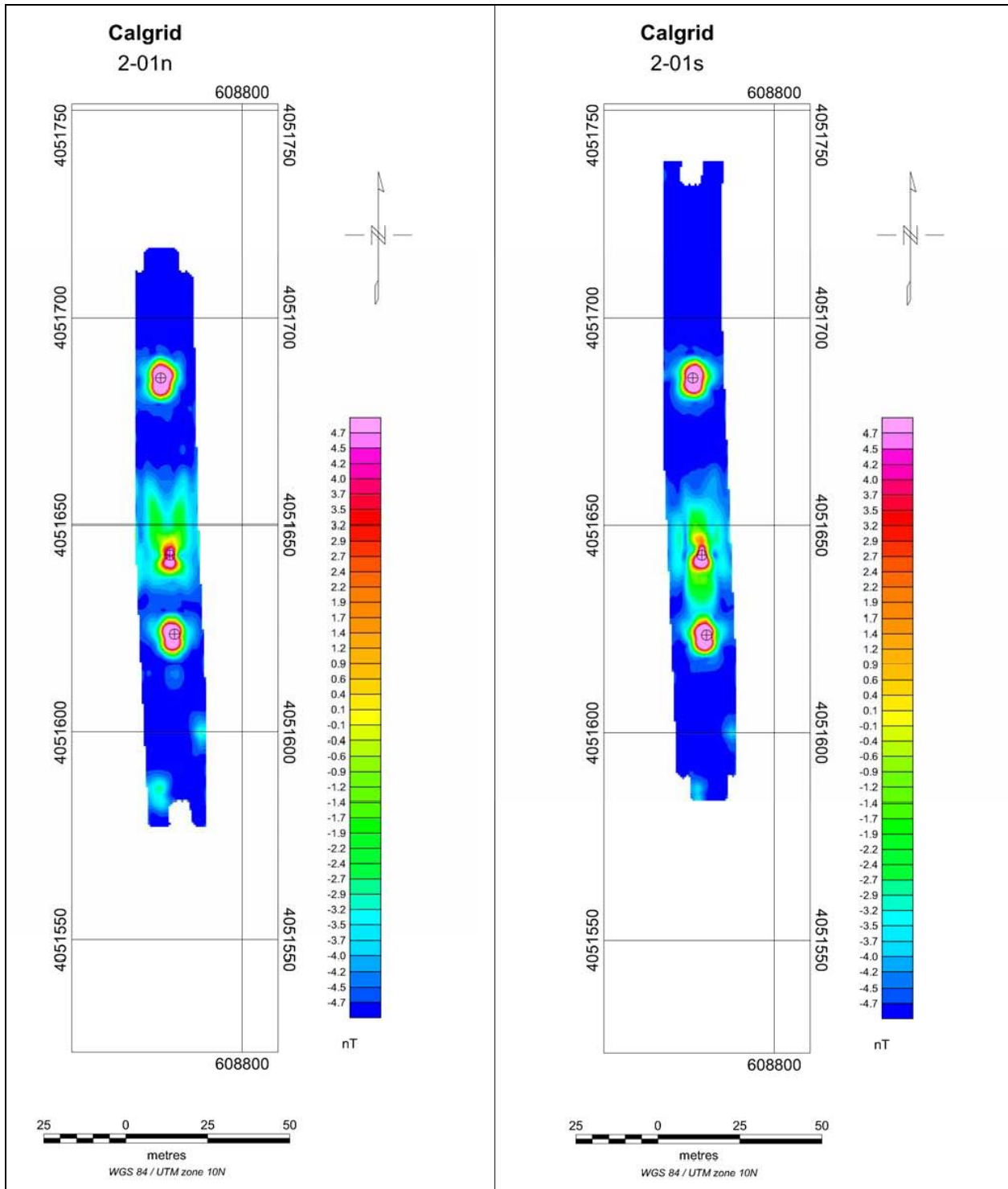


Figure A4. Magnetic QC lines from February 01/05.

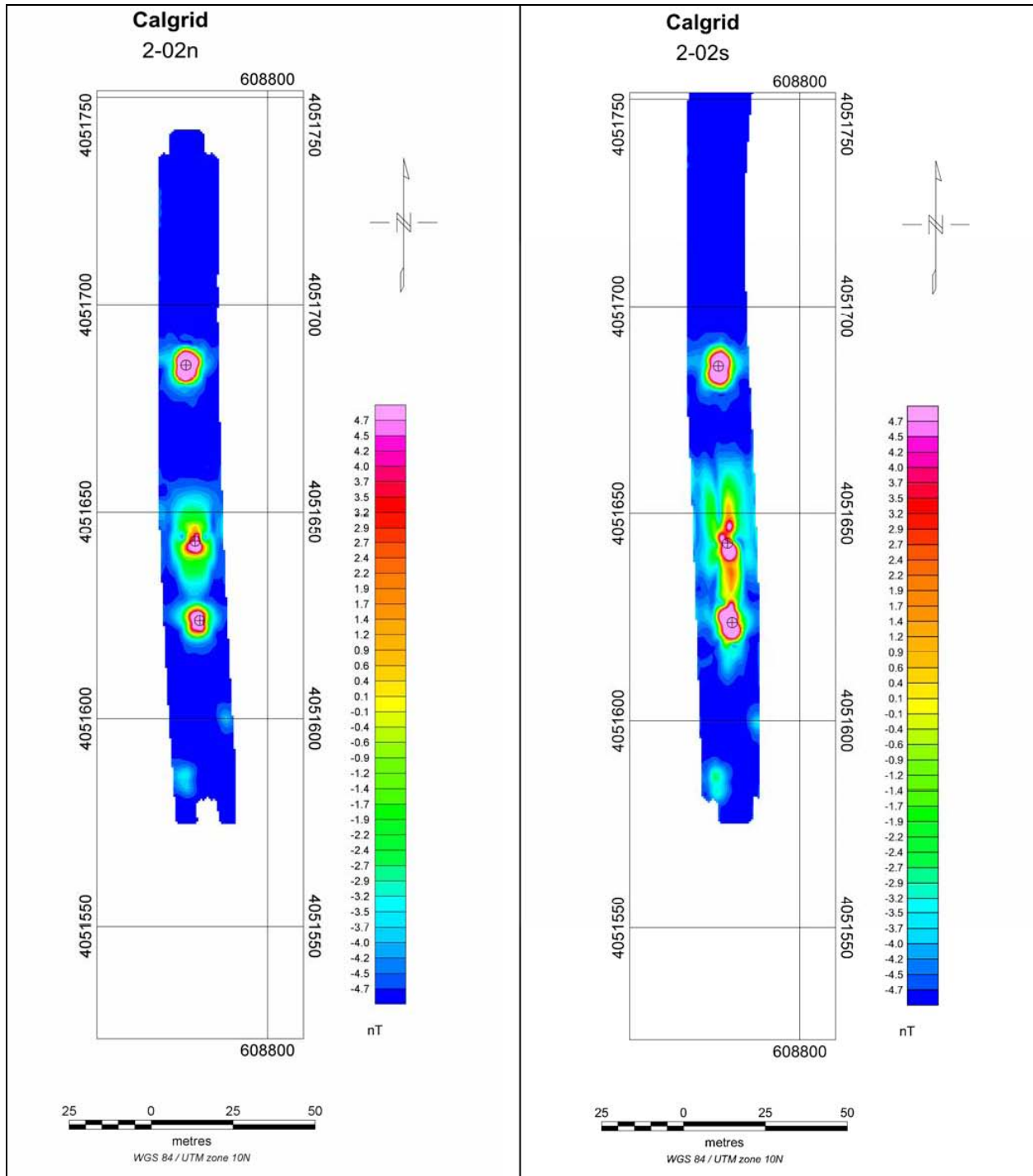


Figure A5. Magnetic QC lines from February 02/05.

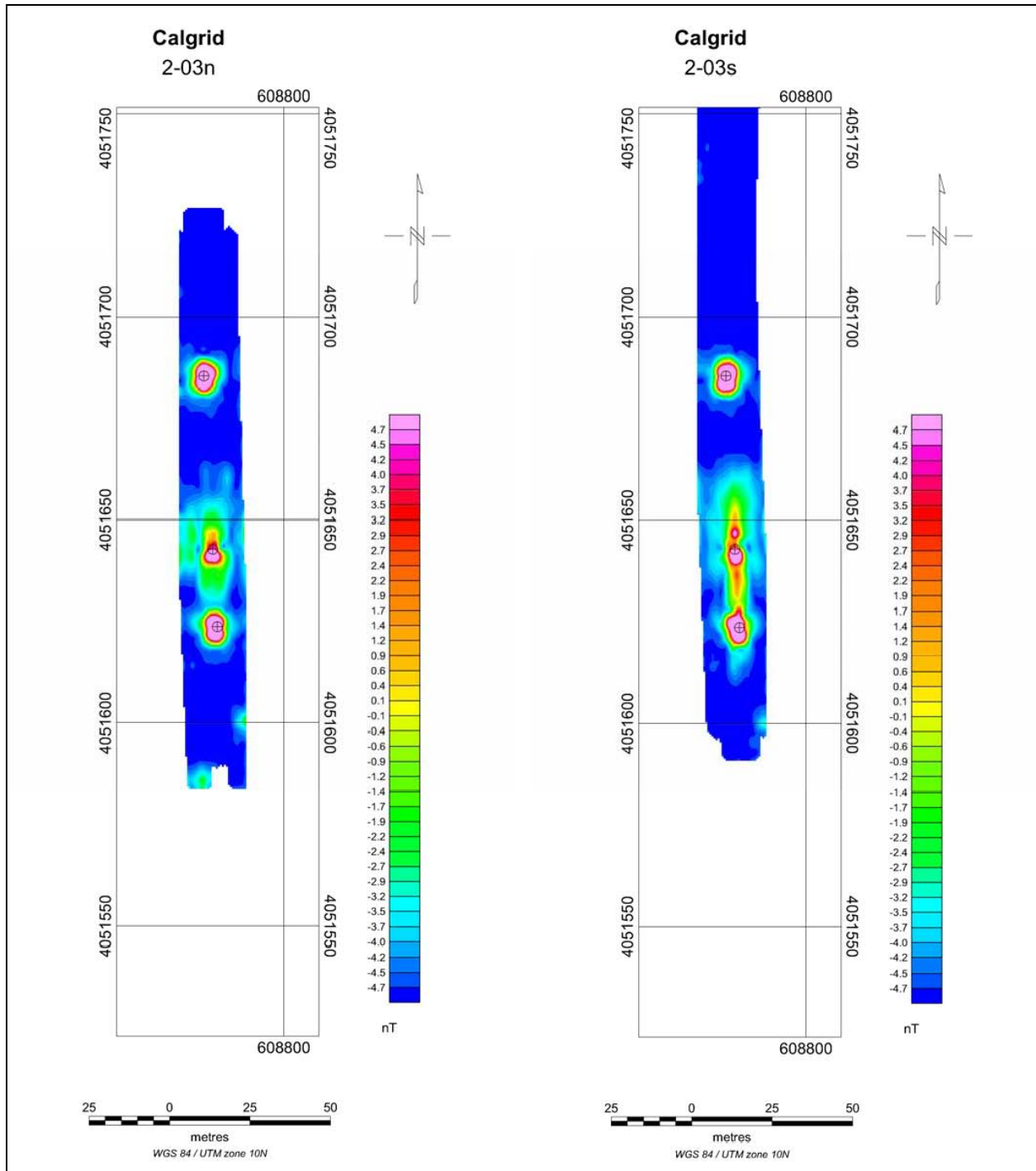


Figure A6. Magnetic QC lines from February 03/05.

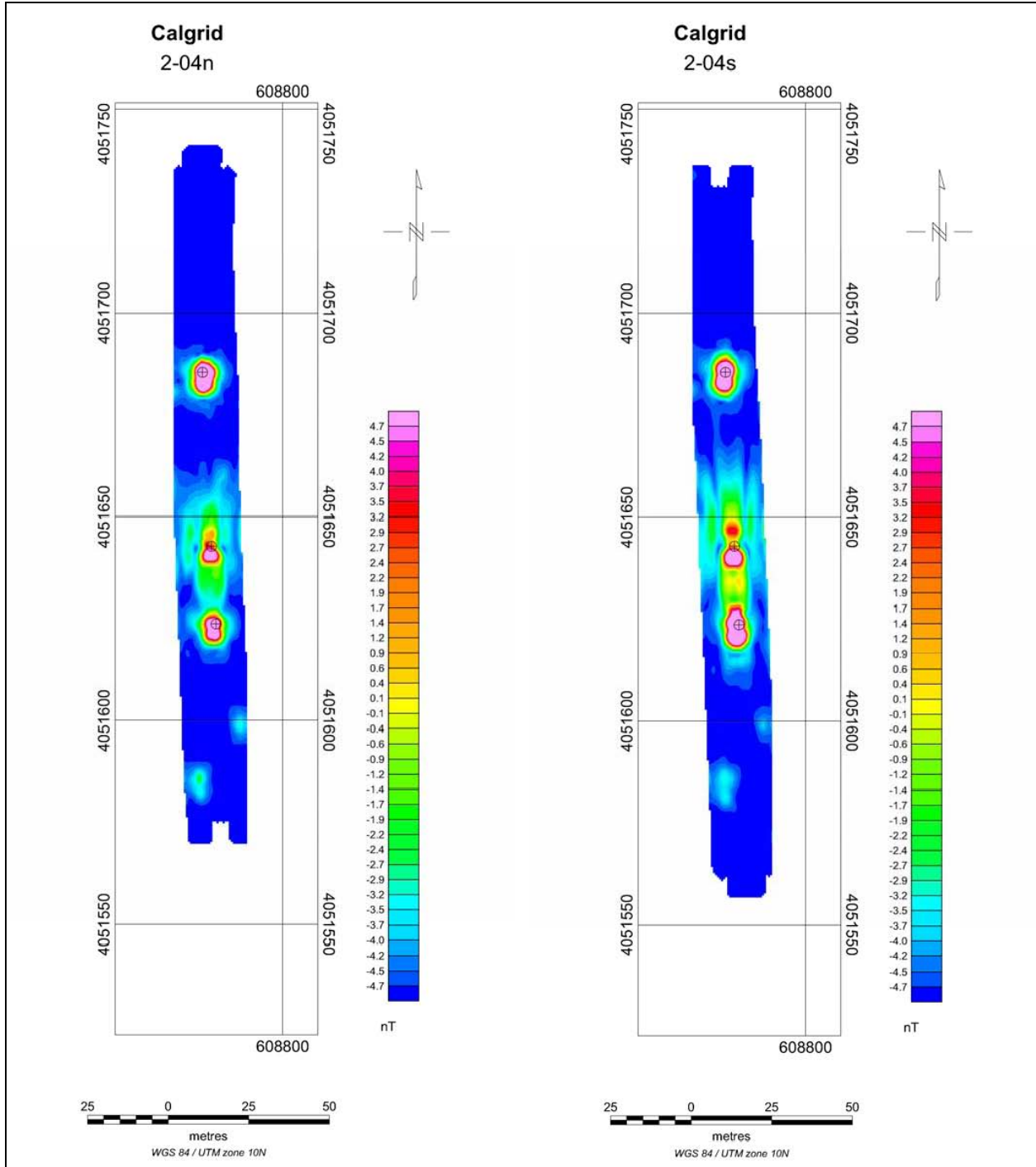


Figure A7. Magnetic QC lines from February 04/05.

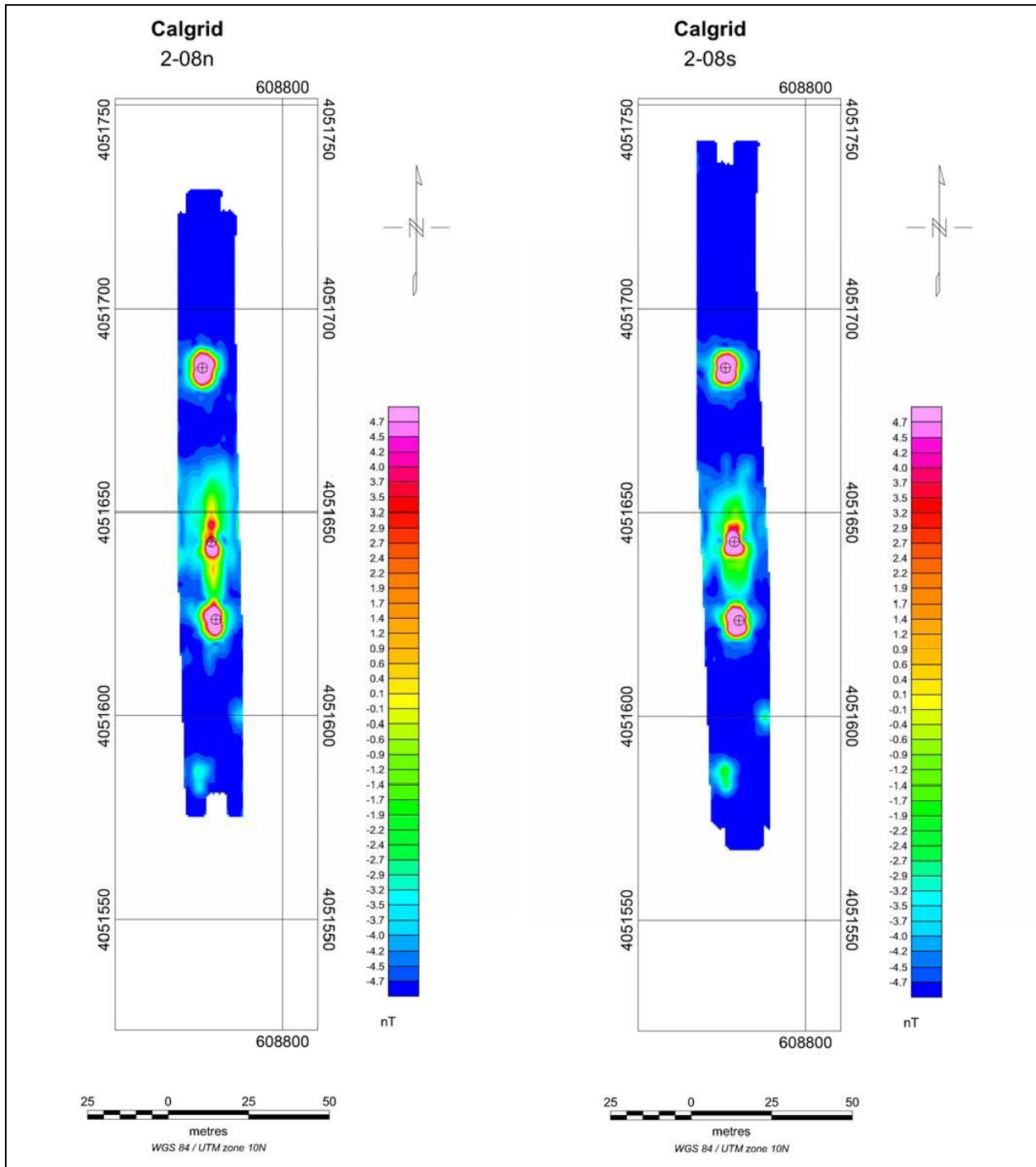


Figure A8. Magnetic QC lines from February 08/05.

# Appendix B: Airborne Geophysical Survey Electromagnetic Data, Fort Ord, CA

The maps shown in this appendix depict six electromagnetic (EM) time-decay snapshots (bins 1-6), EM sensor altitude above ground level, and analytic signal data from the EM blocks A and B.

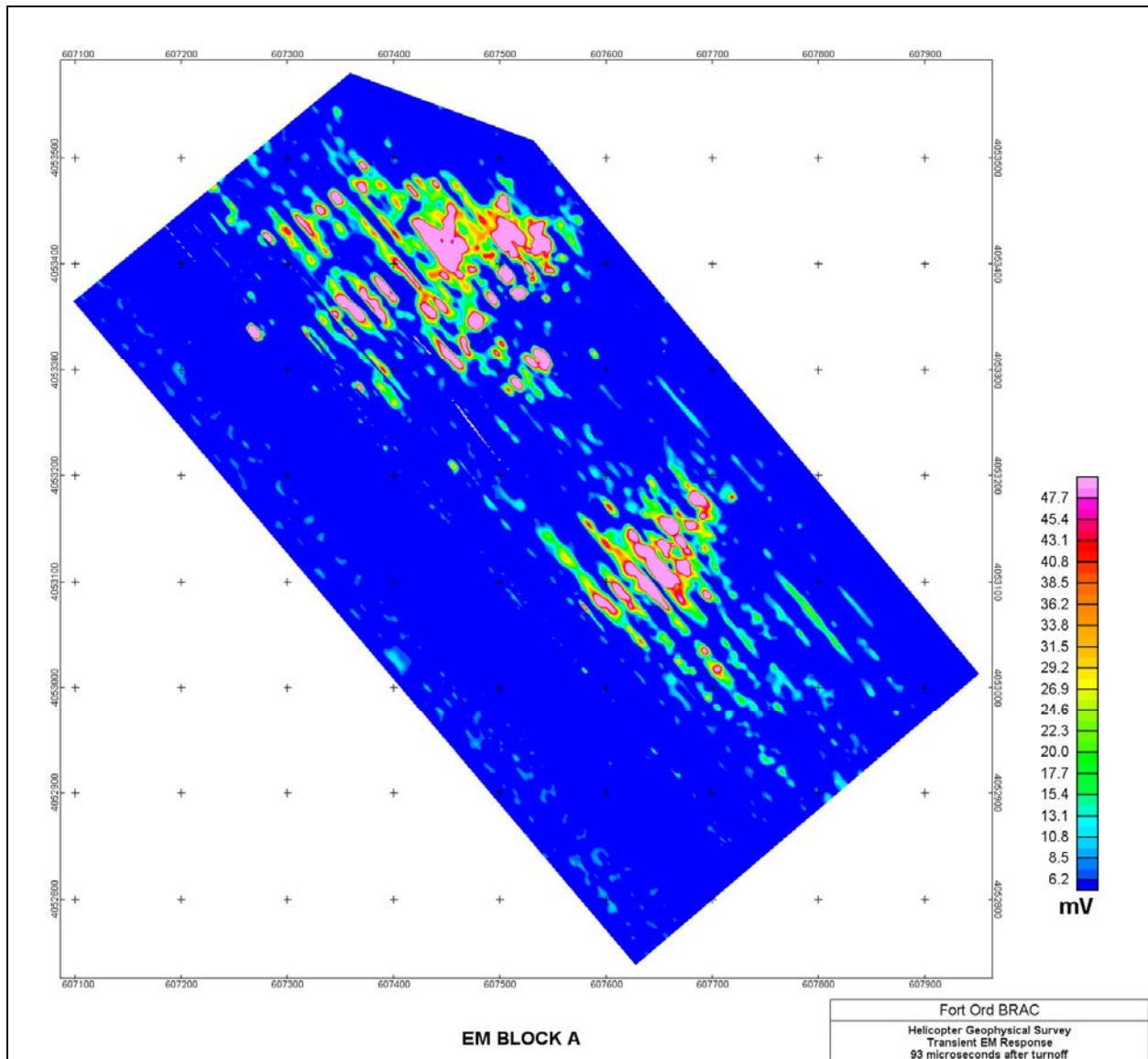


Figure B1. EM response (mV), time bin 1-93 microseconds after turnoff, EM Block A.

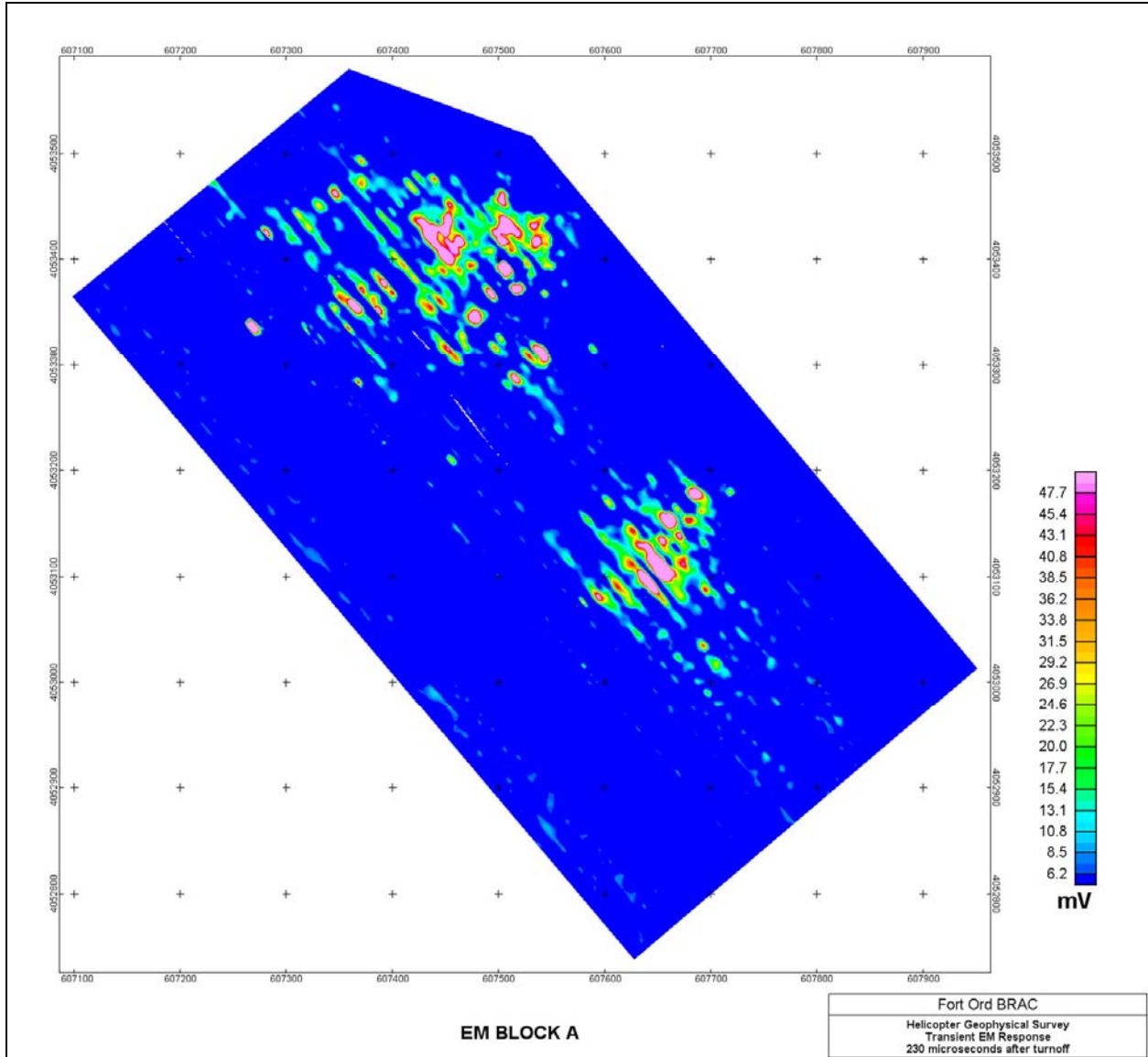


Figure B2. EM response (mV), time bin 2-230 microseconds after turnoff, EM Block A.

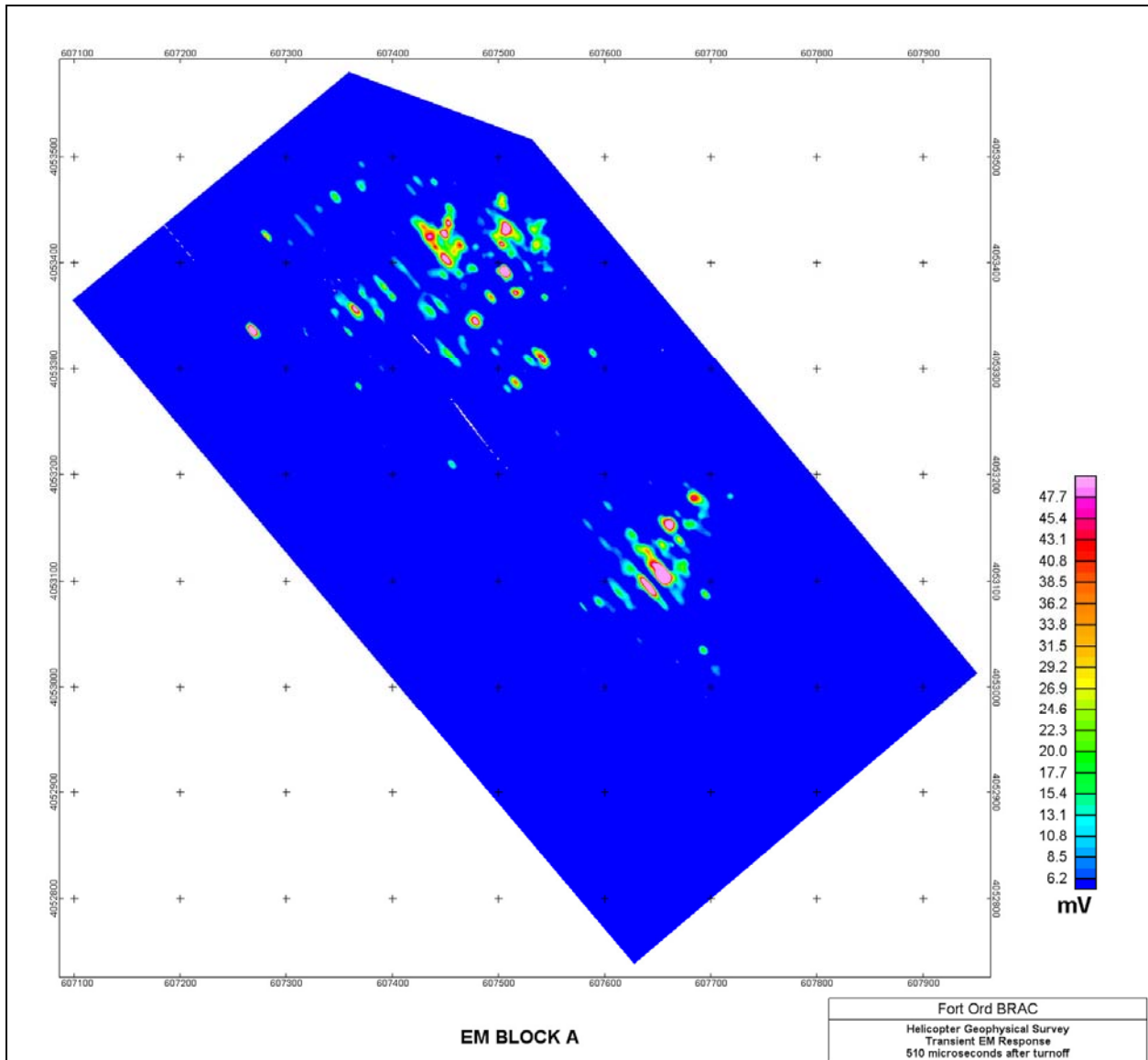


Figure B3. EM response (mV), time bin 3-510 microseconds after turnoff, EM Block A.

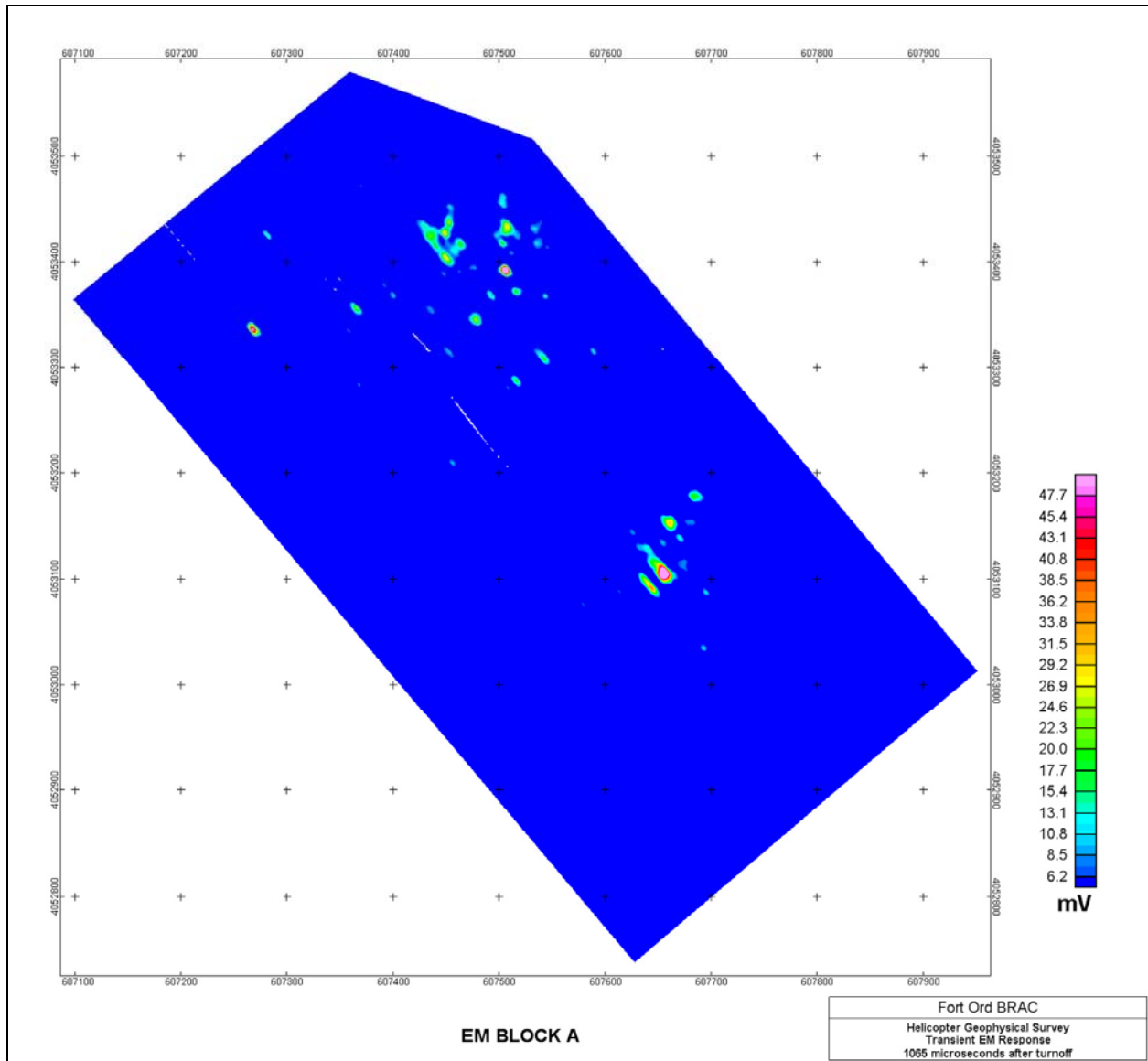


Figure B4. EM response (mV), time bin 4 - 1065 microseconds after turnoff, EM Block A.

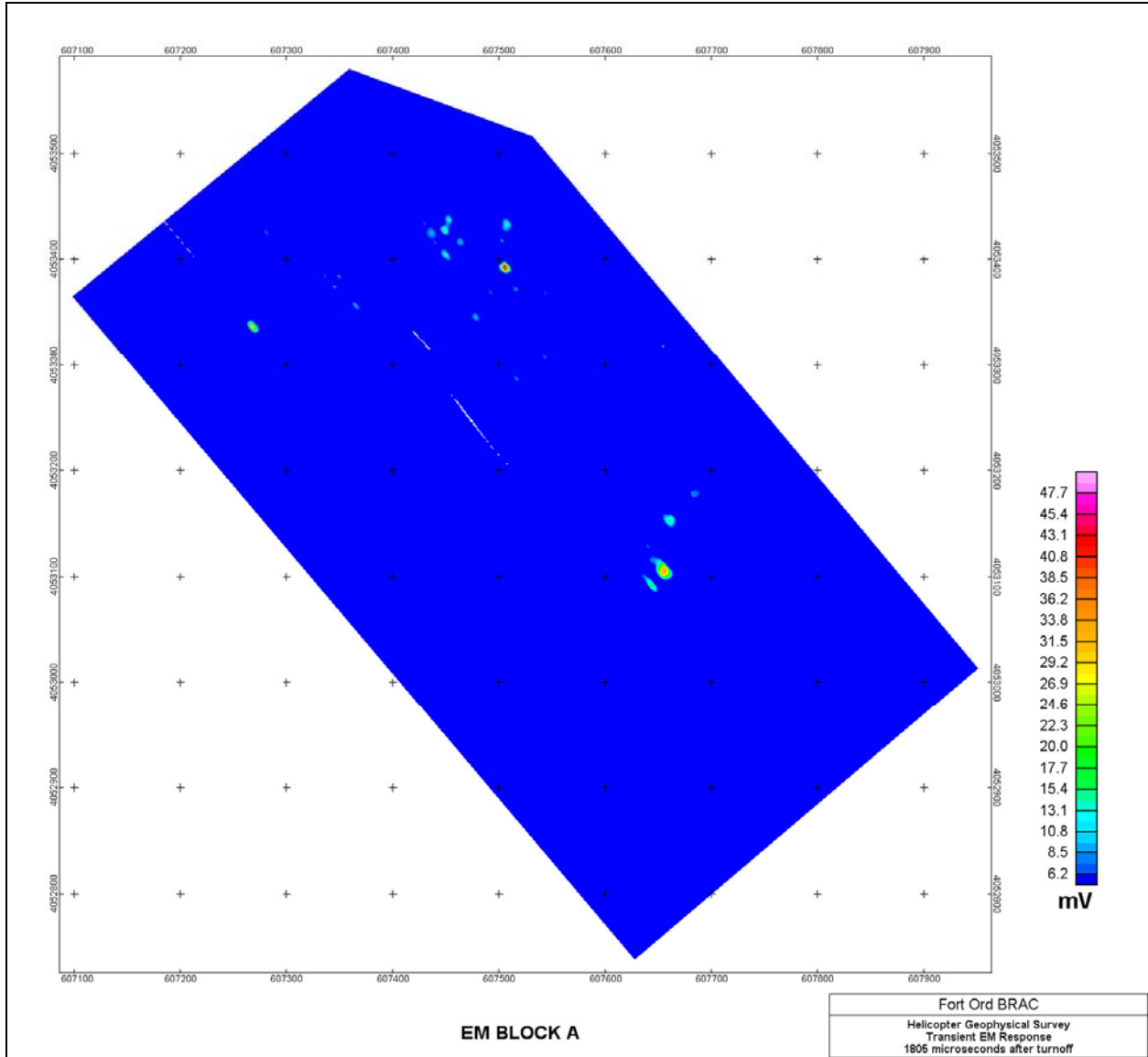


Figure B5. EM response (mV), time bin 5-1805 microseconds after turnoff, EM Block A.

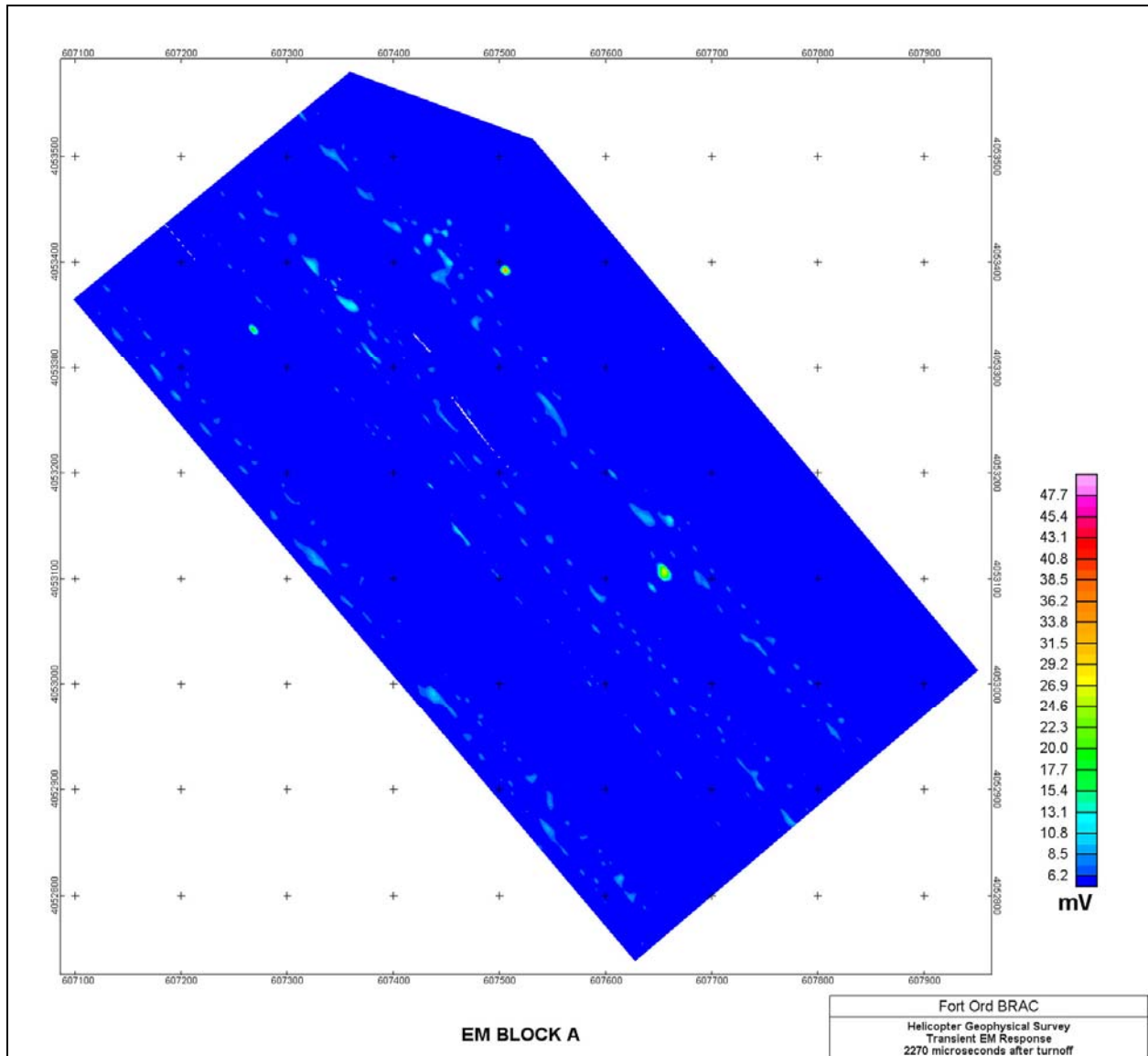


Figure B6. EM response (mV), time bin 6-2270 microseconds after turnoff, EM Block A.

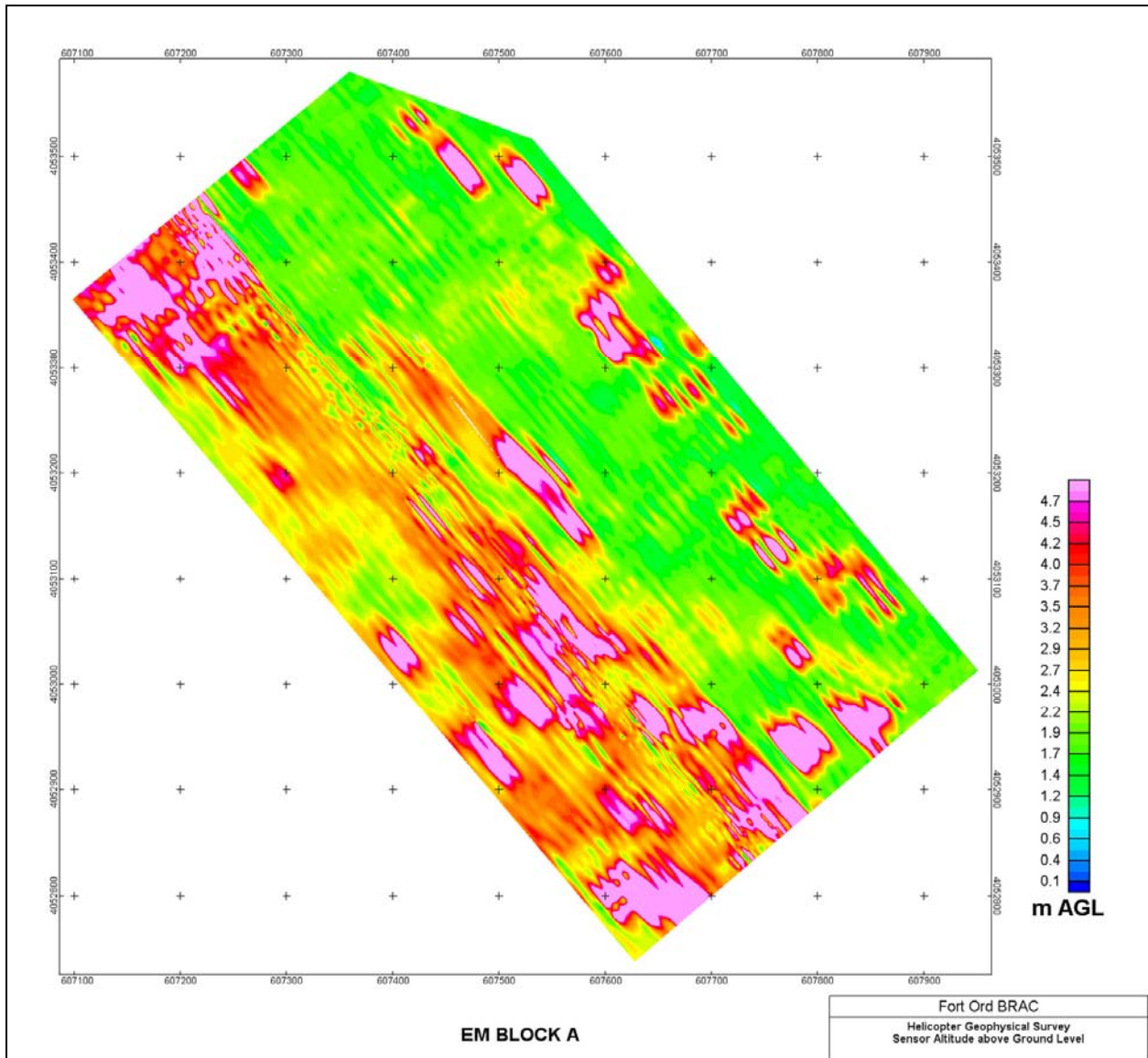


Figure B7. EM sensor altitude, EM Block A.

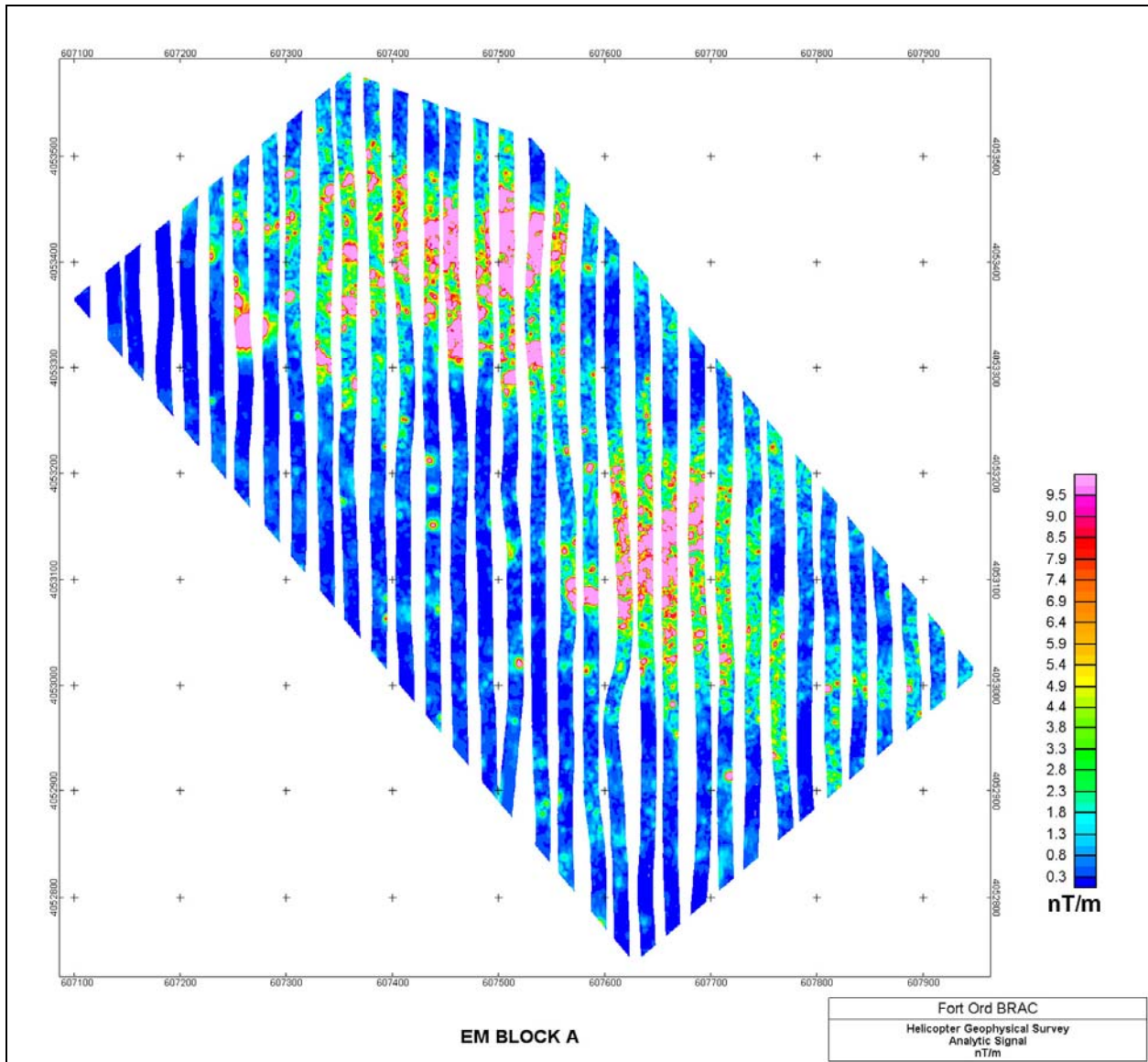


Figure B8. Analytic signal computed from total magnetic field data, EM Block A.

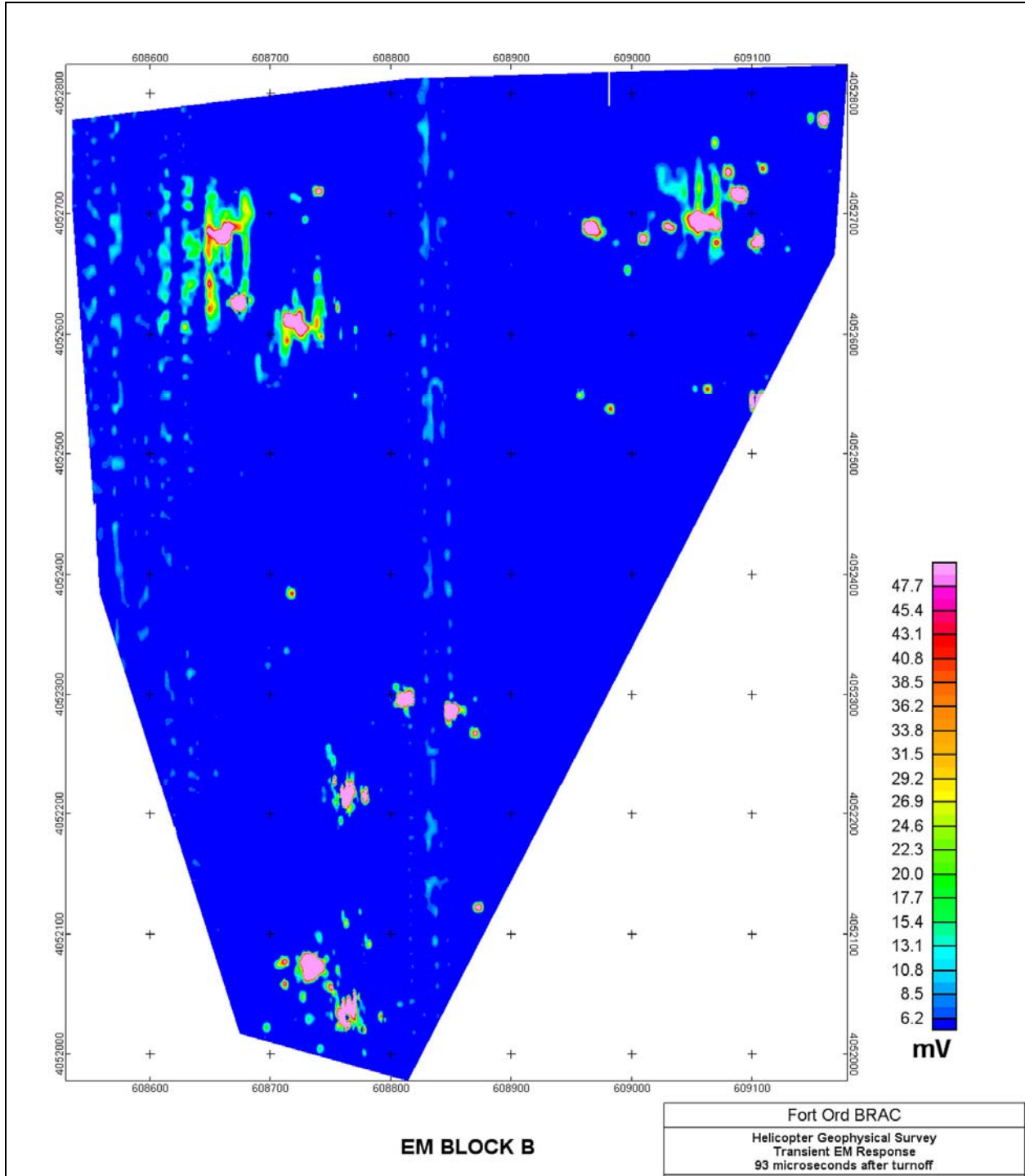


Figure B9. EM response (mV), time bin 1-93 microseconds after turnoff, EM Block B.

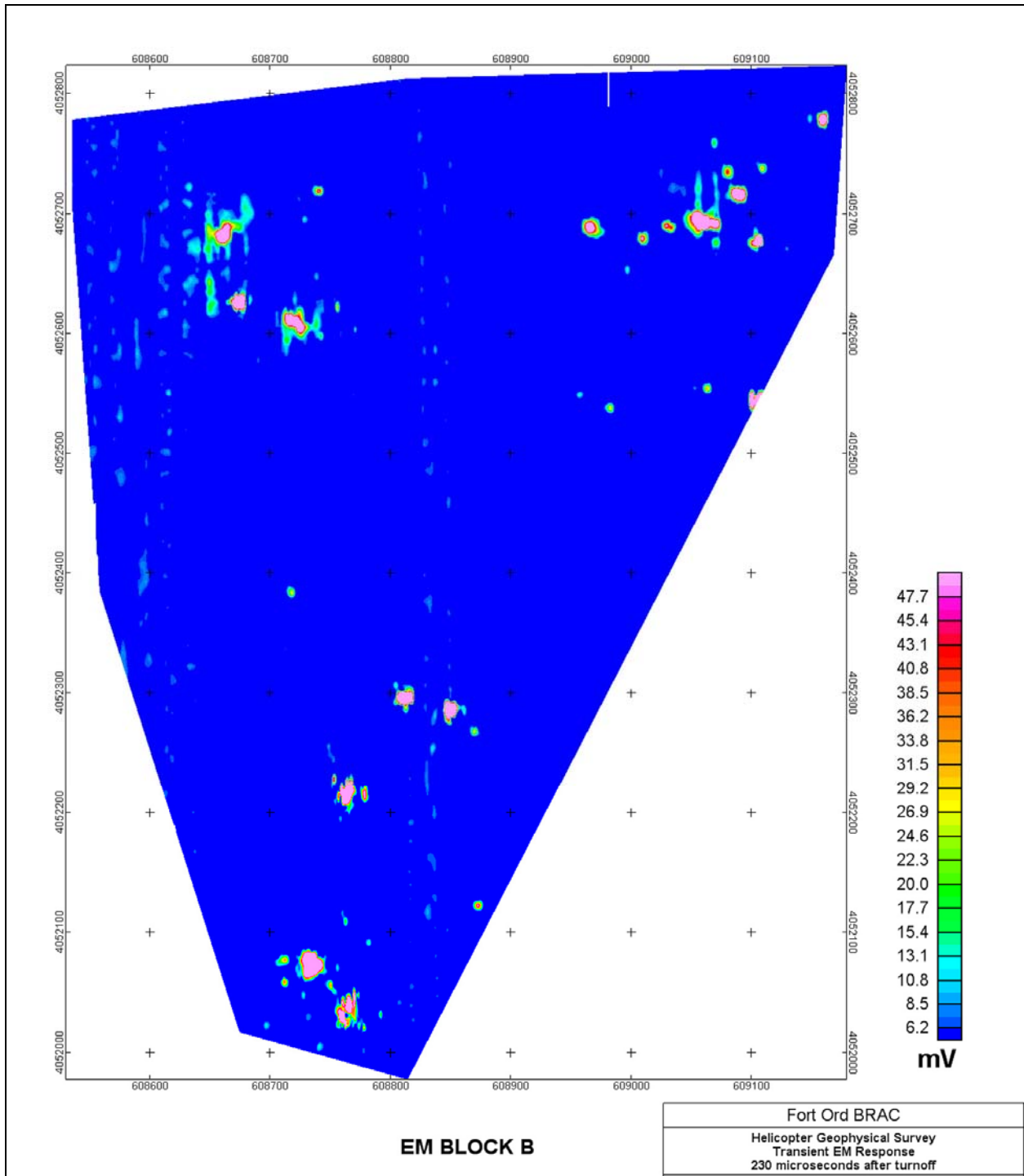


Figure B10. EM response (mV), time bin 2-230 microseconds after turnoff, EM Block B.

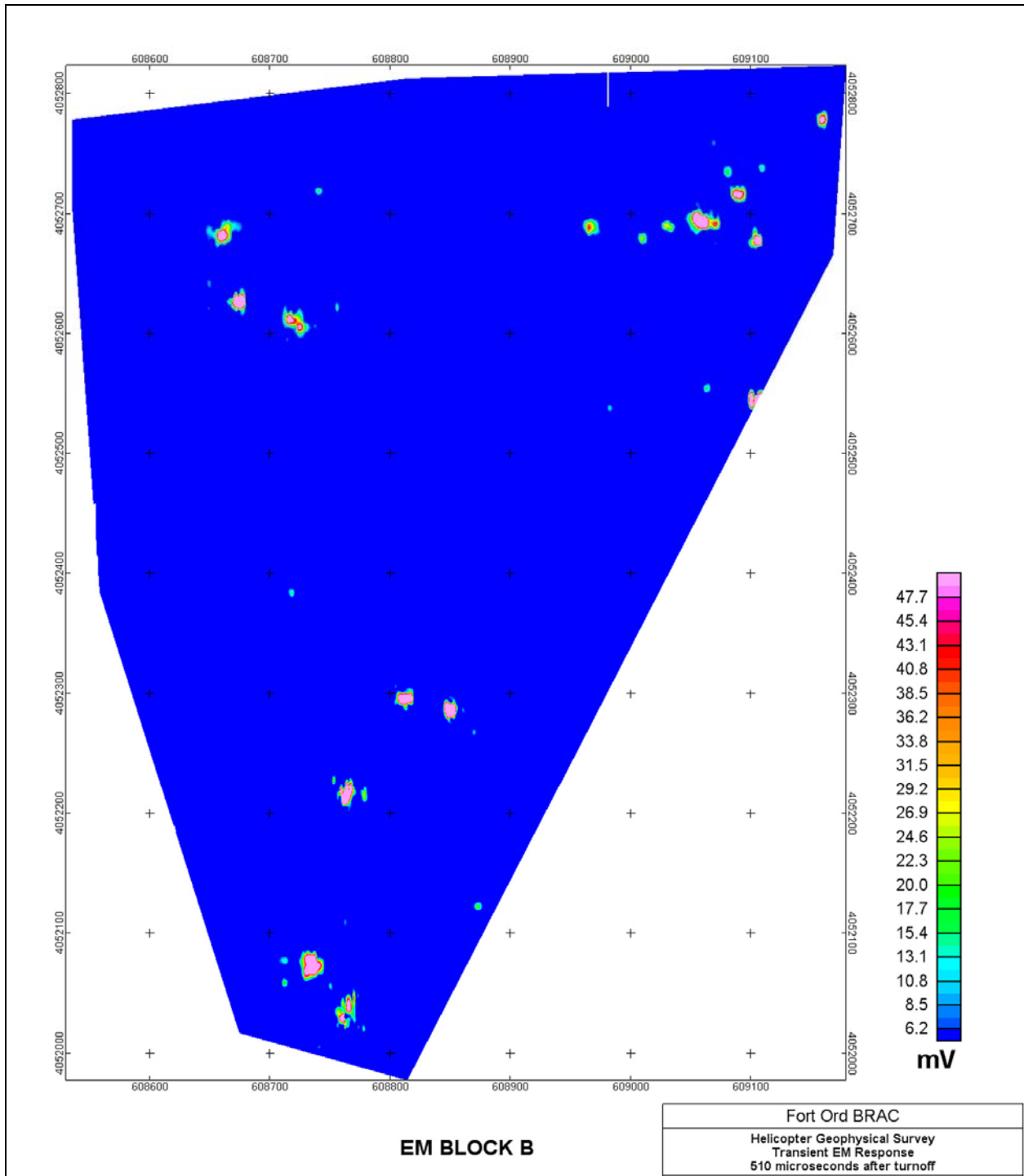


Figure B11. EM response (mV), time bin 3-510 microseconds after turnoff, EM Block B.

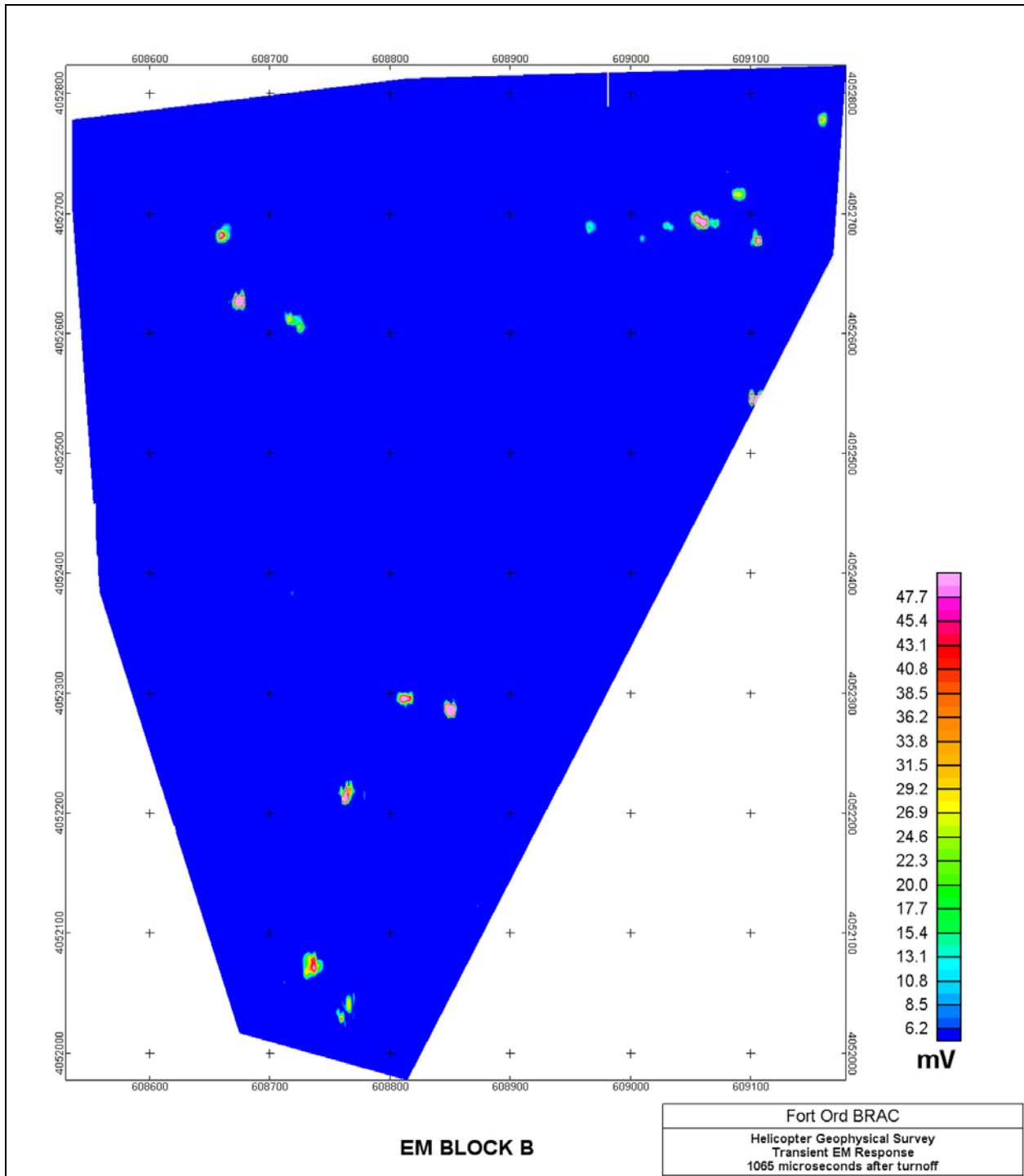


Figure B12. EM response (mV), time bin 4-1065 microseconds after turnoff, EM Block B.

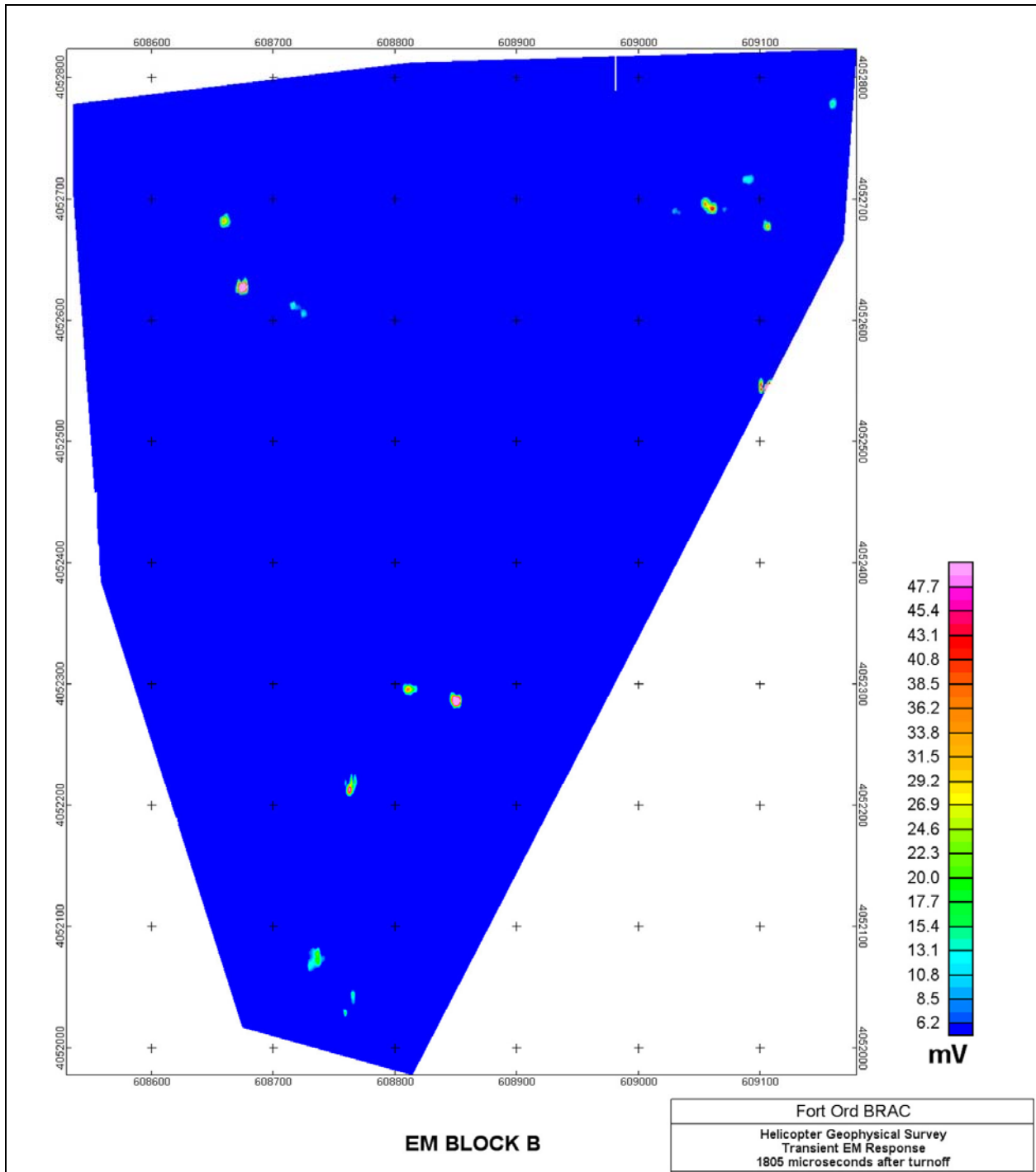


Figure B13. EM response (mV), time bin 5-1805 microseconds after turnoff, EM Block B.

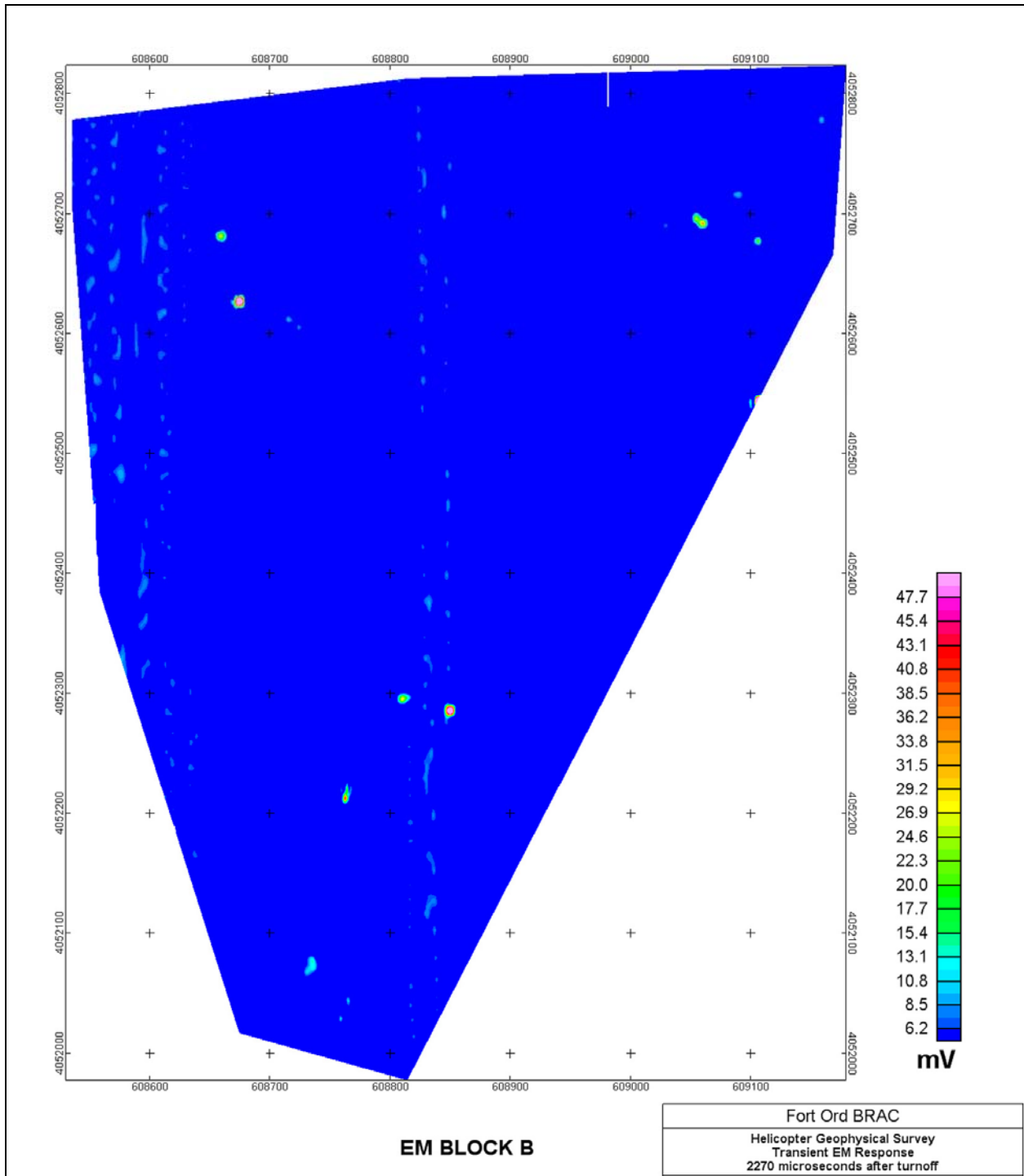


Figure B14. EM response (mV), time bin 6-2270 microseconds after turnoff, EM Block B.

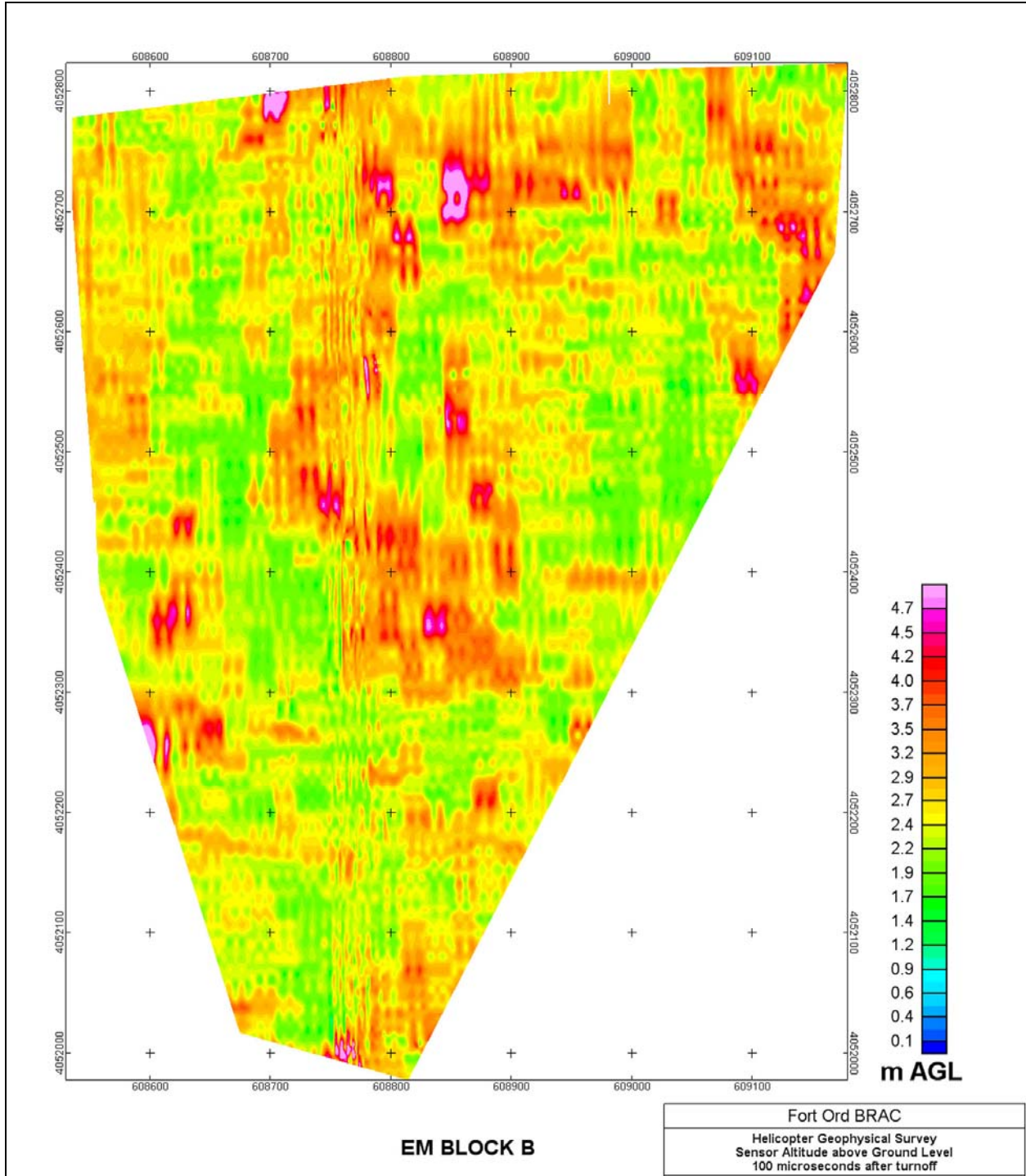


Figure B15. EM sensor altitude, EM Block B.

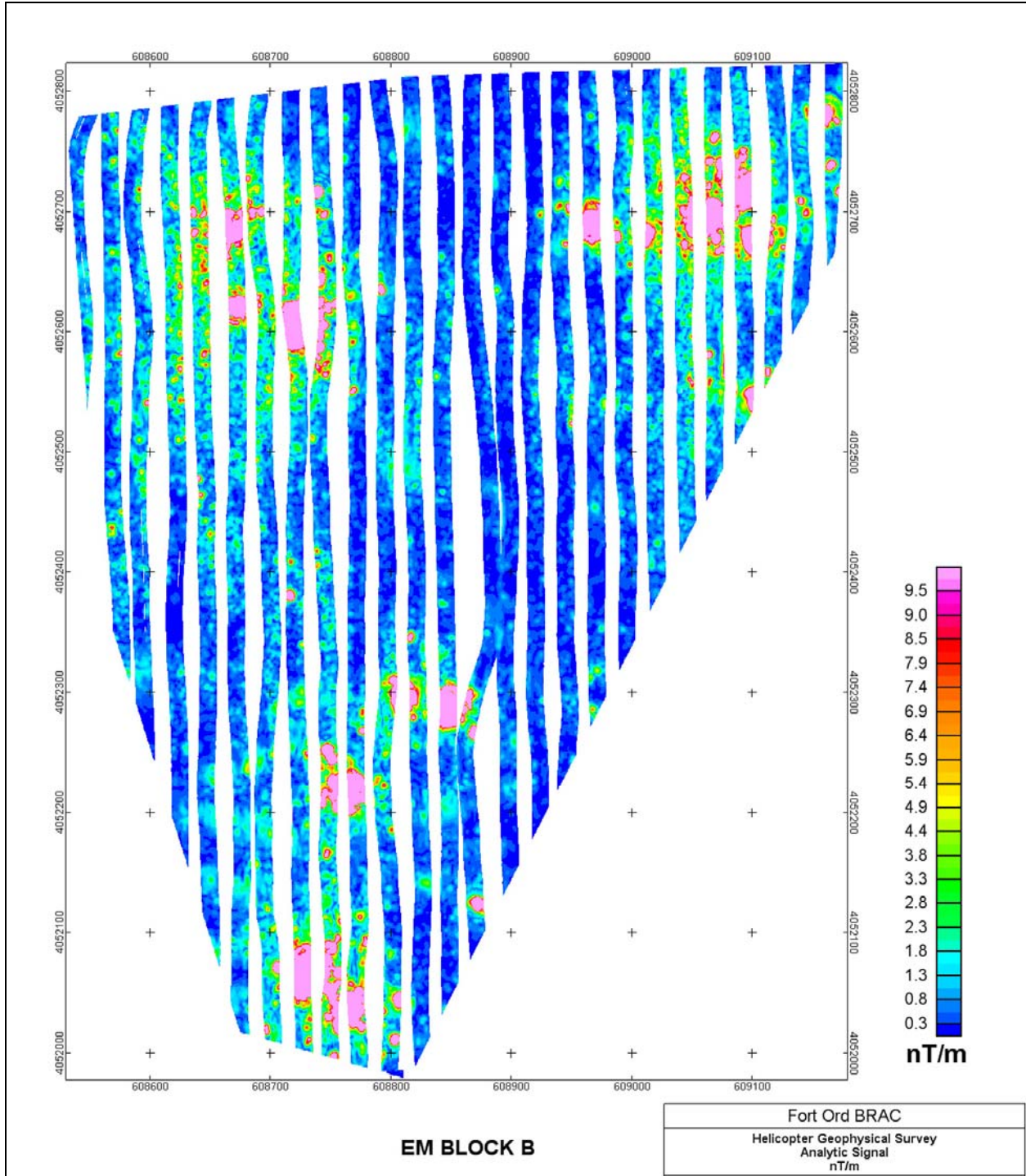


Figure B16. Analytic signal computed from total magnetic field, EM Block B.

# Appendix C: Development of Soil Sampling Plan, Fort Ord, CA

## Introduction

This appendix documents the steps taken to define field soil sampling sites using airborne magnetometer data acquired from the airborne geophysical survey at Fort Ord, CA, January 29 through February 17, 2005 (Chapter 2).

The magnetometer analytic signal data were used to determine soil sampling sites. The analytic signal is a magnetic data form that provides a high-frequency, symmetric response that is centered over source bodies regardless of the effects of remnant magnetization. The analytic signal is a product calculated from the gridded total field data as the square root of the sum of the squares of three orthogonal magnetic gradients (Hrvoic and Pozza 2006). An advantage of the analytic signal is that it is symmetric around targets, while the total field data represent a bipolar signal around small sources. The analytic signal is also a positive value and is generally easier to interpret.

All processing, with the exception of exporting the Geosoft files received from Battelle, was conducted using ArcGIS 9.1 (Environmental Systems Research Institute (ESRI) 2005). The only additional ESRI ArcGIS extension required for processing the data was Spatial Analyst; however, these third-party tools were utilized: Hawth's Analysis Tools (version 3.12), ET Geowizards (version 9.3), a freeware set of tools available from <http://www.ianko.com/>, and a tool called "Pixel Value To Point" downloaded from <http://arcscripts.esri.com>.

The projection of all layers was defined as UTM, Zone 10, NAD83.

## Processing steps

**Step 1.** The Geosoft grid files (GRD) representing magnetometer analytic signal data were first converted to a format usable in ArcGIS (see Chapter 2 for description of magnetometer data collection and analysis).

Using the Oasis Montaj Viewer program, the analytic signal GRD files were exported to "Arcview Binary Raster" format (.FLT extension).

In ArcGIS 9.1, the “.FLT” files were imported into ArcMap using the ArcToolbox → Conversion Tools → Import to Raster → Floating Point Data to Grid conversion tool. This process was used to develop ESRI Grid files. Figure C1 illustrates the raw magnetometer data overlain on a digital orthophoto.

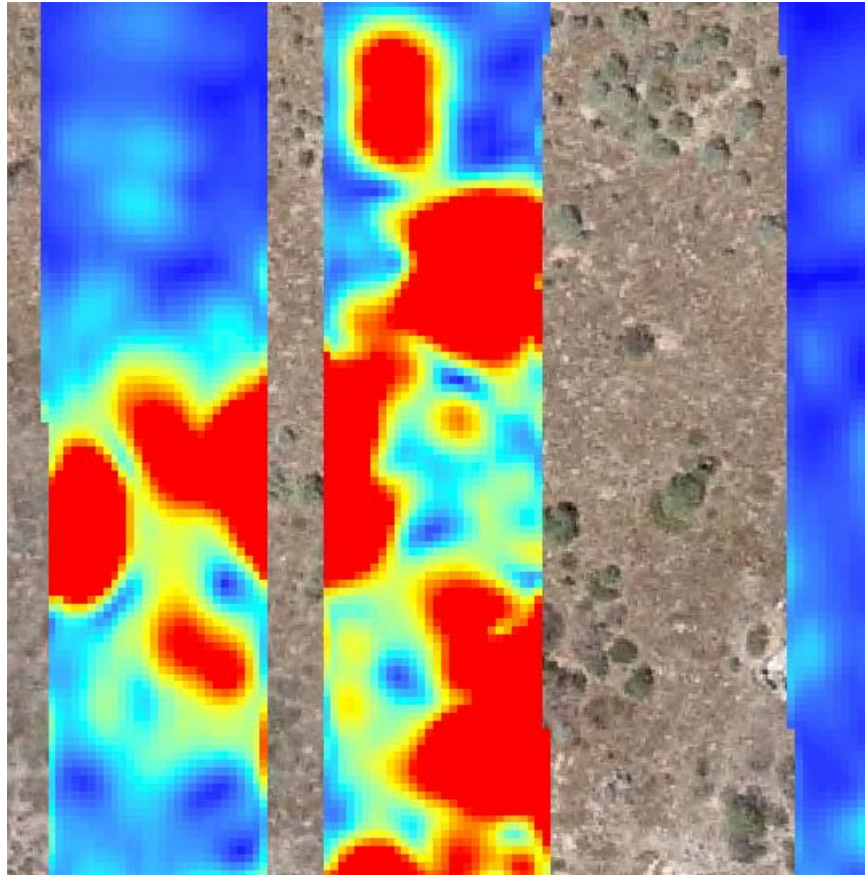
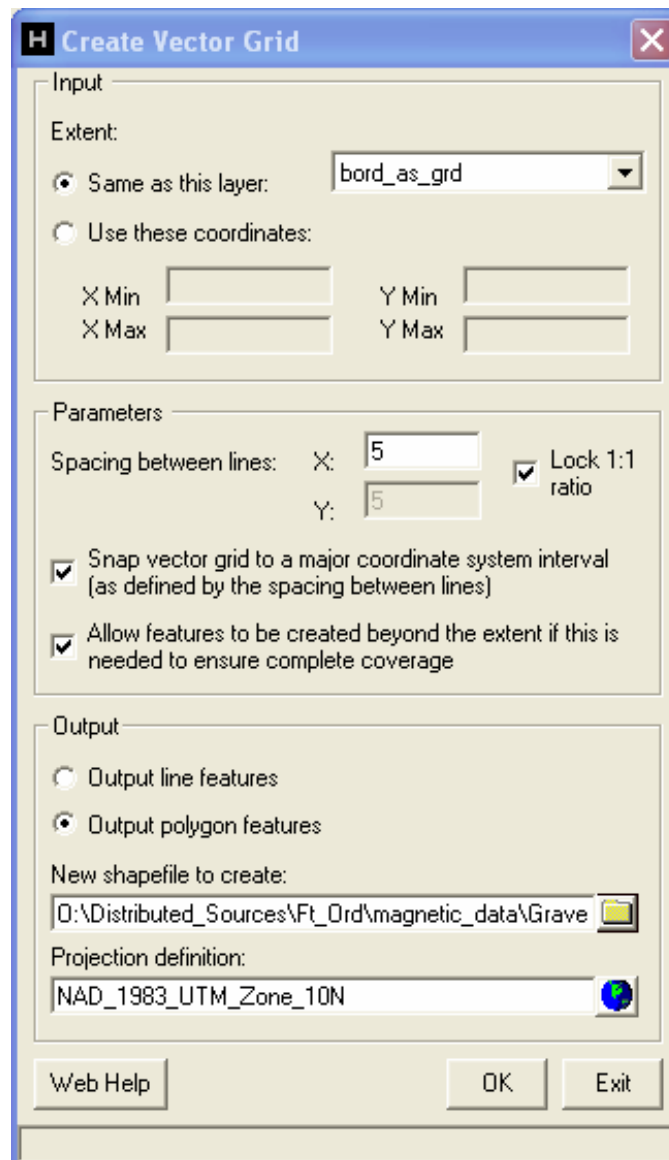


Figure C1. Raw magnetometer data. (Distance from side to side is approximately 55 m).

**Step 2.** A  $5 \times 5$  m polygon layer was developed using Hawth's Analysis tools (Beyer 2004), using the “create vector grid” utility:



This generated a polygon shapefile of  $5 \times 5$  m square cells for the entire area of interest (Figure C2).

**Step 3.** Centroids were generated for each of the  $5 \times 5$  m cells using a utility called “centroid 1.1” downloaded from <http://arcscripts.esri.com>. This utility created a point shapefile, with each point located in the center of each  $5 \times 5$  m grid.

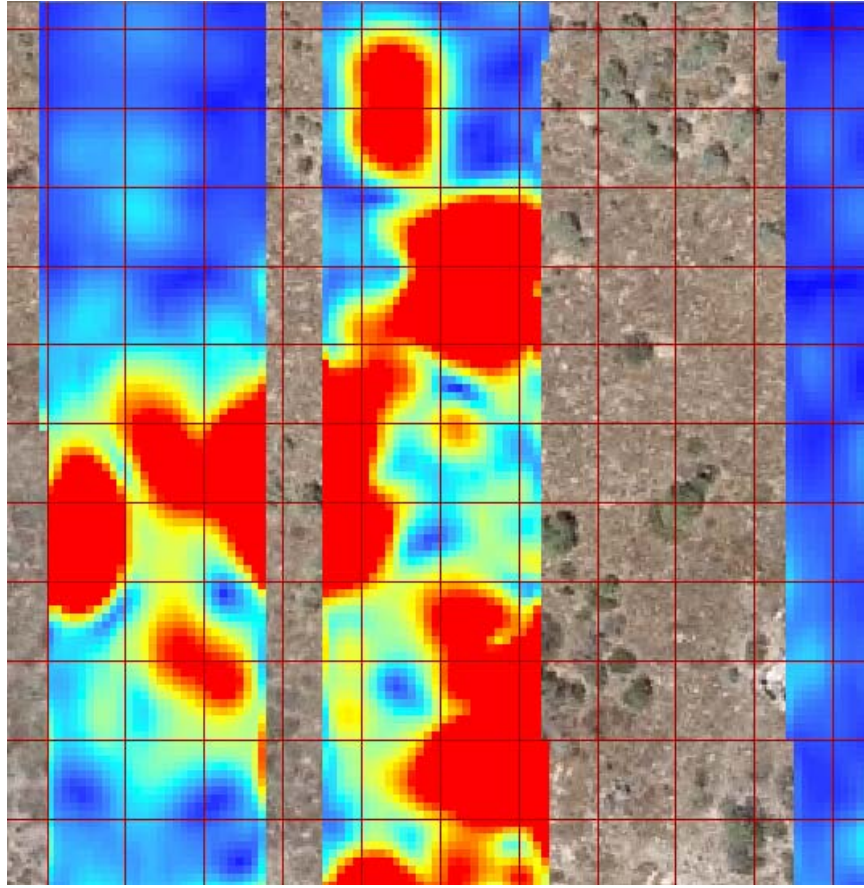
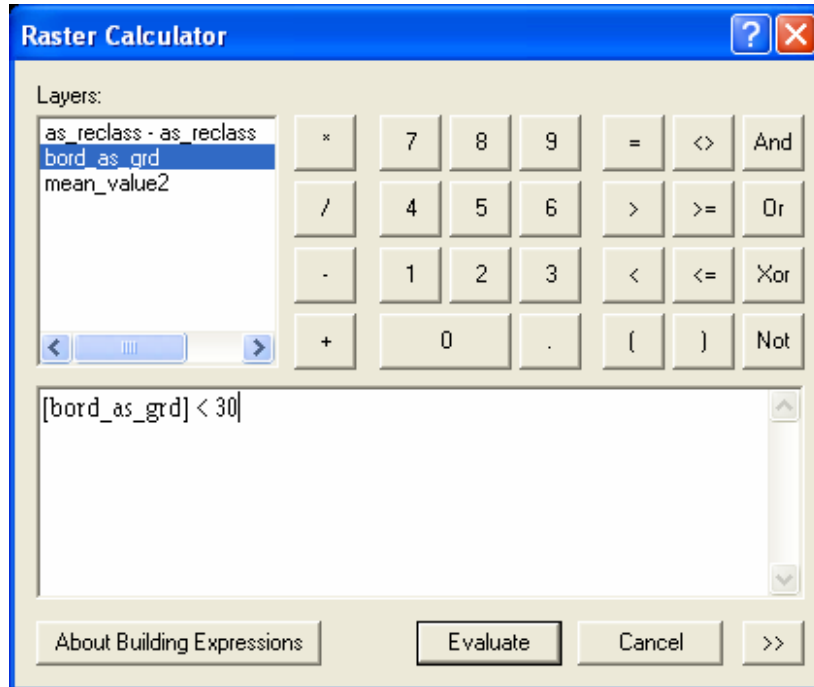


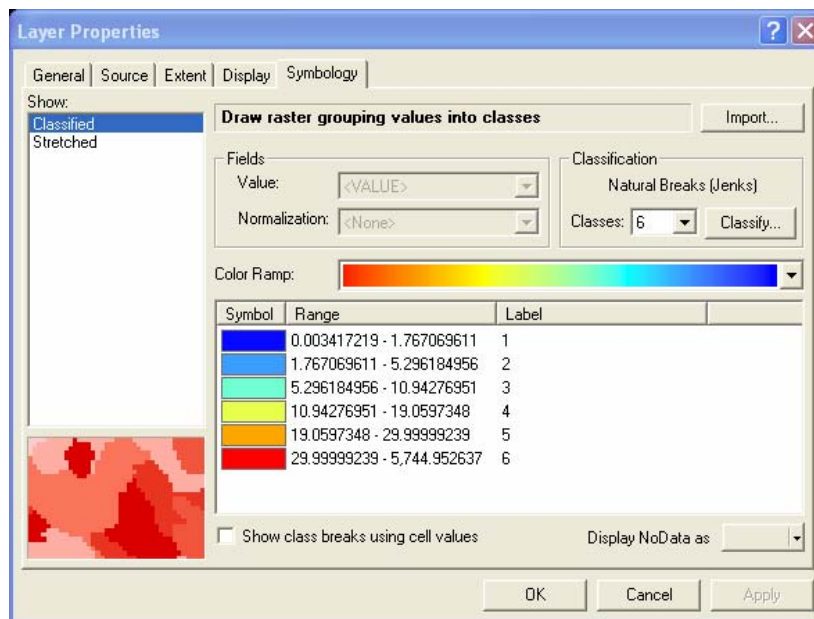
Figure C2. 5-m resolution mesh of polygons generated using Hawth's Analysis Tools.

**Step 4.** Unique identifiers were assigned to each centroid by opening the attribute table and calculating the ID field to be equal to the FID + 1.

**Step 5.** To define the “classes” within the magnetometer data, the histogram was closely analyzed. It was determined that values above 30 nT/m were only located over major targets and represented a very small portion of the total data collected. Therefore, a class > 30 nT/m was selected. All areas with a value greater than 30 nT/m were assigned to this highest class value. Since it was assessed that six classes best categorized the data, these areas (>30 nT/m) were assigned to class 6. Using Spatial Analyst Raster Calculator, all the areas with a value less than 30 nT/m were selected:



**Step 6.** The histogram was then further broken down into five additional classes. This was done automatically by ArcMap using a Jenks Optimization to calculate the natural breaks in the histogram (Figure C3). This technique minimizes within class differences and maximizes between class differences. The final classes were defined as follows:



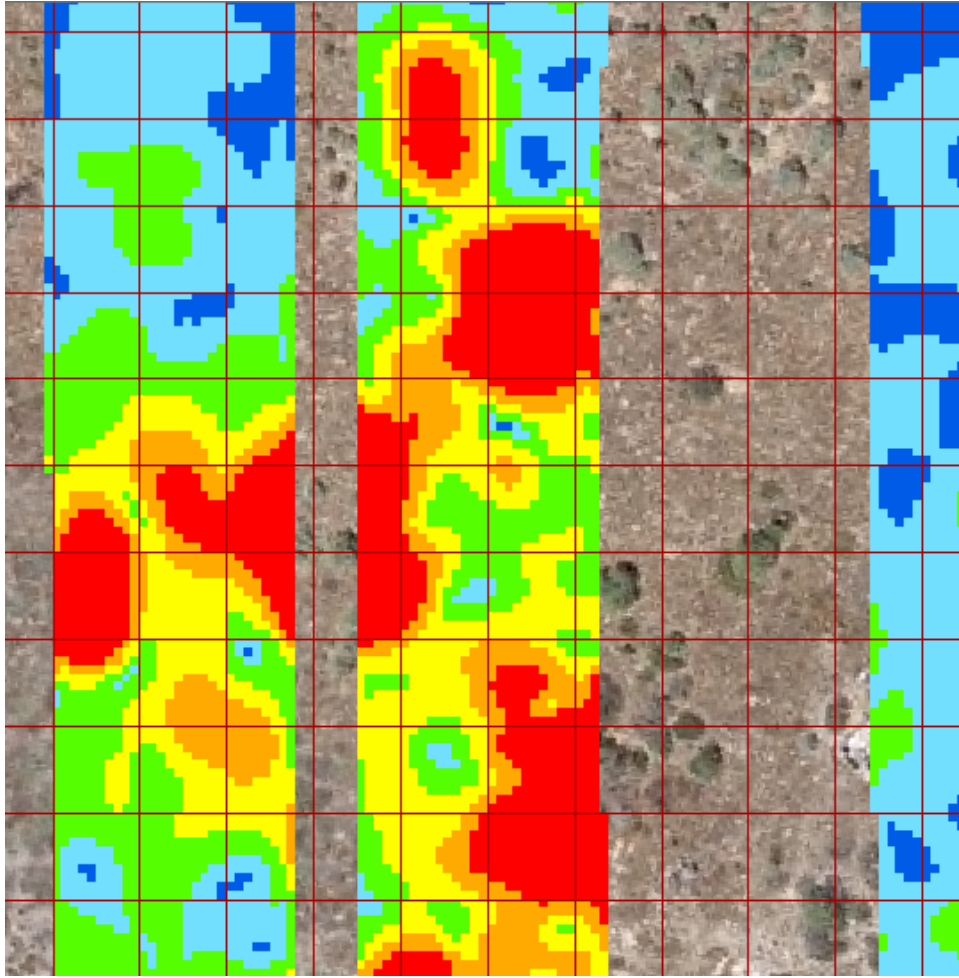
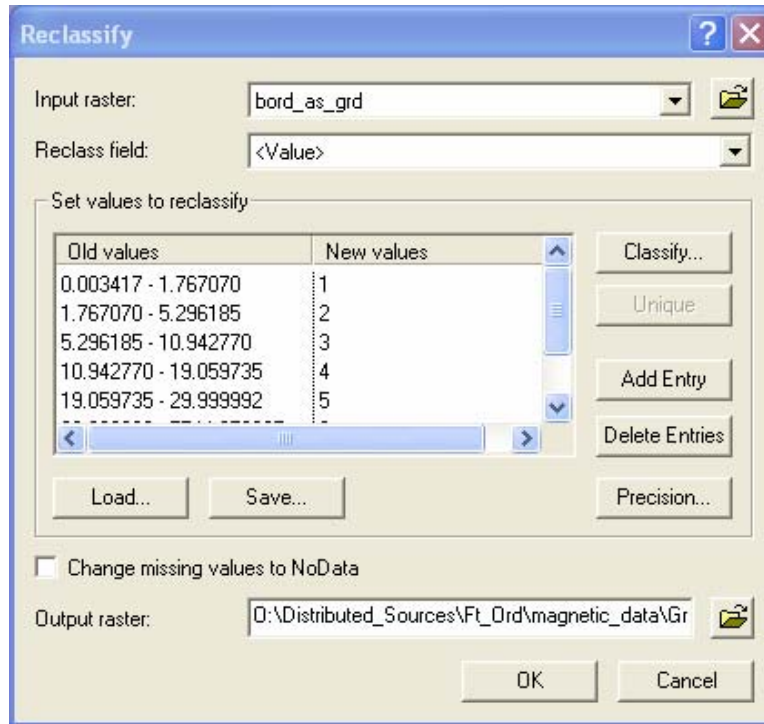
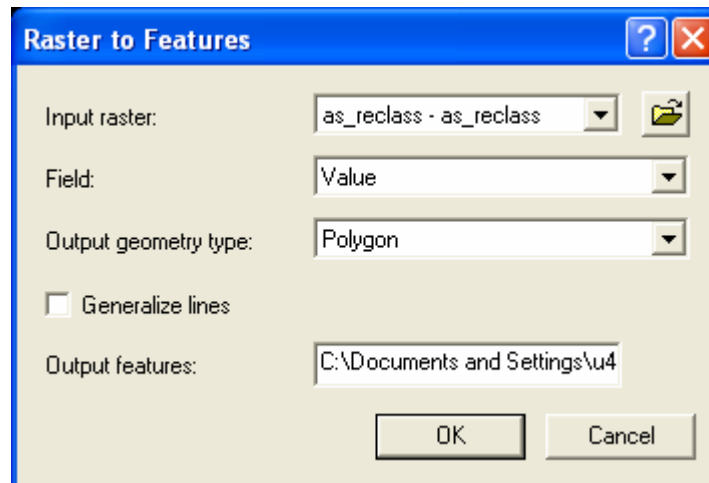


Figure C3. Six classes generated using Jenck's Optimization techniques.

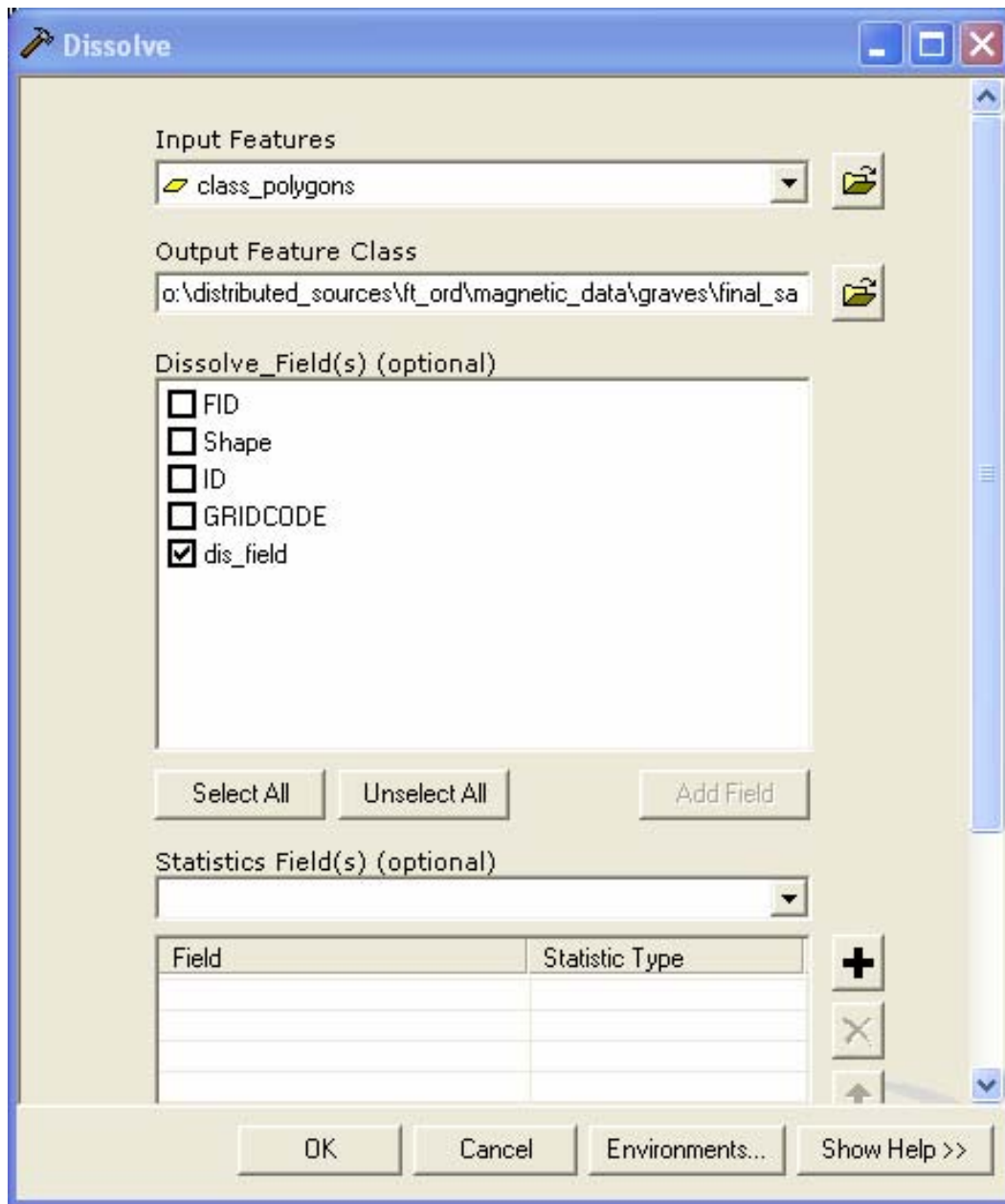
**Step 7.** In order to ensure that sampling was only done in  $5 \times 5$  m cells that fell completely within the data collected by the helicopter, it was necessary to determine which cells met this criterion. Since this type of selection operation cannot be performed on raster data, it was first necessary to convert the classes into vector format. Since this operation cannot be conducted on floating point data, it was first necessary to create an integer raster file that represented the six classes. This was done using the Spatial Analyst "RECLASSIFY" tool:



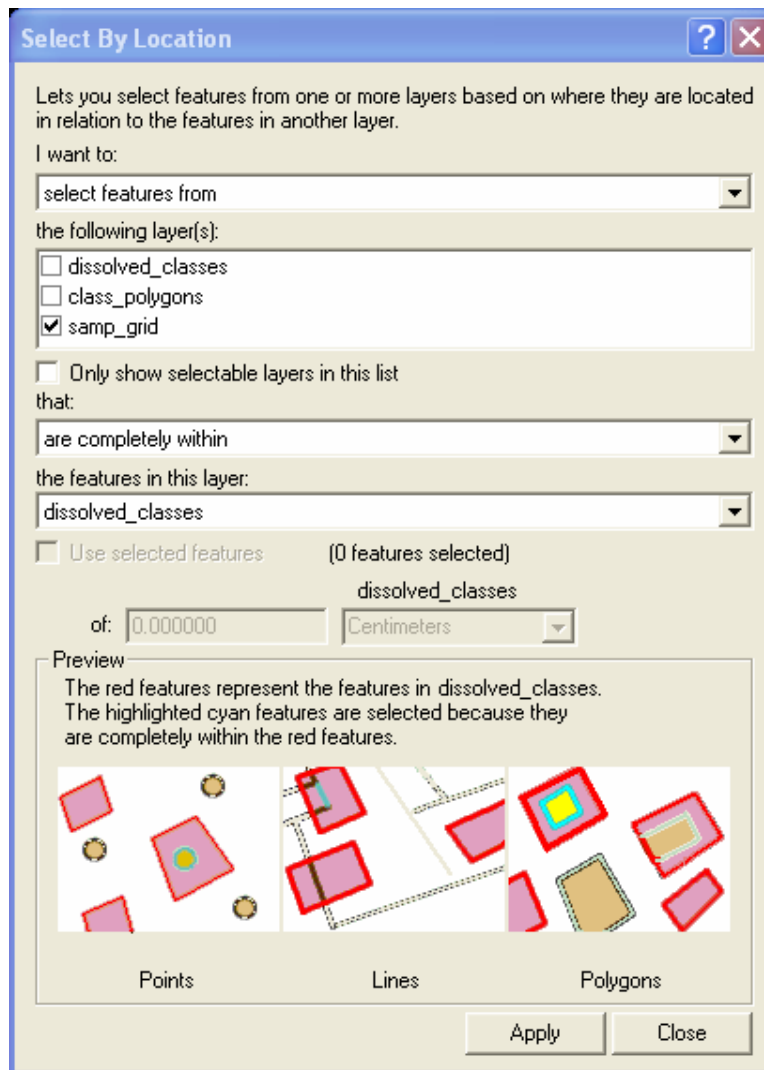
**Step 8.** The output of the RECLASSIFY tool was converted to a shapefile using the Spatial Analyst “Raster to Features” tool (making sure to uncheck the “Generalize Lines” option):



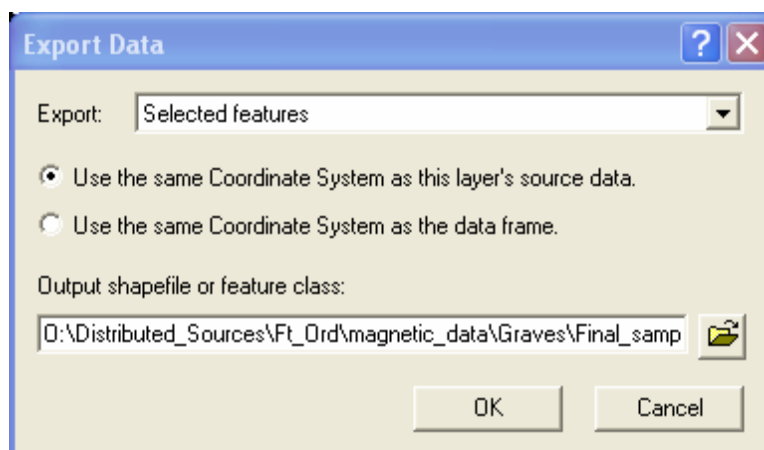
**Step 9.** An attribute (DIS\_FIELD) was then added to the attribute table and a value of “1” assigned to all polygons. This was required as it would be necessary to dissolve (remove) all the lines between classes into one class (representing areas where remote sensing data were collected). The “Dissolve” tool was used to do this:



**Step 10.** Once these preliminary steps were completed, it was possible to select all the  $5 \times 5$  m cells that completely fell within the area covered by the magnetometer. This was done using Selection → Select by Location:



**Step 11.** The selected cells were then exported to create a new shapefile using the “Export Data” tool:



**Step 12.** Centroids were then calculated for each of the potential sampling cells using the ET Geowizards “Polygon to Point” wizard:



The potential sampling sites found to lie totally within areas covered by the flight path are illustrated in Figure C4.

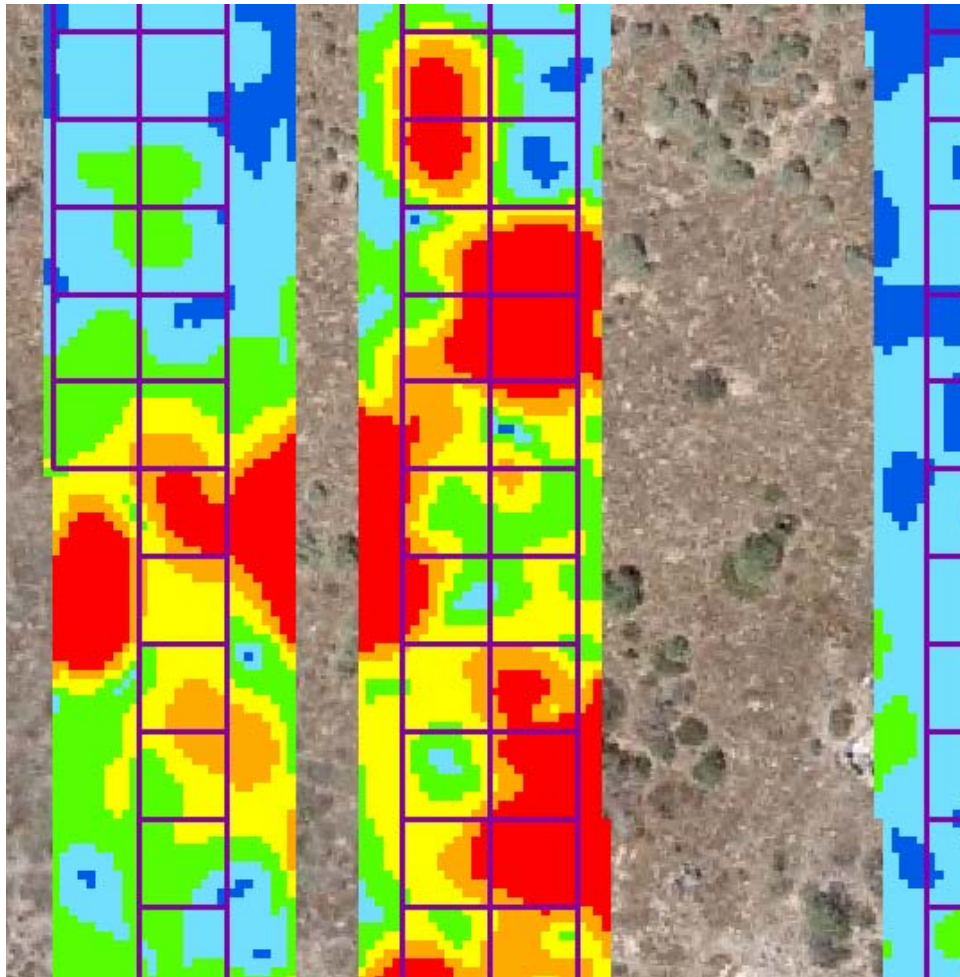
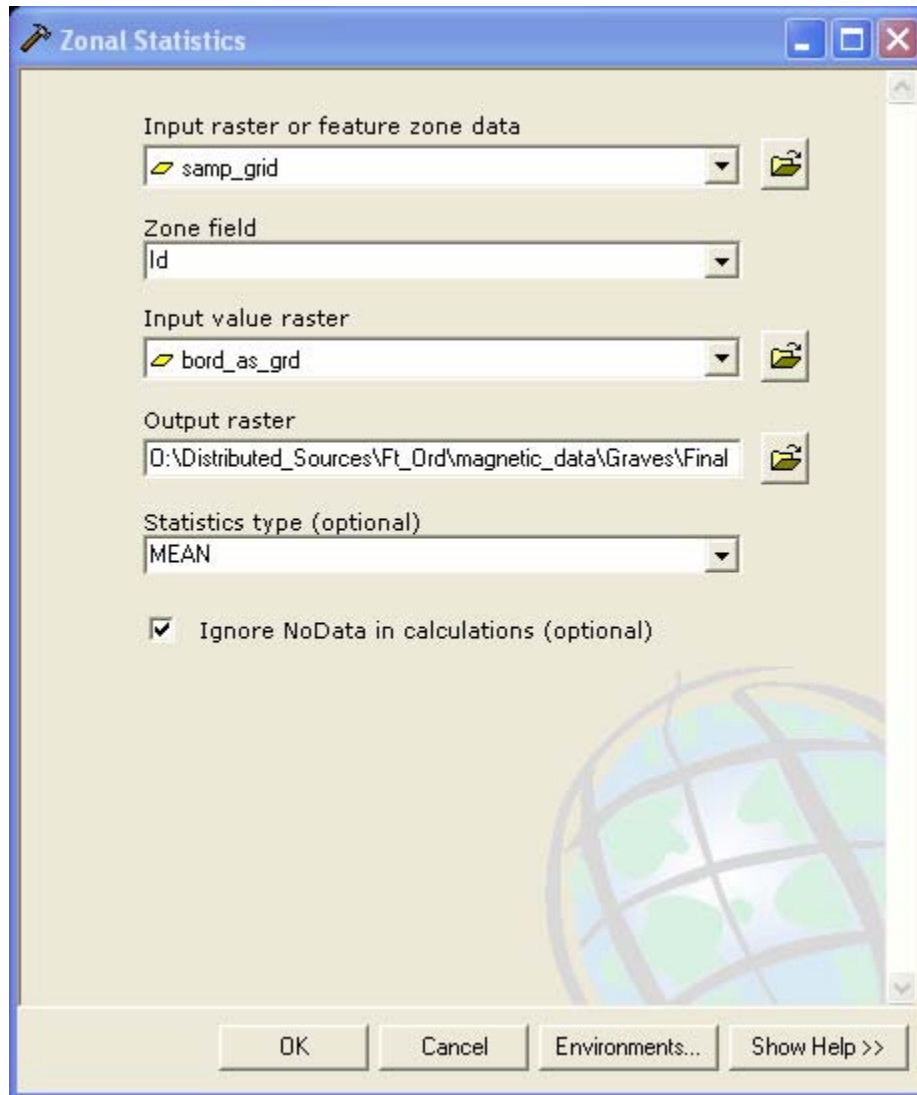


Figure C4. 5-m grids that fell totally within the flight lines.

**Step 13.** Next, the center points had to be associated with the zone they fell within (1-6). To do this, the mean value of magnetometer analytic signal was calculated within each cell. This was done using the Spatial Analyst “Zonal Statistics” tool:



where:

*Input raster or feature zone data = the polygons defining the 5 × 5 m zones*

*Zone field = the unique ID field for each zone (calculated above)*

*Input value raster = the raw gridded analytic signal data*

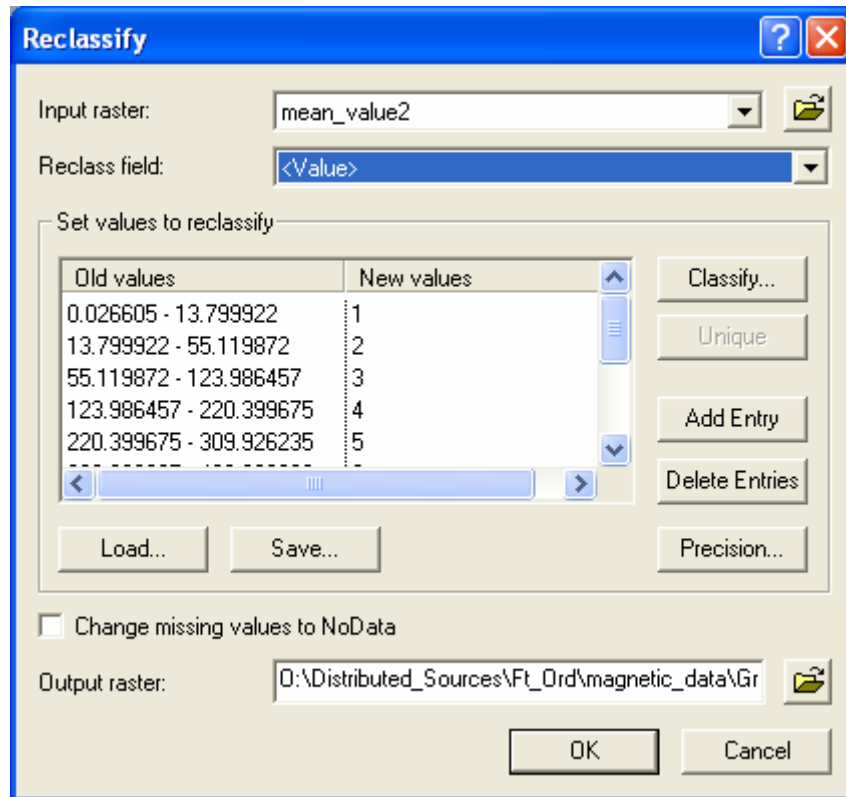
*Output raster = name of the output Grid file containing the mean value within each cell*

*Statistics type = MEAN (calculate the average analytics signal value in each cell)*

*(the “Ignore NoData in calculations” button must be selected)*

The output of this process is the mean of the analytic signal data for each 5 × 5 m cell.

**Step 14.** The mean-value (5 × 5 m) raster file was reclassified to represent values from 1 to 6, using the same procedure as used above for the raw analytic signal data:



This was done in preparation for attaching the class value to the centroid for each cell. Figure C5 illustrates the mean value of magnetometer analytic signal in each 5-m potential sampling site.

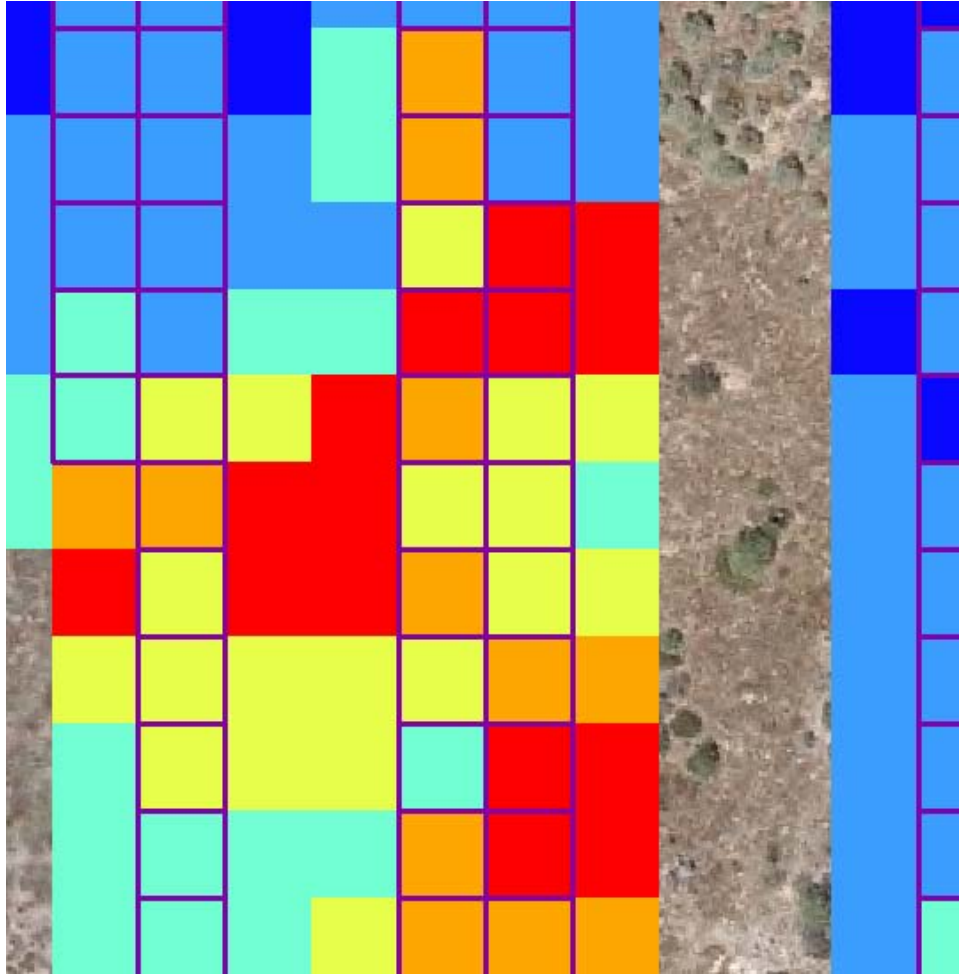
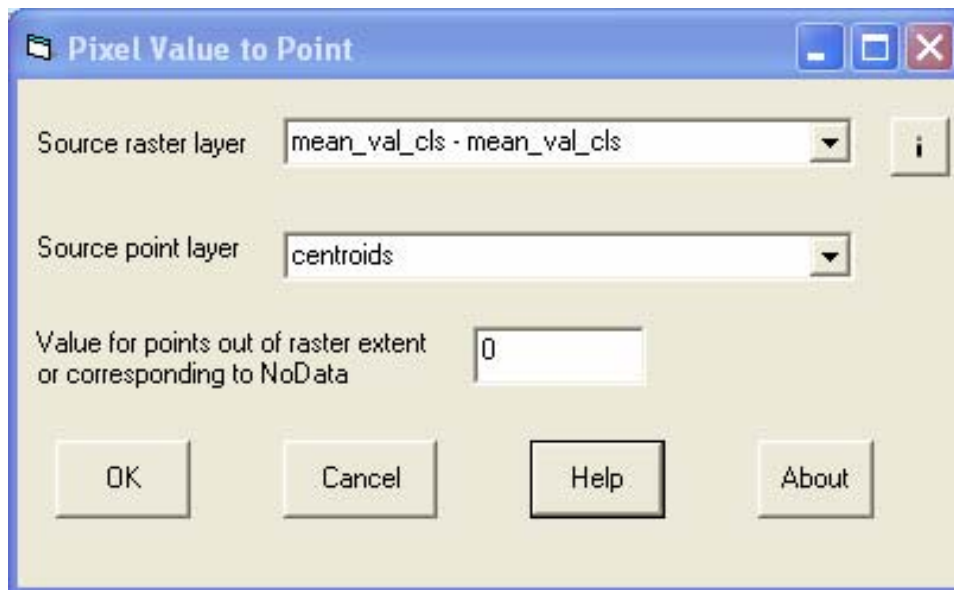
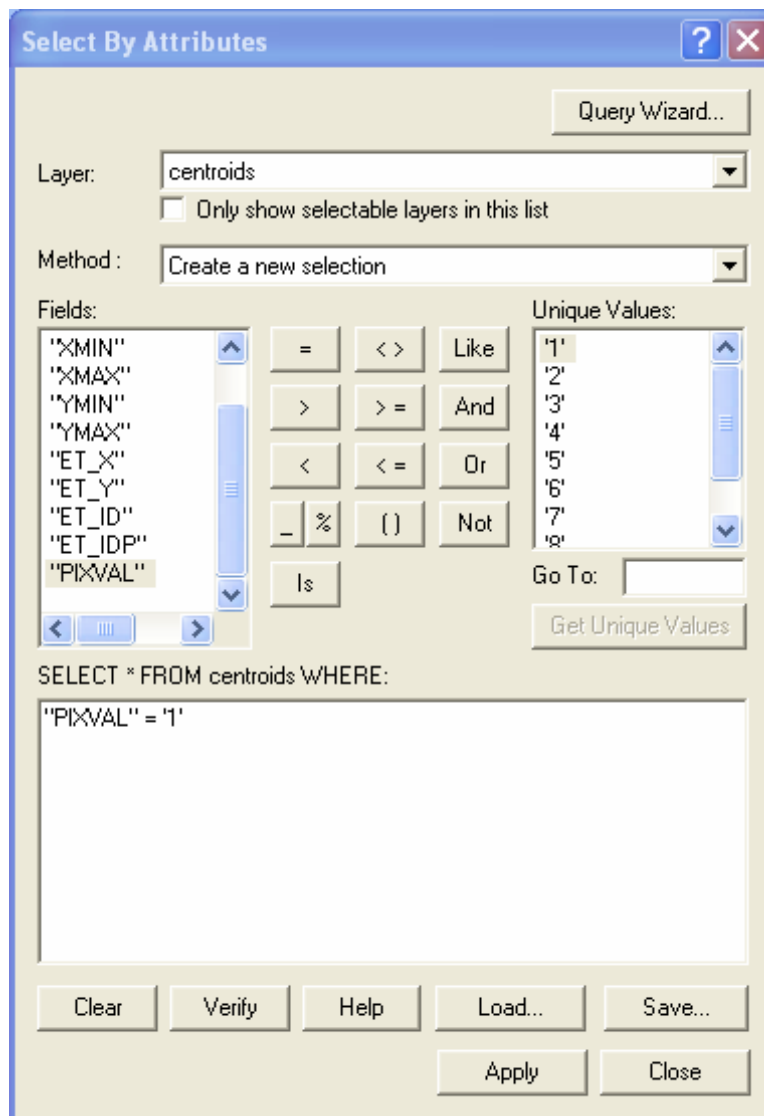


Figure C5. Mean analytic signal value in each 5-m potential sampling area broken into six classes.

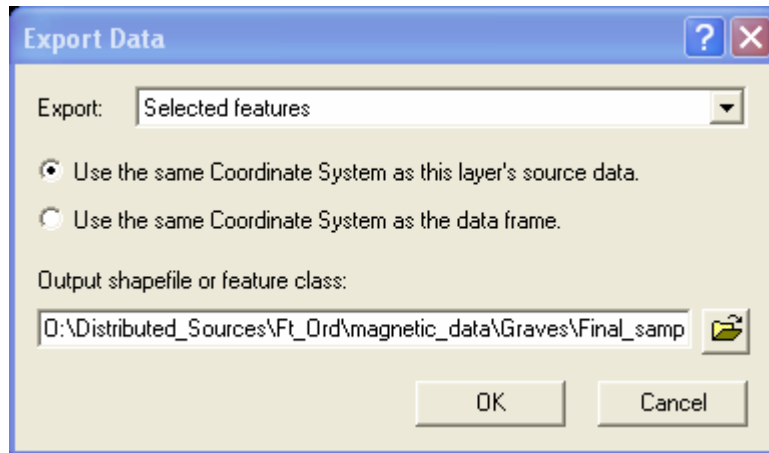
**Step 15.** To attach these mean values with the associated centroid point, a freeware script downloaded from <http://arcscripts.esri.com> called “Pixel Value to Point” was used:



**Step 16.** After the mean class value (1-6) was assigned to each point, a Selection → Selection by Attributes was done to select all the points that had been assigned to each class:

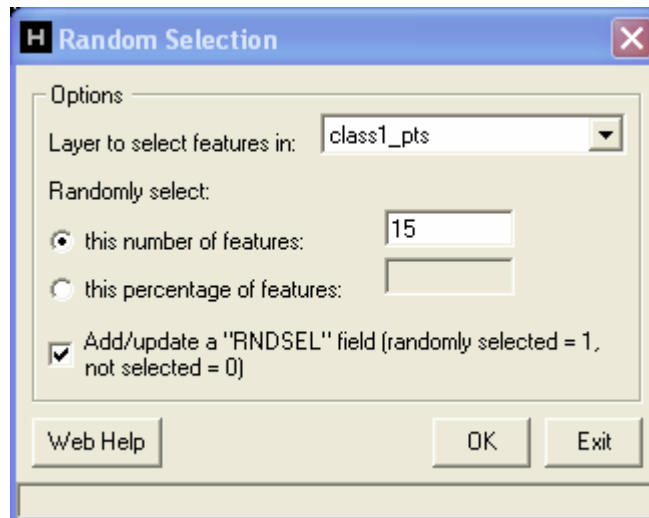


**Step 17.** After all the points from one class were selected, they were exported to a new shapefile:



This was repeated for each remaining class (2-6).

**Step 18.** Once the six shapefiles had been created (one for each class), a random selection was done (using Hawth's Tools) to select 15 cells from each shapefile:



The “Add/update...” button was selected so that a new field would be added to the shapefile recording which sites were selected. This process resulted in 90 samples sites (15 per class).

Figure C6 depicts the location of all sampling sites selected using the procedure described in this chapter.

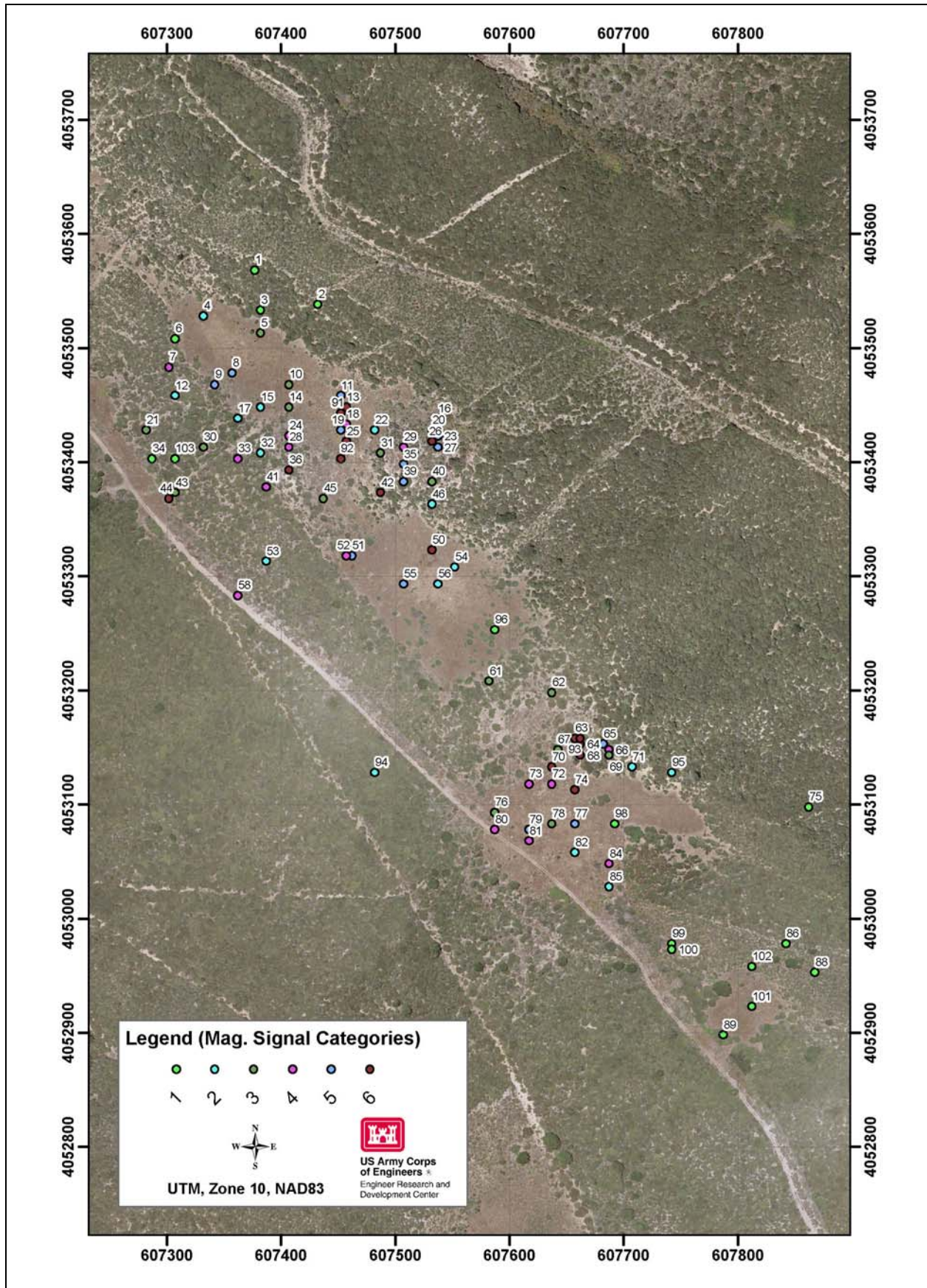


Figure C6. Soil sampling sites selected from airborne magnetometer data, Fort Ord, CA.

## Appendix D: SAS Program (All Observations Included)

```

*****;
*** Analysis of Fort Ord Energetics / Analytic Signal Relationship
      ***;
*** All observations included
      ***;
*****;

dm'log;clear;output;clear';
options nodate nocenter nonumber ps=512 ls=99 nolabel;
ODS HTML style=minimal rs=none body='C:\ Mark R
Graves\Analysis01_All.html' ;

Title1 'Analysis of Fort Ord data (all observations included)';
filename input1 'C:\ Mark R Graves\analyzed_data2.csv';

data Contaminants;
  infile input1 missover DSD dlm="," firstobs=2;
  input X_COOR Y_COOR GRIDCODE MEAN IDENTIFIER OID_GRID TNT RDX
        TETRYL TNB_135 DNT_4_AM DNT_2_AM NG DNT_2_4 HMX TOT_ENER $
        ENERGETICS DETECTABLE $;
  LENERGETICS = log(ENERGETICS+1);
  LMean = log(mean);
datalines;
run;

PROC PRINT DATA=Contaminants; TITLE2 'Data Listing'; RUN;

options ps=60 ls=132;
proc plot data=Contaminants; TITLE2 'scatter plots with group variable';
  plot ENERGETICS * mean = GridCode;
  plot TNT * mean = GridCode;
RUN; OPTIONS PS=256 ls=132;

proc means DATA=Contaminants;
  TITLE2 'Variable means';
  var MEAN TNT RDX TETRYL TNB_135 DNT_4_AM DNT_2_AM NG DNT_2_4 HMX
  ENERGETICS LENERGETICS LMEAN;
run;

*-----;
options ps=52;
proc factor method=prin rotate=varimax ev scree out=factors01 nfact=4;
  TITLE2 'Factor analysis using of various chemical';
  var TNT RDX TETRYL TNB_135 DNT_4_AM DNT_2_AM NG DNT_2_4 HMX;
run;
options ps=512 ls=99;

proc corr data=factors01;
  TITLE2 'Correlations of factors and variables of interest';
  var factor1 factor2 factor3 factor4;
  with MEAN ENERGETICS LENERGETICS LMEAN;
run;

proc mixed DATA=Contaminants;
  TITLE2 'ANCOVA using value of ENERGETICS';
  class gridcode;
  model ENERGETICS = GridCode / htype = 1 3 outp=resid01;

```

```
run;
PROC UNIVARIATE DATA=resid01 NORMAL PLOT; VAR resid;
  TITLE3 'Residual analysis';
RUN;

PROC REG DATA=Contaminants; id GridCode IDENTIFIER ENERGETICS;
  TITLE2 'Regression using value of ENERGETICS';
  MODEL ENERGETICS = mean / clb alpha=0.05;
  output out=next0 r=resid;
RUN;
PROC UNIVARIATE DATA=next0 NORMAL PLOT; VAR resid;
  TITLE3 'Residual analysis';
RUN;

proc mixed DATA=Contaminants;
  TITLE2 'ANCOVA using value of Log(ENERGETICS)';
  class gridcode;
  model LENERGETICS = GridCode / htype = 1 3 outp=resid01;
run;
PROC UNIVARIATE DATA=resid01 NORMAL PLOT; VAR resid;
  TITLE3 'Residual analysis';
RUN;

PROC REG DATA=Contaminants; id GridCode IDENTIFIER ENERGETICS;
  TITLE2 'Regression using value of ENERGETICS';
  MODEL LENERGETICS = mean / clb alpha=0.05;
  output out=next1 r=resid;
RUN;
PROC UNIVARIATE DATA=next1 NORMAL PLOT; VAR resid;
  TITLE3 'Residual analysis';
RUN;

PROC logistic DATA=Contaminants descending;
  TITLE2 'Logistic Regression';
  MODEL DETECTABLE = mean;
  output out=next5 prob=prob lower=lcl upper=ucl;
RUN;
options ps=52;
proc plot data=next5; plot prob*mean; run;
options ps=512;

proc sort data=next5; by mean detectable; run;
proc print data=next5;
  var X_COOR Y_COOR GRIDCODE MEAN IDENTIFIER OID_GRID_TOT_ENER
ENERGETICS DETECTABLE prob lcl ucl;
run;
```

## Appendix E: SAS Program (Large Outlier Deleted)

```

*****;
*** Analysis of Fort Ord Energetics / Analytic Signal Relationship
***;
*** Large Outlier Deleted
***;
*****;

dm'log;clear;output;clear';
options nodate nocenter nonumber ps=512 ls=99 nolabel;
ODS HTML style=minimal rs=none body='C:\ Mark R
Graves\Analysis01_LessOne.html' ;

Title1 'Analysis of Fort Ord data (one observation omitted)';
filename input1 'C:\ analyzed_data2.csv';

data Contaminants;
  infile input1 missover DSD dlm="," firstobs=2;
  input X COOR Y COOR GRIDCODE MEAN IDENTIFIER OID_ GRID TNT RDX
        TETRYL TNB_135 DNT_4 AM DNT_2_AM NG DNT_2_4 HMX TOT_ENER $
        ENERGETICS DETECTABLE $;
  if ENERGETICS gt 100 then delete;
  LENERGETICS = log(ENERGETICS+1);
  LMean = log(mean);
  drop DNT_2_4;
datalines;
run;

PROC PRINT DATA=Contaminants; TITLE2 'Data Listing'; RUN;

options ps=60 ls=132;
proc plot data=Contaminants; TITLE2 'scatter plots with group variable';
  plot ENERGETICS * mean = GridCode;
  plot TNT * mean = GridCode;
RUN; OPTIONS PS=256 ls=132;

proc means DATA=Contaminants;
  TITLE2 'Variable means';
  var MEAN TNT RDX TETRYL TNB_135 DNT_4_AM DNT_2_AM NG HMX ENERGETICS
  LENERGETICS LMEAN;
run;

*-----;
options ps=52;
proc factor method=prin rotate=varimax ev scree out=factors01 nfact=4;
  TITLE2 'Factor analysis using of various chemical';
  var TNT RDX TETRYL TNB_135 DNT_4_AM DNT_2_AM NG HMX;
run;
options ps=512 ls=99;

proc corr data=factors01;
  TITLE2 'Correlations of factors and variables of interest';
  var factor1 factor2 factor3 factor4;
  with MEAN ENERGETICS LENERGETICS LMEAN;
run;

proc mixed DATA=Contaminants;
  TITLE2 'ANCOVA using value of ENERGETICS';
  class gridcode;
  model ENERGETICS = GridCode / htype = 1 3 outp=resid01;
run;
PROC UNIVARIATE DATA=resid01 NORMAL PLOT; VAR resid;
  TITLE3 'Residual analysis';
RUN;

PROC REG DATA=Contaminants; id GridCode IDENTIFIER ENERGETICS;

```

```
TITLE2 'Regression using value of ENERGETICS';
MODEL ENERGETICS = mean / clb alpha=0.05;
output out=next0 r=resid;
RUN;
PROC UNIVARIATE DATA=next0 NORMAL PLOT; VAR resid;
TITLE3 'Residual analysis';
RUN;

proc mixed DATA=Contaminants;
TITLE2 'ANCOVA using value of Log(ENERGETICS)';
class gridcode;
model LENERGETICS = GridCode / htype = 1 3 outp=resid02;
run;
PROC UNIVARIATE DATA=resid02 NORMAL PLOT; VAR resid;
TITLE3 'Residual analysis';
RUN;

PROC REG DATA=Contaminants; id GridCode IDENTIFIER ENERGETICS;
TITLE2 'Regression using value of ENERGETICS';
MODEL LENERGETICS = mean / clb alpha=0.05;
output out=next1 r=resid;
RUN;
PROC UNIVARIATE DATA=next1 NORMAL PLOT; VAR resid;
TITLE3 'Residual analysis';
RUN;

PROC logistic DATA=Contaminants descending;
TITLE2 'Logistic Regression';
MODEL DETECTABLE = mean;
output out=next5 prob=prob lower=lcl upper=ucl;
RUN;
options ps=52;
proc plot data=next5; plot prob*mean; run;
options ps=512;

proc sort data=next5; by mean detectable; run;
proc print data=next5;
var X_COOR Y_COOR GRIDCODE MEAN IDENTIFIER OID_ GRID_ TOT_ENER
ENERGETICS DETECTABLE prob lcl ucl;
run;
```

# Appendix F: SAS Output (All Observations Included)

Analysis of Fort Ord Energetics / Magnetometer Relationship (all observations included)  
Data Listing

Obs	X_COOR	Y_COOR	GRIDCODE	MEAN	IDENTIFIER	OID_	GRID_	TNT	RDX	TETRYL	TNB_135
1	607377.25	4053567.75	1	0.5975	1	0	1	0.000	0.00000	0.00000	0.000
2	607432.25	4053537.75	1	0.3735	2	1	2	0.000	0.00000	0.00000	0.000
3	607382.25	4053532.75	1	0.9051	3	2	3	0.000	0.00000	0.00000	0.000
4	607332.25	4053527.75	2	3.6400	4	3	4	0.000	0.00000	0.00000	0.000
5	607382.25	4053512.75	3	6.3144	5	4	5	0.000	0.00000	0.00000	0.000
6	607307.25	4053507.75	1	0.4086	6	5	6	0.032	0.00000	0.00000	0.000
7	607302.25	4053482.75	4	17.3290	7	6	7	0.024	0.00000	0.00000	0.000
8	607357.25	4053477.75	5	23.3830	8	7	8	0.015	0.00000	0.00000	0.000
9	607342.25	4053467.75	5	28.2375	9	8	9	0.000	0.00000	0.00000	0.000
10	607407.25	4053467.75	3	5.5343	10	9	10	0.000	0.00000	0.40200	0.000
11	607452.25	4053457.75	5	25.8849	11	10	11	0.018	0.03940	0.09800	0.000
12	607307.25	4053457.75	2	2.0160	12	11	12	0.000	0.00000	0.13000	0.000
13	607457.25	4053447.75	6	68.7318	13	12	13	0.130	0.07826	0.00000	0.000
14	607407.25	4053447.75	3	5.5446	14	13	14	0.000	0.00000	0.02000	0.000
15	607382.25	4053447.75	2	3.5198	15	14	15	0.020	0.00000	0.00000	0.000
16	607537.25	4053437.75	5	29.8993	16	15	16	0.038	0.00000	0.00000	0.000
17	607362.25	4053437.75	2	3.0913	17	16	17	0.020	0.00000	0.00000	0.000
18	607457.25	4053432.75	4	11.2894	18	17	18	0.066	0.00000	0.00000	0.000
19	607452.25	4053427.75	5	19.5779	19	18	19	0.108	0.00000	0.00000	0.000
20	607532.25	4053427.75	5	27.6896	20	19	20	0.032	0.00000	0.00000	0.000
21	607282.25	4053427.75	3	5.3924	21	20	21	0.028	0.00000	0.00000	0.000
22	607482.25	4053427.75	2	3.8342	22	21	22	2.500	0.00000	0.00000	0.022
23	607537.25	4053422.75	5	22.3613	23	22	23	0.030	0.00000	0.13533	0.000
24	607407.25	4053422.75	4	14.1836	24	23	24	0.038	0.00000	0.00000	0.000
25	607457.25	4053417.75	6	76.2974	25	24	25	0.079	0.00000	0.00000	0.000
26	607532.25	4053417.75	6	34.4811	26	25	26	0.032	0.00000	0.00000	0.000
27	607537.25	4053412.75	5	20.1159	27	26	27	0.020	0.00000	0.00000	0.000
28	607407.25	4053412.75	4	12.2318	28	27	28	0.036	0.00000	0.16140	0.000
29	607507.25	4053412.75	4	17.1124	29	28	29	0.000	0.00000	0.00000	0.000
30	607332.25	4053412.75	3	6.7223	30	29	30	0.040	0.00000	0.00000	0.000
31	607487.25	4053407.75	3	7.1761	31	30	31	0.104	0.00000	0.00000	0.000
32	607382.25	4053407.75	2	1.9434	32	31	32	0.000	0.00000	0.00000	0.000
33	607362.25	4053402.75	4	12.5499	33	32	33	0.000	0.00000	0.00000	0.000
34	607287.25	4053402.75	1	0.3073	34	33	34	0.000	0.00000	0.00000	0.000
35	607507.25	4053397.75	5	21.2925	35	34	35	0.090	0.00000	0.00000	0.000
36	607407.25	4053392.75	6	35.1617	36	35	36	0.000	0.00000	0.00000	0.000
37	607507.25	4053382.75	5	26.3907	37	36	37	0.151	0.00000	0.00000	0.000
38	607532.25	4053382.75	3	9.3090	38	37	38	0.240	0.00000	0.00000	0.000
39	607387.25	4053377.75	4	15.8233	39	38	39	0.000	0.00000	0.00000	0.000
40	607487.25	4053372.75	6	36.2997	40	39	40	0.000	0.00000	0.00000	0.000
41	607307.25	4053372.75	3	5.3780	41	40	41	0.000	0.00000	0.00000	0.000
42	607302.25	4053367.75	6	48.5423	42	41	42	0.000	0.00000	0.02000	0.000
43	607437.25	4053367.75	3	7.7568	43	42	43	0.000	0.00000	0.15200	0.000
44	607532.25	4053362.75	2	1.8374	44	43	44	0.093	0.00000	0.26000	0.000
45	607532.25	4053322.75	6	37.8995	45	44	45	0.000	0.00000	0.24800	0.000
46	607462.25	4053317.75	5	23.8641	46	45	46	0.015	0.00000	0.24400	0.000
47	607457.25	4053317.75	4	13.5964	47	46	47	0.000	0.00000	0.22400	0.000
48	607387.25	4053312.75	2	2.7404	48	47	48	0.000	0.00000	0.77733	0.000
49	607552.25	4053307.75	2	2.4750	49	48	49	0.000	0.00000	1.97000	0.000
50	607507.25	4053292.75	5	27.2801	50	49	50	0.044	0.00000	1.99000	0.000
51	607537.25	4053292.75	2	2.8409	51	50	51	0.000	0.00000	0.25200	0.000
52	607362.25	4053282.75	4	15.8211	52	51	52	0.000	0.00000	0.25000	0.000
53	607582.25	4053207.75	3	5.4322	53	52	53	0.000	0.00000	0.24600	0.000
54	607637.25	4053197.75	3	6.0226	54	53	54	0.017	0.00000	0.04440	0.000
55	607657.25	4053157.75	6	47.9550	55	54	55	1.226	0.00000	0.00000	0.000
56	607662.25	4053152.75	6	34.6362	56	55	56	0.392	0.00000	0.11400	0.000
57	607682.25	4053152.75	5	22.1332	57	56	57	0.000	0.00000	0.07606	0.000
58	607687.25	4053147.75	4	12.9211	58	57	58	0.000	0.00000	0.03260	0.000
59	607642.25	4053147.75	3	8.9993	59	58	59	0.000	0.00000	0.04760	0.000
60	607662.25	4053142.75	6	42.8153	60	59	60	0.000	0.00000	0.06960	0.000
61	607687.25	4053142.75	3	6.9134	61	60	61	0.000	0.00000	0.06000	0.000
62	607637.25	4053132.75	6	37.4711	62	61	62	0.085	0.00000	0.00000	0.000
63	607707.25	4053132.75	2	1.9725	63	62	63	0.000	0.00000	0.00000	0.000
64	607637.25	4053117.75	4	13.2006	64	63	64	0.040	0.00000	0.00000	0.000
65	607617.25	4053117.75	4	18.6911	65	64	65	0.057	0.00000	0.00000	0.000
66	607657.25	4053112.75	6	47.7244	66	65	66	0.050	0.00000	0.00000	0.000
67	607862.25	4053097.75	1	0.2298	67	66	67	0.000	0.00000	0.00000	0.000
68	607587.25	4053092.75	3	8.6438	68	67	68	0.043	0.00000	0.00000	0.000
69	607657.25	4053082.75	5	23.5714	69	68	69	145.400	0.00000	0.00000	0.136
70	607637.25	4053082.75	3	6.0146	70	69	70	0.948	0.00000	0.02340	0.000
71	607617.25	4053077.75	5	27.3248	71	70	71	0.018	0.00000	0.00000	0.000
72	607587.25	4053077.75	4	17.4712	72	71	72	0.000	0.00000	0.00000	0.000
73	607617.25	4053067.75	4	16.6639	73	72	73	0.057	0.00000	0.00000	0.000
74	607657.25	4053057.75	2	4.0242	74	73	74	0.000	0.00000	0.00000	0.000
75	607687.25	4053047.75	4	12.2959	75	74	75	0.000	0.00000	0.00000	0.000
76	607687.25	4053027.75	2	1.9734	76	75	76	0.000	0.00000	0.00000	0.000
77	607842.25	4052977.75	1	0.3653	77	76	77	0.000	0.00000	0.00000	0.000
78	607867.25	4052952.75	1	0.6905	78	77	78	0.000	0.00000	0.00000	0.000

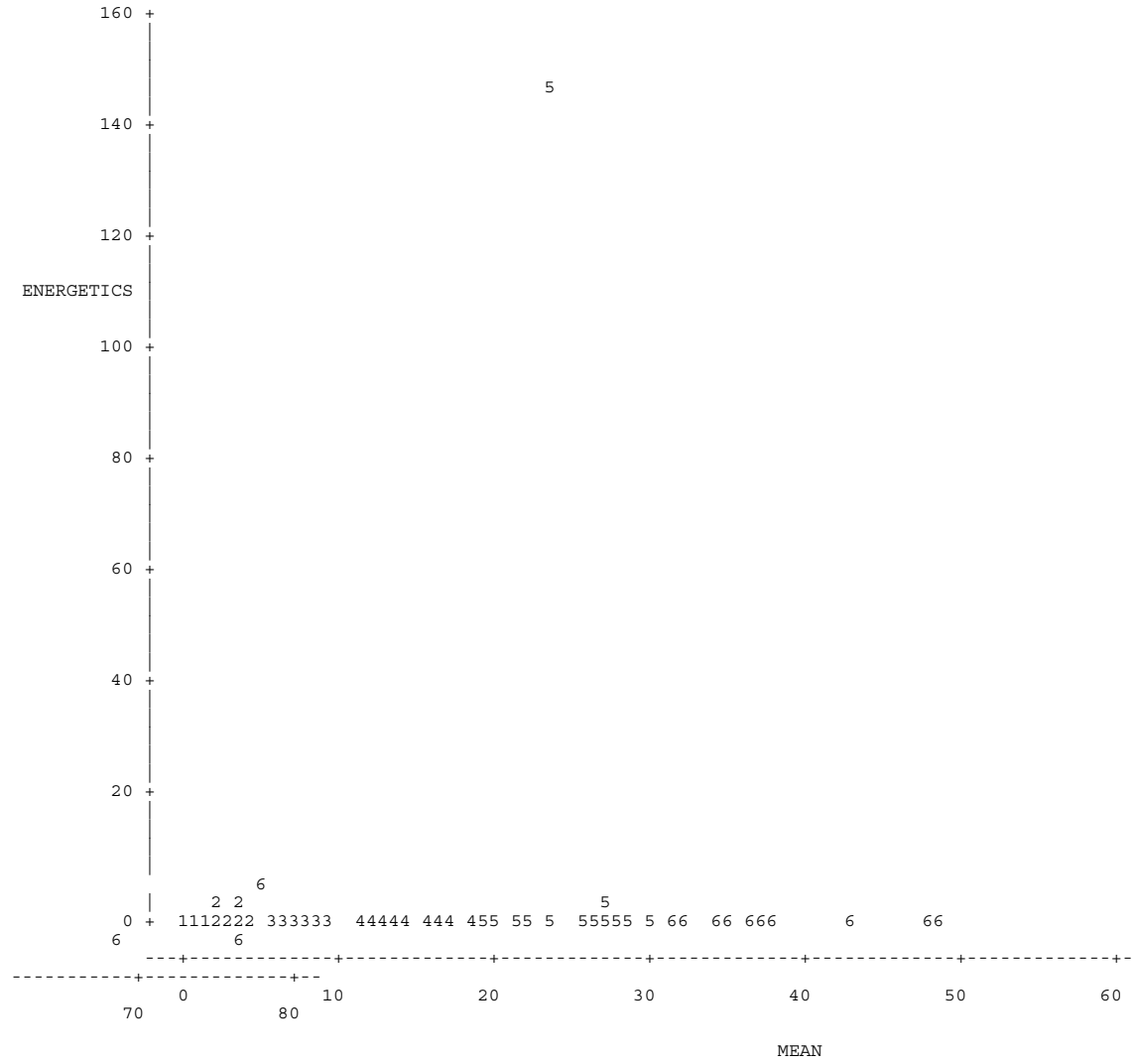
79	607787.25	4052897.75	1	0.1060	89	78	89	0.000	0.00000	0.00000	0.000
80	607452.25	4053442.75	6	31.1573	91	79	91	0.061	0.00000	0.00000	0.000
81	607452.25	4053402.75	6	32.3068	92	80	92	0.055	0.00000	0.00000	0.000
82	607662.25	4053157.75	6	77.5767	93	81	93	7.260	0.00000	0.00000	0.000
83	607482.25	4053127.75	2	0.2474	94	82	94	0.000	0.00000	0.00000	0.000
84	607742.25	4053127.75	2	4.4785	95	83	95	0.029	0.00000	0.00000	0.000
85	607587.25	4053252.75	1	1.2364	96	84	96	0.000	0.00000	0.00000	0.000
86	607692.25	4053082.75	1	1.6145	98	85	98	0.000	0.00000	0.00000	0.000
87	607742.25	4052977.75	1	1.4408	99	86	99	0.000	0.00000	0.00000	0.000
88	607742.25	4052972.75	1	1.5788	100	87	100	0.000	0.00000	0.00000	0.000
89	607812.25	4052922.75	1	1.0437	101	88	101	0.000	0.00000	0.00000	0.000
90	607812.25	4052957.75	1	1.3164	102	89	102	0.000	0.00000	0.00000	0.000
91	607307.25	4053402.75	1	1.3045	103	90	103	0.000	0.00000	0.00000	0.000

Obs	DNT_4_AM	DNT_2_AM	NG	DNT_2_4	HMX	TOT_ENER	ENERGETICS	DETECTABLE	LENERGETICS	LMean
1	0.00000	0.0000	0.0000	0.000	0.000	<0.02	0.000	NO	0.00000	-0.51503
2	0.00000	0.0000	0.0000	0.000	0.000	<0.02	0.000	NO	0.00000	-0.98484
3	0.00000	0.0000	0.0000	0.000	0.000	<0.02	0.000	NO	0.00000	-0.09967
4	0.00000	0.0000	0.0000	0.000	0.000	<0.02	0.000	NO	0.00000	1.29197
5	0.00000	0.0000	0.0000	0.000	0.000	<0.02	0.000	NO	0.00000	1.84283
6	0.00000	0.0000	0.0000	0.000	0.000	0.0322	0.032	YES	0.03169	-0.89497
7	0.00000	0.0000	0.0000	0.000	0.000	0.024	0.024	YES	0.02372	2.85238
8	0.00000	0.0000	0.0000	0.000	0.000	0.0154	0.015	NO	0.01528	3.15201
9	0.00000	0.0000	0.0000	0.000	0.000	<0.02	0.000	NO	0.00000	3.34065
10	0.00000	0.0000	0.0000	0.000	0.000	0.402	0.402	YES	0.33790	1.71097
11	0.00000	0.0000	0.0000	0.000	0.000	0.1552	0.155	YES	0.14427	3.25366
12	0.00000	0.0000	0.0000	0.000	0.000	0.13	0.130	YES	0.12222	0.70110
13	0.00000	0.0000	0.0000	0.000	0.000	0.208266	0.208	YES	0.18918	4.23021
14	0.00000	0.0000	0.0000	0.000	0.000	0.02	0.020	NO	0.01980	1.71283
15	0.00000	0.0000	0.0000	0.000	0.000	0.0204	0.020	YES	0.02019	1.25842
16	0.08600	0.0820	0.0000	0.000	0.024	0.23	0.230	YES	0.20701	3.39783
17	0.00000	0.0000	0.0000	0.000	0.000	0.02	0.020	NO	0.01980	1.12859
18	0.00000	0.0000	0.0000	0.000	0.000	0.0656	0.066	YES	0.06354	2.42386
19	0.02920	0.0278	0.0000	0.000	0.000	0.1646	0.165	YES	0.15238	2.97440
20	0.07000	0.0560	0.0000	0.000	0.000	0.158	0.158	YES	0.14669	3.32106
21	0.00000	0.0000	0.0000	0.000	0.000	0.028	0.028	YES	0.02762	1.68499
22	0.12400	0.1060	0.0000	0.000	0.000	2.752	2.752	YES	1.32229	1.34397
23	0.00000	0.0260	0.0000	0.000	0.000	0.191333	0.191	YES	0.17507	3.10733
24	0.00000	0.0000	0.0000	0.000	0.000	0.0384	0.038	YES	0.03768	2.65209
25	0.00000	0.0000	0.0000	0.000	0.000	0.0788	0.079	YES	0.07585	4.33464
26	0.00000	0.0000	0.0000	0.000	0.000	0.032	0.032	YES	0.03150	3.54041
27	0.00000	0.0000	0.0000	0.000	0.000	0.02	0.020	NO	0.01980	3.00151
28	0.00000	0.0000	0.0000	0.000	0.000	0.1974	0.197	YES	0.18015	2.50404
29	0.00000	0.0000	0.0000	0.000	0.000	<0.02	0.000	NO	0.00000	2.83980
30	0.00000	0.0000	0.0000	0.000	0.000	0.04	0.040	YES	0.03922	1.90543
31	0.04020	0.0000	0.6000	0.000	0.000	0.74	0.740	YES	0.55389	1.97075
32	0.00000	0.0000	0.0000	0.000	0.000	<0.02	0.000	NO	0.00000	0.66445
33	0.00000	0.0000	0.0000	0.000	0.000	<0.02	0.000	NO	0.00000	2.52971
34	0.00000	0.0000	0.0000	0.000	0.000	<0.02	0.000	NO	0.00000	-1.17996
35	0.04520	0.0000	0.0000	0.000	0.000	0.135	0.135	YES	0.12663	3.05836
36	0.00000	0.0000	0.0000	0.000	0.000	<0.02	0.000	NO	0.00000	3.55996
37	0.05380	0.0096	0.0000	0.000	0.000	0.214	0.214	YES	0.19392	3.27301
38	0.09600	0.0000	0.0000	0.000	0.000	0.336	0.336	YES	0.28968	2.23099
39	0.00000	0.0000	0.0000	0.000	0.000	<0.02	0.000	NO	0.00000	2.76148
40	0.00000	0.0000	0.0000	0.000	0.000	<0.02	0.000	NO	0.00000	3.59181
41	0.00000	0.0000	0.0000	0.000	0.000	<0.02	0.000	NO	0.00000	1.68232
42	0.00000	0.0000	0.0000	0.000	0.000	0.02	0.020	YES	0.01980	3.88244
43	0.00000	0.0000	0.0000	0.000	0.000	0.152	0.152	YES	0.14150	2.04857
44	0.03180	0.0000	0.0000	0.000	0.000	0.3844	0.384	YES	0.32527	0.60834
45	0.00000	0.0000	0.0000	0.000	0.000	0.248	0.248	YES	0.22154	3.63494
46	0.00000	0.0000	0.0000	0.000	0.000	0.2592	0.259	YES	0.23048	3.17238
47	0.00000	0.0000	0.0000	0.000	0.000	0.224	0.224	YES	0.20212	2.60981
48	0.00000	0.0000	0.0300	0.000	0.000	0.807333	0.807	YES	0.59185	1.00809
49	0.00000	0.0000	0.0000	0.000	0.000	1.97	1.970	YES	1.08856	0.90625
50	0.08780	0.0000	0.0000	0.000	0.000	2.1218	2.122	YES	1.13841	3.30616
51	0.00000	0.0000	0.0000	0.000	0.000	0.252	0.252	YES	0.22474	1.04413
52	0.00000	0.0000	0.0258	0.000	0.000	0.2758	0.276	YES	0.24357	2.76135
53	0.00000	0.0000	0.0000	0.000	0.000	0.246	0.246	YES	0.21994	1.69234
54	0.01980	0.0000	0.0000	0.000	0.000	0.0816	0.082	YES	0.07844	1.79552
55	0.09422	0.0900	0.0000	0.000	0.000	1.41	1.410	YES	0.87963	3.87026
56	0.15400	0.1560	0.0000	0.000	0.000	0.816	0.816	YES	0.59664	3.54490
57	0.00000	0.0000	0.0000	0.000	0.000	0.076066	0.076	YES	0.07331	3.09708
58	0.00000	0.0000	0.0000	0.000	0.000	0.0326	0.033	YES	0.03208	2.55886
59	0.00000	0.0168	0.0000	0.000	0.000	0.0644	0.064	YES	0.06241	2.19715
60	0.00000	0.0000	0.0000	0.000	0.000	0.0696	0.070	YES	0.06728	3.75690
61	0.00000	0.0000	0.0000	0.000	0.000	0.06	0.060	YES	0.05827	1.93346
62	0.00000	0.0000	0.0000	0.000	0.000	0.0852	0.085	YES	0.08176	3.62357
63	0.00000	0.0000	0.0000	0.000	0.000	<0.02	0.000	NO	0.00000	0.67931
64	0.02000	0.0000	0.4600	0.000	0.000	0.52	0.520	YES	0.41871	2.58026
65	0.03720	0.0238	0.0000	0.000	0.000	0.1182	0.118	YES	0.11172	2.92805
66	0.03035	0.0222	0.0000	0.000	0.000	0.103022	0.103	YES	0.09805	3.86544
67	0.00000	0.0000	0.0000	0.000	0.000	<0.02	0.000	NO	0.00000	-1.47072
68	0.03200	0.0000	0.0000	0.000	0.000	0.0754	0.075	YES	0.07269	2.15684
69	1.21000	0.9440	0.0000	0.066	0.000	147.756	147.756	YES	5.00231	3.16003
70	0.02240	0.0246	0.0000	0.000	0.000	1.0184	1.018	YES	0.70231	1.79419
71	0.00000	0.0000	0.0000	0.000	0.000	0.018	0.018	NO	0.01784	3.30779
72	0.00000	0.0186	0.0000	0.000	0.000	0.0186	0.019	NO	0.01843	2.86056
73	0.13360	0.1514	0.0000	0.000	0.000	0.3418	0.342	YES	0.29401	2.81324
74	0.00000	0.0000	0.0000	0.000	0.000	<0.02	0.000	NO	0.00000	1.39233
75	0.00000	0.0000	0.0000	0.000	0.000	<0.02	0.000	NO	0.00000	2.50927
76	0.00000	0.0196	0.0000	0.000	0.000	0.0196	0.020	NO	0.01941	0.67974
77	0.00000	0.0000	0.0000	0.000	0.000	<0.02	0.000	NO	0.00000	-1.00701
78	0.00000	0.0000	0.0000	0.000	0.000	<0.02	0.000	NO	0.00000	-0.37030
79	0.00000	0.0000	0.0000	0.000	0.000	<0.02	0.000	NO	0.00000	-2.24479

80	0.00000	0.0000	0.0000	0.000	0.0614	0.061	YES	0.05959	3.43905
81	0.03460	0.0200	0.000	0.000	0.1094	0.109	YES	0.10382	3.47528
82	0.21400	0.2280	0.000	0.000	7.702	7.702	YES	2.16355	4.35127
83	0.00000	0.0000	0.000	0.000	<0.02	0.000	NO	0.00000	-1.39667
84	0.00000	0.0000	0.000	0.000	0.0288	0.029	YES	0.02839	1.49929
85	0.00000	0.0000	0.000	0.000	<0.02	0.000	NO	0.00000	0.21217
86	0.00000	0.0000	0.000	0.000	<0.02	0.000	NO	0.00000	0.47899
87	0.00000	0.0000	0.000	0.000	<0.02	0.000	NO	0.00000	0.36518
88	0.00000	0.0000	0.000	0.000	<0.02	0.000	NO	0.00000	0.45668
89	0.00000	0.0000	0.000	0.000	<0.02	0.000	NO	0.00000	0.04278
90	0.00000	0.0000	0.000	0.000	<0.02	0.000	NO	0.00000	0.27489
91	0.00000	0.0000	0.000	0.000	<0.02	0.000	NO	0.00000	0.26581

Analysis of Fort Ord data (all observations included)  
scatter plots with group variable

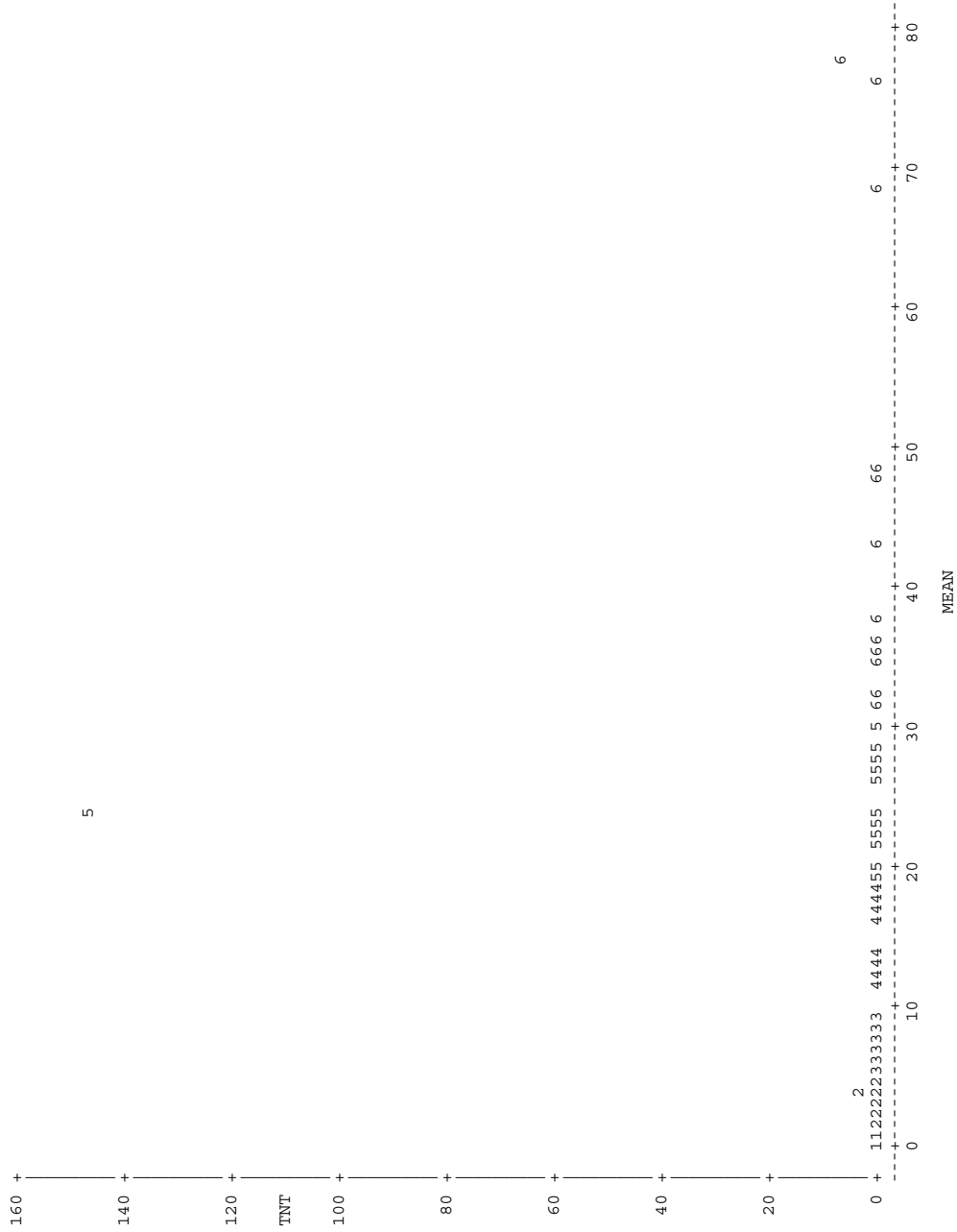
Plot of ENERGETICS\*MEAN. Symbol is value of GRIDCODE.



NOTE: 41 obs hidden.

Analysis of Fort Ord data (all observations included)  
scatter plots with group variable

Plot of TNT\*MEAN . Symbol is value of GRIDCODE .



NOTE: 45 obs hidden.

Analysis of Fort Ord data (all observations included)  
Variable means

The MEANS Procedure

Variable	N	Mean	Std Dev	Minimum	Maximum
MEAN	91	15.7642831	16.9710250	0.1059500	77.5767000
TNT	91	1.7558457	15.2469711	0	145.4000000
RDX	91	0.0012930	0.0091438	0	0.0782600
TETRYL	91	0.0884365	0.3063824	0	1.9900000
TNB_135	91	0.0017363	0.0144167	0	0.1360000
DNT_4_AM	91	0.0292986	0.1308544	0	1.2100000
DNT_2_AM	91	0.0222242	0.1043097	0	0.9440000
NG	91	0.0122615	0.0788447	0	0.6000000
DNT_2_4	91	0.000725275	0.0069187	0	0.0660000
HMX	91	0.000263736	0.0025159	0	0.0240000
ENERGETICS	91	1.9120352	15.4851037	0	147.7560000
LENERGETICS	91	0.2225871	0.6051682	0	5.0023074
LMean	91	1.9704045	1.5203162	-2.2447880	4.3512671

Analysis of Fort Ord data (all observations included)  
Factor analysis using of various chemical

The FACTOR Procedure

Initial Factor Method: Principal Components

Prior Communality Estimates: ONE

Eigenvalues of the Correlation Matrix: Total = 9 Average = 1

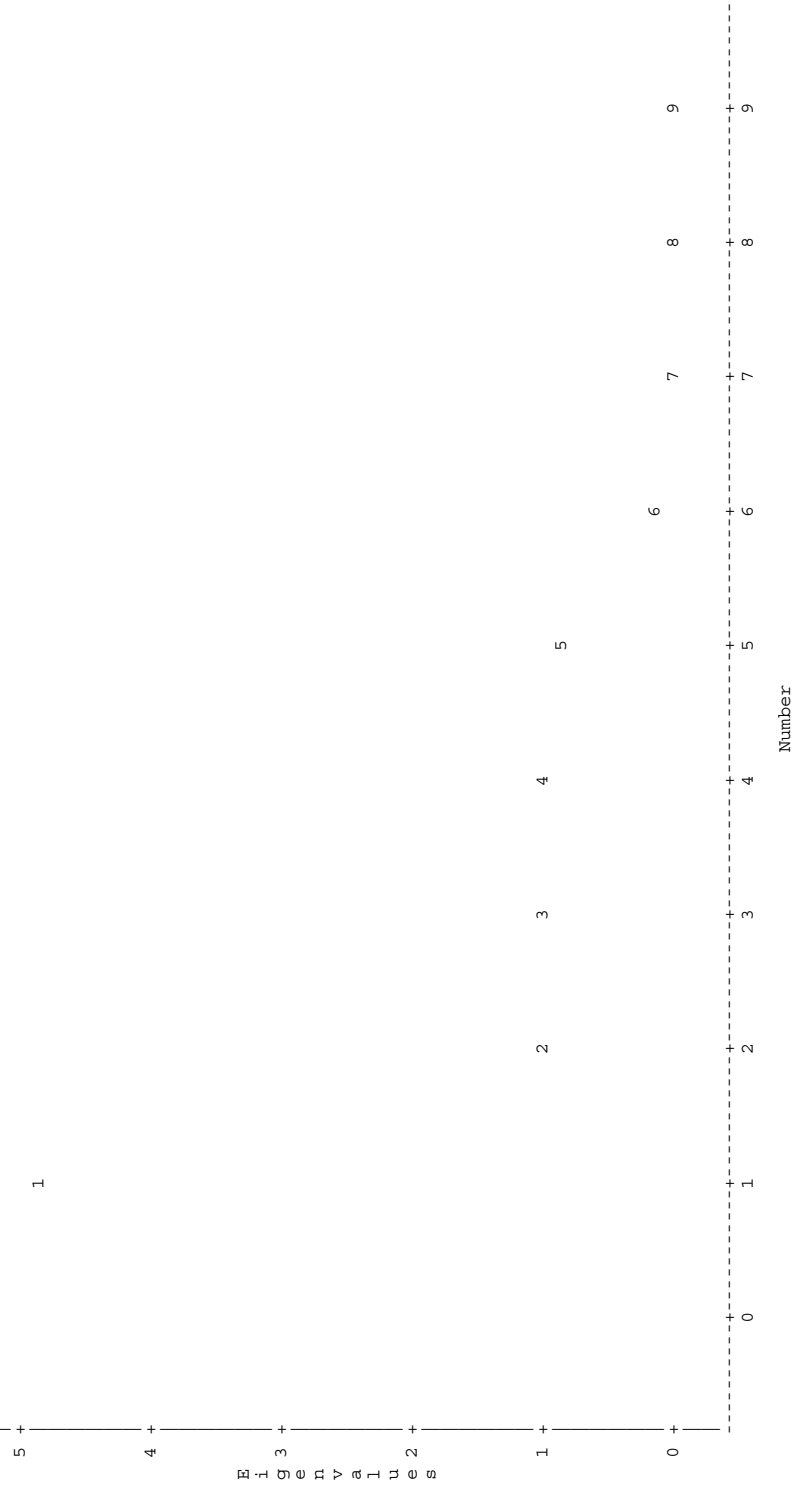
	Eigenvalue	Difference	Proportion	Cumulative
1	4.86952304	3.83177511	0.5411	0.5411
2	1.03774793	0.01525396	0.1153	0.6564
3	1.02249396	0.00573666	0.1136	0.7700
4	1.01675730	0.08857397	0.1130	0.8829
5	0.92818333	0.82839538	0.1031	0.9861
6	0.09978795	0.08388552	0.0111	0.9972
7	0.01590243	0.00697118	0.0018	0.9989
8	0.00893125	0.00825844	0.0010	0.9999
9	0.00067281		0.0001	1.0000

4 factors will be retained by the NFACTOR criterion.

Analysis of Fort Ord data (all observations included)  
Factor analysis using of various chemical

The FACTOR Procedure  
Initial Factor Method: Principal Components

Scree Plot of Eigenvalues



Analysis of Fort Ord data (all observations included)  
Factor analysis using of various chemical

The FACTOR Procedure  
Initial Factor Method: Principal Components

Eigenvectors				
	1	2	3	4
TNT	0.45023	-0.01812	-0.00270	-0.03014
RDX	-0.01257	0.13137	0.65567	-0.57232
TETRYL	-0.01866	-0.78266	-0.08698	0.20236
TNB_135	0.44765	-0.01777	-0.00267	-0.02991
DNT_4_AM	0.44702	-0.00200	-0.01441	0.02493
DNT_2_AM	0.44225	0.02806	0.01813	0.03812
NG	-0.00968	0.37081	-0.71395	-0.31720
DNT_2_4	0.44813	-0.01957	-0.00304	-0.03031
HMX	0.00833	0.48048	0.22859	0.72532

Factor Pattern				
	Factor1	Factor2	Factor3	Factor4
TNT	0.99351	-0.01846	-0.00273	-0.03039
RDX	-0.02775	0.13383	0.66300	-0.57710
TETRYL	-0.04117	-0.79730	-0.08795	0.20405
TNB_135	0.98783	-0.01810	-0.00270	-0.03016
DNT_4_AM	0.98643	-0.00204	-0.01458	0.02514
DNT_2_AM	0.97592	0.02859	0.01834	0.03844
NG	-0.02136	0.37775	-0.72193	-0.31985
DNT_2_4	0.98889	-0.01993	-0.00307	-0.03056
HMX	0.01839	0.48946	0.23115	0.73137

Variance Explained by Each Factor

Factor1	Factor2	Factor3	Factor4
4.8695230	1.0377479	1.0224940	1.0167573

Final Communality Estimates: Total = 7.946522

TNT	RDX	TETRYL	TNB_135	DNT_4_AM	DNT_2_AM	NG
0.98834284	0.79128742	0.68675086	0.97706098	0.97389982	0.95504714	0.76663768
0.97924936	0.82824612					

Analysis of Fort Ord data (all observations included)  
 Factor analysis using of various chemical

The FACTOR Procedure  
 Rotation Method: Varimax

## Orthogonal Transformation Matrix

	1	2	3	4
1	0.99986	0.00032	0.01610	-0.00473
2	-0.00921	0.66130	0.66225	0.35216
3	-0.00085	-0.65104	0.27360	0.70802
4	-0.01401	-0.37260	0.69735	-0.61211

## Rotated Factor Pattern

	Factor1	Factor2	Factor3	Factor4
TNT	0.99397	0.00121	-0.01816	0.00547
RDX	-0.02145	-0.12812	-0.13286	0.86992
TETRYL	-0.03660	-0.54604	-0.41044	-0.46775
TNB_135	0.98829	0.00134	-0.01785	0.00550
DNT_4_AM	0.98597	-0.00091	0.02808	-0.03109
DNT_2_AM	0.97496	-0.00704	0.06647	-0.00510
NG	-0.01975	0.83898	-0.17075	-0.18223
DNT_2_4	0.98937	0.00053	-0.01943	0.00484
HMX	0.00343	-0.09930	0.89771	-0.11174

## Variance Explained by Each Factor

Factor1	Factor2	Factor3	Factor4
4.8684391	1.0283688	1.0273920	1.0223223

Final Communality Estimates: Total = 7.946522

TNT	RDX	TETRYL	TNB_135	DNT_4_AM	DNT_2_AM	NG
0.98834284	0.79128742	0.68675086	0.97706098	0.97389982	0.95504714	0.76663768
0.97924936	0.82824612					

Analysis of Fort Ord data (all observations included)  
 Factor analysis using of various chemical

The FACTOR Procedure  
 Rotation Method: Varimax

Scoring Coefficients Estimated by Regression

Squared Multiple Correlations of the Variables with Each Factor

Factor1	Factor2	Factor3	Factor4
1.0000000	1.0000000	1.0000000	1.0000000

Standardized Scoring Coefficients

	Factor1	Factor2	Factor3	Factor4
TNT	0.20458	0.00118	-0.03007	0.00918
RDX	0.00051	-0.12538	-0.13309	0.85195
TETRYL	-0.00411	-0.52685	-0.39253	-0.45427
TNB_135	0.20341	0.00130	-0.02969	0.00918
DNT_4_AM	0.20223	-0.00116	0.01530	-0.02688
DNT_2_AM	0.19959	-0.00748	0.05274	-0.00169
NG	-0.00274	0.81759	-0.17155	-0.17914
DNT_2_4	0.20365	0.00052	-0.03123	0.00855
HMX	-0.01084	-0.10328	0.87589	-0.11416

Analysis of Fort Ord data (all observations included)  
 Correlations of factors and variables of interest

The CORR Procedure

4 With Variables: MEAN ENERGETICS LENERGETICS LMean  
 4 Variables: Factor1 Factor2 Factor3 Factor4

Simple Statistics

Variable	N	Mean	Std Dev	Sum	Minimum	Maximum
MEAN	91	15.76428	16.97102	1435	0.10595	77.57670
ENERGETICS	91	1.91204	15.48510	173.99520	0	147.75600
LENERGETICS	91	0.22259	0.60517	20.25543	0	5.00231
LMean	91	1.97040	1.52032	179.30681	-2.24479	4.35127
Factor1	91	0	1.00000	0	-0.18098	9.33425
Factor2	91	0	1.00000	0	-3.36777	6.27644
Factor3	91	0	1.00000	0	-2.47671	8.46953
Factor4	91	0	1.00000	0	-2.91473	7.34555

Pearson Correlation Coefficients, N = 91  
 Prob > |r| under H0: Rho=0

	Factor1	Factor2	Factor3	Factor4
MEAN	0.09833 0.3538	-0.07638 0.4718	0.06616 0.5332	0.29176 0.0050
ENERGETICS	0.99411 <.0001	-0.00550 0.9587	-0.02614 0.8057	-0.00458 0.9656
LENERGETICS	0.88765 <.0001	-0.06756 0.5246	-0.11843 0.2635	-0.12977 0.2202
LMean	0.11899 0.2613	-0.02313 0.8277	0.05580 0.5993	0.12824 0.2257

Analysis of Fort Ord data (all observations included)  
ANCOVA using value of ENERGETICS

The Mixed Procedure

Model Information

Data Set	WORK.CONTAMINANTS
Dependent Variable	ENERGETICS
Covariance Structure	Diagonal
Estimation Method	REML
Residual Variance Method	Profile
Fixed Effects SE Method	Model-Based
Degrees of Freedom Method	Residual

Class Level Information

Class	Levels	Values
GRIDCODE	6	1 2 3 4 5 6

Dimensions

Covariance Parameters	1
Columns in X	7
Columns in Z	0
Subjects	1
Max Obs Per Subject	91

Number of Observations

Number of Observations Read	91
Number of Observations Used	91
Number of Observations Not Used	0

Covariance Parameter  
Estimates

Cov Parm	Estimate
Residual	239.67

Fit Statistics

-2 Res Log Likelihood	723.3
AIC (smaller is better)	725.3
AICC (smaller is better)	725.3
BIC (smaller is better)	727.7

Type 1 Tests of Fixed Effects

Effect	Num DF	Den DF	F Value	Pr > F
GRIDCODE	5	85	1.01	0.4174

Type 3 Tests of Fixed Effects

Effect	Num DF	Den DF	F Value	Pr > F
GRIDCODE	5	85	1.01	0.4174

Analysis of Fort Ord data (all observations included)  
 ANCOVA using value of ENERGETICS  
 Residual analysis

The UNIVARIATE Procedure  
 Variable: Resid

## Moments

N	91	Sum Weights	91
Mean	0	Sum Observations	0
Std Deviation	15.044954	Variance	226.350642
Skewness	8.65829367	Kurtosis	80.1661628
Uncorrected SS	20371.5578	Corrected SS	20371.5578
Coeff Variation	.	Std Error Mean	1.57713972

## Basic Statistical Measures

Location		Variability	
Mean	0.00000	Std Deviation	15.04495
Median	-0.13599	Variance	226.35064
Mode	-0.00201	Range	147.75600
		Interquartile Range	0.62455

## Tests for Location: Mu0=0

Test	-Statistic-	-----p Value-----
Student's t	t 0	Pr >  t  1.0000
Sign	M -27.5	Pr >=  M  <.0001
Signed Rank	S -1218	Pr >=  S  <.0001

## Tests for Normality

Test	--Statistic--	-----p Value-----
Shapiro-Wilk	W 0.207276	Pr < W <0.0001
Kolmogorov-Smirnov	D 0.434819	Pr > D <0.0100
Cramer-von Mises	W-Sq 4.818858	Pr > W-Sq <0.0050
Anderson-Darling	A-Sq 23.54813	Pr > A-Sq <0.0050

## Quantiles (Definition 5)

Quantile	Estimate
100% Max	137.6550273
99%	137.6550273
95%	0.8008133
90%	0.2180400
75% Q3	-0.0020125
50% Median	-0.1359867
25% Q1	-0.6265587
10%	-9.9096427
5%	-10.0249127
1%	-10.1009727
0% Min	-10.1009727

## Extreme Observations

-----Lowest-----		-----Highest-----	
Value	Obs	Value	Obs
-10.1010	9	0.800813	70
-10.0856	8	1.544365	49
-10.0830	71	2.326365	22
-10.0810	27	6.972421	82
-10.0249	57	137.655027	69



Analysis of Fort Ord data (all observations included)  
 Regression using value of ENERGETICS

The REG Procedure  
 Model: MODEL1  
 Dependent Variable: ENERGETICS

Number of Observations Read 91  
 Number of Observations Used 91

Analysis of Variance

Source	DF	Sum of Squares	Mean Square	F Value	Pr > F
Model	1	104.84626	104.84626	0.43	0.5115
Error	89	21476	241.30464		
Corrected Total	90	21581			

Root MSE 15.53398 R-Square 0.0049  
 Dependent Mean 1.91204 Adj R-Sq -0.0063  
 Coeff Var 812.43189

Parameter Estimates

Variable	DF	Parameter Estimate	Standard Error	t Value	Pr >  t	95% Confidence Limits	
Intercept	1	0.90945	2.22826	0.41	0.6841	-3.51805	5.33695
MEAN	1	0.06360	0.09648	0.66	0.5115	-0.12811	0.25531

Analysis of Fort Ord data (all observations included)  
 Regression using value of ENERGETICS  
 Residual analysis

The UNIVARIATE Procedure  
 Variable: resid

## Moments

N	91	Sum Weights	91
Mean	0	Sum Observations	0
Std Deviation	15.4474424	Variance	238.623478
Skewness	9.46062244	Kurtosis	89.9911643
Uncorrected SS	21476.113	Corrected SS	21476.113
Coeff Variation	.	Std Error Mean	1.61933197

## Basic Statistical Measures

Location		Variability	
Mean	0.00000	Std Deviation	15.44744
Median	-1.28913	Variance	238.62348
Mode	.	Range	151.03050
		Interquartile Range	1.19296

## Tests for Location: Mu0=0

Test	-Statistic-	-----p Value-----
Student's t	t 0	Pr >  t  1.0000
Sign	M -41.5	Pr >=  M  <.0001
Signed Rank	S -1885	Pr >=  S  <.0001

## Tests for Normality

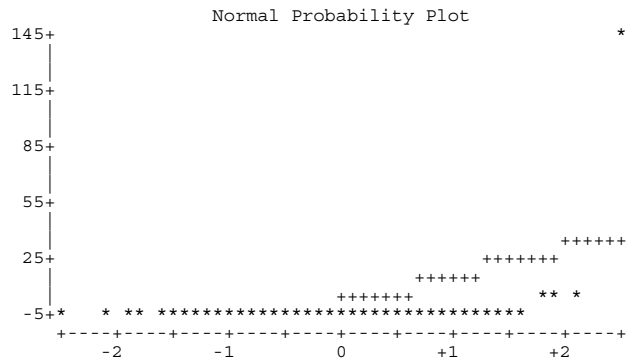
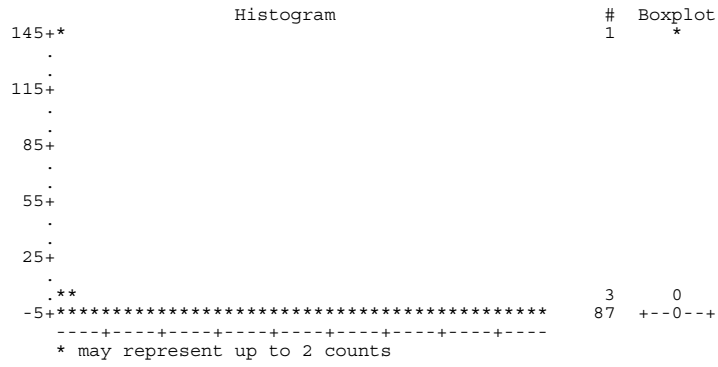
Test	--Statistic--	-----p Value-----
Shapiro-Wilk	W 0.122703	Pr < W <0.0001
Kolmogorov-Smirnov	D 0.463109	Pr > D <0.0100
Cramer-von Mises	W-Sq 6.197476	Pr > W-Sq <0.0050
Anderson-Darling	A-Sq 29.66568	Pr > A-Sq <0.0050

## Quantiles (Definition 5)

Quantile	Estimate
100% Max	145.347445
99%	145.347445
95%	-0.273570
90%	-0.838129
75% Q3	-0.975828
50% Median	-1.289133
25% Q1	-2.168791
10%	-3.070394
5%	-3.562842
1%	-5.683052
0% Min	-5.683052

## Extreme Observations

-----Lowest-----		-----Highest-----	
Value	Obs	Value	Obs
-5.68305	25	-0.273570	70
-5.07243	13	0.903143	49
-3.97667	42	1.598699	22
-3.84163	66	1.858785	82
-3.56284	60	145.347445	69



Analysis of Fort Ord data (all observations included)  
ANCOVA using value of Log(ENERGETICS)

The Mixed Procedure

Model Information

Data Set	WORK.CONTAMINANTS
Dependent Variable	LENERGETICS
Covariance Structure	Diagonal
Estimation Method	REML
Residual Variance Method	Profile
Fixed Effects SE Method	Model-Based
Degrees of Freedom Method	Residual

Class Level Information

Class	Levels	Values
GRIDCODE	6	1 2 3 4 5 6

Dimensions

Covariance Parameters	1
Columns in X	7
Columns in Z	0
Subjects	1
Max Obs Per Subject	91

Number of Observations

Number of Observations Read	91
Number of Observations Used	91
Number of Observations Not Used	0

Covariance Parameter  
Estimates

Cov Parm	Estimate
Residual	0.3600

Fit Statistics

-2 Res Log Likelihood	170.7
AIC (smaller is better)	172.7
AICC (smaller is better)	172.7
BIC (smaller is better)	175.1

Type 1 Tests of Fixed Effects

Effect	Num DF	Den DF	F Value	Pr > F
GRIDCODE	5	85	1.31	0.2666

Type 3 Tests of Fixed Effects

Effect	Num DF	Den DF	F Value	Pr > F
GRIDCODE	5	85	1.31	0.2666

Analysis of Fort Ord data (all observations included)  
 ANCOVA using value of Log(ENERGETICS)  
 Residual analysis

The UNIVARIATE Procedure  
 Variable: Resid

Moments

N	91	Sum Weights	91
Mean	0	Sum Observations	0
Std Deviation	0.58308444	Variance	0.33998746
Skewness	5.64151831	Kurtosis	40.2596449
Uncorrected SS	30.5988715	Corrected SS	30.5988715
Coeff Variation	.	Std Error Mean	0.06112386

Basic Statistical Measures

Location		Variability	
Mean	0.00000	Std Deviation	0.58308
Median	-0.10088	Variance	0.33999
Mode	-0.00198	Range	5.00231
		Interquartile Range	0.24431

Tests for Location: Mu0=0

Test	-Statistic-	-----p Value-----
Student's t	t 0	Pr >  t  1.0000
Sign	M -24.5	Pr >=  M  <.0001
Signed Rank	S -883	Pr >=  S  0.0003

Tests for Normality

Test	--Statistic--	-----p Value-----
Shapiro-Wilk	W 0.493438	Pr < W <0.0001
Kolmogorov-Smirnov	D 0.277936	Pr > D <0.0100
Cramer-von Mises	W-Sq 2.141464	Pr > W-Sq <0.0050
Anderson-Darling	A-Sq 11.41735	Pr > A-Sq <0.0050

Quantiles (Definition 5)

Quantile	Estimate
100% Max	4.49274681
99%	4.49274681
95%	0.62884919
90%	0.31032784
75% Q3	-0.00198078
50% Median	-0.10088471
25% Q1	-0.24629115
10%	-0.33449024
5%	-0.43625435
1%	-0.50956057
0% Min	-0.50956057

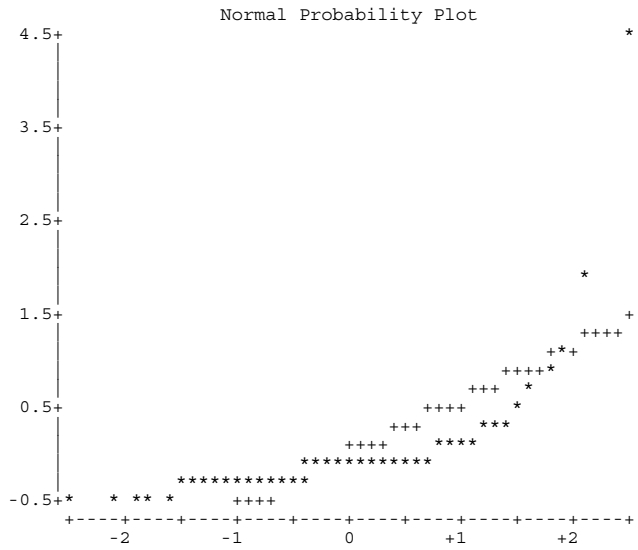
Extreme Observations

-----Lowest-----		-----Highest-----	
Value	Obs	Value	Obs
-0.509561	9	0.628849	50
-0.494278	8	0.837713	49
-0.491721	71	1.071440	22
-0.489758	27	1.857673	82
-0.436254	57	4.492747	69

Stem Leaf	#	Boxplot
44 9	1	*
42		
40		
38		
36		
34		
32		
30		
28		
26		
24		
22		
20		
18 6	1	*
16		
14		
12		
10 7	1	*

```
8 4
6 3
4 37
2 9148
0 0357792469
-0 775533221111100988874330000000000000000
-2 876632110987555555433332210
-4 19994
-----+-----+-----+-----+-----+-----+
Multiply Stem.Leaf by 10**-1
```

1	*
1	0
2	0
4	0
10	+
38	+-----+
27	+-----+
5	



Analysis of Fort Ord data (all observations included)  
 Regression using value of ENERGETICS

The REG Procedure  
 Model: MODEL1  
 Dependent Variable: LENERGETICS

Number of Observations Read 91  
 Number of Observations Used 91

Analysis of Variance

Source	DF	Sum of Squares	Mean Square	F Value	Pr > F
Model	1	1.46724	1.46724	4.15	0.0447
Error	89	31.49333	0.35386		
Corrected Total	90	32.96057			

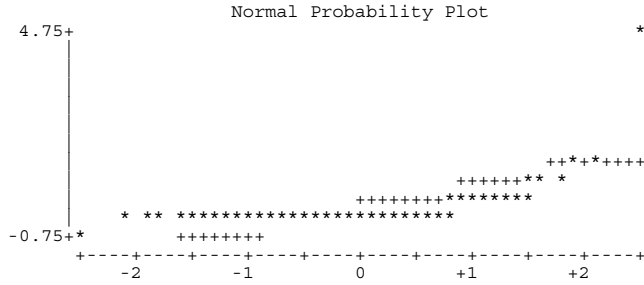
  

Root MSE	0.59486	R-Square	0.0445
Dependent Mean	0.22259	Adj R-Sq	0.0338
Coeff Var	267.24788		

Parameter Estimates

Variable	DF	Parameter Estimate	Standard Error	t Value	Pr >  t	95% Confidence Limits	
Intercept	1	0.10398	0.08533	1.22	0.2262	-0.06556	0.27353
MEAN	1	0.00752	0.00369	2.04	0.0447	0.00018213	0.01486





Analysis of Fort Ord data (all observations included)  
Logistic Regression

The LOGISTIC Procedure

Model Information

Data Set WORK.CONTAMINANTS  
 Response Variable DETECTABLE  
 Number of Response Levels 2  
 Model binary logit  
 Optimization Technique Fisher's scoring

Number of Observations Read 91  
 Number of Observations Used 91

Response Profile

Ordered Value	DETECTABLE	Total Frequency
1	YES	55
2	NO	36

Probability modeled is DETECTABLE='YES'.

Model Convergence Status

Convergence criterion (GCONV=1E-8) satisfied.

Model Fit Statistics

Criterion	Intercept Only	Intercept and Covariates
AIC	124.156	110.630
SC	126.667	115.652
-2 Log L	122.156	106.630

Testing Global Null Hypothesis: BETA=0

Test	Chi-Square	DF	Pr > ChiSq
Likelihood Ratio	15.5264	1	<.0001
Score	12.1575	1	0.0005
Wald	10.3661	1	0.0013

Analysis of Maximum Likelihood Estimates

Parameter	DF	Estimate	Standard Error	Wald Chi-Square	Pr > ChiSq
Intercept	1	-0.4754	0.3257	2.1296	0.1445
MEAN	1	0.0691	0.0215	10.3661	0.0013

Odds Ratio Estimates

Effect	Point Estimate	95% Wald Confidence Limits	
MEAN	1.072	1.027	1.118



Analysis of Fort Ord data (all observations included)  
Logistic Regression

Obs	X		Y	G	D	E	N	E	T	R	E	T	G	E	T	p	l	u
	C	C																
	O	O	O	O	O	O	O	O	O	O	O	O	O	O	O	O	O	O
	R	R	R	R	R	R	R	R	R	R	R	R	R	R	R	R	R	R
1	607787.25	4052897.75	1	0.1060	89	78	89	<0.02	0.000	NO	0.38508	0.24911	0.54173					
2	607862.25	4053097.75	1	0.2298	75	66	75	<0.02	0.000	NO	0.38711	0.25140	0.54295					
3	607482.25	4053127.75	2	0.2474	94	82	94	<0.02	0.000	NO	0.38740	0.25172	0.54313					
4	607287.25	4053402.75	1	0.3073	34	33	34	<0.02	0.000	NO	0.38838	0.25283	0.54372					
5	607842.25	4052977.75	1	0.3653	86	76	86	<0.02	0.000	NO	0.38933	0.25391	0.54430					
6	607432.25	4053537.75	1	0.3735	2	1	2	<0.02	0.000	NO	0.38947	0.25406	0.54438					
7	607307.25	4053507.75	1	0.4086	6	5	6	0.0322	0.032	YES	0.39005	0.25471	0.54473					
8	607377.25	4053567.75	1	0.5975	1	0	1	<0.02	0.000	NO	0.39315	0.25823	0.54662					
9	607867.25	4052952.75	1	0.6905	88	77	88	<0.02	0.000	NO	0.39469	0.25998	0.54756					
10	607382.25	4053532.75	1	0.9051	3	2	3	<0.02	0.000	NO	0.39824	0.26401	0.54973					
11	607812.25	4052922.75	1	1.0437	101	88	101	<0.02	0.000	NO	0.40053	0.26664	0.55114					
12	607587.25	4053252.75	1	1.2364	96	84	96	<0.02	0.000	NO	0.40373	0.27030	0.55311					
13	607307.25	4053402.75	1	1.3045	103	90	103	<0.02	0.000	NO	0.40487	0.27160	0.55381					
14	607812.25	4052957.75	1	1.3164	102	89	102	<0.02	0.000	NO	0.40506	0.27182	0.55393					
15	607742.25	4052977.75	1	1.4408	99	86	99	<0.02	0.000	NO	0.40714	0.27420	0.55522					
16	607742.25	4052972.75	1	1.5788	100	87	100	<0.02	0.000	NO	0.40944	0.27685	0.55665					
17	607692.25	4053082.75	1	1.6145	98	85	98	<0.02	0.000	NO	0.41004	0.27754	0.55702					
18	607532.25	4053362.75	2	1.8374	46	43	46	0.3844	0.384	YES	0.41377	0.28184	0.55935					
19	607382.25	4053407.75	2	1.9434	32	31	32	<0.02	0.000	NO	0.41555	0.28389	0.56047					
20	607707.25	4053132.75	2	1.9725	71	62	71	<0.02	0.000	NO	0.41603	0.28446	0.56077					
21	607687.25	4053027.75	2	1.9734	85	75	85	0.0196	0.020	NO	0.41605	0.28447	0.56078					
22	607307.25	4053457.75	2	2.0160	12	11	12	0.13	0.130	YES	0.41676	0.28530	0.56123					
23	607552.25	4053307.75	2	2.4750	54	48	54	1.97	1.970	YES	0.42449	0.29426	0.56613					
24	607387.25	4053312.75	2	2.7404	53	47	53	0.807333	0.807	YES	0.42898	0.29947	0.56900					
25	607537.25	4053292.75	2	2.8409	56	50	56	0.252	0.252	YES	0.43068	0.30145	0.57009					
26	607362.25	4053437.75	2	3.0913	17	16	17	0.02	0.020	NO	0.43492	0.30639	0.57284					
27	607382.25	4053447.75	2	3.5198	15	14	15	0.0204	0.020	YES	0.44221	0.31489	0.57761					
28	607332.25	4053527.75	2	3.6400	4	3	4	<0.02	0.000	NO	0.44426	0.31728	0.57896					
29	607482.25	4053427.75	2	3.8342	22	21	22	2.752	2.752	YES	0.44758	0.32115	0.58117					
30	607657.25	4053057.75	2	4.0242	82	73	82	<0.02	0.000	NO	0.45083	0.32494	0.58334					
31	607742.25	4053127.75	2	4.4785	95	83	95	0.0288	0.029	YES	0.45861	0.33401	0.58860					
32	607307.25	4053372.75	3	5.3780	43	40	43	<0.02	0.000	NO	0.47407	0.35198	0.59935					
33	607282.25	4053427.75	3	5.3924	21	20	21	0.028	0.028	YES	0.47432	0.35227	0.59952					
34	607582.25	4053207.75	3	5.4322	61	52	61	0.246	0.246	YES	0.47500	0.35306	0.60001					
35	607407.25	4053467.75	3	5.5343	10	9	10	0.402	0.402	YES	0.47676	0.35509	0.60126					
36	607407.25	4053447.75	3	5.5446	14	13	14	0.02	0.020	NO	0.47694	0.35530	0.60138					
37	607637.25	4053082.75	3	6.0146	78	69	78	0.0184	1.018	YES	0.48505	0.36464	0.60722					
38	607637.25	4053197.75	3	6.0226	62	53	62	0.0816	0.082	YES	0.48518	0.36479	0.60732					
39	607382.25	4053512.75	3	6.3144	5	4	5	<0.02	0.000	NO	0.49022	0.37057	0.61101					
40	607332.25	4053412.75	3	6.7223	30	29	30	0.04	0.040	YES	0.49727	0.37859	0.61625					
41	607687.25	4053142.75	3	6.9134	69	60	69	0.06	0.060	YES	0.50057	0.38233	0.61874					
42	607487.25	4053407.75	3	7.1761	31	30	31	0.74	0.740	YES	0.50510	0.38745	0.62219					
43	607437.25	4053367.75	3	7.7568	45	42	45	0.152	0.152	YES	0.51513	0.39865	0.62999					
44	607587.25	4053092.75	3	8.6438	76	67	76	0.0754	0.075	YES	0.53041	0.41540	0.64228					
45	607642.25	4053147.75	3	8.9993	67	58	67	0.0644	0.064	YES	0.53653	0.42198	0.64735					
46	607532.25	4053382.75	3	9.3090	40	37	40	0.336	0.336	YES	0.54184	0.42763	0.65182					
47	607457.25	4053432.75	4	11.2894	18	17	18	0.0656	0.066	YES	0.57556	0.46203	0.68165					
48	607407.25	4053412.75	4	12.2318	28	27	28	0.1974	0.197	YES	0.59138	0.47721	0.69648					
49	607687.25	4053047.75	4	12.2959	84	74	84	<0.02	0.000	NO	0.59245	0.47822	0.69750					
50	607362.25	4053402.75	4	12.5499	33	32	33	<0.02	0.000	NO	0.59668	0.48216	0.70155					
51	607687.25	4053147.75	4	12.9211	66	57	66	0.0326	0.033	YES	0.60284	0.48782	0.70751					
52	607637.25	4053117.75	4	13.2006	72	63	72	0.52	0.520	YES	0.60745	0.49200	0.71202					
53	607457.25	4053317.75	4	13.5964	52	46	52	0.224	0.224	YES	0.61395	0.49781	0.71843					
54	607407.25	4053422.75	4	14.1836	24	23	24	0.0384	0.038	YES	0.62352	0.50617	0.72797					
55	607362.25	4053282.75	4	15.8211	58	51	58	0.2758	0.276	YES	0.64969	0.52800	0.75459					
56	607387.25	4053377.75	4	15.8233	41	38	41	<0.02	0.000	NO	0.64972	0.52802	0.75462					
57	607617.25	4053067.75	4	16.6639	81	72	81	0.3418	0.342	YES	0.66282	0.53843	0.76812					
58	607507.25	4053412.75	4	17.1124	29	28	29	<0.02	0.000	NO	0.66971	0.54378	0.77524					
59	607302.25	4053482.75	4	17.3290	7	6	7	0.024	0.024	YES	0.67301	0.54632	0.77866					
60	607587.25	4053077.75	4	17.4712	80	71	80	0.0186	0.019	NO	0.67517	0.54797	0.78089					
61	607617.25	4053117.75	4	18.6911	73	64	73	0.1182	0.118	YES	0.69337	0.56161	0.79966					
62	607452.25	4053427.75	5	19.5779	19	18	19	0.1646	0.165	YES	0.70624	0.57100	0.81282					
63	607537.25	4053412.75	5	20.1159	27	26	27	0.02	0.020	NO	0.71389	0.57651	0.82058					
64	607507.25	4053397.75	5	21.2925	35	34	35	0.135	0.135	YES	0.73020	0.58809	0.83689					
65	607682.25	4053152.75	5	22.1332	65	56	65	0.076066	0.076	YES	0.74149	0.59601	0.84795					
66	607537.25	4053422.75	5	22.3613	23	22	23	0.191333	0.191	YES	0.74450	0.59811	0.85086					
67	607357.25	4053477.75	5	23.3830	8	7	8	0.0154	0.015	NO	0.75769	0.60731	0.86343					
68	607657.25	4053082.75	5	23.5714	77	68	77	147.756	147.756	YES	0.76007	0.60897	0.86567					
69	607462.25	4053317.75	5	23.8641	51	45	51	0.2592	0.259	YES	0.76374	0.61153	0.86909					
70	607452.25	4053457.75	5	25.8849	11	10	11	0.1552	0.155	YES	0.78800	0.62849	0.89091					
71	607507.25	4053382.75	5	26.3907	39	36	39	0.214	0.214	YES	0.79378	0.63257	0.89590					
72	607507.25	4053292.75	5	27.2801	55	49	55	2.1218	2.122	YES	0.80366	0.63959	0.90422					
73	607617.25	4053077.75	5	27.3248	79	70	79	0.018	0.018	NO	0.80414	0.63994	0.90462					
74	607532.25	4053427.75	5	27.6896	20	19	20	0.158	0.158	YES	0.80808	0.64277	0.90786					
75	607342.25	4053467.75	5	28.2375	9	8	9	<0.02	0.000	NO	0.81388	0.64697	0.91255					
76	607537.25	4053437.75	5	29.8993	16	15	16	0.23	0.230	YES	0.83065	0.65933	0.92555					
77	607452.25	4053442.75	6	31.1573	91	79	91	0.0614	0.061	YES	0.84253	0.66835	0.93423					
78	607452.25	4053402.75	6	32.3068	92	80	92	0.1094	0.109	YES	0.85278	0.67637	0.94136					
79	607532.25	4053417.75	6	34.4811	26	25	26	0.032	0.032	YES	0.87066	0.69101	0.95297					
80	607662.25	4053152.75	6	34.6362	64	55	64	0.816	0.816	YES	0.87186	0.69202	0.95371					
81	607407.25	4053392.75	6	35.1617	36	35	36	<0.02	0.000	NO	0.87586	0.69545	0.95614					

82	607487.25	4053372.75	6	36.2997	42	39	42	<0.02	0.000	NO	0.88416	0.70275	0.96100
83	607637.25	4053132.75	6	37.4711	70	61	70	0.0852	0.085	YES	0.89219	0.71009	0.96547
84	607532.25	4053322.75	6	37.8995	50	44	50	0.248	0.248	YES	0.89501	0.71273	0.96699
85	607662.25	4053142.75	6	42.8153	68	59	68	0.0696	0.070	YES	0.92291	0.74157	0.98037
86	607657.25	4053112.75	6	47.7244	74	65	74	0.103022	0.103	YES	0.94384	0.76786	0.98842
87	607657.25	4053157.75	6	47.9550	63	54	63	1.41	1.410	YES	0.94468	0.76904	0.98871
88	607302.25	4053367.75	6	48.5423	44	41	44	0.02	0.020	YES	0.94676	0.77202	0.98940
89	607457.25	4053447.75	6	68.7318	13	12	13	0.208266	0.208	YES	0.98625	0.85658	0.99884
90	607457.25	4053417.75	6	76.2974	25	24	25	0.0788	0.079	YES	0.99180	0.88042	0.99950
91	607662.25	4053157.75	6	77.5767	93	81	93	7.702	7.702	YES	0.99249	0.88409	0.99956

# Appendix G: SAS Output (Large Outlier Deleted)

Analysis of Fort Ord data (one observation omitted)  
Data Listing

Obs	X_COOR	Y_COOR	GRIDCODE	MEAN	IDENTIFIER	OID_	GRID_	TNT	RDX	TETRYL	TNB_135
1	607377.25	4053567.75	1	0.5975	1	0	1	0.00000	0.00000	0.00000	0.000
2	607432.25	4053537.75	1	0.3735	2	1	2	0.00000	0.00000	0.00000	0.000
3	607382.25	4053532.75	1	0.9051	3	2	3	0.00000	0.00000	0.00000	0.000
4	607332.25	4053527.75	2	3.6400	4	3	4	0.00000	0.00000	0.00000	0.000
5	607382.25	4053512.75	3	6.3144	5	4	5	0.00000	0.00000	0.00000	0.000
6	607307.25	4053507.75	1	0.4086	6	5	6	0.03220	0.00000	0.00000	0.000
7	607302.25	4053482.75	4	17.3290	7	6	7	0.02400	0.00000	0.00000	0.000
8	607357.25	4053477.75	5	23.3830	8	7	8	0.01540	0.00000	0.00000	0.000
9	607342.25	4053467.75	5	28.2375	9	8	9	0.00000	0.00000	0.00000	0.000
10	607407.25	4053467.75	3	5.5343	10	9	10	0.00000	0.00000	0.40200	0.000
11	607452.25	4053457.75	5	25.8849	11	10	11	0.01780	0.03940	0.09800	0.000
12	607307.25	4053457.75	2	2.0160	12	11	12	0.00000	0.00000	0.13000	0.000
13	607457.25	4053447.75	6	68.7318	13	12	13	0.13000	0.07826	0.00000	0.000
14	607407.25	4053447.75	3	5.5446	14	13	14	0.00000	0.00000	0.02000	0.000
15	607382.25	4053447.75	2	3.5198	15	14	15	0.02040	0.00000	0.00000	0.000
16	607537.25	4053437.75	5	29.8993	16	15	16	0.03800	0.00000	0.00000	0.000
17	607362.25	4053437.75	2	3.0913	17	16	17	0.02000	0.00000	0.00000	0.000
18	607457.25	4053432.75	4	11.2894	18	17	18	0.06560	0.00000	0.00000	0.000
19	607452.25	4053427.75	5	19.5779	19	18	19	0.10760	0.00000	0.00000	0.000
20	607532.25	4053427.75	5	27.6896	20	19	20	0.03200	0.00000	0.00000	0.000
21	607282.25	4053427.75	3	5.3924	21	20	21	0.02800	0.00000	0.00000	0.000
22	607482.25	4053427.75	2	3.8342	22	21	22	2.50000	0.00000	0.00000	0.022
23	607537.25	4053422.75	5	22.3613	23	22	23	0.03000	0.00000	0.13533	0.000
24	607407.25	4053422.75	4	14.1836	24	23	24	0.03840	0.00000	0.00000	0.000
25	607457.25	4053417.75	6	76.2974	25	24	25	0.07880	0.00000	0.00000	0.000
26	607532.25	4053417.75	6	34.4811	26	25	26	0.03200	0.00000	0.00000	0.000
27	607537.25	4053412.75	5	20.1159	27	26	27	0.02000	0.00000	0.00000	0.000
28	607407.25	4053412.75	4	12.2318	28	27	28	0.03600	0.00000	0.16140	0.000
29	607507.25	4053412.75	4	17.1124	29	28	29	0.00000	0.00000	0.00000	0.000
30	607332.25	4053412.75	3	6.7223	30	29	30	0.04000	0.00000	0.00000	0.000
31	607487.25	4053407.75	3	7.1761	31	30	31	0.10366	0.00000	0.00000	0.000
32	607382.25	4053407.75	2	1.9434	32	31	32	0.00000	0.00000	0.00000	0.000
33	607362.25	4053402.75	4	12.5499	33	32	33	0.00000	0.00000	0.00000	0.000
34	607287.25	4053402.75	1	0.3073	34	33	34	0.00000	0.00000	0.00000	0.000
35	607507.25	4053397.75	5	21.2925	35	34	35	0.08980	0.00000	0.00000	0.000
36	607407.25	4053392.75	6	35.1617	36	35	36	0.00000	0.00000	0.00000	0.000
37	607507.25	4053382.75	5	26.3907	39	36	39	0.15060	0.00000	0.00000	0.000
38	607532.25	4053382.75	3	9.3090	40	37	40	0.24000	0.00000	0.00000	0.000
39	607387.25	4053377.75	4	15.8233	41	38	41	0.00000	0.00000	0.00000	0.000
40	607487.25	4053372.75	6	36.2997	42	39	42	0.00000	0.00000	0.00000	0.000
41	607307.25	4053372.75	3	5.3780	43	40	43	0.00000	0.00000	0.00000	0.000
42	607302.25	4053367.75	6	48.5423	44	41	44	0.00000	0.00000	0.02000	0.000
43	607437.25	4053367.75	3	7.7568	45	42	45	0.00000	0.00000	0.15200	0.000
44	607532.25	4053362.75	2	1.8374	46	43	46	0.09260	0.00000	0.26000	0.000
45	607532.25	4053322.75	6	37.8995	50	44	50	0.00000	0.00000	0.24800	0.000
46	607462.25	4053317.75	5	23.8641	51	45	51	0.01520	0.00000	0.24400	0.000
47	607457.25	4053317.75	4	13.5964	52	46	52	0.00000	0.00000	0.22400	0.000
48	607387.25	4053312.75	2	2.7404	53	47	53	0.00000	0.00000	0.77733	0.000
49	607552.25	4053307.75	2	2.4750	54	48	54	0.00000	0.00000	1.97000	0.000
50	607507.25	4053292.75	5	27.2801	55	49	55	0.04400	0.00000	1.99000	0.000
51	607537.25	4053292.75	2	2.8409	56	50	56	0.00000	0.00000	0.25200	0.000
52	607362.25	4053282.75	4	15.8211	58	51	58	0.00000	0.00000	0.25000	0.000
53	607582.25	4053207.75	3	5.4322	61	52	61	0.00000	0.00000	0.24600	0.000
54	607637.25	4053197.75	3	6.0226	62	53	62	0.01740	0.00000	0.04440	0.000
55	607657.25	4053157.75	6	47.9550	63	54	63	1.22644	0.00000	0.00000	0.000
56	607662.25	4053152.75	6	34.6362	64	55	64	0.39200	0.00000	0.11400	0.000
57	607682.25	4053152.75	5	22.1332	65	56	65	0.00000	0.00000	0.07606	0.000
58	607687.25	4053147.75	4	12.9211	66	57	66	0.00000	0.00000	0.03260	0.000
59	607642.25	4053147.75	3	8.9993	67	58	67	0.00000	0.00000	0.04760	0.000
60	607662.25	4053142.75	6	42.8153	68	59	68	0.00000	0.00000	0.06960	0.000
61	607687.25	4053142.75	3	6.9134	69	60	69	0.00000	0.00000	0.06000	0.000
62	607637.25	4053132.75	6	37.4711	70	61	70	0.08520	0.00000	0.00000	0.000
63	607707.25	4053132.75	2	1.9725	71	62	71	0.00000	0.00000	0.00000	0.000
64	607637.25	4053117.75	4	13.2006	72	63	72	0.04000	0.00000	0.00000	0.000
65	607617.25	4053117.75	4	18.6911	73	64	73	0.05720	0.00000	0.00000	0.000
66	607657.25	4053112.75	6	47.7244	74	65	74	0.05046	0.00000	0.00000	0.000
67	607862.25	4053097.75	1	0.2298	75	66	75	0.00000	0.00000	0.00000	0.000
68	607587.25	4053092.75	3	8.6438	76	67	76	0.04340	0.00000	0.00000	0.000
69	607637.25	4053082.75	3	6.0146	78	69	78	0.94800	0.00000	0.02340	0.000
70	607617.25	4053077.75	5	27.3248	79	70	79	0.01800	0.00000	0.00000	0.000
71	607587.25	4053077.75	4	17.4712	80	71	80	0.00000	0.00000	0.00000	0.000
72	607617.25	4053067.75	4	16.6639	81	72	81	0.05680	0.00000	0.00000	0.000
73	607657.25	4053057.75	2	4.0242	82	73	82	0.00000	0.00000	0.00000	0.000
74	607687.25	4053047.75	4	12.2959	84	74	84	0.00000	0.00000	0.00000	0.000
75	607687.25	4053027.75	2	1.9734	85	75	85	0.00000	0.00000	0.00000	0.000
76	607842.25	4052977.75	1	0.3653	86	76	86	0.00000	0.00000	0.00000	0.000

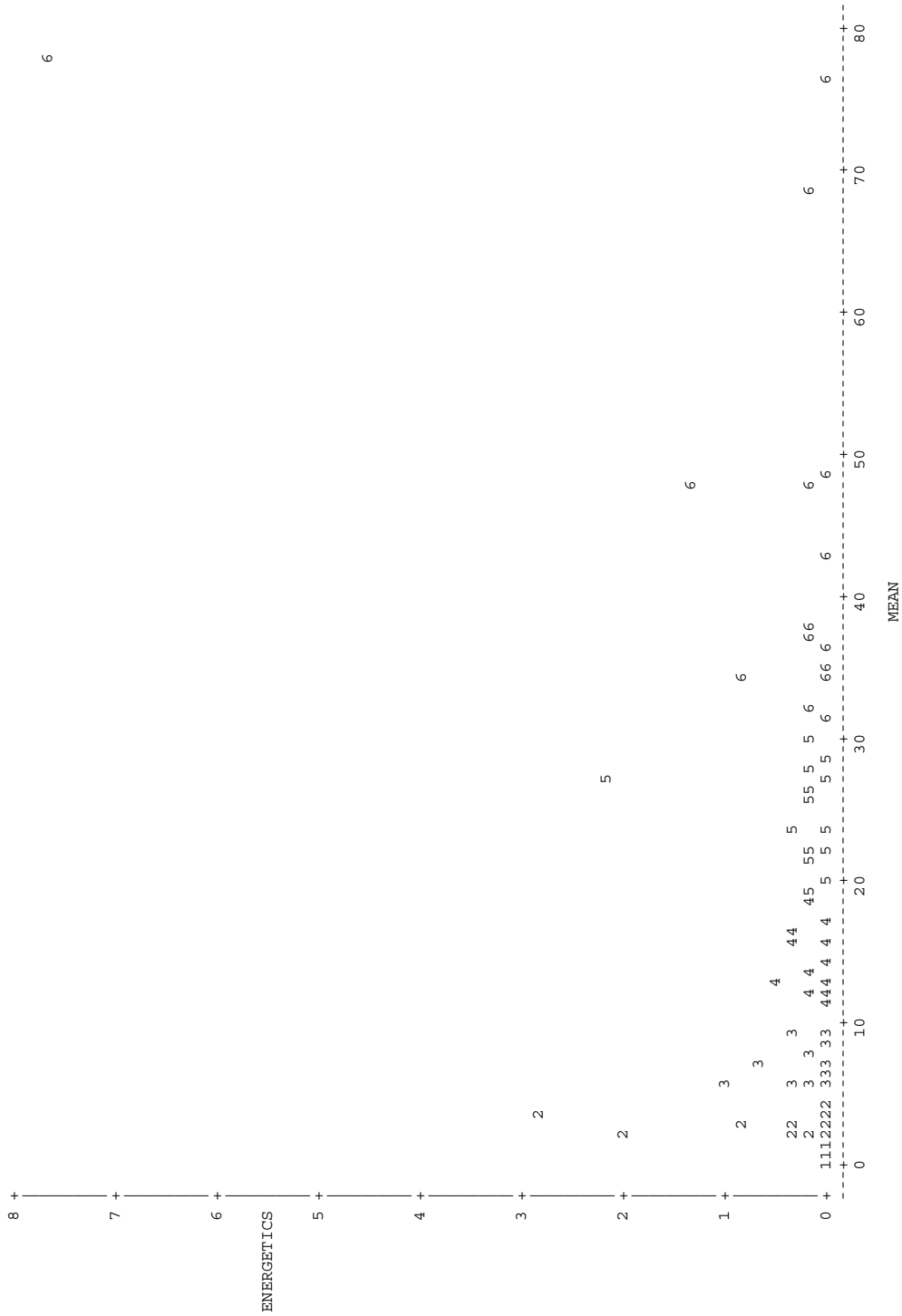
77	607867.25	4052952.75	1	0.6905	88	77	88	0.00000	0.00000	0.00000	0.000
78	607787.25	4052897.75	1	0.1060	89	78	89	0.00000	0.00000	0.00000	0.000
79	607452.25	4053442.75	6	31.1573	91	79	91	0.06140	0.00000	0.00000	0.000
80	607452.25	4053402.75	6	32.3068	92	80	92	0.05480	0.00000	0.00000	0.000
81	607662.25	4053157.75	6	77.5767	93	81	93	7.26000	0.00000	0.00000	0.000
82	607482.25	4053127.75	2	0.2474	94	82	94	0.00000	0.00000	0.00000	0.000
83	607742.25	4053127.75	2	4.4785	95	83	95	0.02880	0.00000	0.00000	0.000
84	607587.25	4053252.75	1	1.2364	96	84	96	0.00000	0.00000	0.00000	0.000
85	607692.25	4053082.75	1	1.6145	98	85	98	0.00000	0.00000	0.00000	0.000
86	607742.25	4052977.75	1	1.4408	99	86	99	0.00000	0.00000	0.00000	0.000
87	607742.25	4052972.75	1	1.5788	100	87	100	0.00000	0.00000	0.00000	0.000
88	607812.25	4052922.75	1	1.0437	101	88	101	0.00000	0.00000	0.00000	0.000
89	607812.25	4052957.75	1	1.3164	102	89	102	0.00000	0.00000	0.00000	0.000
90	607307.25	4053402.75	1	1.3045	103	90	103	0.00000	0.00000	0.00000	0.000

Obs	DNT_4_AM	DNT_2_AM	NG	HMX	TOT_ENER	ENERGETICS	DETECTABLE	LENERGETICS	LMean
1	0.00000	0.0000	0.0000	0.000	<0.02	0.00000	NO	0.00000	-0.51503
2	0.00000	0.0000	0.0000	0.000	<0.02	0.00000	NO	0.00000	-0.98484
3	0.00000	0.0000	0.0000	0.000	<0.02	0.00000	NO	0.00000	-0.09967
4	0.00000	0.0000	0.0000	0.000	<0.02	0.00000	NO	0.00000	1.29197
5	0.00000	0.0000	0.0000	0.000	<0.02	0.00000	NO	0.00000	1.84283
6	0.00000	0.0000	0.0000	0.000	0.0322	0.03220	YES	0.03169	-0.89497
7	0.00000	0.0000	0.0000	0.000	0.024	0.02400	YES	0.02372	2.85238
8	0.00000	0.0000	0.0000	0.000	0.0154	0.01540	NO	0.01528	3.15201
9	0.00000	0.0000	0.0000	0.000	<0.02	0.00000	NO	0.00000	3.34065
10	0.00000	0.0000	0.0000	0.000	0.402	0.40200	YES	0.33790	1.71097
11	0.00000	0.0000	0.0000	0.000	0.1552	0.15520	YES	0.14427	3.25366
12	0.00000	0.0000	0.0000	0.000	0.13	0.13000	YES	0.12222	0.70110
13	0.00000	0.0000	0.0000	0.000	0.208266	0.20826	YES	0.18918	4.23021
14	0.00000	0.0000	0.0000	0.000	0.02	0.02000	NO	0.01980	1.71283
15	0.00000	0.0000	0.0000	0.000	0.0204	0.02040	YES	0.02019	1.25842
16	0.08600	0.0820	0.0000	0.024	0.23	0.23000	YES	0.20701	3.39783
17	0.00000	0.0000	0.0000	0.000	0.02	0.02000	NO	0.01980	1.12859
18	0.00000	0.0000	0.0000	0.000	0.0656	0.06560	YES	0.06354	2.42386
19	0.02920	0.0278	0.0000	0.000	0.1646	0.16460	YES	0.15238	2.97440
20	0.07000	0.0560	0.0000	0.000	0.158	0.15800	YES	0.14669	3.32106
21	0.00000	0.0000	0.0000	0.000	0.028	0.02800	YES	0.02762	1.68499
22	0.12400	0.1060	0.0000	0.000	2.752	2.75200	YES	1.32229	1.34397
23	0.00000	0.0260	0.0000	0.000	0.191333	0.19133	YES	0.17507	3.10733
24	0.00000	0.0000	0.0000	0.000	0.0384	0.03840	YES	0.03768	2.65209
25	0.00000	0.0000	0.0000	0.000	0.0788	0.07880	YES	0.07585	4.33464
26	0.00000	0.0000	0.0000	0.000	0.032	0.03200	YES	0.03150	3.54041
27	0.00000	0.0000	0.0000	0.000	0.02	0.02000	NO	0.01980	3.00151
28	0.00000	0.0000	0.0000	0.000	0.1974	0.19740	YES	0.18015	2.50404
29	0.00000	0.0000	0.0000	0.000	<0.02	0.00000	NO	0.00000	2.83980
30	0.00000	0.0000	0.0000	0.000	0.04	0.04000	YES	0.03922	1.90543
31	0.04020	0.0000	0.6000	0.000	0.74	0.74000	YES	0.55389	1.97075
32	0.00000	0.0000	0.0000	0.000	<0.02	0.00000	NO	0.00000	0.66445
33	0.00000	0.0000	0.0000	0.000	<0.02	0.00000	NO	0.00000	2.52971
34	0.00000	0.0000	0.0000	0.000	<0.02	0.00000	NO	0.00000	-1.17996
35	0.04520	0.0000	0.0000	0.000	0.135	0.13500	YES	0.12663	3.05836
36	0.00000	0.0000	0.0000	0.000	<0.02	0.00000	NO	0.00000	3.55996
37	0.05380	0.0096	0.0000	0.000	0.214	0.21400	YES	0.19392	3.27301
38	0.09600	0.0000	0.0000	0.000	0.336	0.33600	YES	0.28968	2.23099
39	0.00000	0.0000	0.0000	0.000	<0.02	0.00000	NO	0.00000	2.76148
40	0.00000	0.0000	0.0000	0.000	<0.02	0.00000	NO	0.00000	3.59181
41	0.00000	0.0000	0.0000	0.000	<0.02	0.00000	NO	0.00000	1.68232
42	0.00000	0.0000	0.0000	0.000	0.02	0.02000	YES	0.01980	3.88244
43	0.00000	0.0000	0.0000	0.000	0.152	0.15200	YES	0.14150	2.04857
44	0.03180	0.0000	0.0000	0.000	0.3844	0.38440	YES	0.32527	0.60834
45	0.00000	0.0000	0.0000	0.000	0.248	0.24800	YES	0.22154	3.63494
46	0.00000	0.0000	0.0000	0.000	0.2592	0.25920	YES	0.23048	3.17238
47	0.00000	0.0000	0.0000	0.000	0.224	0.22400	YES	0.20212	2.60981
48	0.00000	0.0000	0.0300	0.000	0.807333	0.80733	YES	0.59185	1.00809
49	0.00000	0.0000	0.0000	0.000	1.97	1.97000	YES	1.08856	0.90625
50	0.08780	0.0000	0.0000	0.000	2.1218	2.12180	YES	1.13841	3.30616
51	0.00000	0.0000	0.0000	0.000	0.252	0.25200	YES	0.22474	1.04413
52	0.00000	0.0000	0.0258	0.000	0.2758	0.27580	YES	0.24357	2.76135
53	0.00000	0.0000	0.0000	0.000	0.246	0.24600	YES	0.21994	1.69234
54	0.01980	0.0000	0.0000	0.000	0.0816	0.08160	YES	0.07844	1.79552
55	0.09422	0.0900	0.0000	0.000	1.41	1.41000	YES	0.87963	3.87026
56	0.15400	0.1560	0.0000	0.000	0.816	0.81600	YES	0.59664	3.54490
57	0.00000	0.0000	0.0000	0.000	0.076066	0.07606	YES	0.07331	3.09708
58	0.00000	0.0000	0.0000	0.000	0.0326	0.03260	YES	0.03208	2.55886
59	0.00000	0.0168	0.0000	0.000	0.0644	0.06440	YES	0.06241	2.19715
60	0.00000	0.0000	0.0000	0.000	0.0696	0.06960	YES	0.06728	3.75690
61	0.00000	0.0000	0.0000	0.000	0.06	0.06000	YES	0.05827	1.93346
62	0.00000	0.0000	0.0000	0.000	0.0852	0.08520	YES	0.08176	3.62357
63	0.00000	0.0000	0.0000	0.000	<0.02	0.00000	NO	0.00000	0.67931
64	0.02000	0.0000	0.4600	0.000	0.52	0.52000	YES	0.41871	2.58026
65	0.03720	0.0238	0.0000	0.000	0.1182	0.11820	YES	0.11172	2.92805
66	0.03035	0.0222	0.0000	0.000	0.103022	0.10302	YES	0.09805	3.86544
67	0.00000	0.0000	0.0000	0.000	<0.02	0.00000	NO	0.00000	-1.47072
68	0.03200	0.0000	0.0000	0.000	0.0754	0.07540	YES	0.07269	2.15684
69	0.02240	0.0246	0.0000	0.000	1.0184	1.01840	YES	0.70231	1.79419
70	0.00000	0.0000	0.0000	0.000	0.018	0.01800	NO	0.01784	3.30779
71	0.00000	0.0186	0.0000	0.000	0.0186	0.01860	NO	0.01843	2.86056
72	0.13360	0.1514	0.0000	0.000	0.3418	0.34180	YES	0.29401	2.81324
73	0.00000	0.0000	0.0000	0.000	<0.02	0.00000	NO	0.00000	1.39233
74	0.00000	0.0000	0.0000	0.000	<0.02	0.00000	NO	0.00000	2.50927
75	0.00000	0.0196	0.0000	0.000	0.0196	0.01960	NO	0.01941	0.67974
76	0.00000	0.0000	0.0000	0.000	<0.02	0.00000	NO	0.00000	-1.00701
77	0.00000	0.0000	0.0000	0.000	<0.02	0.00000	NO	0.00000	-0.37030
78	0.00000	0.0000	0.0000	0.000	<0.02	0.00000	NO	0.00000	-2.24479

79	0.00000	0.0000	0.0000	0.000	0.0614	0.06140	YES	0.05959	3.43905
80	0.03460	0.0200	0.0000	0.000	0.1094	0.10940	YES	0.10382	3.47528
81	0.21400	0.2280	0.0000	0.000	7.702	7.70200	YES	2.16355	4.35127
82	0.00000	0.0000	0.0000	0.000	<0.02	0.00000	NO	0.00000	-1.39667
83	0.00000	0.0000	0.0000	0.000	0.0288	0.02880	YES	0.02839	1.49929
84	0.00000	0.0000	0.0000	0.000	<0.02	0.00000	NO	0.00000	0.21217
85	0.00000	0.0000	0.0000	0.000	<0.02	0.00000	NO	0.00000	0.47899
86	0.00000	0.0000	0.0000	0.000	<0.02	0.00000	NO	0.00000	0.36518
87	0.00000	0.0000	0.0000	0.000	<0.02	0.00000	NO	0.00000	0.45668
88	0.00000	0.0000	0.0000	0.000	<0.02	0.00000	NO	0.00000	0.04278
89	0.00000	0.0000	0.0000	0.000	<0.02	0.00000	NO	0.00000	0.27489
90	0.00000	0.0000	0.0000	0.000	<0.02	0.00000	NO	0.00000	0.26581

Analysis of Fort Ord data (one observation omitted)  
 scatter plots with group variable

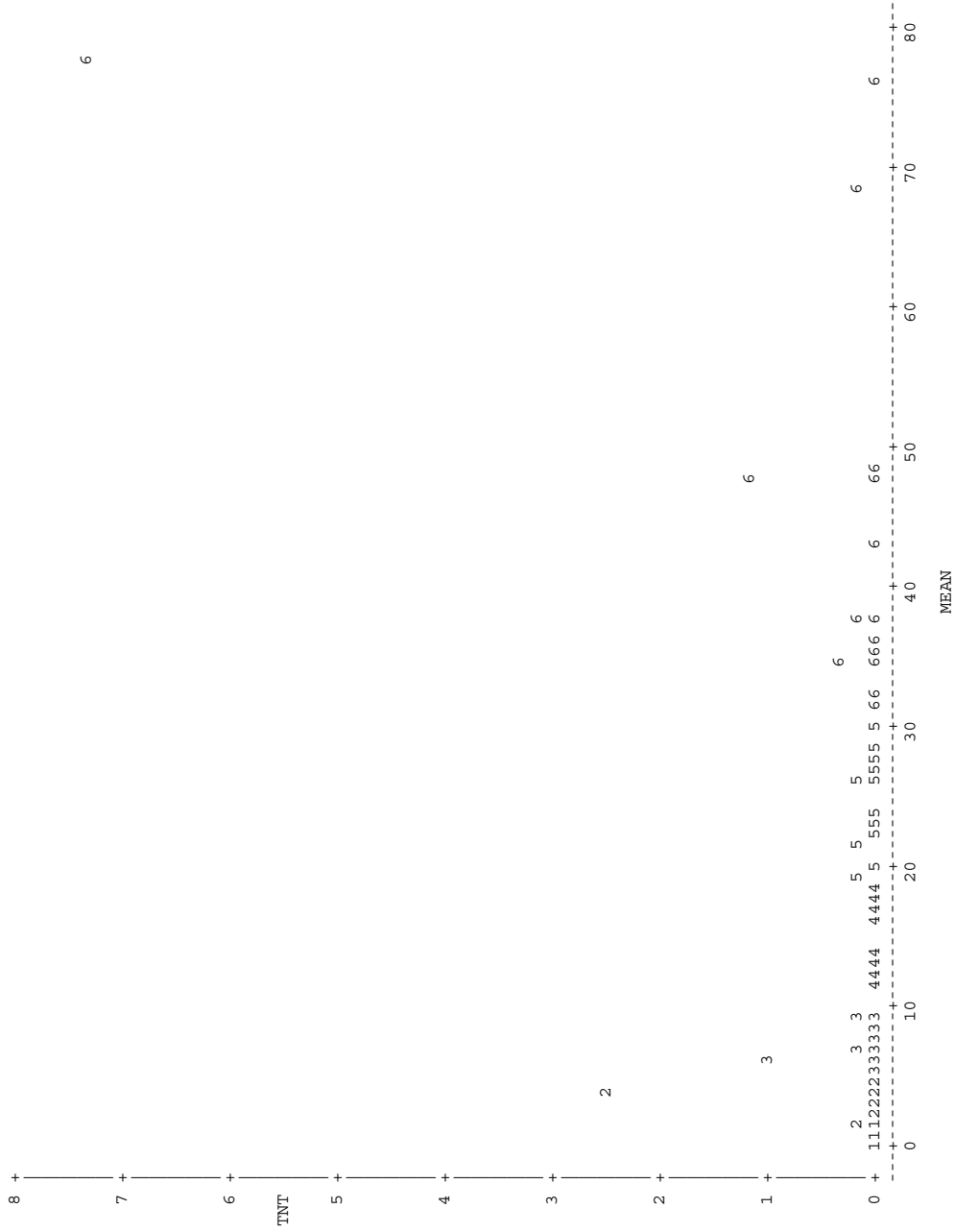
Plot of ENERGETICS\*MEAN. Symbol is value of GRIDCODE.



NOTE: 25 obs hidden.

Analysis of Fort Ord data (one observation omitted)  
 scatter plots with group variable

Plot of TNT\*MEAN. Symbol is value of GRIDCODE.



NOTE: 37 obs hidden.

Analysis of Fort Ord data (one observation omitted)  
 Variable means

The MEANS Procedure

Variable	N	Mean	Std Dev	Minimum	Maximum
MEAN	90	15.6775376	17.0458022	0.1059500	77.5767000
TNT	90	0.1597996	0.8169941	0	7.2600000
RDX	90	0.0013073	0.0091940	0	0.0782600
TETRYL	90	0.0894191	0.3079546	0	1.9900000
TNB_135	90	0.000244444	0.0023190	0	0.0220000
DNT_4_AM	90	0.0161797	0.0384404	0	0.2140000
DNT_2_AM	90	0.0119822	0.0367399	0	0.2280000
NG	90	0.0123978	0.0792757	0	0.6000000
HMX	90	0.000266667	0.0025298	0	0.0240000
ENERGETICS	90	0.2915467	0.9128221	0	7.7020000
LENERGETICS	90	0.1694791	0.3328630	0	2.1635529
LMean	90	1.9571864	1.5235662	-2.2447880	4.3512671

Analysis of Fort Ord data (one observation omitted)  
 Factor analysis using of various chemical

The FACTOR Procedure

Initial Factor Method: Principal Components

Prior Communality Estimates: ONE

Eigenvalues of the Correlation Matrix: Total = 8 Average = 1

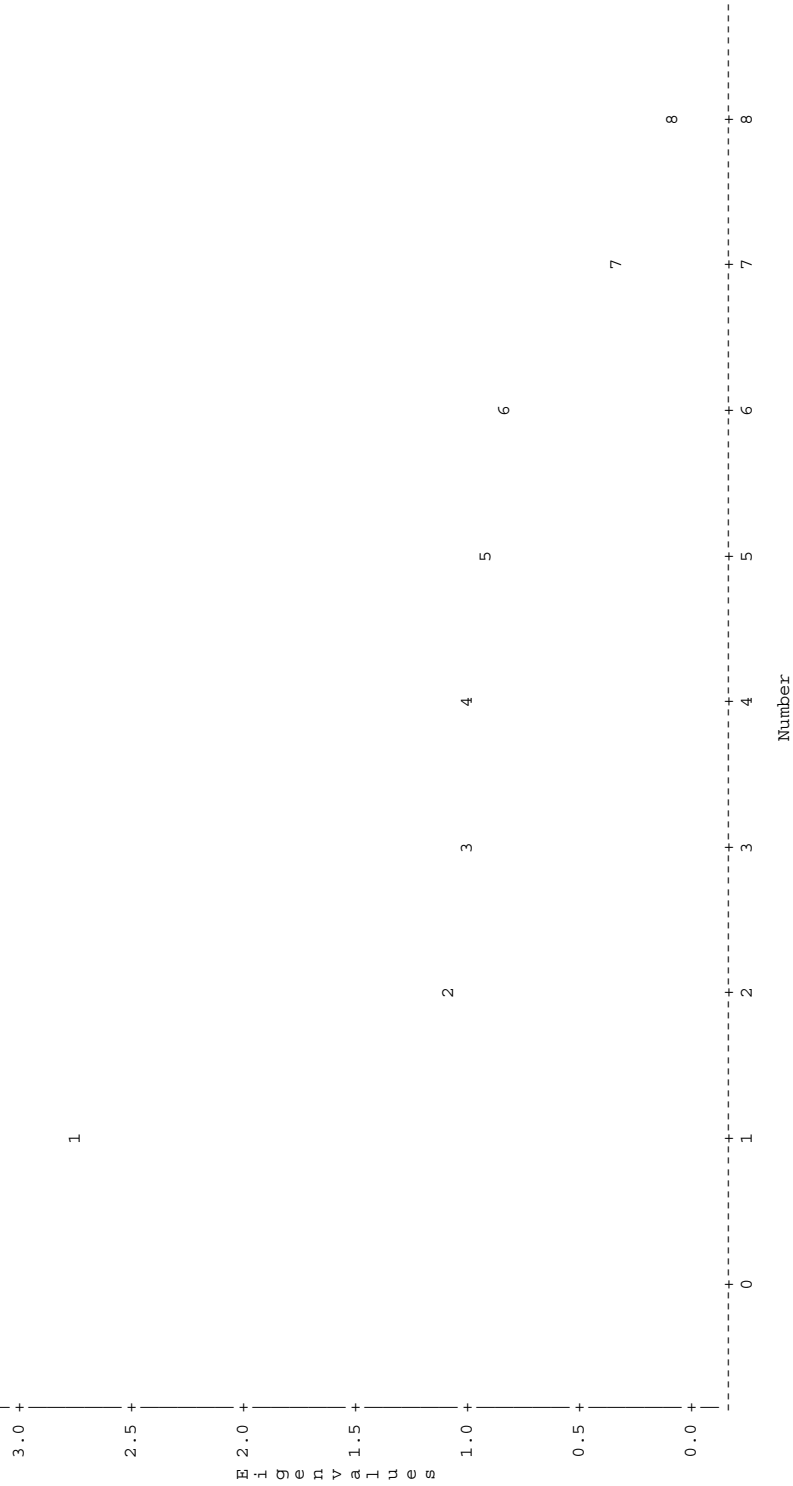
	Eigenvalue	Difference	Proportion	Cumulative
1	2.72423523	1.67202726	0.3405	0.3405
2	1.05220797	0.01347480	0.1315	0.4721
3	1.03873317	0.01193120	0.1298	0.6019
4	1.02680197	0.07291095	0.1284	0.7302
5	0.95389103	0.14134119	0.1192	0.8495
6	0.81254984	0.50497603	0.1016	0.9511
7	0.30757381	0.22356684	0.0384	0.9895
8	0.08400697		0.0105	1.0000

4 factors will be retained by the NFACTOR criterion.

Analysis of Fort Ord data (one observation omitted)  
Factor analysis using of various chemical

The FACTOR Procedure  
Initial Factor Method: Principal Components

Scree Plot of Eigenvalues



Analysis of Fort Ord data (one observation omitted)  
Factor analysis using of various chemical

The FACTOR Procedure  
Initial Factor Method: Principal Components

	Eigenvectors			
	1	2	3	4
TNT	0.51374	-0.20267	0.00353	0.00819
RDX	-0.04185	-0.30986	-0.46259	-0.47605
TETRYL	-0.02309	0.06650	0.83468	-0.14916
TNB_135	0.27860	-0.38594	0.01327	0.02596
DNT_4_AM	0.56092	0.09119	0.07786	0.03774
DNT_2_AM	0.57095	0.07981	-0.03825	-0.04746
NG	-0.00674	0.03500	-0.17015	0.84382
HMX	0.12455	0.83284	-0.22945	-0.18623

	Factor Pattern			
	Factor1	Factor2	Factor3	Factor4
TNT	0.84795	-0.20790	0.00360	0.00830
RDX	-0.06908	-0.31784	-0.47147	-0.48239
TETRYL	-0.03812	0.06821	0.85070	-0.15115
TNB_135	0.45983	-0.39589	0.01353	0.02631
DNT_4_AM	0.92581	0.09354	0.07936	0.03824
DNT_2_AM	0.94236	0.08187	-0.03898	-0.04809
NG	-0.01112	0.03591	-0.17341	0.85505
HMX	0.20557	0.85431	-0.23385	-0.18871

Variance Explained by Each Factor

Factor1	Factor2	Factor3	Factor4
2.7242352	1.0522080	1.0387332	1.0268020

Final Communality Estimates: Total = 5.841978

	TNT	RDX	TETRYL	TNB_135	DNT_4_AM	DNT_2_AM
NG						
		HMX				
0.76231933		0.56077643	0.75263335	0.36904847	0.87363585	0.89857767
0.76259350		0.86239375				

Analysis of Fort Ord data (one observation omitted)  
Factor analysis using of various chemical

The FACTOR Procedure  
Rotation Method: Varimax

Orthogonal Transformation Matrix

	1	2	3	4
1	0.99174	0.12706	0.00571	0.01651
2	-0.12629	0.95555	0.21431	0.15825
3	0.02182	-0.20726	0.97657	-0.05360
4	0.00485	-0.16679	0.01860	0.98580

Rotated Factor Pattern

	Factor1	Factor2	Factor3	Factor4
TNT	0.86732	-0.09305	-0.03604	-0.01091
RDX	-0.04100	-0.13432	-0.53790	-0.50171
TETRYL	-0.02859	-0.09077	0.84236	-0.18443
TNB_135	0.50645	-0.32706	-0.06851	-0.02985
DNT_4_AM	0.90827	0.18419	0.10354	0.06353
DNT_2_AM	0.92315	0.21407	-0.01604	-0.01681
NG	-0.01520	-0.07377	-0.14582	0.85770
HMX	0.08996	0.92240	-0.04762	-0.03491

Variance Explained by Each Factor

Factor1	Factor2	Factor3	Factor4
2.6967258	1.0779145	1.0394029	1.0279351

Final Communality Estimates: Total = 5.841978

	TNT	RDX	TETRYL	TNB_135	DNT_4_AM	DNT_2_AM
NG						
		HMX				
0.76231933		0.56077643	0.75263335	0.36904847	0.87363585	0.89857767
0.76259350		0.86239375				

Analysis of Fort Ord data (one observation omitted)  
 Factor analysis using of various chemical

The FACTOR Procedure  
 Rotation Method: Varimax

Scoring Coefficients Estimated by Regression

Squared Multiple Correlations of the Variables with Each Factor

	Factor1	Factor2	Factor3	Factor4
	1.0000000	1.0000000	1.0000000	1.0000000

Standardized Scoring Coefficients

	Factor1	Factor2	Factor3	Factor4
TNT	0.33376	-0.15132	-0.03703	-0.01835
RDX	0.00082	-0.11944	-0.51687	-0.48703
TETRYL	-0.00491	-0.08502	0.81086	-0.17898
TNB_135	0.21532	-0.34505	-0.06647	-0.03219
DNT_4_AM	0.32766	0.10608	0.09629	0.05230
DNT_2_AM	0.33219	0.13389	-0.01887	-0.02614
NG	-0.00796	-0.07220	-0.14026	0.83519
HMX	-0.03350	0.86273	-0.04884	-0.03938

Analysis of Fort Ord data (one observation omitted)  
 Correlations of factors and variables of interest

The CORR Procedure

4 With Variables: MEAN ENERGETICS LENERGETICS LMean  
 4 Variables: Factor1 Factor2 Factor3 Factor4

Simple Statistics

Variable	N	Mean	Std Dev	Sum	Minimum	Maximum
MEAN	90	15.67754	17.04580	1411	0.10595	77.57670
ENERGETICS	90	0.29155	0.91282	26.23920	0	7.70200
LENERGETICS	90	0.16948	0.33286	15.25312	0	2.16355
LMean	90	1.95719	1.52357	176.14677	-2.24479	4.35127
Factor1	90	0	1.00000	0	-0.35953	6.52328
Factor2	90	0	1.00000	0	-3.06831	8.65339
Factor3	90	0	1.00000	0	-4.56051	5.30274
Factor4	90	0	1.00000	0	-4.16026	6.36177

Pearson Correlation Coefficients, N = 90  
 Prob > |r| under H0: Rho=0

	Factor1	Factor2	Factor3	Factor4
MEAN	0.35910 0.0005	0.10364 0.3310	-0.17693 0.0953	-0.19731 0.0623
ENERGETICS	0.84182 <.0001	-0.10354 0.3315	0.23730 0.0243	-0.00103 0.9923
LENERGETICS	0.80182 <.0001	-0.11845 0.2662	0.36099 0.0005	0.03775 0.7239
LMean	0.24170 0.0217	0.11823 0.2671	-0.06646 0.5337	-0.06793 0.5247

Analysis of Fort Ord data (one observation omitted)  
ANCOVA using value of ENERGETICS

The Mixed Procedure

Model Information

Data Set	WORK.CONTAMINANTS
Dependent Variable	ENERGETICS
Covariance Structure	Diagonal
Estimation Method	REML
Residual Variance Method	Profile
Fixed Effects SE Method	Model-Based
Degrees of Freedom Method	Residual

Class Level Information

Class	Levels	Values
GRIDCODE	6	1 2 3 4 5 6

Dimensions

Covariance Parameters	1
Columns in X	7
Columns in Z	0
Subjects	1
Max Obs Per Subject	90

Number of Observations

Number of Observations Read	90
Number of Observations Used	90
Number of Observations Not Used	0

Covariance Parameter  
Estimates

Cov Parm	Estimate
Residual	0.8233

Fit Statistics

-2 Res Log Likelihood	238.3
AIC (smaller is better)	240.3
AICC (smaller is better)	240.3
BIC (smaller is better)	242.7

Type 1 Tests of Fixed Effects

Effect	Num DF	Den DF	F Value	Pr > F
GRIDCODE	5	84	1.21	0.3094

Type 3 Tests of Fixed Effects

Effect	Num DF	Den DF	F Value	Pr > F
GRIDCODE	5	84	1.21	0.3094

Analysis of Fort Ord data (one observation omitted)  
 ANCOVA using value of ENERGETICS  
 Residual analysis

The UNIVARIATE Procedure  
 Variable: Resid

## Moments

N	90	Sum Weights	90
Mean	0	Sum Observations	0
Std Deviation	0.88150717	Variance	0.77705489
Skewness	6.01506607	Kurtosis	44.9387683
Uncorrected SS	69.1578851	Corrected SS	69.1578851
Coeff Variation	.	Std Error Mean	0.09291901

## Basic Statistical Measures

Location		Variability	
Mean	0.00000	Std Deviation	0.88151
Median	-0.10452	Variance	0.77705
Mode	-0.00201	Range	7.70200
		Interquartile Range	0.26646

## Tests for Location: Mu0=0

Test	-Statistic-	-----p Value-----
Student's t	t 0	Pr >  t  1.0000
Sign	M -27	Pr >=  M  <.0001
Signed Rank	S -1024.5	Pr >=  S  <.0001

## Tests for Normality

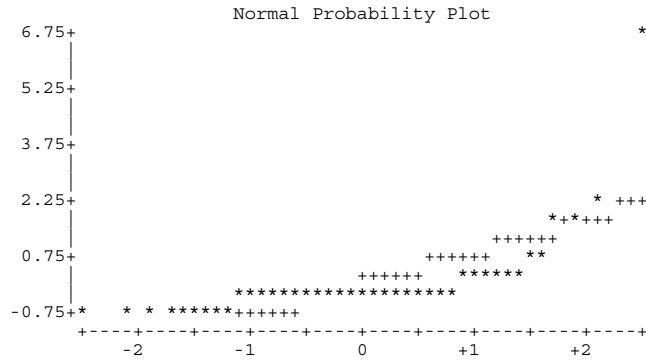
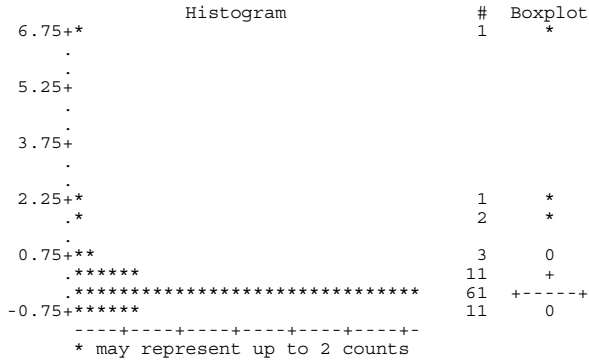
Test	--Statistic--	-----p Value-----
Shapiro-Wilk	W 0.452558	Pr < W <0.0001
Kolmogorov-Smirnov	D 0.313237	Pr > D <0.0100
Cramer-von Mises	W-Sq 2.51675	Pr > W-Sq <0.0050
Anderson-Darling	A-Sq 13.01356	Pr > A-Sq <0.0050

## Quantiles (Definition 5)

Quantile	Estimate
100% Max	6.9724213
99%	6.9724213
95%	0.8008133
90%	0.2998673
75% Q3	-0.0020125
50% Median	-0.1045154
25% Q1	-0.2684707
10%	-0.6233687
5%	-0.6681787
1%	-0.7295787
0% Min	-0.7295787

Extreme Observations

-----Lowest-----		-----Highest-----	
Value	Obs	Value	Obs
-0.729579	40	0.800813	69
-0.729579	36	1.544365	49
-0.709579	42	1.853329	50
-0.697579	26	2.326365	22
-0.668179	79	6.972421	81



Analysis of Fort Ord data (one observation omitted)  
 Regression using value of ENERGETICS

The REG Procedure  
 Model: MODEL1  
 Dependent Variable: ENERGETICS

Number of Observations Read 90  
 Number of Observations Used 90

Analysis of Variance

Source	DF	Sum of Squares	Mean Square	F Value	Pr > F
Model	1	9.56319	9.56319	13.03	0.0005
Error	88	64.59555	0.73404		
Corrected Total	89	74.15873			

Root MSE 0.85676 R-Square 0.1290  
 Dependent Mean 0.29155 Adj R-Sq 0.1191  
 Coeff Var 293.86771

Parameter Estimates

Variable	DF	Parameter Estimate	Standard Error	t Value	Pr >  t	95% Confidence Limits	
Intercept	1	-0.00994	0.12302	-0.08	0.9358	-0.25441	0.23453
MEAN	1	0.01923	0.00533	3.61	0.0005	0.00864	0.02982

Analysis of Fort Ord data (one observation omitted)  
 Regression using value of ENERGETICS  
 Residual analysis

The UNIVARIATE Procedure  
 Variable: resid

Moments

N	90	Sum Weights	90
Mean	0	Sum Observations	0
Std Deviation	0.85193466	Variance	0.72579266
Skewness	4.92862266	Kurtosis	32.9183482
Uncorrected SS	64.595547	Corrected SS	64.595547
Coeff Variation	.	Std Error Mean	0.0898018

Basic Statistical Measures

Location		Variability	
Mean	0.00000	Std Deviation	0.85193
Median	-0.05372	Variance	0.72579
Mode	.	Range	7.59860
		Interquartile Range	0.30333

Tests for Location: Mu0=0

Test	-Statistic-	-----p Value-----
Student's t	t 0	Pr >  t  1.0000
Sign	M -20	Pr >=  M  <.0001
Signed Rank	S -889.5	Pr >=  S  0.0002

Tests for Normality

Test	--Statistic--	-----p Value-----
Shapiro-Wilk	W 0.544243	Pr < W <0.0001
Kolmogorov-Smirnov	D 0.306173	Pr > D <0.0100
Cramer-von Mises	W-Sq 2.177488	Pr > W-Sq <0.0050
Anderson-Darling	A-Sq 11.14498	Pr > A-Sq <0.0050

Quantiles (Definition 5)

Quantile	Estimate
100% Max	6.22010612
99%	6.22010612
95%	0.91267554
90%	0.33225858
75% Q3	0.00402973
50% Median	-0.05372167
25% Q1	-0.29930441
10%	-0.57711343
5%	-0.74381795
1%	-1.37849220
0% Min	-1.37849220

Extreme Observations

-----Lowest-----		-----Highest-----	
Value	Obs	Value	Obs
-1.378492	25	0.912676	69
-1.103543	13	1.607131	50
-0.903550	42	1.932343	49
-0.804801	66	2.688205	22
-0.743818	60	6.220106	81



Analysis of Fort Ord data (one observation omitted)  
 ANCOVA using value of Log(ENERGETICS)

The Mixed Procedure

Model Information

Data Set	WORK.CONTAMINANTS
Dependent Variable	LENERGETICS
Covariance Structure	Diagonal
Estimation Method	REML
Residual Variance Method	Profile
Fixed Effects SE Method	Model-Based
Degrees of Freedom Method	Residual

Class Level Information

Class	Levels	Values
GRIDCODE	6	1 2 3 4 5 6

Dimensions

Covariance Parameters	1
Columns in X	7
Columns in Z	0
Subjects	1
Max Obs Per Subject	90

Number of Observations

Number of Observations Read	90
Number of Observations Used	90
Number of Observations Not Used	0

Covariance Parameter Estimates

Cov Parm	Estimate
Residual	0.1068

Fit Statistics

-2 Res Log Likelihood	66.7
AIC (smaller is better)	68.7
AICC (smaller is better)	68.8
BIC (smaller is better)	71.2

Type 1 Tests of Fixed Effects

Effect	Num DF	Den DF	F Value	Pr > F
GRIDCODE	5	84	1.66	0.1523

Type 3 Tests of Fixed Effects

Effect	Num DF	Den DF	F Value	Pr > F
GRIDCODE	5	84	1.66	0.1523

Analysis of Fort Ord data (one observation omitted)  
 ANCOVA using value of Log(ENERGETICS)  
 Residual analysis

The UNIVARIATE Procedure  
 Variable: Resid

Moments

N	90	Sum Weights	90
Mean	0	Sum Observations	0
Std Deviation	0.31751012	Variance	0.10081267
Skewness	3.31379841	Kurtosis	14.4686825
Uncorrected SS	8.972328	Corrected SS	8.972328
Coeff Variation	.	Std Error Mean	0.0334685

Basic Statistical Measures

Location		Variability	
Mean	0.00000	Std Deviation	0.31751
Median	-0.05343	Variance	0.10081
Mode	-0.00198	Range	2.16355
		Interquartile Range	0.17671

Tests for Location: Mu0=0

Test	-Statistic-	-----p Value-----
Student's t	t 0	Pr >  t  1.0000
Sign	M -22	Pr >=  M  <.0001
Signed Rank	S -757.5	Pr >=  S  0.0019

Tests for Normality

Test	--Statistic--	-----p Value-----
Shapiro-Wilk	W 0.664959	Pr < W <0.0001
Kolmogorov-Smirnov	D 0.260045	Pr > D <0.0100
Cramer-von Mises	W-Sq 1.487878	Pr > W-Sq <0.0050
Anderson-Darling	A-Sq 8.131023	Pr > A-Sq <0.0050

Quantiles (Definition 5)

Quantile	Estimate
100% Max	1.85767294
99%	1.85767294
95%	0.57374680
90%	0.30054209
75% Q3	0.00333776
50% Median	-0.05343095
25% Q1	-0.17336746
10%	-0.24856988
5%	-0.25084861
1%	-0.30587994
0% Min	-0.30587994

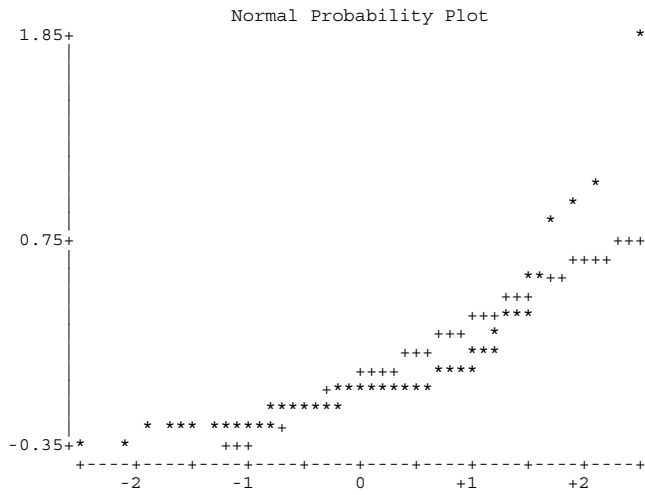
Extreme Observations

-----Lowest-----		-----Highest-----	
Value	Obs	Value	Obs
-0.305880	40	0.573747	55
-0.305880	36	0.837713	49
-0.286077	42	0.949760	50
-0.274381	26	1.071440	22
-0.250849	82	1.857673	81

Stem Leaf	#	Boxplot
18 6	1	*
17		
16		
15		
14		
13		
12		
11		
10 7	1	*
9 5	1	*
8 4	1	*
7		
6		
5 37	2	0
4		
3 148	3	0
2 9	1	0
1 2469	4	

```

0 012345779          9  +---+--+
-0 98887644443310000000000000000000 28 *-----*
-1 9777755332221111100          20  +-----+
-2 9755555433332210           17   |
-3 11                    2     |
-----+-----+-----+-----+-----+
Multiply Stem.Leaf by 10**-1
    
```



Analysis of Fort Ord data (one observation omitted)  
 Regression using value of ENERGETICS

The REG Procedure  
 Model: MODEL1  
 Dependent Variable: LENERGETICS

Number of Observations Read 90  
 Number of Observations Used 90

Analysis of Variance

Source	DF	Sum of Squares	Mean Square	F Value	Pr > F
Model	1	0.95670	0.95670	9.45	0.0028
Error	88	8.90430	0.10119		
Corrected Total	89	9.86100			

Root MSE 0.31810 R-Square 0.0970  
 Dependent Mean 0.16948 Adj R-Sq 0.0868  
 Coeff Var 187.69053

Parameter Estimates

Variable	DF	Parameter Estimate	Standard Error	t Value	Pr >  t	95% Confidence Limits	
Intercept	1	0.07412	0.04567	1.62	0.1082	-0.01664	0.16489
MEAN	1	0.00608	0.00198	3.07	0.0028	0.00215	0.01001





Analysis of Fort Ord data (one observation omitted)  
 Logistic Regression

The LOGISTIC Procedure

Model Information

Data Set WORK.CONTAMINANTS  
 Response Variable DETECTABLE  
 Number of Response Levels 2  
 Model binary logit  
 Optimization Technique Fisher's scoring

Number of Observations Read 90  
 Number of Observations Used 90

Response Profile

Ordered Value	DETECTABLE	Total Frequency
1	YES	54
2	NO	36

Probability modeled is DETECTABLE='YES'.

Model Convergence Status

Convergence criterion (GCONV=1E-8) satisfied.

Model Fit Statistics

Criterion	Intercept Only	Intercept and Covariates
AIC	123.142	110.074
SC	125.642	115.073
-2 Log L	121.142	106.074

Testing Global Null Hypothesis: BETA=0

Test	Chi-Square	DF	Pr > ChiSq
Likelihood Ratio	15.0684	1	0.0001
Score	11.8662	1	0.0006
Wald	10.0669	1	0.0015

Analysis of Maximum Likelihood Estimates

Parameter	DF	Estimate	Standard Error	Wald Chi-Square	Pr > ChiSq
Intercept	1	-0.4732	0.3249	2.1217	0.1452
MEAN	1	0.0676	0.0213	10.0669	0.0015

Odds Ratio Estimates

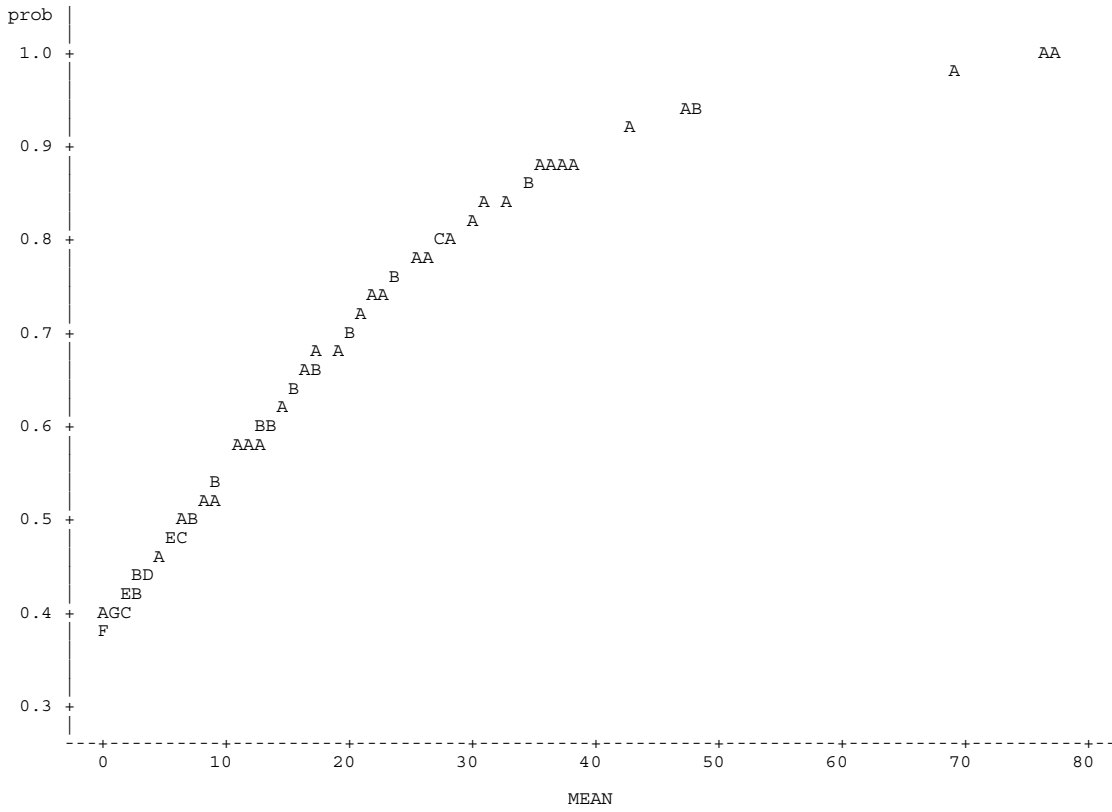
Effect	Point Estimate	95% Wald Confidence Limits	
MEAN	1.070	1.026	1.116

Association of Predicted Probabilities and Observed Responses

Percent Concordant	77.2	Somers' D	0.546
Percent Discordant	22.6	Gamma	0.547
Percent Tied	0.2	Tau-a	0.265
Pairs	1944	c	0.773

Analysis of Fort Ord data (one observation omitted)  
Logistic Regression

Plot of prob\*MEAN. Legend: A = 1 obs, B = 2 obs, etc.



Analysis of Fort Ord data (one observation omitted)  
 Logistic Regression

Obs	X		G R I D E	I D E N T I F I C A T O R S			E N T R E T C T I C L E S	D E T E R M I N I N G	p	l	u		
	$\bar{C}$ O R	$\bar{C}$ O R		M E A N	F O R	O I D						G R E E N	
1	607787.25	4052897.75	1	0.1060	89	78	89	<0.02	0.00000	NO	0.38555	0.24978	0.54181
2	607862.25	4053097.75	1	0.2298	75	66	75	<0.02	0.00000	NO	0.38753	0.25203	0.54300
3	607482.25	4053127.75	2	0.2474	94	82	94	<0.02	0.00000	NO	0.38782	0.25235	0.54317
4	607287.25	4053402.75	1	0.3073	34	33	34	<0.02	0.00000	NO	0.38878	0.25344	0.54375
5	607842.25	4052977.75	1	0.3653	86	76	86	<0.02	0.00000	NO	0.38971	0.25450	0.54431
6	607432.25	4053537.75	1	0.3735	2	1	2	<0.02	0.00000	NO	0.38984	0.25465	0.54439
7	607307.25	4053507.75	1	0.4086	6	5	6	0.0322	0.03220	YES	0.39041	0.25529	0.54473
8	607377.25	4053567.75	1	0.5975	1	0	1	<0.02	0.00000	NO	0.39345	0.25875	0.54657
9	607867.25	4052952.75	1	0.6905	88	77	88	<0.02	0.00000	NO	0.39496	0.26047	0.54748
10	607382.25	4053532.75	1	0.9051	3	2	3	<0.02	0.00000	NO	0.39843	0.26444	0.54959
11	607812.25	4052922.75	1	1.0437	101	88	101	<0.02	0.00000	NO	0.40068	0.26701	0.55096
12	607587.25	4053252.75	1	1.2364	96	84	96	<0.02	0.00000	NO	0.40381	0.27061	0.55288
13	607307.25	4053402.75	1	1.3045	103	90	103	<0.02	0.00000	NO	0.40492	0.27189	0.55356
14	607812.25	4052957.75	1	1.3164	102	89	102	<0.02	0.00000	NO	0.40512	0.27211	0.55368
15	607742.25	4052977.75	1	1.4408	99	86	99	<0.02	0.00000	NO	0.40715	0.27445	0.55493
16	607742.25	4052972.75	1	1.5788	100	87	100	<0.02	0.00000	NO	0.40940	0.27705	0.55633
17	607692.25	4053082.75	1	1.6145	98	85	98	<0.02	0.00000	NO	0.40999	0.27772	0.55669
18	607532.25	4053362.75	2	1.8374	46	43	46	0.3844	0.38440	YES	0.41364	0.28195	0.55896
19	607382.25	4053407.75	2	1.9434	32	31	32	<0.02	0.00000	NO	0.41538	0.28396	0.56005
20	607707.25	4053132.75	2	1.9725	71	62	71	<0.02	0.00000	NO	0.41586	0.28452	0.56034
21	607687.25	4053027.75	2	1.9734	85	75	85	0.0196	0.01960	NO	0.41587	0.28453	0.56035
22	607307.25	4053457.75	2	2.0160	12	11	12	0.13	0.13000	YES	0.41657	0.28535	0.56079
23	607552.25	4053307.75	2	2.4750	54	48	54	1.97	1.97000	YES	0.42414	0.29414	0.56556
24	607387.25	4053312.75	2	2.7404	53	47	53	0.807333	0.80733	YES	0.42853	0.29925	0.56836
25	607537.25	4053292.75	2	2.8409	56	50	56	0.252	0.25200	YES	0.43020	0.30119	0.56943
26	607362.25	4053437.75	2	3.0913	17	16	17	0.02	0.02000	NO	0.43435	0.30604	0.57211
27	607382.25	4053447.75	2	3.5198	15	14	15	0.0204	0.02040	YES	0.44149	0.31437	0.57676
28	607332.25	4053527.75	2	3.6400	4	3	4	<0.02	0.00000	NO	0.44349	0.31671	0.57808
29	607482.25	4053427.75	2	3.8342	22	21	22	2.752	2.75200	YES	0.44674	0.32051	0.58023
30	607657.25	4053057.75	2	4.0242	82	73	82	<0.02	0.00000	NO	0.44992	0.32422	0.58235
31	607742.25	4053127.75	2	4.4785	95	83	95	0.0288	0.02880	YES	0.45753	0.33311	0.58749
32	607307.25	4053372.75	3	5.3780	43	40	43	<0.02	0.00000	NO	0.47267	0.35070	0.59800
33	607282.25	4053427.75	3	5.3924	21	20	21	0.028	0.02800	YES	0.47291	0.35098	0.59817
34	607582.25	4053207.75	3	5.4322	61	52	61	0.246	0.24600	YES	0.47358	0.35175	0.59864
35	607407.25	4053467.75	3	5.5343	10	9	10	0.402	0.40200	YES	0.47531	0.35374	0.59987
36	607407.25	4053447.75	3	5.5446	14	13	14	0.02	0.02000	NO	0.47548	0.35394	0.59999
37	607637.25	4053082.75	3	6.0146	78	69	78	1.0184	1.01840	YES	0.48341	0.36308	0.60570
38	607637.25	4053197.75	3	6.0226	62	53	62	0.0816	0.08160	YES	0.48355	0.36324	0.60580
39	607382.25	4053512.75	3	6.3144	5	4	5	<0.02	0.00000	NO	0.48848	0.36888	0.60941
40	607332.25	4053412.75	3	6.7223	30	29	30	0.04	0.04000	YES	0.49538	0.37674	0.61454
41	607687.25	4053142.75	3	6.9134	69	60	69	0.06	0.06000	YES	0.49861	0.38039	0.61698
42	607487.25	4053407.75	3	7.1761	31	30	31	0.74	0.74000	YES	0.50305	0.38540	0.62037
43	607437.25	4053367.75	3	7.7568	45	42	45	0.152	0.15200	YES	0.51287	0.39635	0.62801
44	607587.25	4053092.75	3	8.6438	76	67	76	0.0754	0.07540	YES	0.52784	0.41273	0.64007
45	607642.25	4053147.75	3	8.9993	67	58	67	0.0644	0.06440	YES	0.53383	0.41915	0.64504
46	607532.25	4053382.75	3	9.3090	40	37	40	0.336	0.33600	YES	0.53904	0.42468	0.64944
47	607457.25	4053432.75	4	11.2894	18	17	18	0.0656	0.06560	YES	0.57211	0.45829	0.67877
48	607407.25	4053412.75	4	12.2318	28	27	28	0.1974	0.19740	YES	0.58764	0.47313	0.69338
49	607687.25	4053047.75	4	12.2959	84	74	84	<0.02	0.00000	NO	0.58869	0.47411	0.69439
50	607362.25	4053402.75	4	12.5499	33	32	33	<0.02	0.00000	NO	0.59284	0.47797	0.69839
51	607687.25	4053147.75	4	12.9211	66	57	66	0.0326	0.03260	YES	0.59889	0.48350	0.70427
52	607637.25	4053117.75	4	13.2006	72	63	72	0.52	0.52000	YES	0.60342	0.48758	0.70872
53	607457.25	4053317.75	4	13.5964	52	46	52	0.224	0.22400	YES	0.60981	0.49326	0.71504
54	607407.25	4053422.75	4	14.1836	24	23	24	0.0384	0.03840	YES	0.61922	0.50143	0.72448
55	607362.25	4053282.75	4	15.8211	58	51	58	0.2758	0.27580	YES	0.64497	0.52275	0.75082
56	607387.25	4053377.75	4	15.8233	41	38	41	<0.02	0.00000	NO	0.64501	0.52277	0.75085
57	607617.25	4053067.75	4	16.6639	81	72	81	0.3418	0.34180	YES	0.65792	0.53294	0.76424
58	607507.25	4053412.75	4	17.1124	29	28	29	<0.02	0.00000	NO	0.66471	0.53817	0.77132
59	607302.25	4053482.75	4	17.3290	7	6	7	0.024	0.02400	YES	0.66797	0.54064	0.77471
60	607587.25	4053077.75	4	17.4712	80	71	80	0.0186	0.01860	NO	0.67010	0.54226	0.77693
61	607617.25	4053117.75	4	18.6911	73	64	73	0.1182	0.11820	YES	0.68808	0.55557	0.79561
62	607452.25	4053427.75	5	19.5779	19	18	19	0.1646	0.16460	YES	0.70081	0.56474	0.80874
63	607537.25	4053412.75	5	20.1159	27	26	27	0.02	0.02000	NO	0.70838	0.57012	0.81649
64	607507.25	4053397.75	5	21.2925	35	34	35	0.135	0.13500	YES	0.72455	0.58142	0.83281
65	607682.25	4053152.75	5	22.1332	65	56	65	0.07606	0.07606	YES	0.73575	0.58915	0.84390
66	607537.25	4053422.75	5	22.3613	23	22	23	0.19133	0.19133	YES	0.73874	0.59120	0.84683
67	607357.25	4053477.75	5	23.3830	8	7	8	0.0154	0.01540	NO	0.75186	0.60017	0.85947
68	607462.25	4053317.75	5	23.8641	51	45	51	0.2592	0.25920	YES	0.75788	0.60428	0.86516
69	607452.25	4053457.75	5	25.8849	11	10	11	0.1552	0.15520	YES	0.78207	0.62083	0.88721
70	607507.25	4053382.75	5	26.3907	39	36	39	0.214	0.21400	YES	0.78785	0.62481	0.89226
71	607507.25	4053292.75	5	27.2801	55	49	55	2.1218	2.12180	YES	0.79773	0.63166	0.90070
72	607617.25	4053077.75	5	27.3248	79	70	79	0.018	0.01800	NO	0.79822	0.63200	0.90111
73	607532.25	4053427.75	5	27.6896	20	19	20	0.158	0.15800	YES	0.80216	0.63476	0.90440
74	607342.25	4053467.75	5	28.2375	9	8	9	<0.02	0.00000	NO	0.80798	0.63885	0.90917
75	607537.25	4053437.75	5	29.8993	16	15	16	0.23	0.23000	YES	0.82482	0.65092	0.92242
76	607452.25	4053442.75	6	31.1573	91	79	91	0.0614	0.06140	YES	0.83678	0.65973	0.93130
77	607452.25	4053402.75	6	32.3068	92	80	92	0.1094	0.10940	YES	0.84712	0.66675	0.93861
78	607532.25	4053417.75	6	34.4811	26	25	26	0.032	0.03200	YES	0.86521	0.68187	0.95056
79	607662.25	4053152.75	6	34.6362	64	55	64	0.816	0.81600	YES	0.86643	0.68287	0.95132
80	607407.25	4053392.75	6	35.1617	36	35	36	<0.02	0.00000	NO	0.87049	0.68622	0.95383
81	607487.25	4053372.75	6	36.2997	42	39	42	<0.02	0.00000	NO	0.87893	0.69336	0.95886



# REPORT DOCUMENTATION PAGE

*Form Approved*  
OMB No. 0704-0188

Public reporting burden for this collection of information is estimated to average 1 hour per response, including the time for reviewing instructions, searching existing data sources, gathering and maintaining the data needed, and completing and reviewing this collection of information. Send comments regarding this burden estimate or any other aspect of this collection of information, including suggestions for reducing this burden to Department of Defense, Washington Headquarters Services, Directorate for Information Operations and Reports (0704-0188), 1215 Jefferson Davis Highway, Suite 1204, Arlington, VA 22202-4302. Respondents should be aware that notwithstanding any other provision of law, no person shall be subject to any penalty for failing to comply with a collection of information if it does not display a currently valid OMB control number. **PLEASE DO NOT RETURN YOUR FORM TO THE ABOVE ADDRESS.**

<b>1. REPORT DATE (DD-MM-YYYY)</b> September 2007		<b>2. REPORT TYPE</b> Final report		<b>3. DATES COVERED (From - To)</b>	
<b>4. TITLE AND SUBTITLE</b>  Evaluation of Airborne Remote Sensing Techniques for Predicting the Distribution of Energetic Compounds on Impact Areas				<b>5a. CONTRACT NUMBER</b>	
				<b>5b. GRANT NUMBER</b>	
				<b>5c. PROGRAM ELEMENT NUMBER</b>	
<b>6. AUTHOR(S)</b>  Mark R. Graves, Linda Peyman Dove, Thomas F. Jenkins, Susan Bigl, Marianne E. Walsh, Alan D. Hewitt, Dennis Lambert, Nancy Perron, Charles Ramsey, Jeff Gamey, Les Beard, William E. Doll, and Dale Magoun				<b>5d. PROJECT NUMBER</b>	
				<b>5e. TASK NUMBER</b>	
				<b>5f. WORK UNIT NUMBER</b>	
<b>7. PERFORMING ORGANIZATION NAME(S) AND ADDRESS(ES)</b>  See reverse.				<b>8. PERFORMING ORGANIZATION REPORT NUMBER</b>  ERDC TR-07-13	
<b>9. SPONSORING / MONITORING AGENCY NAME(S) AND ADDRESS(ES)</b> Office of the Assistant Secretary of the Army (Acquisition, Logistics, and Technology); U.S. Army Corps of Engineers Washington, DC 20314-1000				<b>10. SPONSOR/MONITOR'S ACRONYM(S)</b>	
				<b>11. SPONSOR/MONITOR'S REPORT NUMBER(S)</b>	
<b>12. DISTRIBUTION / AVAILABILITY STATEMENT</b>  Approved for public release; distribution is unlimited.					
<b>13. SUPPLEMENTARY NOTES</b>					
<b>14. ABSTRACT</b> <p>The characterization of impact area munitions constituents has typically employed traditional soil sampling approaches. These sampling approaches do not accurately account for the distribution of such contaminants over the landscape due to the distributed nature of explosive compound sources throughout impact areas, the highly localized distribution of contaminants surrounding these sources, and inaccurate records of historical target locations.</p> <p>Remote sensing and geographic information system (GIS) technologies were utilized to assist in the development of enhanced sampling strategies to better predict the landscape-scale distribution of energetic compounds. Remotely sensed magnetometer and electromagnetic (EM) data were used to detect and delineate areas of high densities of anomalies. The anomalies were considered to be related to targets and/or ranges likely to be highly contaminated with surface and subsurface ordnance and explosive items and artifacts. The Oak Ridge Airborne Geophysical System airborne magnetometer and time-domain EM systems were used.</p> <p>The magnetometer data were analyzed using GIS technology to develop a soil sampling plan based on varying levels of metal content in the ground. Soil samples were then collected and analyzed for energetic compounds. Statistical techniques found that a possible relationship (correlation) between analytic signal and the energetics measured in the soil may exist.</p>					
<b>15. SUBJECT TERMS</b> See reverse.					
<b>16. SECURITY CLASSIFICATION OF:</b>			<b>17. LIMITATION OF ABSTRACT</b>	<b>18. NUMBER OF PAGES</b>	<b>19a. NAME OF RESPONSIBLE PERSON</b>
<b>a. REPORT</b> UNCLASSIFIED	<b>b. ABSTRACT</b> UNCLASSIFIED	<b>c. THIS PAGE</b> UNCLASSIFIED			201

**7. (Concluded)**

Environmental Laboratory  
U.S. Army Engineer Research and Development Center  
3909 Halls Ferry Road  
Vicksburg, MS 39180-6199

Cold Regions Research and Engineering Laboratory  
U.S. Army Engineer Research and Development Center  
Hanover, NH 03755

EnviroStat, Inc.  
P.O. Box 636  
Fort Collins, CO 80522

Battelle  
105 Mitchell Road, Suite 103  
Oak Ridge, TN 37830

University of Louisiana at Monroe, Dept. of Mathematics and Physics  
700 University Avenue  
Monroe, LA 71209

**15. (Concluded)**

Analytic signal  
Anomalies  
Contaminants  
Electromagnetic  
EM  
Energetic compounds  
Energetics  
Explosive compounds  
Fort Ord  
Magnetometer  
Munitions  
Ordnance  
ORAGS